

Monitoring of the impact of the extraction of marine aggregates, in casu sand, in the zone of the Hinder Banks

Scientific Report 2 – January - December 2014

Vera Van Lancker, Matthias Baeye, Dimitris Evangelinos, Dries Van den Eynde

MOZ4-ZAGRI/I/VVL/201502/EN/SR01

Prepared for

- Flemish Authorities, Agency Maritime Services & Coast, Coast. Contract 211.177 <MOZ4>
- ZAGRI



Table of contents

Abbreviations	3
Executive summary	4
Samenvatting	5
Preface	6
1. Introduction	7
2. Study area	8
3. Materials and methods	10
3.1. Measurements and spatial observations	10
3.1.1. Longer-term measurements at a fixed location	10
3.1.2. Short-term spatial observations (<i>RV Belgica</i>)	12
3.1.3. In-situ measurements and sampling	13
3.1.4. Visual observations	14
3.1.5. Data analyses	19
3.1.6. Water column properties derived from water samples	19
3.1.7. Water column properties derived from optical measurements	19
3.1.8. Water column properties derived from ADCPs	20
3.1.9. Seabed properties derived from acoustical measurements	22
3.1.10. Seabed properties derived from sampling	22
3.1.11. External data	22
3.2. Modelling of changing hydrographic conditions	23
3.2.1. Validation of the hydrodynamic model OPTOS-FIN	23
3.2.2. Validation of the sand transport models MU-SEDIM	23
3.2.3. Validation of advection-diffusion sediment transport models MU-STM	24
4. Results	25
4.1. Natural variation in sediment processes	25
4.2. Human-induced variation	45
4.2.1. Introduction	45
4.2.2. Extraction practices	46
4.2.3. Near-field impacts	47
4.2.4. Far-field impacts	53
4.3. Modelling of changing hydrographic conditions	59
4.3.1. Validation of advection-diffusion sediment transport models	59
4.3.2. Validation of sand transport models	63
5. Conclusions	66

5.1. General conclusions	66
5.2. Recommendations for future measurements	67
5.3. Outreach	68
6. Acknowledgments	69
7. References	71
8. Annexes	73

Annex A. RV Belgica Campaign Reports

Annex B. Sediment sample analyses

Annex C. Validation of modelled bottom shear stresses

Annex D. Technical specifications of the TSHDs

Annex E. Publications

Reference to this report

Van Lancker, V., Baeye, M., Evangelinos, D. & Van den Eynde, D. (2015). Monitoring of the impact of the extraction of marine aggregates, in casu sand, in the zone of the Hinder Banks. Period 1/1 - 31/12 2014. Brussels, RBINS-OD Nature. Report <MOZ4-ZAGRI/I/VVL/201502/EN/SR01>, 74 pp. (+5 Annexes, 109 pp).

Abbreviations

ADCP	Acoustic Doppler Current Profiler
AUMS	Autonomous Underway Measurement System
BM-ADCP	Bottom-mounted Acoustic Doppler Current Profiler
BPNS	Belgian Part of the North Sea
COPCO	Continental Shelf Service of FPS Economy
CTD	Conductivity-Depth-Temperature
DGPS	Differential Global Positioning System
DoY	Day of Year
EMS	Electronic Monitoring System
FPS Economy	Federal Public Service Economy, SMEs, Self-Employed and Energy
HM-ADCP	Hull-mounted Acoustic Doppler Current Profiler
Hs	Significant wave height
ILVO	Institute for Agricultural and Fisheries Research
LISST	Laser In-Situ Scattering and Transmissometry
Mab:	Depth in Meter above bottom
MSFD	European Marine Strategy Framework Directive
NE	Northeast-directed (flood)
OBS	Optical Back Scatter
ODAS	Oceanographic Data and Acquisition System
OPTOS-BCZ	Hydrodynamic model applied to the Belgian coastal zone
POC	Particulate Organic Carbon
PON	Particulate Organic Nitrogen
RHIB	Rigid Hull Inflatable Boat
RSSI	Received Signal Strength Indicator
ROV	Remotely operated vehicle
RV	Research Vessel
SPM	Suspended Particulate Matter
SW	Southwest-directed (ebb)
TASS	Turbidity Assessment Software System (www.ecoshape.nl)
TC	Tidal coefficient
Tidal phase (xx)	Spring/Neap/Mid tide, with indication of the tidal coefficient
TSHD	trailing suction hopper dredgers
UTC	Universal Time Coordinates
VLIZ	Flanders Marine Institute

Executive summary

Integrated monitoring of the effects of aggregate extraction is needed to reach Good Environmental Status of the marine environment by 2020 (European Marine Strategy Framework Directive (MSFD); 2008/56/EC). To improve the management of the activity, understanding of the causes of the impact is crucial, as well as insight into natural variability, and therefore increased process and system knowledge is required. Additionally, when exploitation is within or near Habitat Directive areas, appropriate assessments are needed of all stressors (92/43/EEC). In 2012, new extraction activities started in a far offshore sandbank area in the Belgian part of the North Sea, just north of a Habitat Directive area. Here, ecologically valuable gravel beds occur adapted to a clear water regime. Therefore, a dedicated monitoring programme was set-up, with focus on assessing changes in seafloor integrity and hydrographic conditions, two descriptors that define Good Environmental Status. Seafloor integrity relates to the functions that the seabed provides to the ecosystem (e.g., structure; oxygen and nutrient supply), whilst hydrographic conditions refer to currents, turbidity and/or other oceanographic parameters of which changes could adversely impact on benthic ecosystems.

Since 2011, state-of-the-art instrumentation (from RV Belgica) has been used, to measure the 3D current structure, turbidity, depth, backscatter and particle size of the material in the water column, both in-situ and whilst sailing transects over the sandbanks. In the most intense extraction sector, seabed sediments were sampled in detail. In the Habitat Directive area, gravel bed integrity (i.e., epifauna; sand/gravel ratio; grain-sizes; patchiness) was measured as well. Additionally, visual observations were made through scientific divers, video frames and a remote operated vehicle.

Results relate to: (1) quantification of natural variability; (2) sediment plume formation and deposition, differentiating between small and large trailing suction hopper dredgers; (3) far-field impacts, with focus on the gravel beds within the Habitat Directive area, and (4) improvement of models that predict the impact of extraction activities. New insights were revealed on the four levels, though most striking was enrichment of fines in the coarse permeable sands of the gravel area. No direct relationship could yet be made between the intensive extractions and the mud enrichment, but the gravel beds do occur along the tidal stream axis from the southernmost extraction sector and sediment plume modelling shows deposition in the area under calm weather conditions. Further monitoring is required since favourable colonization and growth of epifauna on the gravel beds is critical for the maintenance and increase of biodiversity in the Belgian part of the North Sea.

Samenvatting

Geïntegreerde monitoring van de effecten van aggregaatextractie is nodig om een goede milieutoestand van het mariene milieu te bereiken in 2020 (Europese Kaderrichtlijn Mariene Strategie (KRMS); 2008/56/EG). Om het beheer van de activiteit te optimaliseren, alsook om de oorzaak-gevolg relaties te begrijpen en inzicht te hebben in natuurlijke variabiliteit, is een grotere proces- en systeemkennis nodig. Bovendien, wanneer de exploitatie in, of in de buurt van een Habitatrictlijnengebied valt, is een passende beoordeling nodig van de effecten van alle stressoren (92/43/EEG). In 2012 startten nieuwe extracties op ver zeewaarts gelegen zandbanken in het Belgische deel van de Noordzee, net ten noorden van een Habitatrictlijnengebied. Hier komen ecologisch waardevolle grindbedden voor, aangepast aan helder water. Een gericht monitoringsprogramma werd opgezet, met focus op het beoordelen van veranderingen in de zeebodemintegriteit en hydrografische condities, twee KRMS descriptoren om de mariene milieutoestand te evalueren. Zeebodemintegriteit betreft de functies die de bodem biedt voor het ecosysteem (bv. structuur, zuurstof en toevoer van voedingsstoffen), terwijl hydrografische condities verwijzen naar stromingen, turbiditeit en/of andere oceanografische parameters waarvan veranderingen een negatieve invloed kunnen hebben op bentische ecosystemen.

Sinds 2011, wordt state-of-the-art instrumentatie (aan boord R/V Belgica) ingezet om de 3D-stroomsnelheidsstructuur, troebelheid, diepte, backscatter en deeltjesgrootte van het materiaal in de waterkolom te meten. In de meest intensief ontgonnen sectoren werd het zeebodemsubstraat in detail onderzocht. In het Habitatrictlijnengebied werd ook de grindbedintegriteit (o.a. epifauna; zand/grind verhouding; heterogeniteit) gemeten. Aanvullend werden visuele observaties uitgevoerd, gebruikmakende van wetenschappelijke duikers, videoframes, alsook van een computergestuurd onderwatervoertuig.

De resultaten hebben betrekking op: (1) het kwantificeren van de natuurlijke variabiliteit; (2) de vorming en afzetting van sedimentpluimen, met onderscheid tussen de effecten van kleine tot grote sleepopperzuigers; (3) ver-veld effecten, met de nadruk op de grindbedden binnen het Habitatrictlijnengebied, en (4) verbetering van modellen die de impact van de extracties voorspellen. Nieuwe inzichten werden bekomen op de vier niveaus. Meest opvallend was de aanrijking van fijn materiaal in de permeabele grove zanden in het grindgebied. Geen directe relatie kon worden gemaakt tussen de extracties en de verfijning, maar de grindbedden liggen wel in het stroomgebied van de meest zuidelijke extractiesector en modellen tonen aan dat afzetting mogelijk is onder kalme condities. Dit dient verder opgevolgd te worden gezien het belang van een gunstige kolonisatie en groei van epifauna op grindbedden dat van cruciaal belang is voor het behoud en de toename van de biodiversiteit in het Belgische deel van de Noordzee.

Preface

Results presented in this report relate to the monitoring of intensive aggregate extraction in zone 4, Hinder Banks (MOZ4), for the year 2014. Since 2013, the monitoring activities are financially supported by the Flemish Authorities, Agency Maritime Services and Coast, Coast. The monitoring programme ZAGRI, funded by the revenues of the private sector, and covering all concession zones in the Belgian part of the North Sea, provides a continuous support to MOZ4, as well as for the measurements that commenced in 2011, as for the model development. In 2014, emphasis was placed on a first quantification of the generation and dispersal of sediment plumes. Potential deposition areas of the fine material from the plumes were studied also, with focus on the ecologically valuable gravel beds in the nearby Habitat Directive area. In 2015, data will be integrated with results from the morphological and biological monitoring, respectively carried out by the Continental Shelf Service of FPS Economy (COPCO) and the Institute for Agricultural and Fisheries Research (ILVO).

1. Introduction

A monitoring programme, with focus on hydrodynamics and sediment transport, has been designed allowing testing hypotheses on the impact of marine aggregate extraction in the far offshore Hinder Banks. Hypotheses were based on findings in the Flemish Banks area where 30-yr of extraction practices, and related research on the effects, were available (Van Lancker et al. 2010, for an overview). They have been adapted to incorporate descriptors of good environmental status, as stipulated within the European Marine Strategy Framework Directive (MSFD) (Belgische Staat, 2012). In the context of the present monitoring, main targets are assessing changes in seafloor integrity (descriptor 6) and hydrographic conditions (descriptor 7), two key descriptors of good environmental status, to be reached in 2020.

Summarized, main hypotheses are: (1) Seabed recovery processes are very slow; (2) Large-scale extraction leads to seafloor depressions; these do not impact on the spatial connectedness of habitats (MSFD descriptor 6); (3) Impacts are local, no far field effects are expected; (4) Resuspension, and/or turbidity from overflow during the extraction process, will not lead to an important fining of sediments (e.g., siltation); (5) Marine aggregate extraction has no significant impact on seafloor integrity, nor it will significantly lead to permanent alterations of the hydrographical conditions (MSFD descriptor 7); (6) Cumulative impacts with other sectors (e.g., fisheries) are minimal; and (7) Large-scale extraction does not lead to changes in wave energy dissipation that impact on more coastwards occurring habitats.

The monitoring follows a tiered approach, consisting of in-situ measurements and modelling (Figure 1). Critical is to assess potential changes in hydrographic conditions (MSFD, descriptor 7), as a consequence of multiple seabed perturbations (e.g., depressions in the seabed) and their interactions. This could lead to changes in bottom shear stresses, a MSFD indicator that should remain within defined boundaries¹. Therefore, considerable effort went to current and turbidity measurements along transects crossing the sandbanks, as also on point locations for longer periods. These data serve as a reference and are compared to datasets

¹ For descriptor 7 on hydrographic conditions, the monitoring programme should allow evaluating the following specifications (Belgische Staat, 2012):

- (1) Based upon calculated bottom shear stresses over a 14-days spring-neap tidal cycle, using validated mathematical models, an impact should be evaluated when one of the following conditions is met:
 - (i) There is an increase of more than 10% of the mean bottom shear stress;
 - (ii) The variation of the ratio between the duration of sedimentation and the duration of erosion is beyond the “-5%, +5%” range.
- (2) The impact under consideration should remain within a distance equal to the square root of the area occupied by this activity and calculated from the inherent outermost border.
- (3) All developments need compliance with existing regulations (e.g., EIA, SEA, and Habitat Directive Guidelines) and legislative evaluations are necessary in such a way that an eventual potential impact of permanent changes in hydrographic conditions is accounted for, including cumulative effects. This should be evaluated with relevance to the most suitable spatial scale (ref. OSPAR common language).

recorded under the events of intensive aggregate extraction. The extraction gives rise to sediment plumes and subsequent release of fines in the water column. As such, dispersion of the fines and the probability of siltation in the nearby Habitat Directive area is studied, since this may cause deterioration of the integrity of gravel beds present in this area. This relates directly to Belgium’s commitments within the MSFD stating that the ratio of the hard substrata surface area versus the soft sediment surface area should increase in time (Belgische Staat, 2012). Furthermore, abrasion of the sandbank and/or enrichment of finer material, could lead to habitat changes², another indicator within MSFD (descriptor 6 Seafloor Integrity).

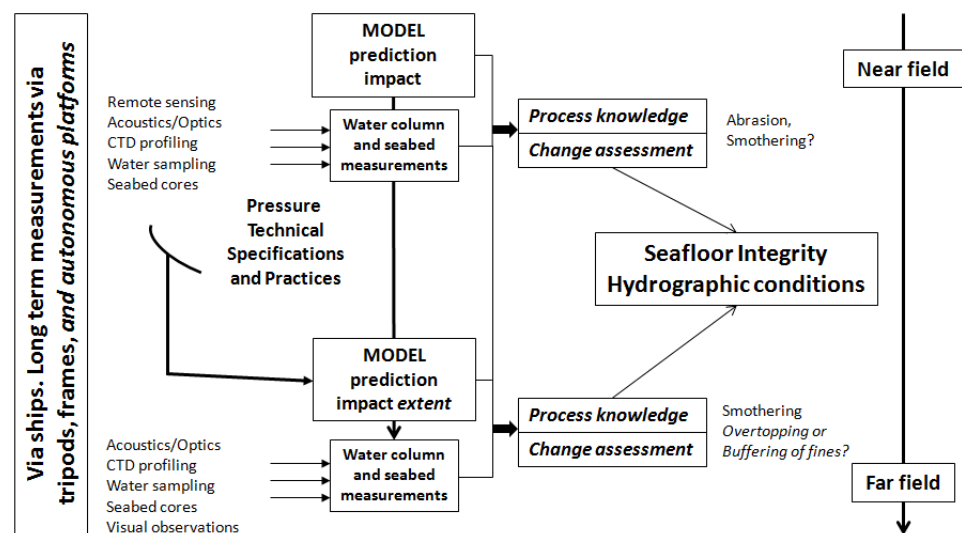


Figure 1. Overview of the research strategy aiming at quantifying both near- and far-field impacts of marine aggregate extraction.

2. Study area

The Hinder Banks form part of a sandbank complex, located 40 km offshore in the Belgian part of the North Sea (BPNS). On the sandbanks, depths range from -8 m to -30 m (Figure 2); they are superimposed with a hierarchy of dune forms, often more than 6 m in height. The channels in-between the sandbanks reach 40 m of water depth. At present, extraction of aggregates takes place mainly on the Oosthinder sandbank. Sediments are medium- to coarse sands, including shell hash, with less than 1 % of silt-clay enrichment (Van Lancker, 2009 @SediCURVE database).

² For descriptor 6 this monitoring programme contributes to the evaluation of the following environmental targets and associated indicators (Belgische Staat, 2012):

- (1) The areal extent and distribution of EUNIS level 3 Habitats (sandy mud to mud; muddy sand to sand and coarse sediments), as well as of the gravel beds, remain within the margin of uncertainty of the sediment distribution, with reference to the Initial Assessment.
- (2) Within the gravel beds (test zones to be defined), the ratio of the surface of hard substrate (i.e., surface colonized by hard substrata epifauna) against the ratio of soft sediment (i.e., surface on top of the hard substrate that prevents the development of hard substrata fauna), does not show a negative trend.

Tidal currents reach more than 1 ms⁻¹; waves are easily more than 1 m in height (44 % of the time). These offshore sandbanks are the first wave energy dissipaters in the BPNS.

Over a 10-yr period intensive extraction of marine aggregates (up to 2.9 million m³ over 3 months) is allowed in this area, with a maximum of 35 million m³ over a period of 10 years. Large trailing suction hopper dredgers (TSHD) can be used, extracting up to 12,500 m³ per run. Present-day yearly extraction levels recently surpassed 3 million m³, the majority of which was extracted with vessels of 1500 m³. Such intensive extraction is new practice in the BPNS and the environmental impact is yet to be determined. South of the Hinder Banks concession, a Habitat Directive area is present, hosting ecologically valuable gravel beds (Houziaux et al., 2008) (Figure 2). For these, it is critical to assess the effect of multiple and frequent depositions from dredging-induced sediment plumes.

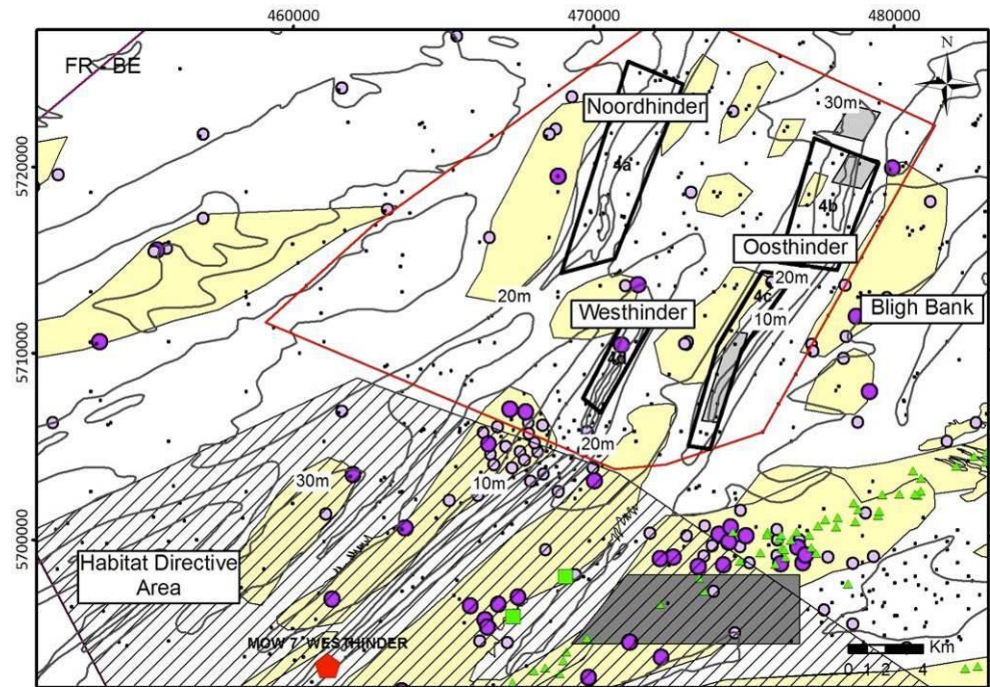


Figure 2. Area of the Hinder Banks, where intensive marine aggregate extraction is allowed in zone 4 (red line) along 4 sectors (black polygons). Within and outside these sectors geomorphological monitoring is carried out by COPCO (light grey polygons). A Habitat Directive area (hatched) is present at a minimum of 2.5 km from the southernmost sectors. Presence of gravel (purple dots) and stones (green triangles) is indicated (size of the dots represents relative amounts of gravel with a minimum of 20 %). In the light yellow areas the probability of finding gravel is high (based on samples, in combination with acoustic imagery). In the gravel refugia (green squares), west of the Oosthinder, ecologically valuable epifauna is present. Indicated also is the position of the Westhinder measuring pole MOW7 (Flanders Hydrography) (red pentagon) where most of the hydro-meteorological data are derived from. Dark grey polygon in the Habitat Directive area is an anchorage zone.

3. Materials and methods

3.1. Measurements and spatial observations

In 2014, three 1-week campaigns were organized, all with RV Belgica. Additionally, Flanders Marine Institute, VLIZ, provided the opportunity to use a Remote Operated Vehicle for visual observations in the Habitat Directive area, with RV Simon Stevin as the deployment platform. Longer term measurements were also conducted along fixed locations. See Table 1 and Figure 3, for an overview of the data periods and research areas.

Table 1. Overview of RV Belgica campaigns in 2014. DoY: Day of Year 2014. Numbering of campaigns continues from the period 2011-2013. HD area: Habitat Directive area; T_coeff: maximum Tidal coefficient. If more than 70: spring tidal conditions.

Nr	Campaign	Area	Time1	Time2	DoY1	DoY2	T_coeff (time max coeff)
13	ST1407*	Sector 4c HD area	2014-03-24	2014-03-28	83	87	70 28/3 10:20
14	ST1417	Sector 4c HD area	2014-06-30	2014-07-04	181	185	78 30/06 01:55
15	ST1425	Sector 4c HD area Bligh Bank	2014-10-13	2014-10-17	286	290	77 13/10 15:20
16	SS14-791	HD area	2014-12-04	2014-12-04	338	338	73 01/12 22:40

*During RV Belgica campaign ST1406 (12-13/3/2014) water samples were taken by COPCO and ILVO close to a TSHD. Vertical profiles of oceanographic parameters were taken as well.

3.1.1. Longer-term measurements at a fixed location

Near-bottom processes (currents and turbidity) were studied using an upward looking bottom-mounted Acoustic Doppler Current Profiler (BM-ADCP; Teledyne/RD Instruments, 1200 kHz Workhorse Sentinel) at 2 locations:

- (1) Eastern steep flank of the Oosthinder sandbank to study the direct impact of the extraction processes. The location was chosen near Sector 4c, outside of main navigation routes and along the steep flank where less beam trawling occurs (see Table 2).
- (2) In the Habitat Directive area: in the trough of a barchan dune where rich gravel beds occur. Aim was to study the relation between the barchan morphology, its fine sediment trapping efficiency (vortices in the lee side?) and deposition of fines on top of the gravel beds (Table 2).

Data were recorded with reference to the bottom; depth in meters above bottom is abbreviated as mab. Positions are given in Table 3.

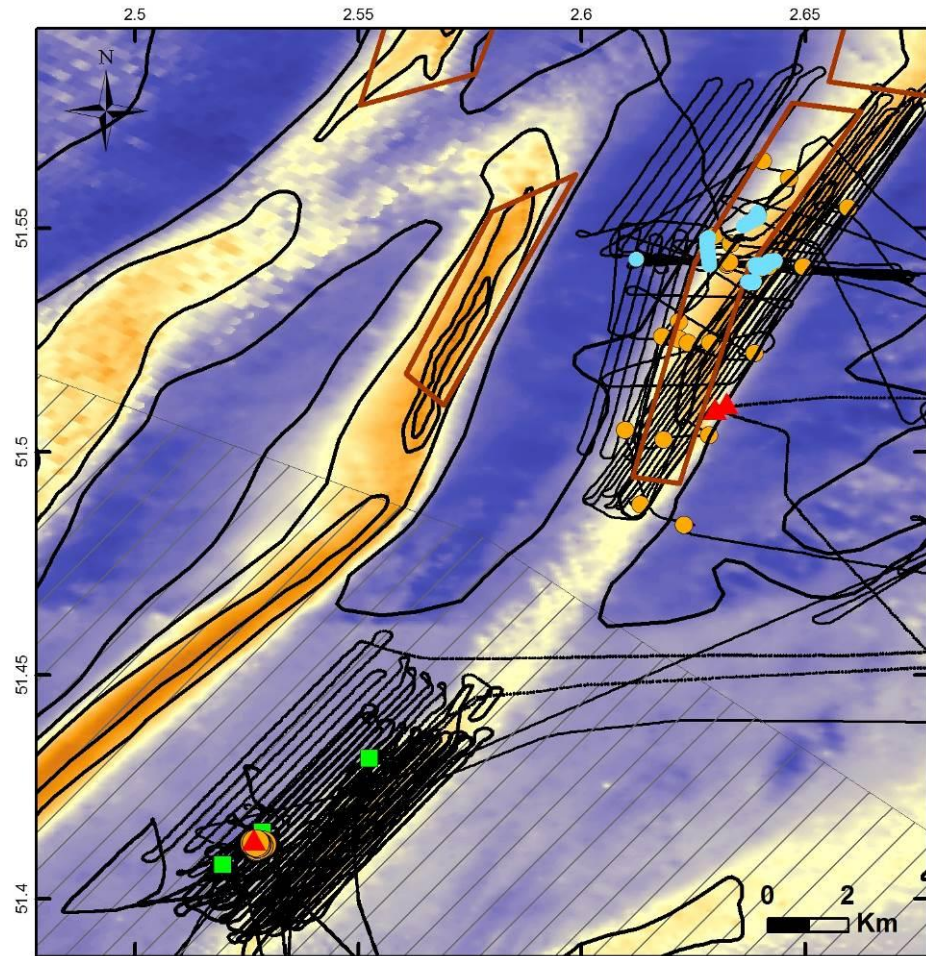


Figure 3. Overview of the 2014 measurements in Sector 4c, Oosthinder sandbank (brown polygon) and south of it, along the gravel beds within the Habitat Directive area (hatched). Along the tracklines multibeam echosounding was performed. Perpendicular to the Oosthinder sandbank, current and backscatter profiling was carried before, during and after extraction, together with water sampling (blue dots). Reineck boxcores were taken in Sector 4c, and Hamon grabs along the gravel beds (orange dots). Longer term measurements with a bottom-mounted ADCP were carried out along the steep side of the Oosthinder sandbank and in the trough of a barchan dune along the gravel beds of the Habitat Directive area (red triangles). Hotspots of biodiversity are indicated also (green squares).

Table 2. Longer term deployments with a BM-ADCP, discussed in this report. Settings of the deployments are given.

Type	Start	End	Bin Size (m)	Remarks
OH-Gravel RDI-BB 1228.8 kHz	2013-07-01 16:45	2013-07-03 09:36 ± 2 days	0.25	Fast pinging mode Bins [0.81-15] mab; average ensemble interval 1.5 s
OH-Impact RDI-BB 1228.8 kHz	2013-10-21 2013-10-26 06:39	2013-10-25 06:38 ± 4 days 2014-04-17 11:39 186 days; ± 6 months	0.25 1*	Fast pinging mode Bins [1.52-12.52] mab ; average ensemble interval: ± 01 h
OH-Gravel RDI-BB 1228.8 kHz	2014-06-30 08:00	2014-07-10 13:32 10 days	0.25	Fast pinging mode Bins [0.81-15] mab; average ensemble interval 10 s

**Originally, the BM-ADCP measured at a bin size of 0.25 m at a high frequency recording interval. However, after 4-days of measurements a short cut took place, resetting the instrument to its default settings of 1 m bin size at an hourly recording rate.*

For optimal range for good quality ADCP measurements (see http://www.rdinstruments.com/datasheets/wh_sentinel.pdf.)

Table 3. Location of the longer term deployments.

ID	Location	Position (WGS84)	Depth
OH-Impact	Oosthinder eastern steep flank	51°30.558'N, 002°37.814'E	± 28 m
OH-Gravel	Oosthinder, western flank. Trough barchan dune	51°24.781'N; 002°31.603'E	± 30 m

The long duration of the ADCP deployment in winter 2013-2014 was unforeseen. Planned duration was approximately 1 month, but the instrument could not be recovered because of no response of the ADCP's transponder. Thanks to dedicated sonar equipment on Belgian Navy's vessel Zr.Ms. URK, the ADCP was detected on 19/12/2013. Navy divers noted that the equipment was for 2/3 buried under the sand. On 15/04/2014, the Navy vessel M923 NARCIS, relocated the ADCP to attach an anchor/buoy system for later recovery of the ADCP. Divers confirmed a 90 % burial of the equipment. RV Belgica recovered the ADCP on 17/04/2014. For the whole duration data has been recorded, though with several data gaps, due to burial of the ADCP, and too low concentrations of SPM in the water column during neap tide.

3.1.2. Short-term spatial observations (*RV Belgica*)

In 2014, the following observations were made:

- (1) Several approaches were tested following a trailer hopper suction dredger (TSHD) (Sector 4c) to quantify dredging-induced sediment plumes. RV Belgica's hull-mounted Acoustic Doppler Current Profiler (HM-ADCP - workhorse RDI, 300 kHz, 1 m bin size) was used at a preferred ship speed of 8 kt. Simultaneously, multibeam echosounding (Kongsberg-Simrad

EM3002 300 kHz; depth, backscatter and water column data) was used, and vertical profiling of oceanographic parameters and water sampling was conducted (see further) (RV Belgica ST1407).

- (2) Very-high resolution acoustic measurements were performed with RV Belgica's multibeam system (Kongsberg-Simrad EM3002, 300 kHz), west and east of Sector 4c, Oosthinder sandbank (RV Belgica ST1407). The system was used also to monitor depth and sediment changes in the Habitat Directive area, south of Sector 4c (RV Belgica ST1417, ST1425). Depth and backscatter data were obtained. Later, results will be combined and compared with bathymetric data from FPS Economy, SME's, Self-Employed and Energy.
- (3) Through-tide (13-hrs cycles) stationary measurements of hull-mounted ADCP (HM-ADCP): currents and turbidity; bin size of 1 m (ST1407, ST1417, Habitat Directive area; ST1425, Sector 4c, gentle and steep side Oosthinder sandbank).
- (4) Throughout all measurements, RV Belgica's Autonomous Underway Measurement System (AUMS) recorded a.o. optical backscatter as a proxy of turbidity. The AUMS instrumentation is linked to a seawater pump system taken water, continuously, at the bow of the ship at 3.2 m. Although, the quality of these data is still under evaluation, their relative values aid in the quantification of turbidity variations in the study area.

See Annex A for the cruise reports ST1407, ST1417 and ST1425, for more details.

3.1.3. In-situ measurements and sampling

Water properties

For calibration of the continuous registrations (HM-ADCP; BM-ADCP; AUMS) water samples were taken using a Niskin bottle of 10 l, mounted on a Seacat profiler (SBE09 CTD system). The latter allowed vertical profiling of oceanographic parameters using CTD for salinity, temperature and depth; and optical backscatter sensor (OBS) for turbidity. Particle-size distribution and volume concentration in the water column was measured using a Sequoia type C 100 X Laser In-Situ Scattering and Transmissometry (LISST). Using an annular ring detector, the instrument derives in-situ particle sizes, in the range 2.5 to 500 μm , from the scattering of particles on 32 rings. The size distribution is presented as concentration (μl^{-1}) in each of the 32 log-spaced size bins. Date and time, optical transmission, water depth and temperature are recorded as supporting measurements (<http://www.sequoiasci.com>). Water samples were filtered on board for suspended particulate matter (SPM) every 30'. Mostly, 1.5 l of water was filtered. Extra filtrations were done, once per hour, for particulate organic carbon (POC/PON) (0.250 l), and a bottle of water (0.33 l) was kept for calibration of the conductivity sensor for salinity.

Dedicated water column measurements were performed for the quantification of sediment plumes arising from TSHDs (see cruise report RV Belgica ST1407). Water samples were taken in the surface plume.

During campaigns ST1407 (Sector 4c, Habitat Directive area), ST1417 (Habitat Directive area) and ST1425 (Sector 4c, gentle and steep side Oosthinder sandbank sediment particles in the water column were retrieved when RV Belgica measured consistently in one area (typically ± 13 h). A centrifuge purifier was used to filter suspended particulate matter from the continuous seawater pump at 3.2 m below the water surface.

See Annex A for the cruise reports ST1407, ST1417 and ST1425, for more details.

Seabed properties

On selected locations seabed sediment samples were taken:

- (1) To characterize, in detail, sediment composition along Sector 4c and to evaluate deposition of the overflow deposits in the near and far field. During ST1407, 16 Reineck boxcore sediment samples were taken and were on-board sliced at a 1-cm interval. Location was defined taken into account: (i) a good spatial representation over the sandbank; (ii) in- and outside intensive dredged areas; (iii) far field areas, where previously plumes were observed (Van Lancker & Baeye, submitted). In the Habitat Directive area, Hamon grabs were taken along the gravel beds with rich epifauna, hence to assess sediment and biological variability (RV Belgica ST1407 (3); ST1417 (12)). Locations were defined on the basis of previous sampling efforts. It is intended to sample these locations each year allowing studying grain-size variation through time, and potentially changes in bottom structure. During ST1417, additional samples (6) were taken by divers: on the top and in the trough of a barchan dune.
- (2) To validate model results, Hamon grabs (3) were also taken in the Bligh Bank area, where long-term simulations of the dispersal of sediment plumes showed deposition of the fines (RV Belgica ST1425).

See Annex A, RV Belgica cruise reports for more details.

3.1.4. Visual observations

Opportunities were sought to investigate the presence and extent of potential smothering of gravel beds in the Habitat Directive area with visual means. To explore the possibilities in future monitoring, a dedicated working group was established within RBINS OD Nature. Arrangements were made with RBINS scientific diving team, led by Alain Norro, and RBINS OD Nature MARECO team for biological validation of the visual observations. VLIZ was contacted for the use of their visual instrumentation: small and large video frame; and the remote operated vehicle (ROV) GENESIS (Figure 4-5). Periods and characteristics of vis-

ual observations are listed in Table 4. The ROV operation was the first deployment of the ROV on RV Simon Stevin. For this first, no separate positioning system was mounted on the ROV and operations were done on drift, with the vessel following the ROV. For both the small video frame and the ROV good imagery was obtained only when the equipment was close to the seafloor. For all operations, imagery deteriorated quickly when currents increased. Only the window of slack tide is suitable.

Table 4. Visual observations in the Habitat Directive area (ROV: Remote Operated Vehicle, RHIB: Rigid Hull Inflatable Boat).

Period	Equipment	Platform	Modus
2014-06-30 to 2014-07-04	Small video frame (VLIZ)	RV Belgica cruise ST1417	Drift
2014-06-30 to 2014-07-04	Hand-held devices by divers	RV Belgica / RHIB cruise ST1417	Drift and stationary
2012-12-04	ROV GENESIS (VLIZ)	RV Simon Stevin cruise 14-791	Drift

Visual observations were made along four areas of interest (Table 5; Figure 6-7). Purpose was to revisit the refugium areas as defined by Houziaux et al. (2008). In the period 2006-2008, gravel beds with exceptional rich epifauna were observed, based on samples with a Gilson type dredge. Area 1 was the northern refugium; area 2 the southern refugium; and area 4 was the location where the scientific diving team dived in 2007. Area 3 was chosen as the outer southern limit of the barchan dune field. Hypothesis was that, if there was a smothering due to extraction activities, there might be a north-to-south trend in the intensity of smothering, hence away from the activity.

Table 5. Locations for visual observations (four different areas, all in the trough of barchan dunes). Per area, a reference position is given.

Sample id	WGS84_NB	WGS84_OL	Remark
Area 1	51°25.8833'	2°33.1500'	Location refugium North
Area 2	51°24.7333'	2°31.6333'	Location refugium South
Area 3	51°24.4501'	2°31.1762'	Similar location refugium; limit of the barchan dune area
Area 4	51°24.8322'	2°31.6590'	Position dive of 2007

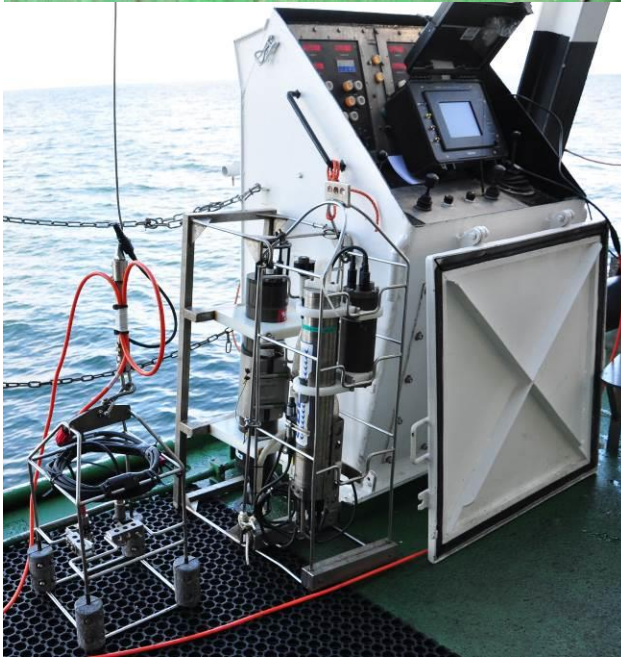
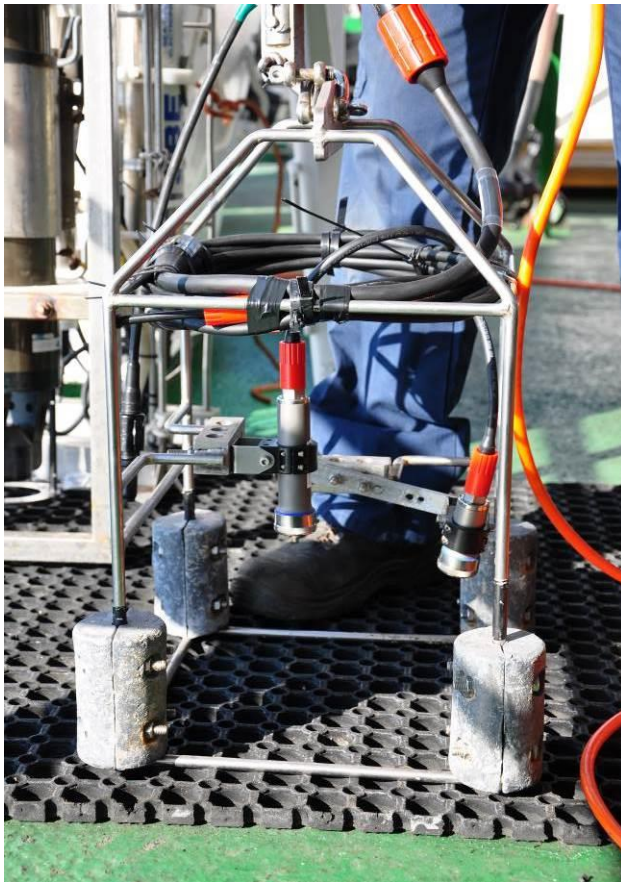


Figure 4. Visual observations during RV Belgica campaign ST1417: small video frame with real-time data visualisation (@VLIZ) and hand-held video imaging by divers (Scientific diving team RBINS OD Nature).

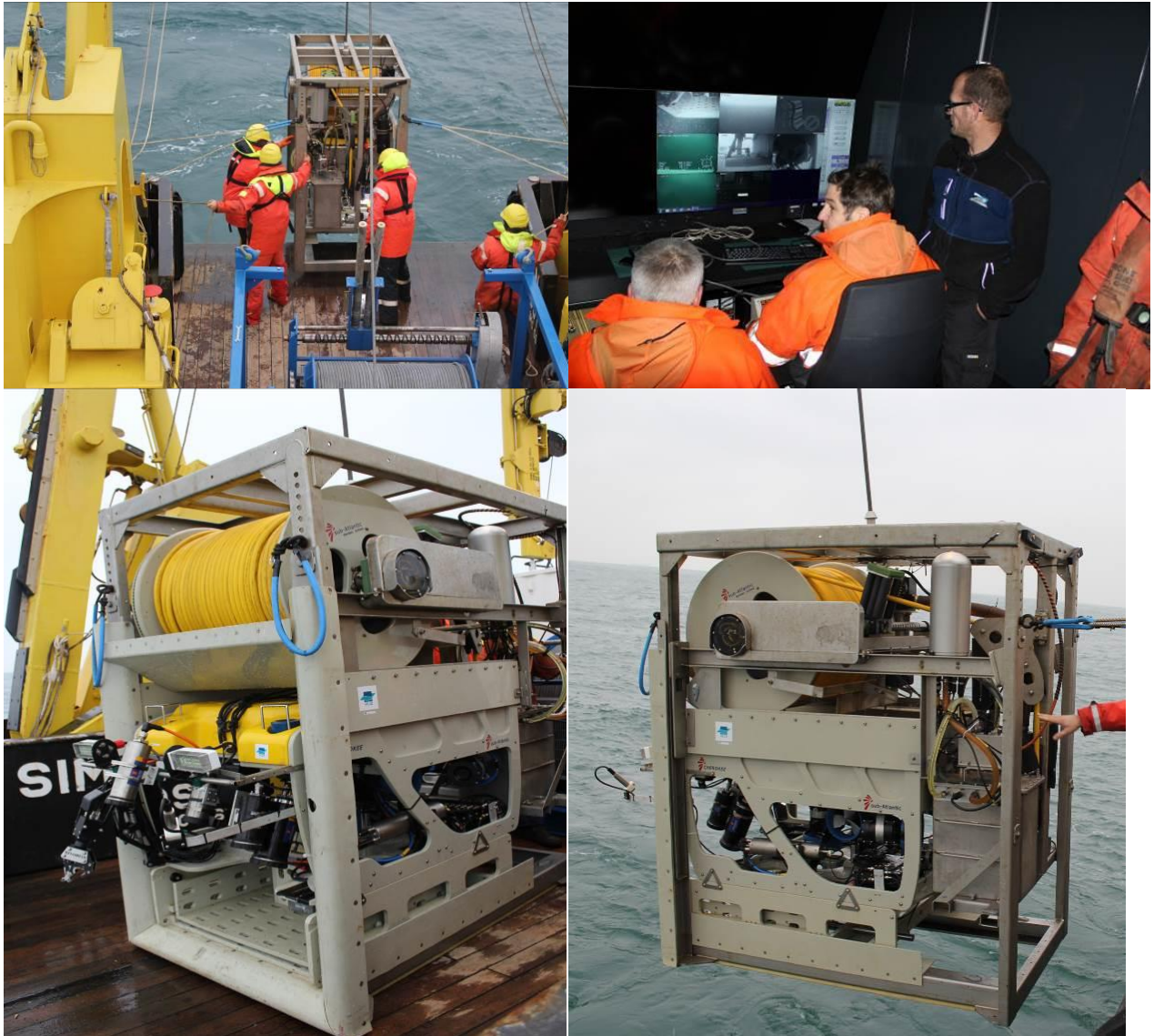


Figure 5. Remote Operated Vehicle GENESIS (@VLIZ), launched from RV Simon Stevin (Pictures @VLIZ). The ROV with 'garage' is first launched; following, the ROV leaves the 'garage' in the mid-water column. Throughout the operations the 'garage' and umbilical float in the water. The drag on the system increases with higher current velocities rendering the operations more difficult.

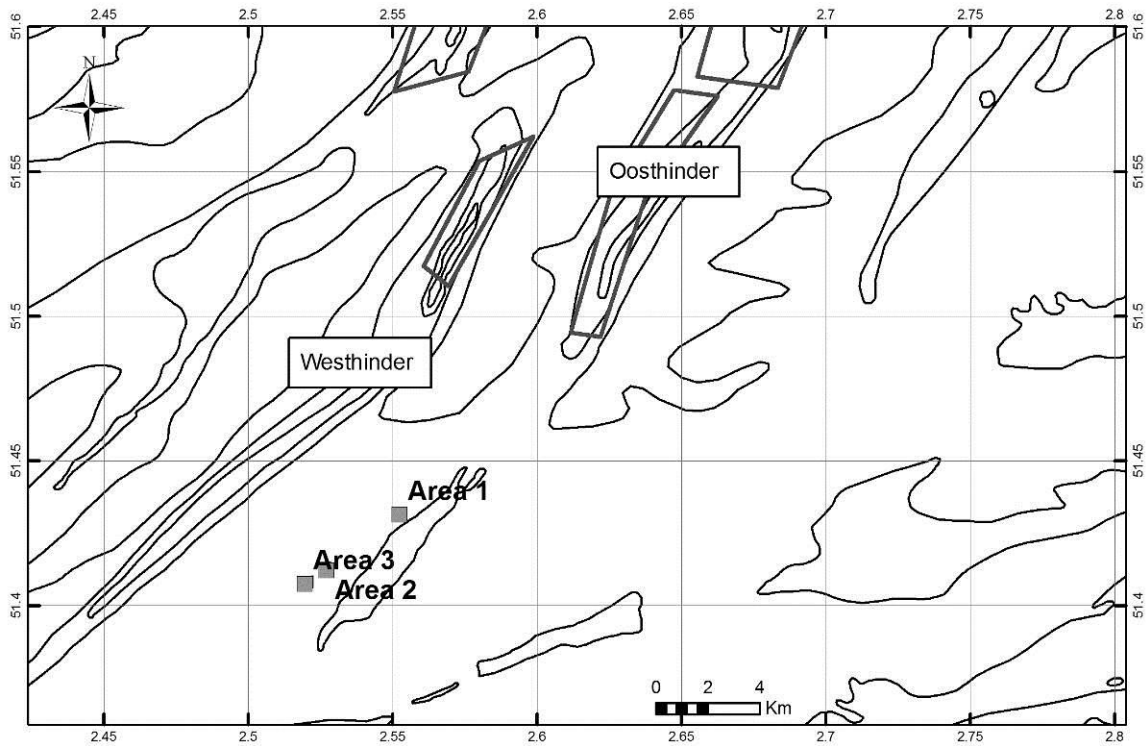


Figure 6. Location of the areas of interest for visual observations. For details, as well as location of Area 4, see Figure 7.

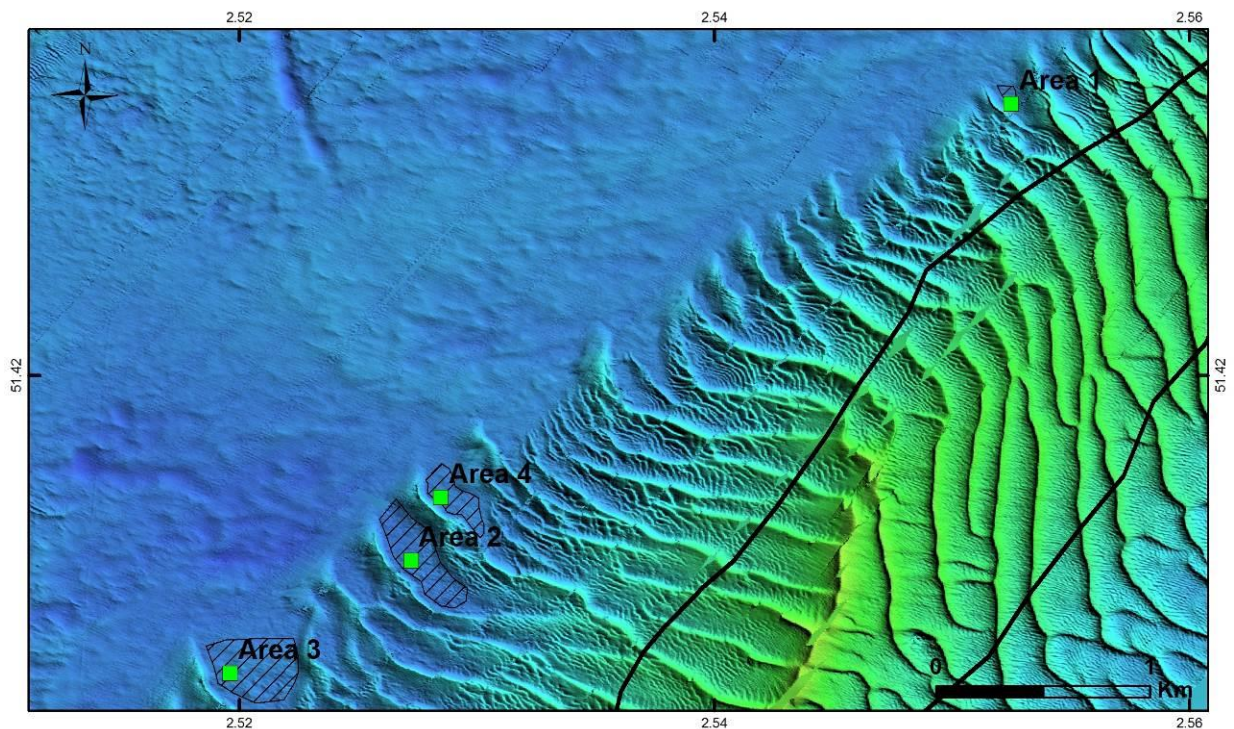


Figure 7. South part of the Oosthinder sandbank where a series of barchan dunes are attached to the main sandbank. In their trough position gravel beds were found and previously 2 refugia were identified (Area 1 and Area 2; Houziaux et al., 2008), which were exceptionally rich in biodiversity. Area 3 was taken as a test area to verify biodiversity at the extremity of the barchan dune field and furthest away from the extraction activities. The four areas were video-imaged with RV Belgica in July 2014, during which also dives were performed in Area 2, 3 and 4. In Area 2 and Area 3 ROV operations were carried out with RV Simon Stevin. Background bathymetry Van Lancker et al., 2007.

3.1.5. Data analyses

Most of the acoustic data, acquired in the period 2014, have been processed. Most of the seabed samples have been analysed.

All data were time-stamped (Universal Time Coordinates, UTC) allowing accurate correlations of various observations. These timestamps were converted to Day of Year (DoY) (1/1/2014 12h=0.5).

3.1.6. Water column properties derived from water samples

On board, water samples were filtered, in three replicates, using pre-weighted Whatmann GFC filters. These were analysed at the Marine Chemistry Lab (OD Nature, ECOCHEM). SPM concentrations (Unit gl^{-1}) were obtained after drying of the filters for 48 hours, after which weight differences were calculated. A deviation of 12 % between the replicates is acceptable (ECOCHEM Standards). Measuring uncertainty of deriving SPM from filtrations is 17 %. Since 2011, 1366 water filtrations have been made in the Hinder Banks area. POC/PON analyses (Unit gl^{-1}) were carried out in the laboratory using an Interscience FlashEA 1112 Series Element Analyser. Measuring uncertainty is 12 % for POC; 18 % for PON (ECOCHEM AK 7.0). For salinity (Unit PSU), a Laboratorium salinometer – Portasal 8410 (Guildline) van Ocean Scientific Int. was used; the measuring uncertainty is 0.15 % (ECOCHEM). It needs emphasis that water samples were taken at different levels in the water column. In ST1407 only the mid-water column was sampled because of technical constraints. Normal procedure is to take a sample 2-4 mab, depending on wave action, hence platform motion. The depth of the water sample is derived from the CTD profiles (see below). Still, there are important uncertainties on the exact sampling depth, as the Seacat frame is easily carried away by the currents. This complicates the match-ups with ADCP data, a necessary step for calibration towards mass concentrations of SPM.

3.1.7. Water column properties derived from optical measurements

Conductivity-depth-temperature (CTD) and optical backscatter (OBS)

CTD data from the Seacat profiler were analysed to derive the depth of the vertical profiles (e.g., link with water sampling and ADCP profiles). OBS data are not yet processed; they will be converted later to mass concentrations of SPM.

In-situ particle size variation from LISST

Data from the LISST-100X were processed following the guidelines “Processing LISST-100 and LISST-100X data in MATLAB”, posted on the Sequoia Scientific website (Sequoia Sci, 2008). After correction for the background (i.e., instrument and ambient water related) binary data from the rings were converted into volume concentrations (μl^{-1}) per ring. This dataset was further analysed in terms of temporal variability (e.g., throughout a 13-hrs tidal cycle) and over the

vertical (i.e., from the surface to 2-3 mab).

Underway optical backscatter measurements (AUMS)

These data were used as they are provided by RV Belgica's Oceanographic Data and Acquisition System (ODAS).

3.1.8. Water column properties derived from ADCPs

ADCPs detect the echoes returned from suspended material (i.e. "sound scatterers") from discrete depths of the water column. Echo intensities, per transmitted pulse, are recorded in counts (also termed the Received Signal Strength Indicator (RSSI), providing indirect information on the currents and density of suspended matter ('backscatter') within each ensonified bin. For the backscatter, the values remain relative as the instrument cannot differentiate the echo intensity from various sources (i.e. suspended sediments, debris, plankton, or air bubbles and high levels of turbulence, e.g. due to waves). This bias complicated interpretation of the datasets, as well as quantitative analyses to find correlation with hydro-meteorological datasets.

Currents and turbidity

For recalculation of bin depth of the HM-ADCP to actual depth values below the water surface, a fixed draught of 4 m was added for RV Belgica. With the blanking distance associated to the type of instrument and the bin size (2 bins are lost), the first depth was around 7 m below the water surface for the hull-mounted profiles with RV Belgica (for 1 m bins). Pulses were averaged into ensembles at a time interval of 60 seconds per sample. The average standard deviation (or accuracy) of current estimates was $\pm 0.018 \text{ ms}^{-1}$ for the 300 kHz ADCP, at 1 m bin size; $\pm 0.009 \text{ ms}^{-1}$ for the 1200 kHz for 0.05 m bin size ADCP (RDI software). For the HM-ADCP data (RV Belgica), also 60 seconds averaging was applied, resulting in a horizontal resolution of $\pm 240 \text{ m}$, at an average ship speed of 8 kt. The horizontal resolution varied with the ship's speed. Errors increased dramatically when using smaller bin sizes for the 300 kHz ADCP.

Algorithms were used to convert the measured RSSI counts to acoustic backscatter in decibels (dB) using the echo intensity scale (dB per RSSI count). The echo intensity was multiplied by 0.42 in order to obtain dB values (instead of counts, and accounting for sound absorption, beam spreading and battery decline). These dB values were then converted to mass concentrations of suspended particulate matter (SPM in gl^{-1}), by calibration against SPM values derived from water filtrations during several field campaigns.

Sediment deposition

Throughout the long-term ADCP deployment, there were several periods of lower quality data that led to the hypothesis that under these conditions sound was attenuated due to a sediment layer on top of the BM-ADCP. From Belgian Navy divers it was known that the trawling resistant system in which the ADCP

was mounted was buried for 90 % in the sand. Whenever additional sand was transported in the area (by migrating sand dunes, or by deposition of sediment plumes, naturally- or human-induced), the instrument itself got buried too, which led to attenuation of the signal, for which the percent good of the four beams is a proxy. As such, echo intensities were plotted for each of the four beams, as well as the averaged beam echo intensity value (see results section). The quality of beam 3 (percentage 'Good'; PG3) was used as a proxy for sediment deposition.

Bottom shear stress from measurements

From the BM-ADCP data, bottom shear stresses were calculated using the 'Law of the Wall' method (e.g., Bergeron and Abrahams, 1992). This method is based on the assumption that the velocity profile in the lower portion (15-20%) of an open channel flow has a logarithmic structure. Hence, a logarithmic profile is fit to the near bottom velocity data in order to obtain the friction velocity u_* and typify the surface texture by a roughness length, z_0 , using the relation:

$$u = \frac{u_*}{\kappa} \ln \frac{z}{z_0}$$

where u is the horizontal mean velocity measured at height z above the bottom and κ is the von Karman's constant. The bed shear stress (τ_0) can then be calculated using the friction velocity as

$$\tau_0 = \rho u_*^2$$

with ρ the water density.

For the long-term BM-ADCP dataset, the first bin was at 1.52 m only, which would not allow these calculations. However, the ADCP recorded initially for about two days with smaller bin sizes (see above), hence for this period detailed calculations were made. In addition, the bottom shear stress was plotted against the current velocity of the 4th bin (at 1.56 mab) (Figure 8). This relationship ($R^2=0.94$, slope=3.7168, and Y-intercept= -0.5946) was then used to obtain the bottom shear stress for the entire deployment. Calculation on the error margins on this indirect calculation is not clear yet.

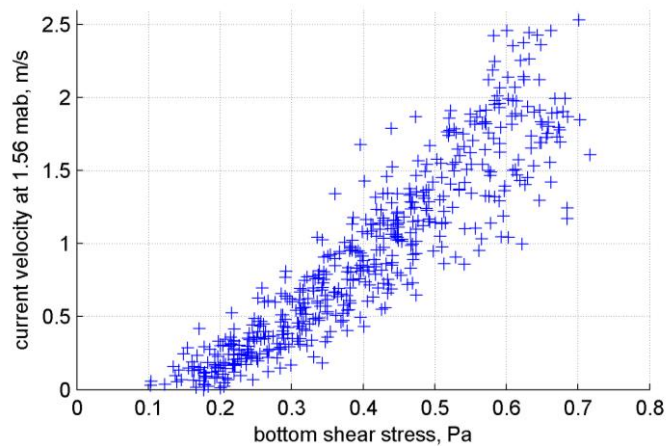


Figure 8. Bottom shear stress versus current velocity at 1.56 mab. This relationship ($R^2=0.94$, slope=3.7168, and Y-intercept= -0.5946) was used to convert current velocities into bottom shear stresses for the entire deployment period (Figure 25).

3.1.9. Seabed properties derived from acoustical measurements

The very-high resolution multibeam bathymetry and backscatter data that were obtained, in full-coverage, along the central part of the Hinder Banks (RV Belgica ST1407) and along the Oosthinder sandbank in the Habitat Directive area (RV Belgica ST1407; ST1417; ST1425) have not been processed yet.

3.1.10. Seabed properties derived from sampling

Sediment samples, from the seabed and the water column, were analysed for grain-size, organic matter and carbonate content. The same applies to the soft sediments within the Hamon grabs. To retrieve sediment from water from a bucket (e.g., from within a sediment plume), a laboratory centrifuge (UGent, Dep. Geology) was used to obtain sufficient material for analyses. OD Nature's MARECO team analysed the epifauna. *See Annex B for sediment analyses procedures.*

3.1.11. External data

Hydro-meteorological data

Wave information (significant wave height in m, direction of low and high frequency waves in degrees, low frequency (0.03 Hz to 0.1 Hz) wave energy in cm^2) were obtained, at 30 min interval, from a Wavec buoy (Westhinder location, Flanders Hydrography) at 18 km southwest of the study area (Figure 2). Sea surface elevation and 3D currents (10 min interval) were extracted from the operational 3D hydrodynamical model OPTOS-BCZ (Luyten et al., 2011). Wind velocity and direction (10 min interval) originated from the fixed Westhinder measur-

ing pole (Flanders Hydrography) (for location, Figure 2). A tidal coefficient³ was calculated to discriminate easily between spring and neap tide and variability in spring tidal levels. Values of more than 70 were regarded spring; 50 mid tide. During the measurements in the period 2011-2013, a maximum of 87 was calculated; in 2014, this increased to 107.

Electronic Monitoring System (EMS)

To detect dredging-induced sediment plumes, the timing of dredging activities was accounted for and was coupled to the relevant time series (Van den Branden et al., 2012, 2013, 2014).

3.2. *Modelling of changing hydrographic conditions*

Focus of the modelling is to assess changes in hydrographic conditions, as within MSFD, Belgium stipulated that variations in bottom shear stresses should remain restricted in the advent of human activities (see footnote 1) (Belgische Staat, 2012). Before such assessments can be made, it is critical to validate the existing mathematical models, which are at the basis of the calculation of bottom shear stress. Furthermore, sediment plume modelling needed to be developed, to assess the probability of deposition of fines in the Habitat Directive area, where ecologically valuable gravel beds occur.

3.2.1. Validation of the hydrodynamic model OPTOS-FIN

See report Year 1.

3.2.2. Validation of the sand transport models MU-SEDIM

MU-SEDIM model (Van den Eynde et al., 2010) calculates bottom shear stresses and sand transport, using a local total-load transport formula, on a grid with a resolution of 250 m x 250 m. A first task consisted of comparing the bottom shear stress, calculated with the numerical model, with the bottom shear stress, derived from field measurements. *See Annex C, for a detailed report on calculations and modelling of bottom shear stresses*

³ For the calculation of the tidal coefficient a methodology was adopted that is commonly used in France, and used by the French Hydrographic Service SHOM (http://fr.wikipedia.org/wiki/Calcul_de_marée). A tidal coefficient represents the amplitude of the tidal level compared to its averaged level and is expressed in hundredths. In France, data is used from tidal levels in Brest where a value of 100 is the maximum astronomical tidal level. For this location, regarded as being representative for the Atlantic coast, the values vary between 20 and 120. Values more than 70 are regarded spring tide; those below neap tide. A coefficient of 95 corresponds to average spring tidal levels; 45 average neap tidal levels. For the calculation of the tidal coefficient for Belgian waters an averaged tidal level (TAW) was taken from a 10-yrns elevation data series (2001-2010) from the tidal gauge at Oostende (Vlaamse Hydrografie, 2011). This value (2.339 m TAW) was subtracted from the high water levels at Oostende (Meetnet Vlaamse Banken, HWO) during each campaign. The outcome was first divided by the averaged value of the most elevated tidal levels (i.e., equinox spring tidal levels; for Oostende this equals to 6/2 m TAW, Vlaamse Hydrografie, 2011) and then multiplied with 100 to obtain the value in hundredths. In short the formula is $[(HWO - 2.339) / 3 * 100]$.

3.2.3. Validation of advection-diffusion sediment transport models MU-STM

The MU-STM model (Fettweis & Van den Eynde, 2003; Van den Eynde, 2004) calculating advection and dispersion, and erosion and deposition of fine-grained material and (fine) sand in the water column, was adapted for its use in sediment plume modelling. To predict the sediment release rate from dredging activities of TSHDs, TASS 4.0 software was used (EcoShape, 2013; www.ecoshape.nl; Spearman et al., 2011). The main sources of input data were: (i) characteristics of the TSHDs; (ii) characteristics of the dredging operation; (iii) hydrodynamic conditions of the dredging site; and (iv) the nature of the *in-situ* sediment being dredged. For each TSHD, the predicted releases were coupled to the effective extraction events (Electronic Monitoring System or EMS data). Additional input parameters were an erosion constant, a critical bottom shear stress for erosion and deposition and settling velocity. A final map of dispersion, including the total mass and concentration of each sediment fraction, was obtained as an outcome of the model simulations. For the whole simulation period, detailed output was generated at selected locations to investigate temporal and spatial variability of the deposition patterns. The workflow is presented in Figure 9.

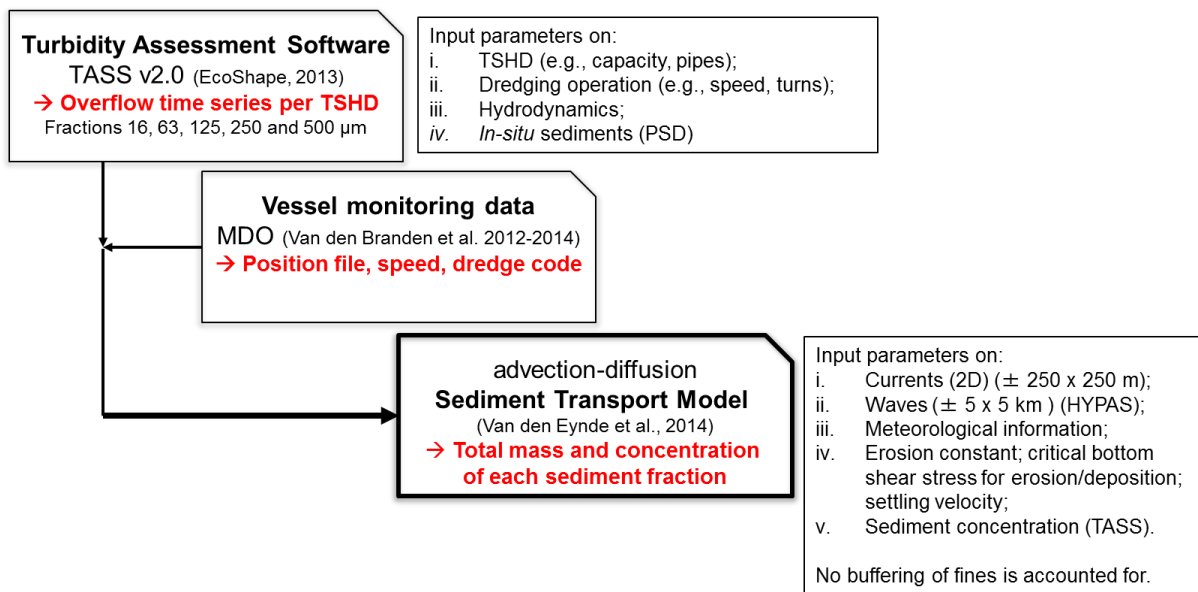


Figure 9. Workflow on sediment plume modelling, based on a combination of the TASS software, vessel monitoring data and the MU-STM advection-diffusion sediment transport model.

Considerable effort went to the compilation of the required technical specifications (input to the TASS software) of the TSHDs. Data were provided by the dredging companies. To become more acquainted with the dredging process, three visits were made to TSHDs (Breughel (DJN), Rio (Groep De Cloedt), Pal-lieter (DEME, 25/11/2014)). See Annex D for the technical specifications of the TSHDs.

4. Results

4.1. Natural variation in sediment processes

Reference is made to Van Lancker et al. (2014) reporting the main natural variations that were current- and wave-induced, based on the 2011-2013 monitoring. Only new insights are reported here, and are mostly based on new 13-hrs measurements and long-time series obtained with the HM-ADCP and BM-ADCP.

Oosthinder sandbank, Sector 4c

During RV Belgica ST1425 (13-17/10/2014), HM-ADCP measurements were conducted whilst sailing over the sandbank areas (snapshot in Figure 10) and two 13-h cycles were measured whilst being anchored on the Oosthinder sandbank. For the latter, the aim was to demonstrate the difference in hydrodynamics and sediment transport along the gentle (stoss) and steep (lee) side of the sandbank (Figure 11; for position of the water samples see Figure 12). Analyses of the data confirmed that along the steep side of the sandbank the ebb current was more dominant (stronger) than the flood current, whilst along the gentle side the flood was more dominant (stronger) than the ebb current. Sediments in the water column, as sampled with the centrifuge purifier, were clearly finer along the gentle slope, as compared to the steep slope. Samples from the latter clearly contained fine sands. This will be confirmed by the grain-size analyses. Water filtrations confirmed higher SPM concentrations along the steep slope (measurements up to 0.020 g l^{-1}) with highest values during slack tide ± 2 h before High Water. Note that during this time sand grains were present in the water samples, giving rise to fluctuations in the SPM concentrations. Compared to the steep slope, SPM variations were smaller along the gentle slope. Highest values ($\pm 0.0075 \text{ g l}^{-1}$) were measured also ± 2 h before High Water. Figure 13 and Figure 14 provide SPM concentration variation derived from HM-ADCP.

Natural variation in sediment processes was further investigated in the Habitat Directive area, particularly along the barchan dunes, where ecologically valuable gravel beds occur. During RV Belgica campaign ST1407, a 13-h cycle was performed measuring current and backscatter information with the HM-ADCP. Similar observations were made during RV Belgica ST1417. See

Figure 15 for the variation in SPM concentrations, obtained from water filtrations. Positions of the water sampling in the trough are indicated in Figure 16 and Figure 17. HM-ADCP data are shown in Figure 18, Figure 19 and Figure 20.

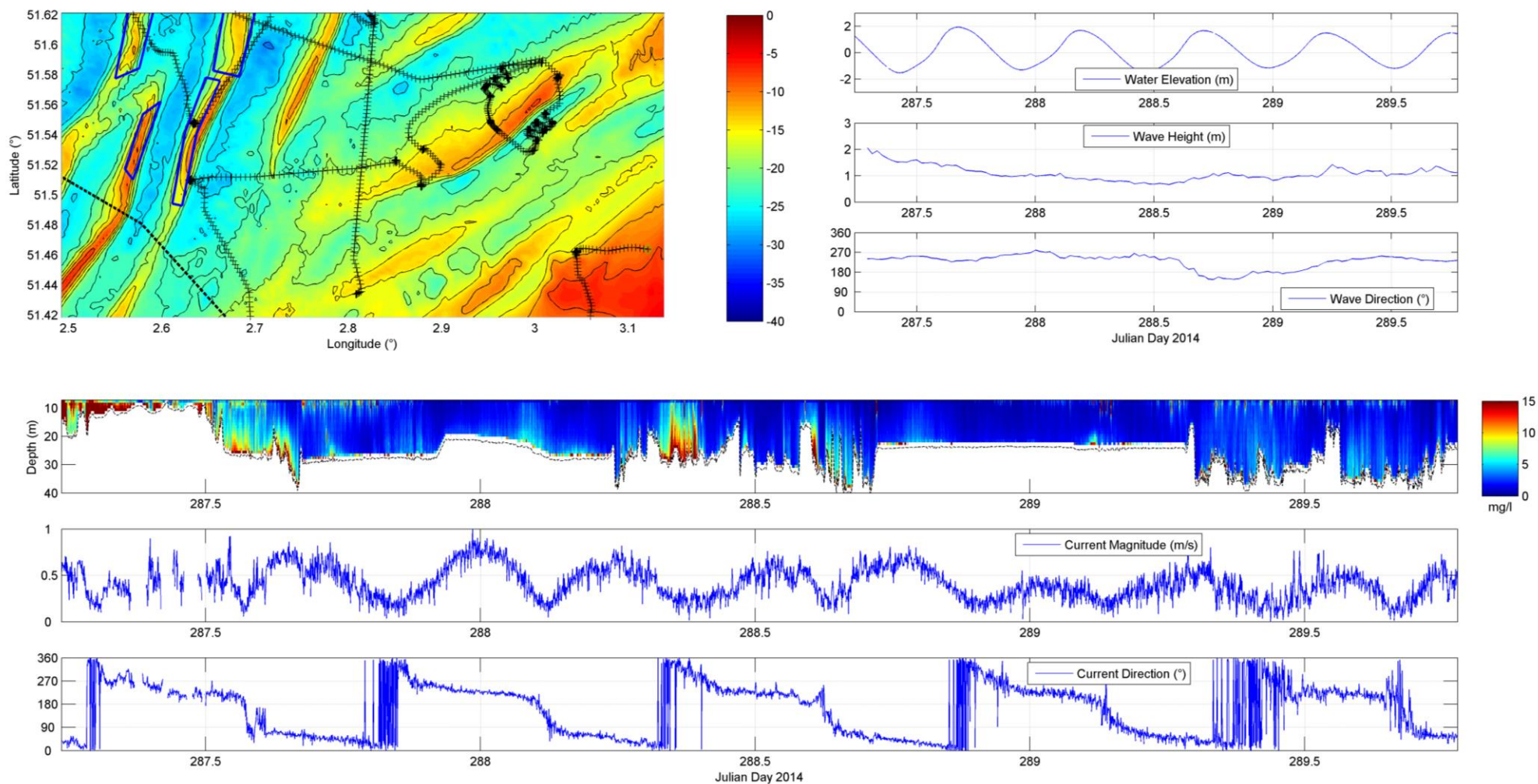


Figure 10. Current and SPM concentration values during RV Belgica campaign ST1425, based on HM-ADCP. Upper left: map of where measurements took place. Upper right subplots: Tide (Wandelaar), wave height (Westhinder), wave direction (Westhinder). Lower 3 subplots: SPM concentration in $\times 10^{-3} \text{ g l}^{-1}$, current magnitude at $\sim 10 \text{ m}$ water depth, current direction at $\sim 10 \text{ m}$ water depth. Note the location of two through-tide measurements at the steep (287.685-288.288) and gentle side (288.729-289.271) of the Oosthinder sandbank, respectively. Highest SPM concentrations were derived at the beginning of the profile corresponding to a transect over the shallow Oostende Bank. The high turbidity event around DoY 288.4 was in the gully north of the Thornton Bank and may be related to ship maneuvering during biological sampling.

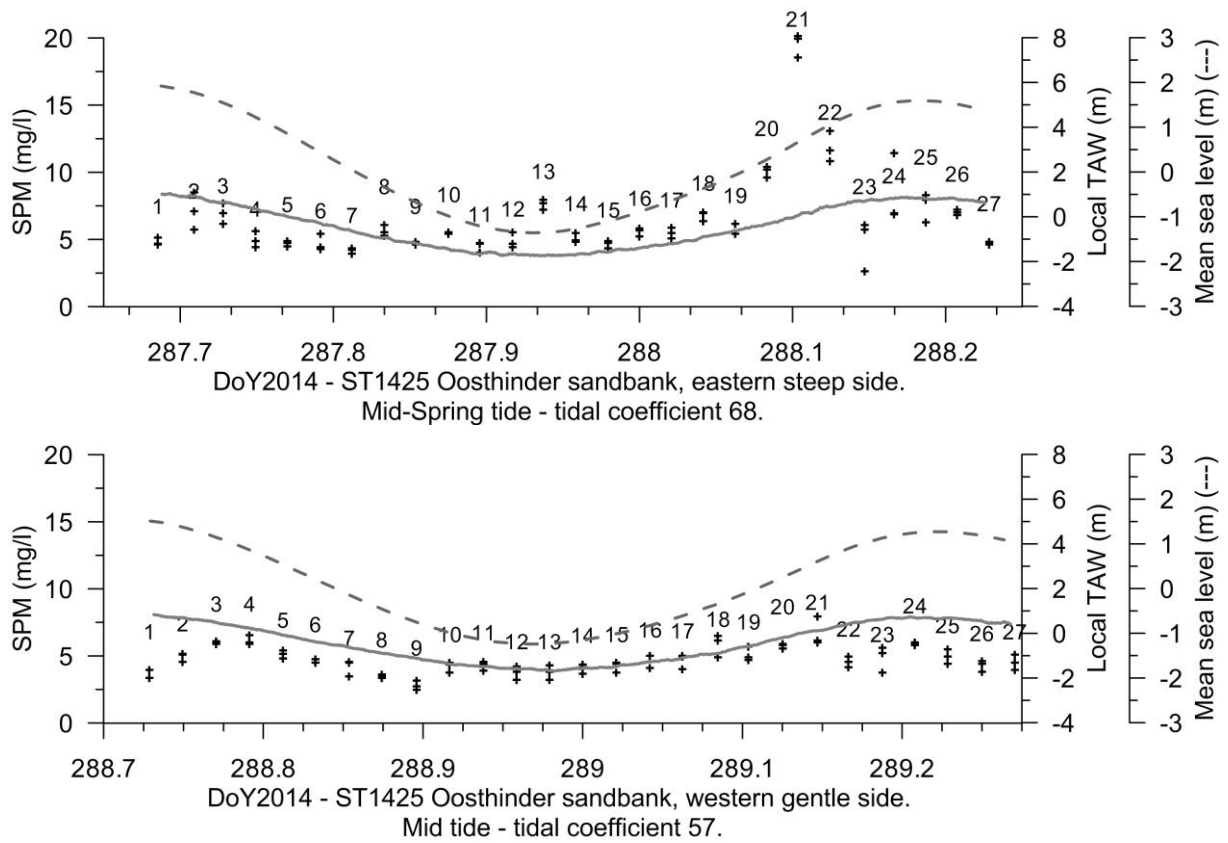


Figure 11. SPM concentrations ('+' markers, left axis) from water filtrations during RV Belgica campaign ST1425, together with local TAW (continuous line, right axis) and mean sea level (dashed line, second right axis). Upper: steep side of the Oosthinder sandbank; Lower: gentle slope. During the upper series significant wave heights ranged between 0.94-1.33 m; during the second series between 1.26-1.41 m.

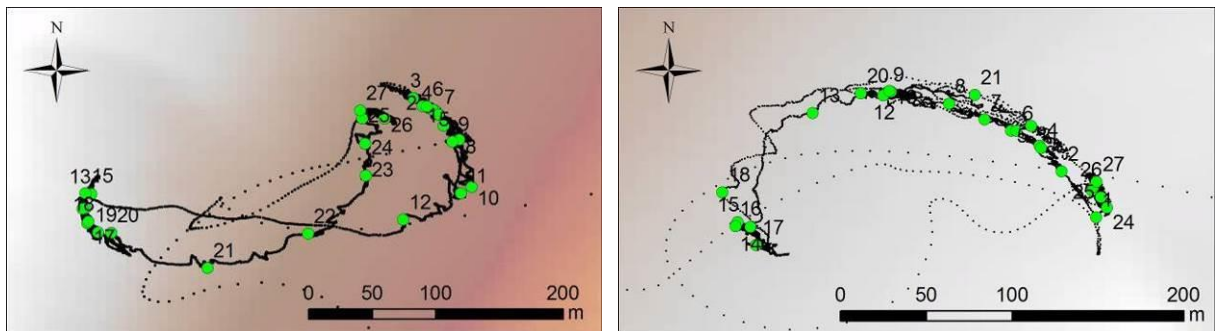


Figure 12: Left: RV Belgica track during 13-hrs cycle along the eastern steep slope Oosthinder sandbank; Right: along western gentle slope. Positions of the water samples are indicated (green dots).

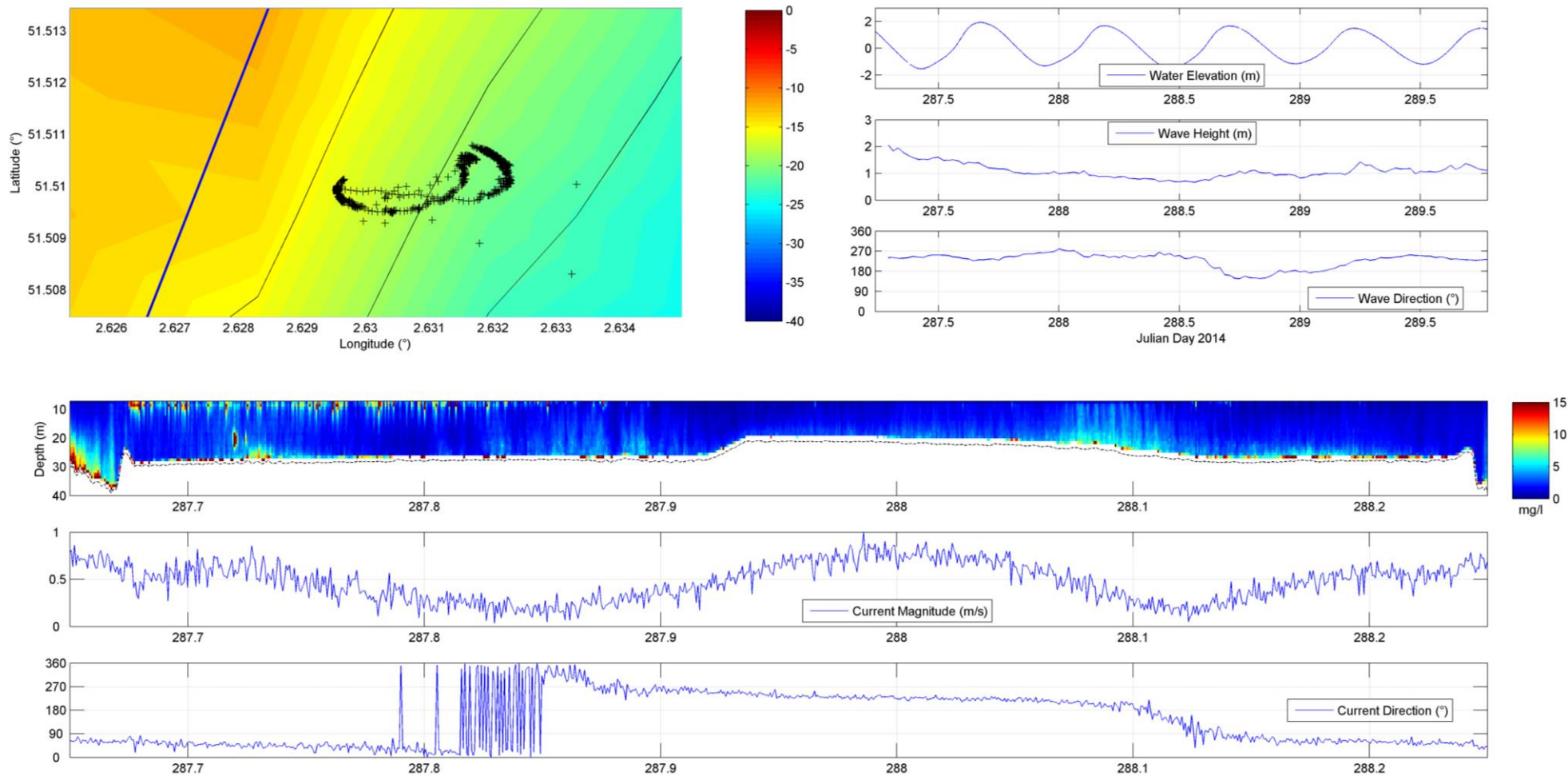


Figure 13. HM-ADCP (anchored) measurements along the steep side of the Oosthinder sandbank. Around DoY 288 (ebb), no significant increase in SPM concentration was observed during maximal current speed, but when currents decelerated, SPM concentration doubled. Possibly, the change in current direction towards the S (180°) advected sediments away from the sandbank top. Advected sediments deposited here, and were then somewhat picked up by the increasing flood current (DoY 288.15-288.2). The band of SPM high concentration values around -10 m likely corresponded to movements of the ship (probably due to the combination of wind blowing from the W and the current direction towards the E). Once the current direction changed (287.85), no more artifacts were present, but also the wave height decreased. Tidal coefficient 68.

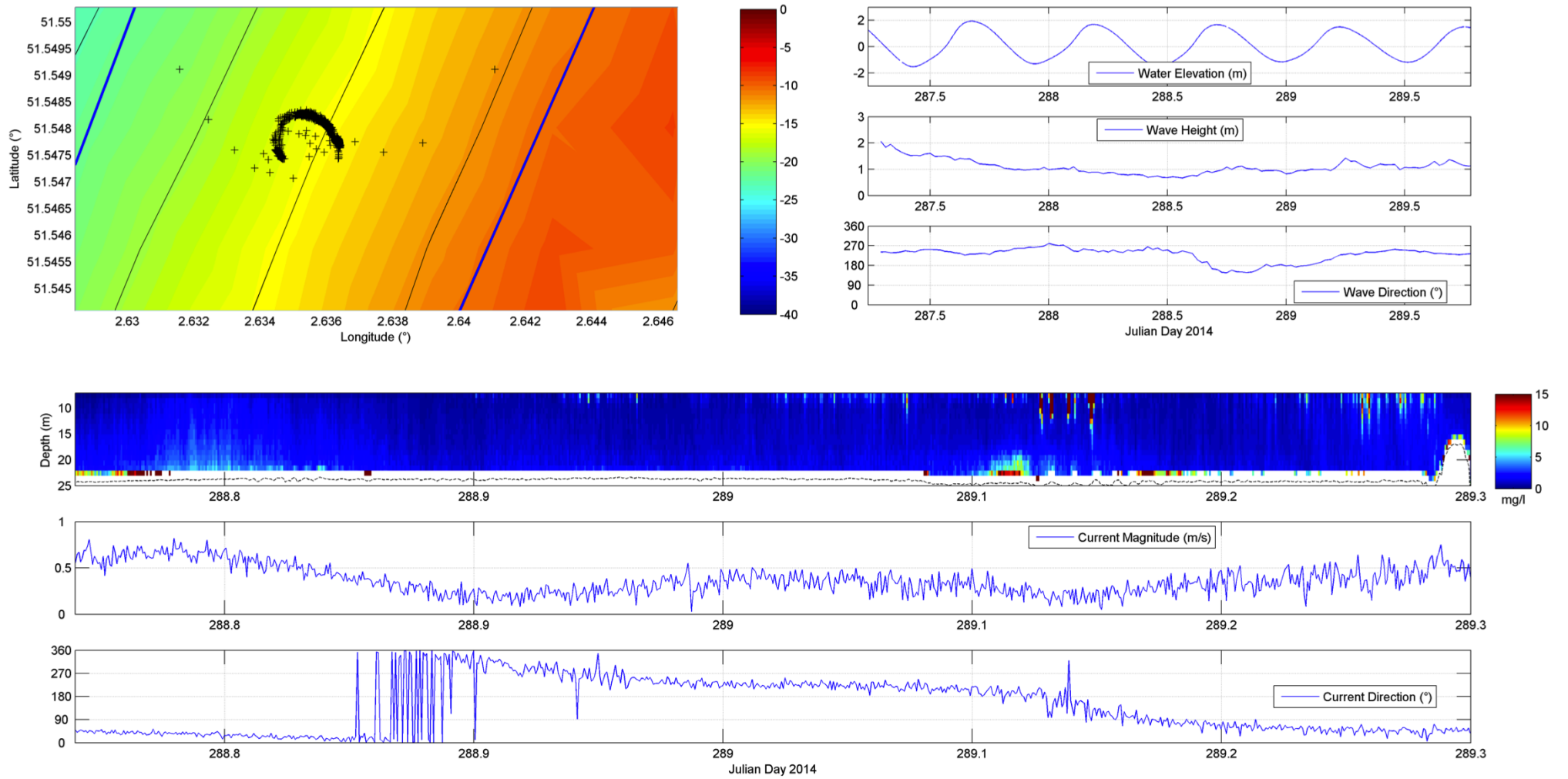


Figure 14. HM-ADCP (anchored) measurements along the gentle (E) side of the Oosthinder sandbank. Note that increased SPM concentrations were observed during flood (45°T) (DoY 288.8), whilst no sediment resuspension occurred during ebb (225°T). Tidal coefficient 57.

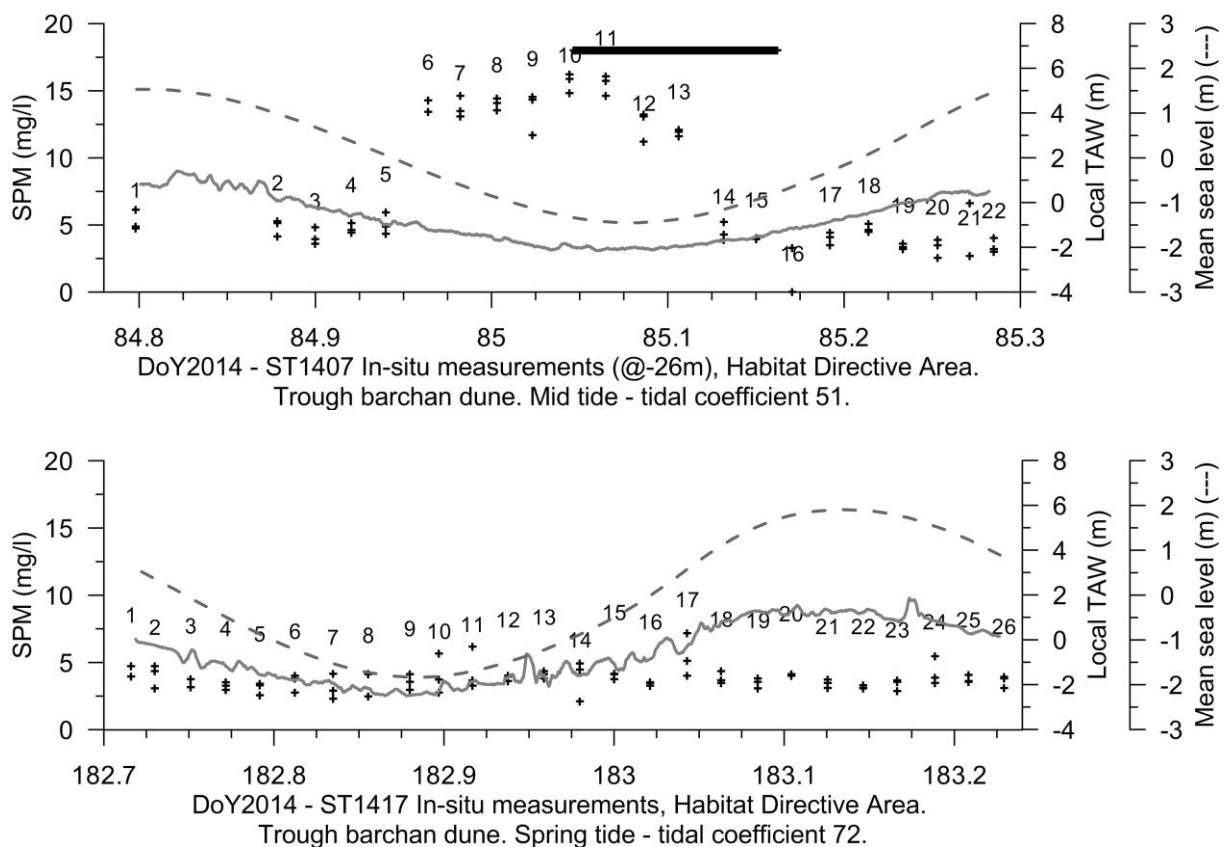


Figure 15. SPM concentrations ('+' markers, left axis) in the Habitat Directive area from water filtrations during RV Belgica campaign ST1407 (upper) and ST1417 (lower), together with local TAW (continuous line, right axis) and mean sea level (dashed line, second right axis). During the upper series significant wave heights ranged between 1.18-1.32 m; during the second series between 0.74-1.02 m. Extraction activities, during the ST1407 campaign (upper), are indicated in a thick black line. Note that during ST1407, higher SPM concentrations were measured during the ebb phase; this was also observed in the HM-ADCP recordings (Figure 18) and were attributed to advection of sediments. Tidal phase was mid tide with current velocities around 0.5 ms^{-1} only. Such an event was not observed under the spring tidal conditions of ST1417. Note also that during the 13-h cycle of ST1407; water samples were taken at a constant depth of -26 m from the water surface, because of technical failure (see campaign report, Annex A). This explains in part the jump in values during the ebbing phase of the tide: water samples were taken closer to the bottom.

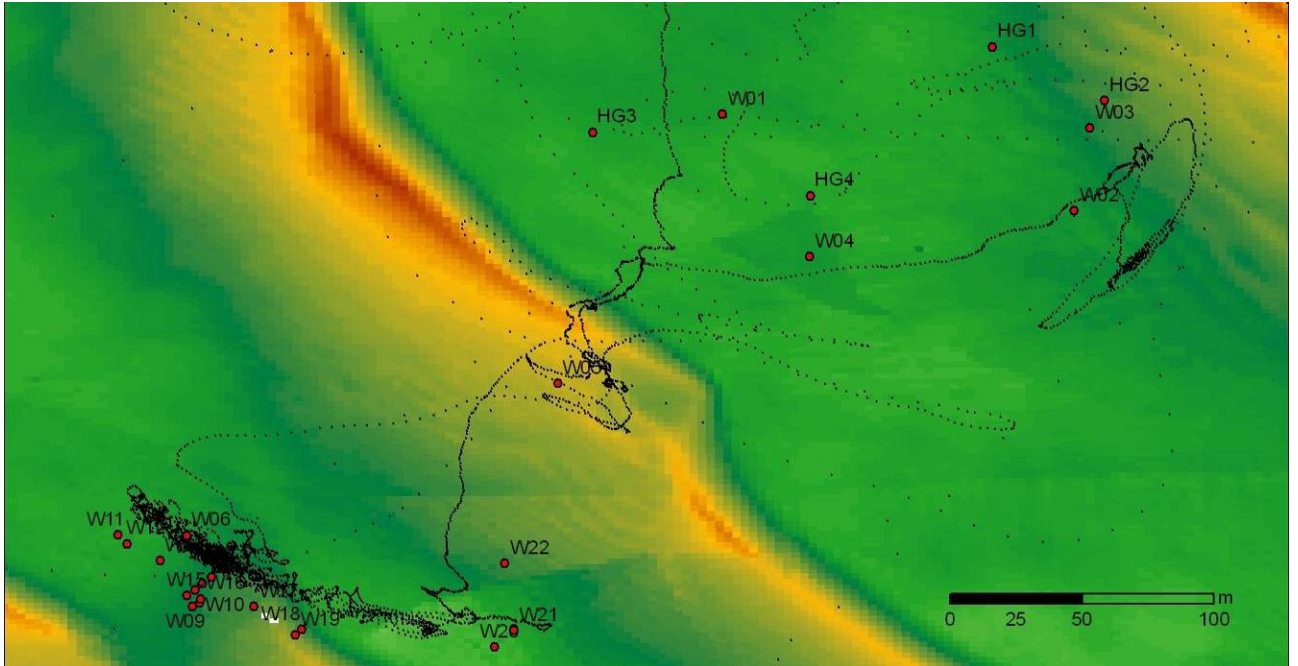


Figure 16: RV Belgica track in the trough of a barchan dune during ST1407, Habitat Directive area, west of the Oosthinder sandbank. Water samples and vertical profiling of oceanographic parameters was conducted at 22 locations (W01 to W22, see also Figure 15). Four Hamon Grabs were taken (HG1 to HG4). Note the strong drift of the ship with the tide.

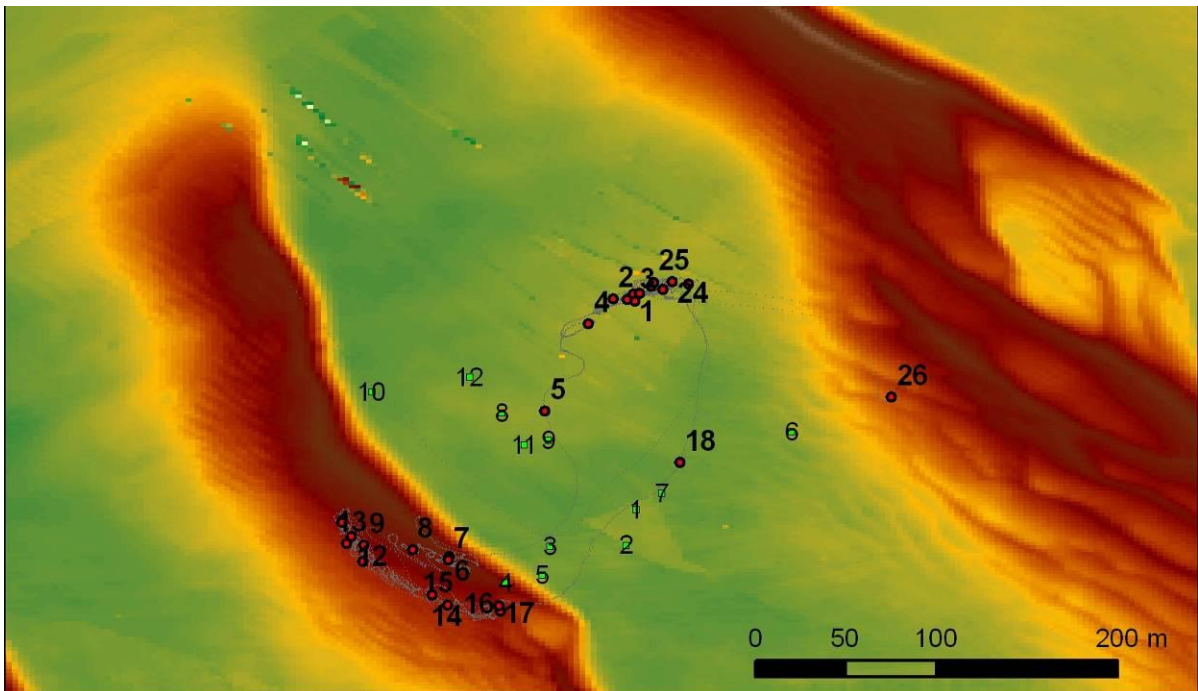


Figure 17: RV Belgica track in the trough of a barchan dune during ST1417, Habitat Directive area, west of the Oosthinder sandbank. Water samples and vertical profiling of oceanographic parameters was conducted at 26 locations (see also Figure 15). Twelve Hamon Grabs were taken.

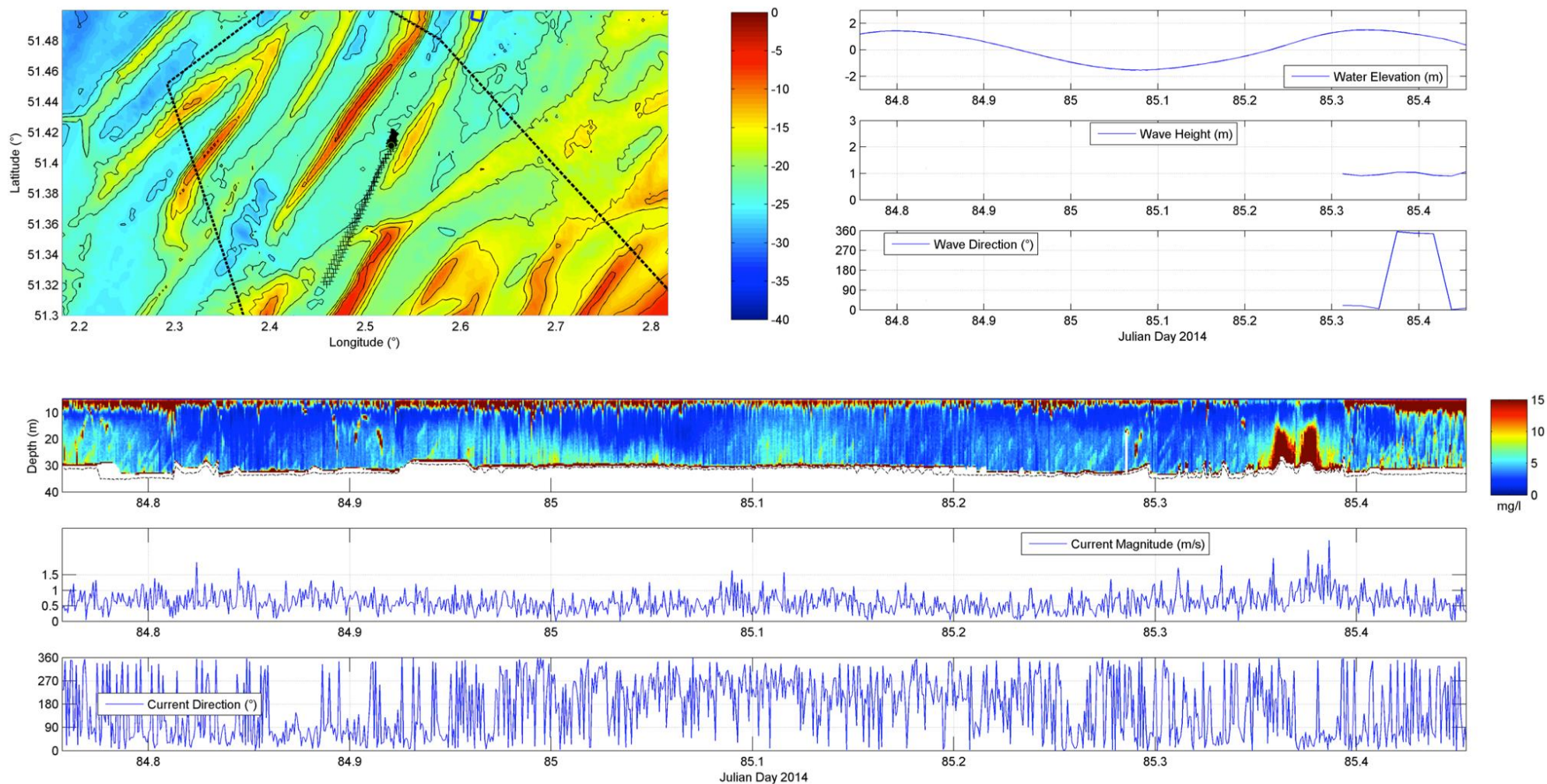


Figure 18. Through-tide measurements (13-h) in the trough of a barchan dune (Habitat Directive area) (DoY 84.8-85.3). Highest SPM concentrations were observed during slack tide after flood (NE directed). Sediments were likely advected away from the sandbank. Re-suspension only during ebb condition. Water filtrations provided SPM concentrations between 0.003-0.016 $g\ l^{-1}$. Highest concentrations in SPM were measured around DoY 85 (advection event) and were derived from both the water samples and the ADCP. Note that the current data were noisy, because of the smaller bin size (0.5 m) used. The “red band” at -10 m is likely an artifact (e.g., ship movement). RV Belgica ST1407. Tidal coefficient 51. Delineation corresponds to Habitat directive area. Reason for high turbidity event around DoY 85.38 is unclear; the ship was sailing away in the direction of the Oostdyck sandbank.

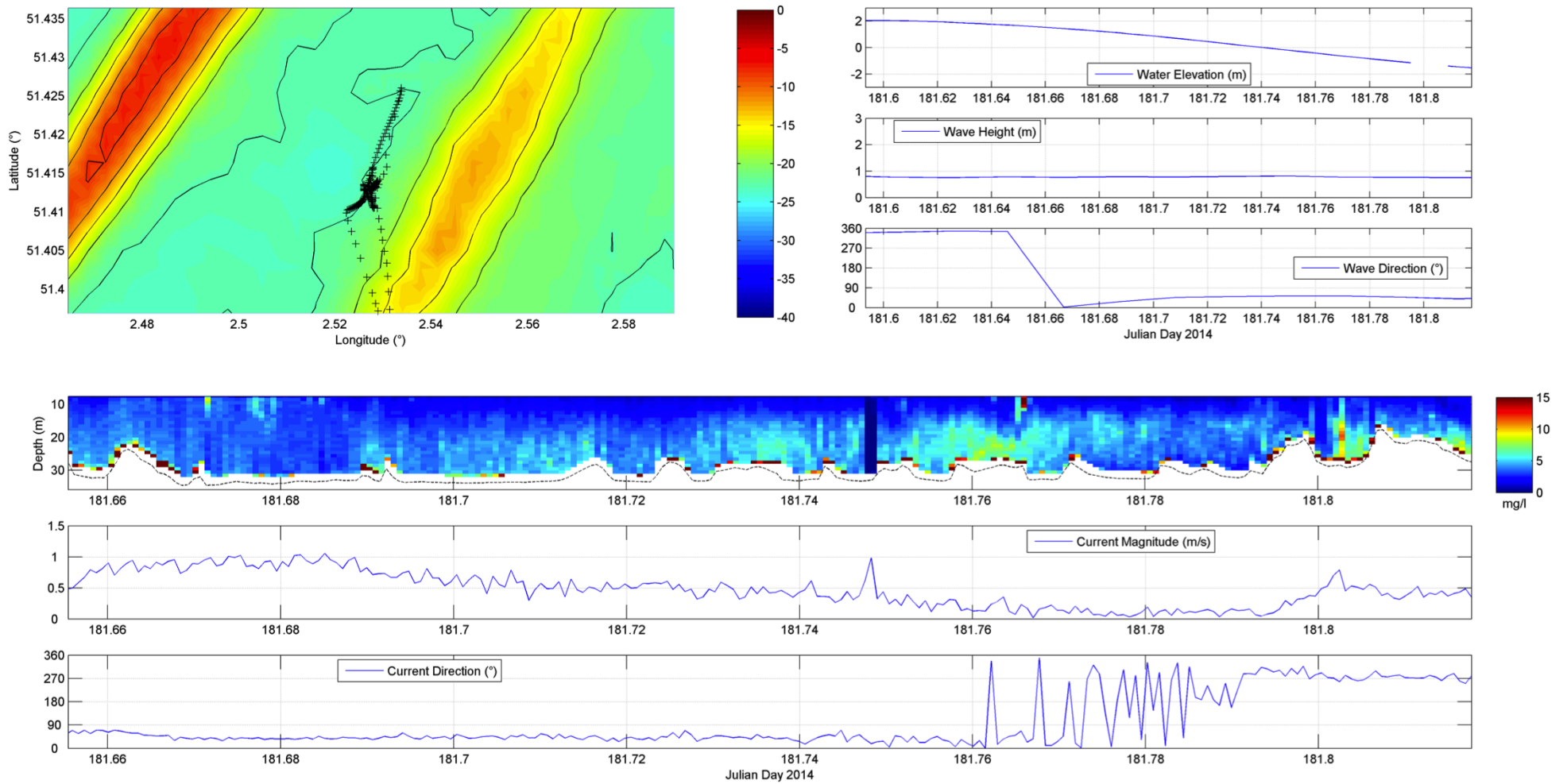


Figure 19. HM-ADCP recording during the period that the BM-ADCP was deployed, from RV Belgica, in the trough of a barchan dune (DoY 181.69-181.78). Campaign ST1417. Sediment suspensions advected away from the sandbank when the current was directed to the N. No clear re-suspension was observed during maximal flood current (45°T) (DoY 181.68). High turbidity event near DoY 181.81 is located at the head of the Oostdyck sandbank. Tidal coefficient 72.

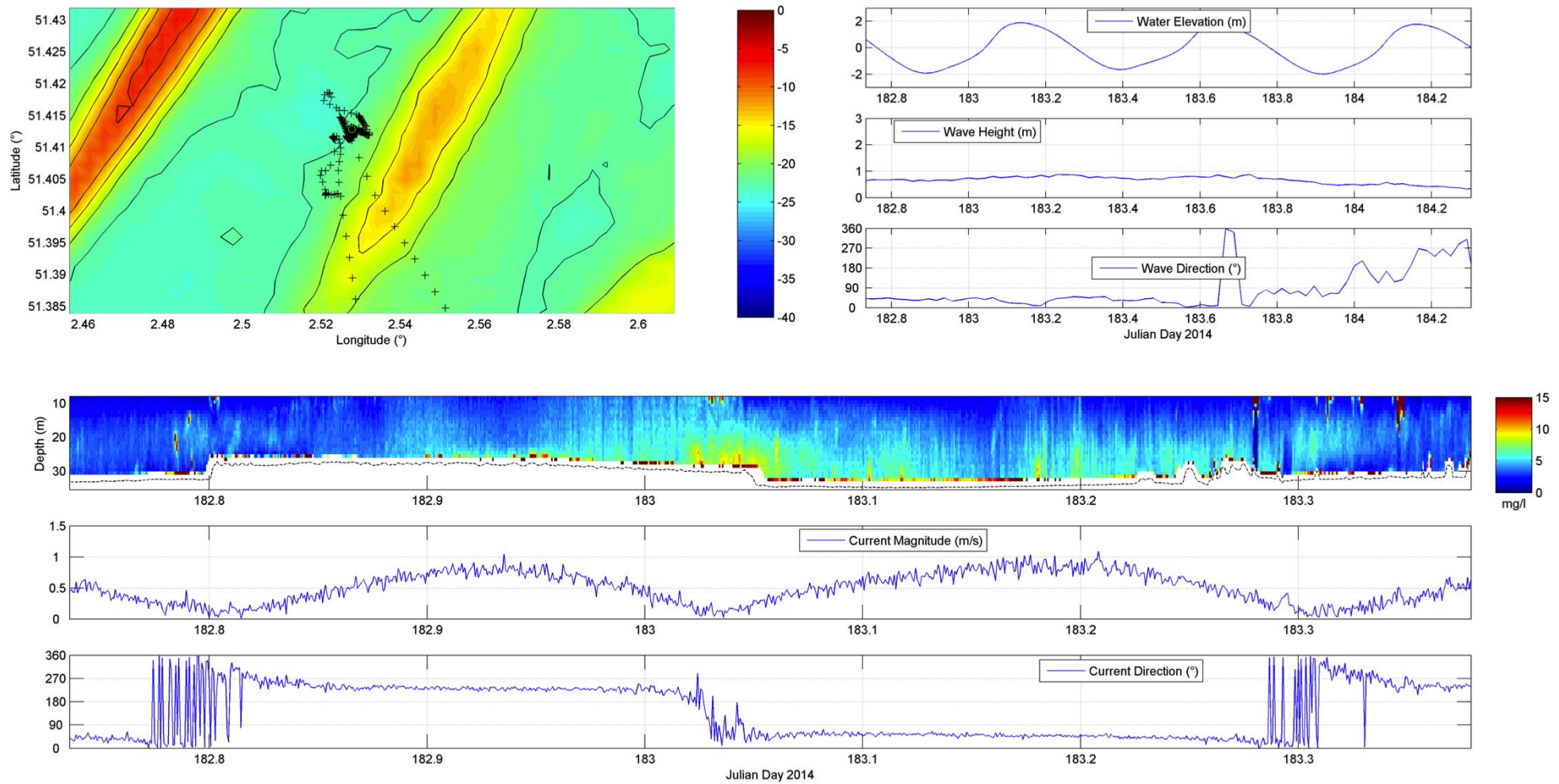


Figure 20. HM-ADCP recordings during the 13-h cycle in the trough of a barchan dune. Moderate re-suspension occurred during ebb (DoY 182.9). High SPM concentrations were observed during slack tide after ebb. During flood, sediments resuspended again and advected away during slack tide. RV Belgica ST1417. Tidal coefficient 72.

The long-term deployment of the BM-ADCP provided additional insight into sediment transport along the steep side of the Oosthinder sandbank in the period 13/10/2013 to 17/04/2014 (186 days, or nearly 6 months of data). First, the currents are described, and subsequently variation in SPM concentration and bottom shear stresses.

Current characterisation

Current characteristics near the seabed (1.52 mab) (Figure 21; Figure 22), confirmed (ref. previous report, Van Lancker et al., 2014):

- Overall strong currents in the area: up to 0.8 ms^{-1} (near bed),
- Flood lasting longer than the ebb,
- Competitive ebb and flood current strengths. Over the 6 months period, the tidal ellipse did show a slight dominance of the flood current, though this is due to the dominance of prevailing SW wind/wave conditions during this period (Figure 25);
- During peak conditions, the ebb current has a higher directionality.

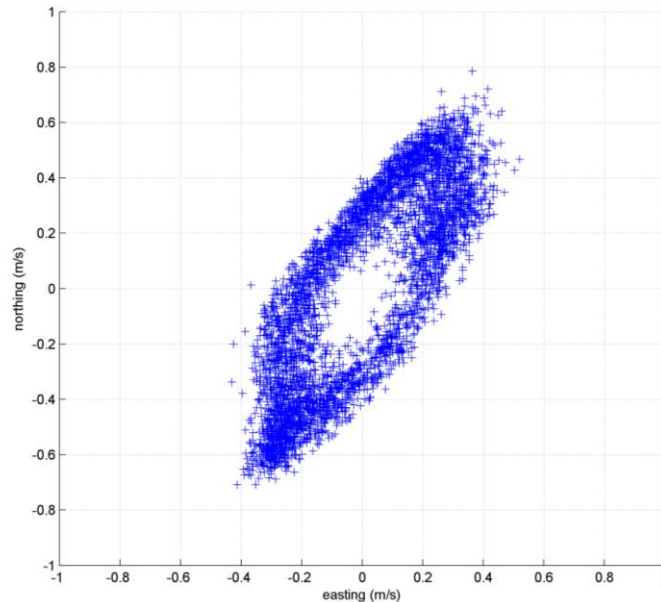


Figure 21. Orientation of tidal ellipse ($\sim 31^\circ$ true north), based on the first bin data (1.52 mab). Currents rotated counterclockwise.

The averaged current profile over the entire period showed an averaged current strength of 0.4 ms^{-1} at 1.52 mab. This is roughly the resuspension threshold of the *in-situ* sediments (following Soulsby, 2007), confirming the high sediment transport capacity in the area.

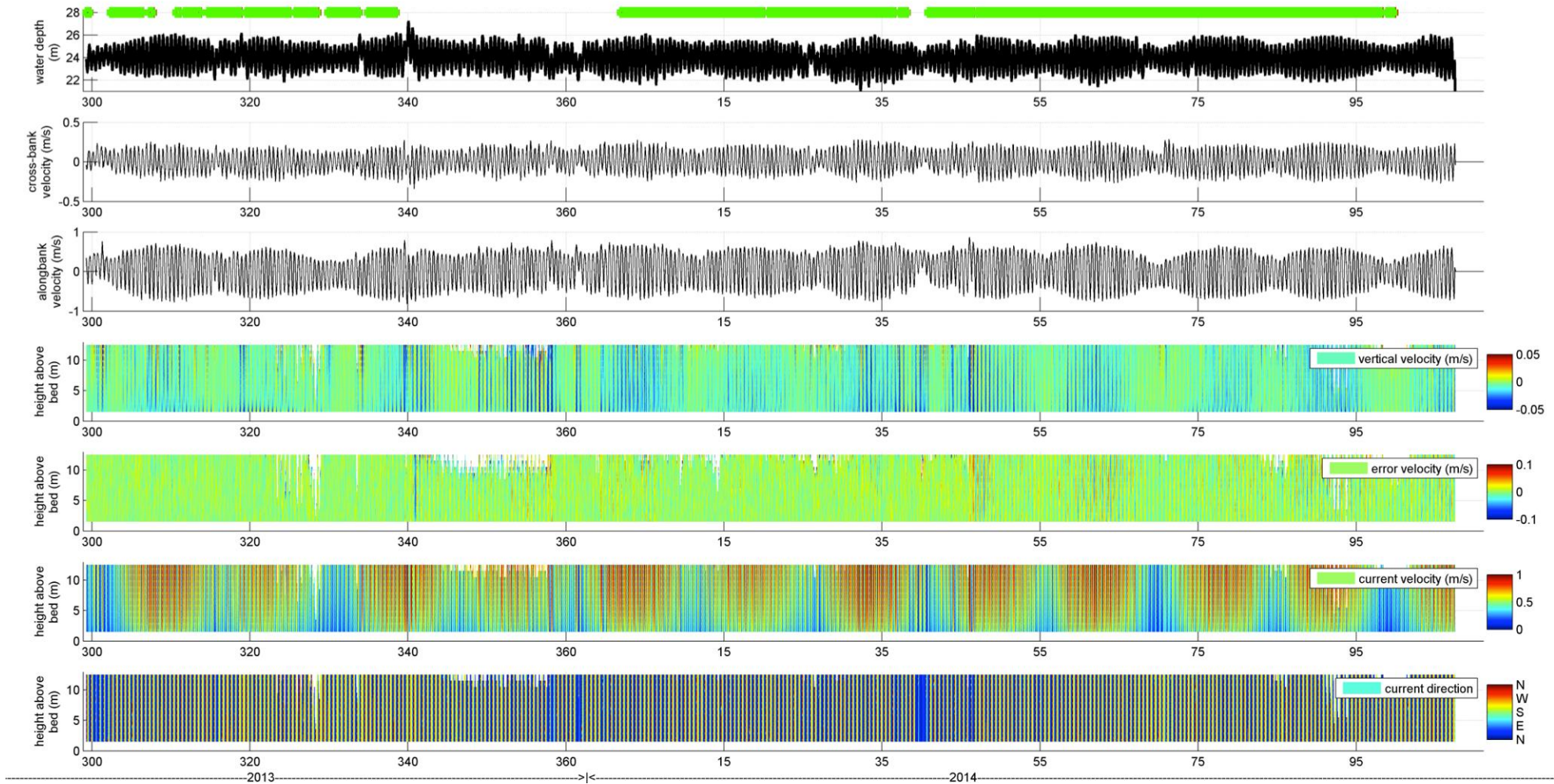


Figure 22. Current characteristics during the long-term BM-ADCP deployment along the steep side of the Oosthinder sandbank. Subplot 1 on water depth showed a variation between -22 and -27 m. A total of 12 spring tides, and 12 neap tides were recorded with tidal amplitudes of about 4 m and 2.5 m respectively. Superimposed on this plot are the extraction events (green markers) in Sector 4c. Subplots 2 and 3 show the cross- and along-bank velocities at 1.52 mab, respectively. Cross-bank velocities varied between -0.2 and 0.2 ms^{-1} (with positive values directed offshore NW, and negative values directed towards the shore SE). Along-bank velocities were stronger, up to 0.6 ms^{-1} (spring tide). Positive values are directed to the NE. Subplots 4 until 7 are the lower water column velocity parameters (subplot 4 is vertical velocity; subplot 5 error velocity; subplot 6 current velocity, and subplot 7 current direction). Blanked areas corresponded to bad quality data. Note the periods with intensified NE-directed currents (blue, in subplot 7).

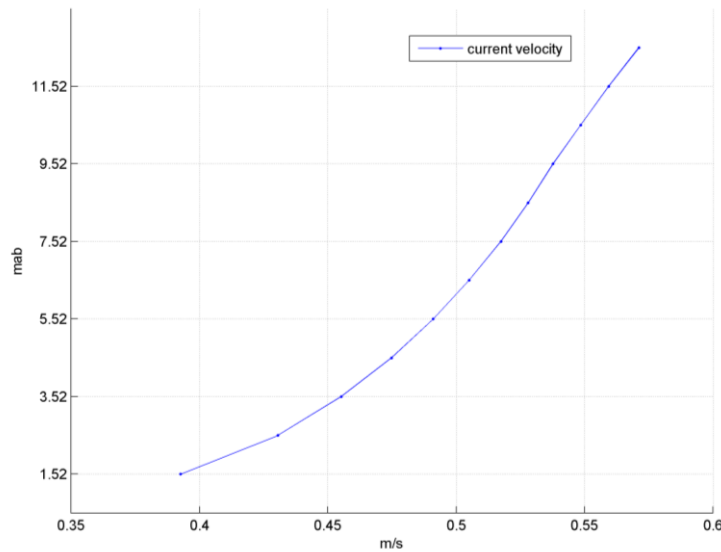


Figure 23. Averaged current profile of the current velocity with a clear decrease towards the sea bed (0.57 -> 0.39 m/s). The near bottom part of the logarithmic profile (~1 m) is not sampled since the first data point is only at 1.52 mab.

An overview of all current characteristics is given in Figure 22-22. Note the reinforcement of the along-bank current under persistent SW conditions in Figure 25 (DoY2013 350 – DoY2014 50). However, first analyses did not show an important impact on SPM concentration values nor bottom shear stresses.

SPM concentrations

SPM variation followed mostly the spring-neap tidal oscillation with values of more than 0.020 gl^{-1} during spring. Highest concentrations were derived in the beginning of the time series when SW conditions give rise to waves of more than 4 m in significant wave height (Hs) (Figure 24; Figure 25; DoY2013 300). Note that this event occurred under neap tide, confirming the importance of waves for the resuspension of sediments (Van Lancker et al., 2014).

Bottom shear stress

Estimated bottom shear stress ranged between 0 and 2 Pa, following the tidal cycle and spring-neap tidal oscillation (Figure 25). When de-tided, the averaged value is around 1 Pa. Note that bottom shear stress values are indicative only, since the low resolution settings of the ADCP did not allow obtaining current profiles near the seabed. Bottom shear stresses were derived indirectly, using a relationship between current strength and bottom shear stress during the first days of the deployment when high-resolution profiles were recorded. Note that Van Lancker et al. (2014) reported values of up to 3-4 Pa under elevated spring tidal conditions (tidal coefficient 85; 30/3/2013 or DoY 89.06).

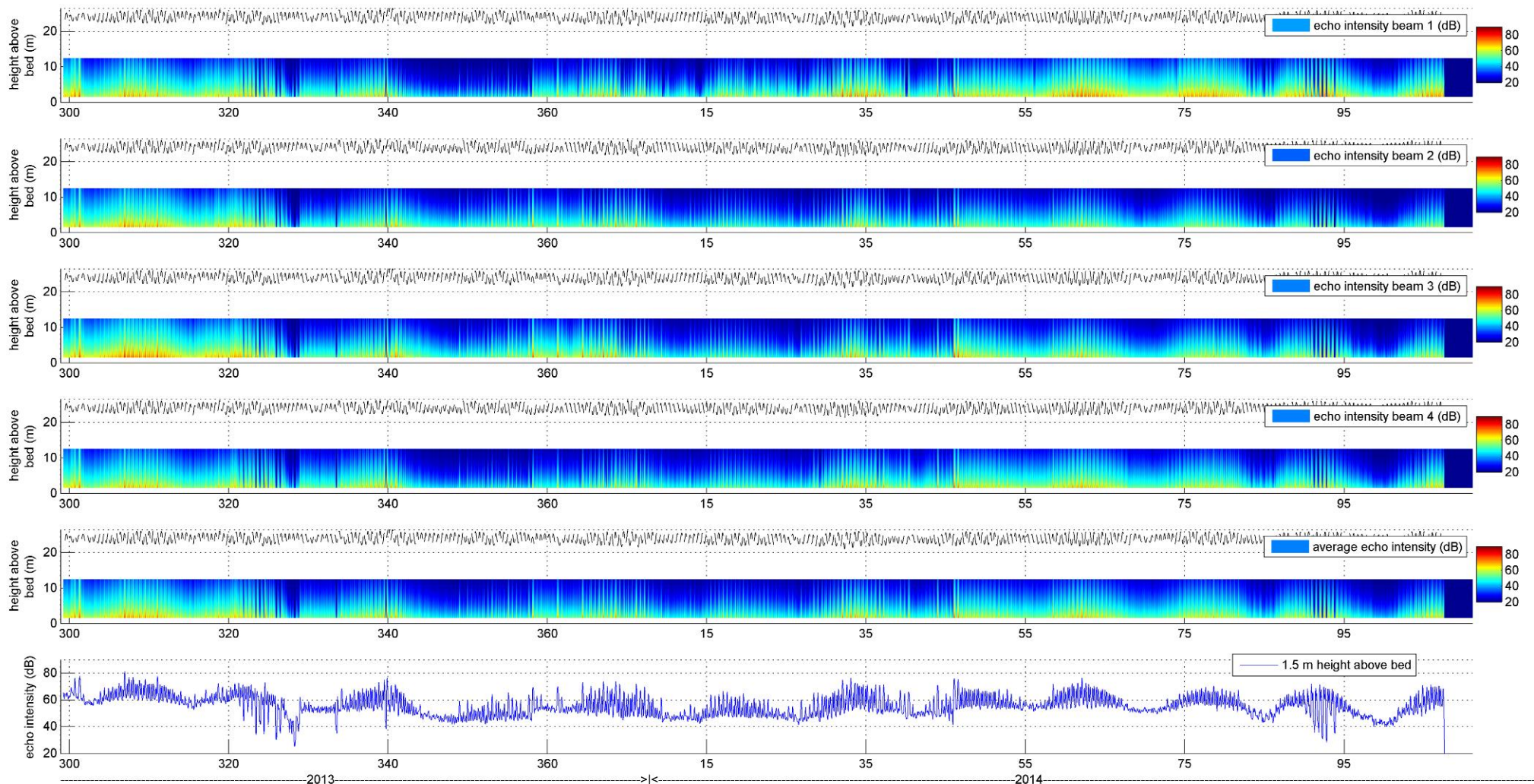


Figure 24. ADCP beam echo intensities in dB (subplot 1 to 4). Subplot 5 is the averaged beam echo intensity. The black line on each subplot is the water depth time-series. Subplot 6 shows the echo intensity (beam-averaged) at 1.52 mab, with a clear resuspension-deposition signal, as well as the spring-neap signal. Sometimes, echo intensity dropped very low (eg., around DoY 325 and between DoY 90 and 95). The echo intensity was multiplied by 0.42 in order to obtain dB values (instead of counts). dB can then be used as a proxy for sediment concentration (Figure 25).

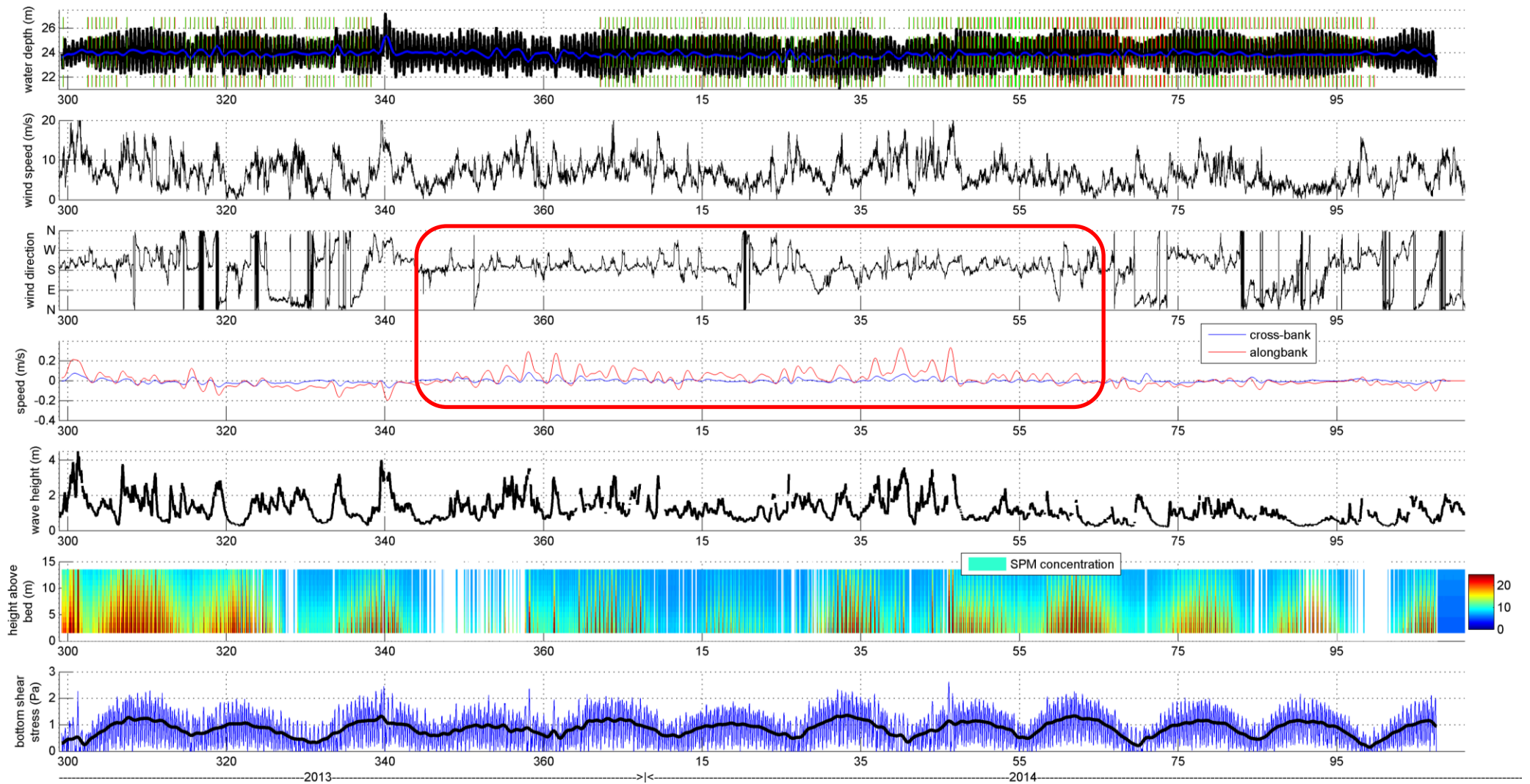


Figure 25. SPM concentration and bottom shear stress variation. Subplot 1 represents water depth and extraction phases. Subplot 2 and 3 are the wind parameters: wind speed and wind direction (“blowing from”). Wind speeds reached 20 ms^{-1} (typically associated with SW and NW winds). NE winds were also common. Subplot 4 is the low-pass filtered (33-hrs) information of the hydrodynamics, mainly influenced by the wind conditions. Along-bank residual velocity (red line) showed highest variance. Positive peaks (directed towards NE) corresponded to phases of SW winds; negative peaks corresponded to N and NE winds. Subplot 5 is significant wave height, measured at Westhinder MW7. Highest waves (up to 4 m) related to strong SW and NW wind conditions. Subplot 6 gives the estimated SPM concentration derived from the dB values, calibrated with SPM concentrations from in-situ water samples. Resuspension-deposition cycles are clearly visible in the data, as well as spring-neap variation. The lower subplot is the estimated bottom shear stress ranging between 0 and 2 Pa, mostly following the tidal cycle and spring-neap variation. Red rectangle indicates a period where persistent SW wind conditions reinforced the along-bank current to the NE.

With reference to sediment processes in the Habitat Directive area, results are shown from measurements in the trough of a barchan dune, important to understand the deposition pattern of fines in this area.

Aim was to demonstrate eddy formation or vortex structures when the current passes over the dune tops, here 6-7 m in height. Hypothesis was that such vortices would trap fine sediments and would lead to enhanced deposition of fines in the trough of the dune where the rich gravel beds occur. Such trapping mechanisms are known in literature and have been modelled (e.g., Omidyeganeh et al., 2013).

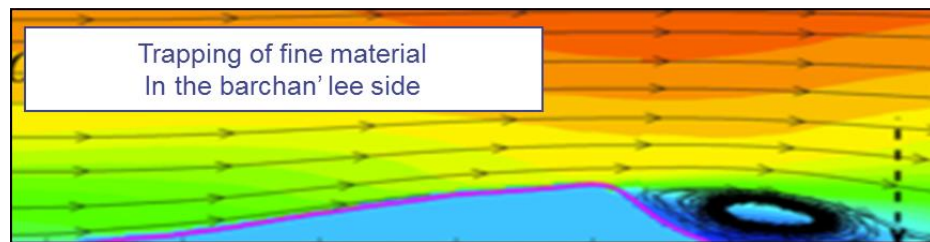


Figure 26. Modelled trapping mechanism along the lee side of a barchan dune (Omidyeganeh et al., 2013).

First, results are shown from 2013 (3-4/7/2013) providing evidence of the current pattern and echo intensity (proxy for SPM concentration) over two tidal cycles. Figure 27 and Figure 28 show the current magnitude and direction over the whole range of 15 m. Maximal ebb current direction was 220T (true north) and reached about 0.5 ms^{-1} , whereas the flood current ($\sim 050\text{T}$) was slightly stronger. In the figures, the depth-averaged current magnitude refers to the mean current magnitude over the lower 15 m of the water column. In Figure 27, the ebbing tide is situated between the vertical black lines. Slack tides are tidal phases with reduced current magnitudes (between 0.2 and 0.25 ms^{-1}). The slack tide window before LW (ebbing tide) has lowest current strengths. Additionally, the current magnitude is given for the first bin cell (i.e. $\sim 1 \text{ mab}$). During the measurement, the tidal range varied between 3 and 3.5 m (mid-tide conditions, TC 59; 3/7 20:30 or DoY 184.86).

The echo intensity at 3 mab did not strictly follow the current magnitude. Water clarity during slack tide before LW was slightly higher than during slack tide before HW.

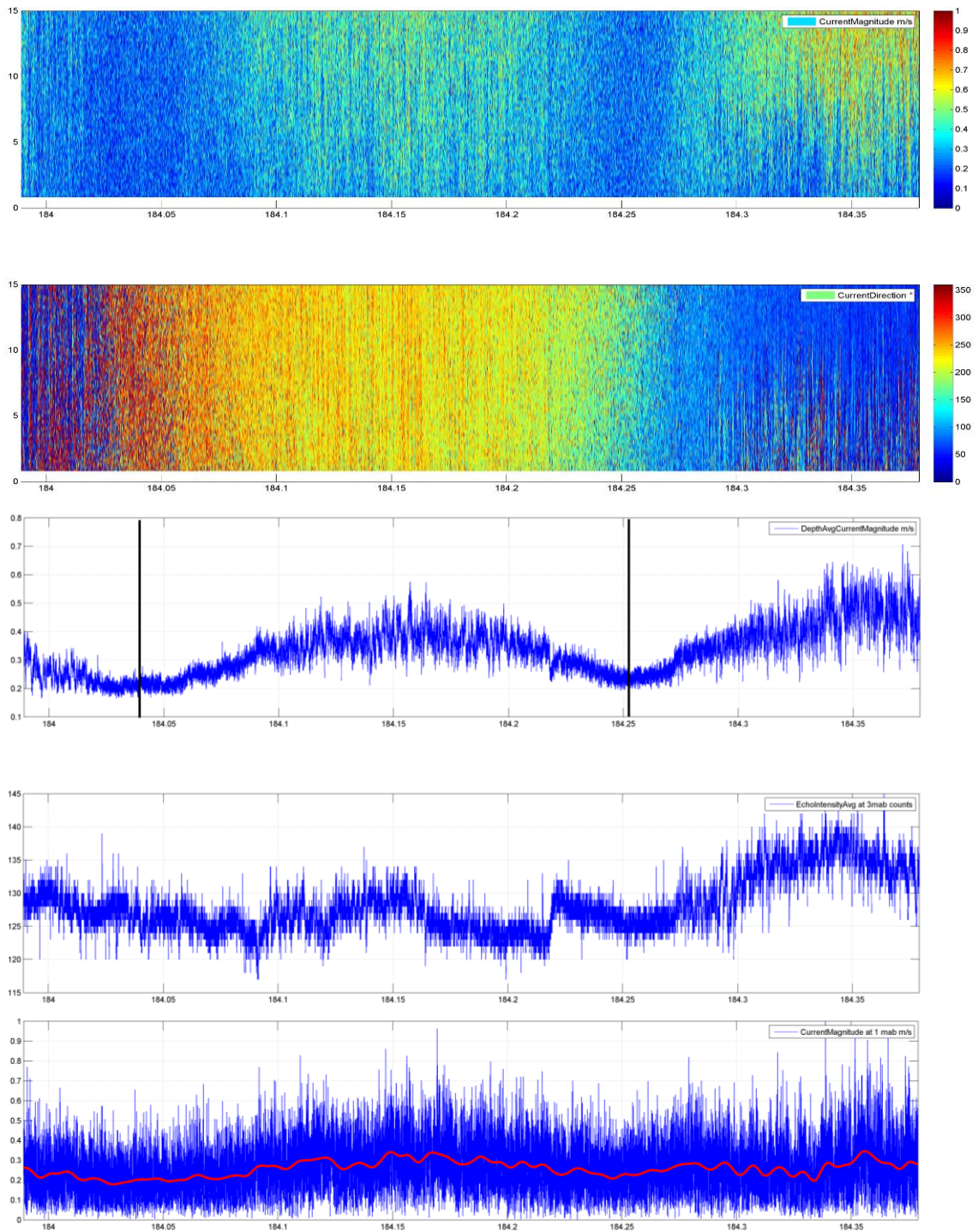


Figure 27. Current information (magnitude, direction, depth averaged) in the trough of a barchan dune (Area 2, Figure 6) (Data from 3/7/2013). Low Water was around DoY 184.09 and High Water around 184.35. The vertical lines indicate the timing of slack water, respectively ± 3 h before Low Water (longest window, lowest currents) and ± 3 h before High Water. Timing between the small ticks is 1.2 h. Depth-averaged currents were clearly higher during flood than ebb, as also the echo intensities at 3 mab. In contrast, the low-pass filtered (moving average of 12.5') current magnitude at 1 mab showed a decelerated flood current, somewhat less in strength than its ebb counterpart. Tidal coefficient 57 (mid tide).

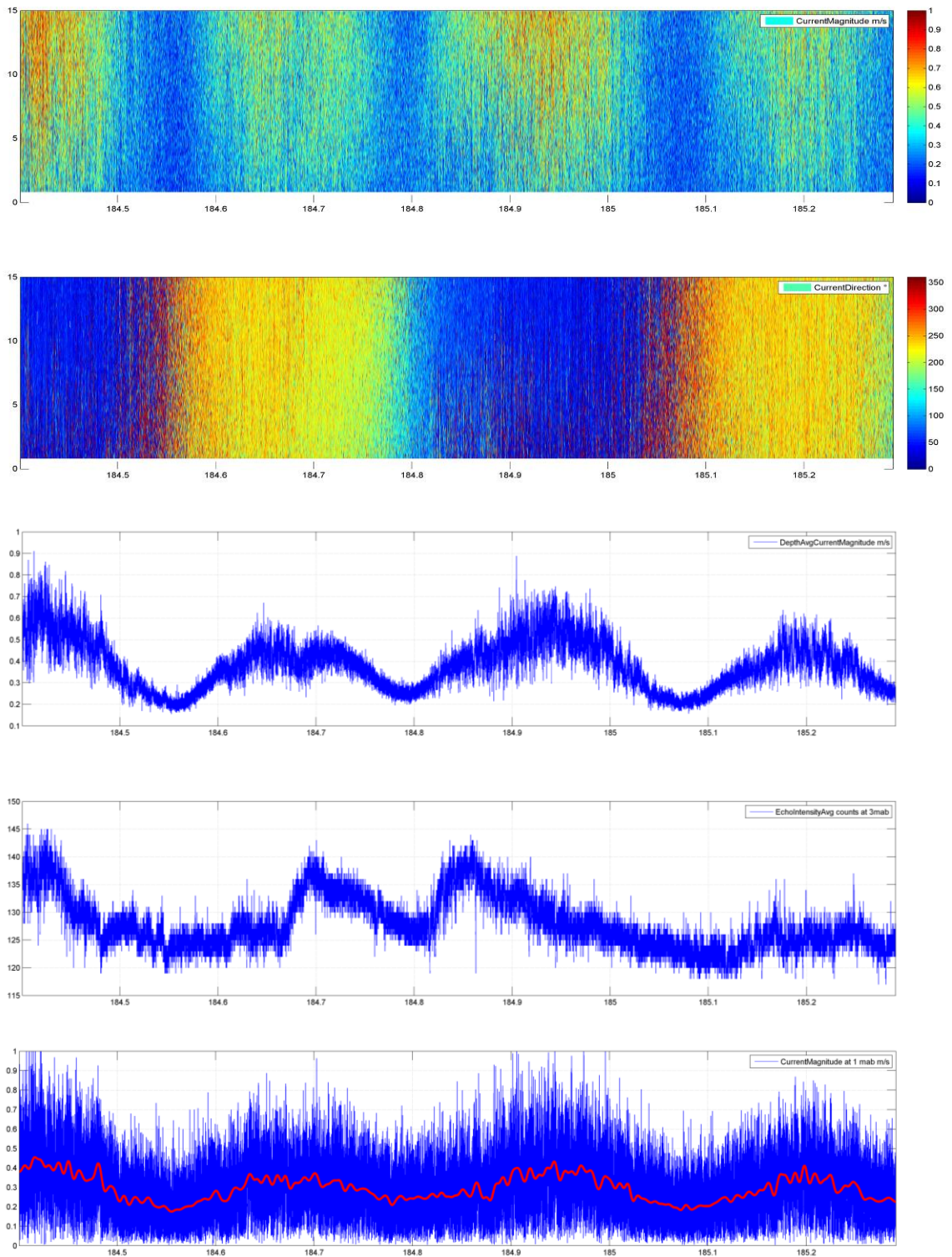


Figure 28. Current information (magnitude, direction, depth averaged) in the trough of a barchan dune (Area 2, Figure 6) (Data from 3-4/7/2013). Low Water was around DoY 184.6 and High Water around 184.86. Timing between the small ticks is 2.4 h. Depth-averaged currents were higher during flood than ebb. Echo intensities (3 mab) showed a peak \pm 2.3 h after Low Water, but also at High Water. Low-pass filtered current magnitude at 1 mab showed values near 0.4 m at peak tidal velocities, the average velocity for sediment resuspension. Tidal coefficient 59, mid tide.

Next, results are shown from an 11-days deployment of a BM-ADCP in the trough of a barchan dune (30/06/2014-10/07/2014; maximum tidal coefficient 78 at DoY 190,896 (30/06 01:55)). Measurements were aimed also at resolving turbulence and vortices in the lee side of the barchans, but unfortunately, measurements only took place at a 10-min interval, which was not sufficient to record such features. Still, good background data were recorded on environmental conditions (Figure 29). Only a moderate correlation (0.52) was derived between the ADCP backscatter and current velocity (Figure 30), implying that currents alone cannot explain variability in turbidity.

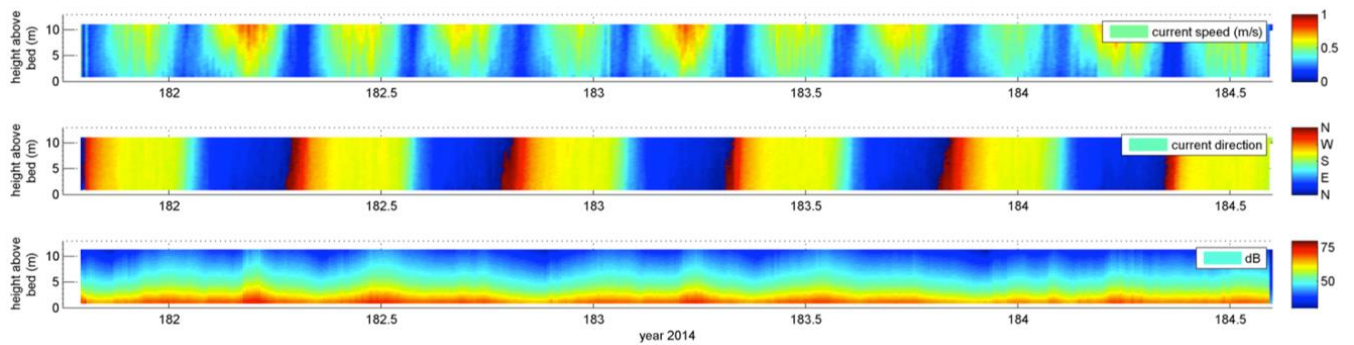


Figure 29. 3-days snapshot (DoY 181.5-184.5; tidal coefficient 76 to 72) of the time series of the BM-ADCP in the trough of a barchan dune. Current speeds were up to 1 ms^{-1} at 11 mab. Current direction rotated counterclockwise. Backscatter (in dB) information (not yet corrected for beam spreading and water attenuation) slightly showed a resuspension-deposition signal, at least up to 5 mab. Note the higher current velocities when currents are NE-directed. Under both flood and ebb higher current velocities sediments were resuspended.

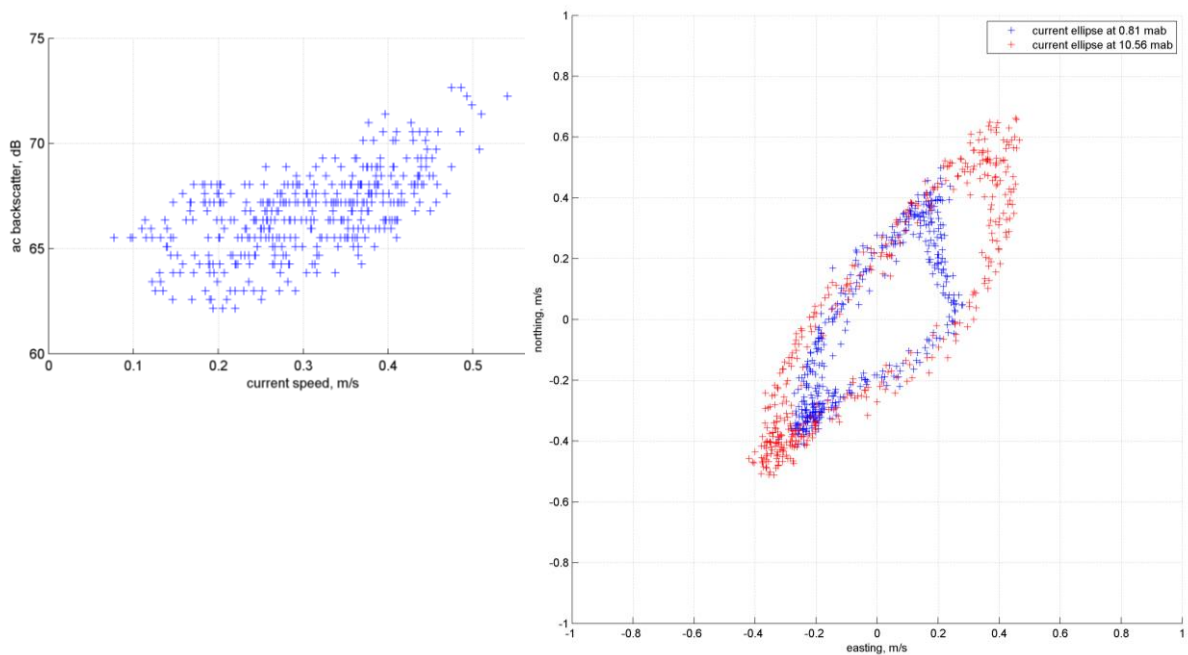


Figure 30. Left: Current speed versus backscatter (dB) at 0.81 mab. Correlation coefficient was 0.52. Right: tidal ellipse at 0.81 mab (bin 1) (blue), plotted together with the tidal ellipse at 10.56 mab (bin 40) (red). The flood phase of the tide (NE-directed) showed two different signatures. Near the bed, flood currents are decelerated compared to higher up in the water column, likely attributed to a reversal of the current near the bed (following the hypothesis of a vortex structure). Around 6.81 mab, there was a transition between the tidal ellipses. During ebb, this effect was not seen. Direction of maximum ebb is 220 T (true North); direction maximum flood is 50 T. Currents rotate counterclockwise. The tidal ellipse is rectilinear implying a strong directionality of maximum flood and ebb currents, but lower currents during slack water, hence more chance for deposition.

Preliminary conclusions for current and turbidity patterns along the barchan dunes:

- Flood clearly dominant in current strength;
- Sediment resuspension under both flood and ebb peak velocities;
- Rectilinear currents, with a strong directionality of the peak currents, but low currents during slack water. Hence in water depths of around 30 m, deposition of fines during slack water is likely;
- Near-bed tidal ellipses that differentiate clearly from those higher in the water column (Figure 30). This might be attributed to the presence of a vortex structure.
- Near-bed deceleration of the flood current, compared to the overall flood dominance higher in the water column.

Summary of new insights of natural variation:

- Current and backscatter data from ADCP measurements, showed increased SPM concentrations, both caused by resuspension and advection.
- The advection event can occur directly after the resuspension, and can deposit at the following slack tide. Sometimes, this occurred after flood; sometimes after ebb. Hitherto, no systematic patterns have been revealed.
- Advection events have been seen under both spring and mid tidal conditions and the source direction is both flood and ebb oriented.
- Importance of wind-driven currents, e.g., persistent winds from the southwest strengthen the flood current and can, for the typical ebb-dominated steep slope of the Oosthinder sandbank, reverse the residual current to flood dominant.
- The gravel fields in the barchan dunes of the Habitat Directive area are subdued to a dominance of the flood current, though the flood current was decelerated near the bed, potentially pointing to a vortex structure along the steep side of the barchans.

4.2. *Human-induced variation*

4.2.1. Introduction

In relation to marine aggregate extraction, one can expect three types of dredge plumes, each having a typical behaviour (Spearman et al., 2011) (Figure 31): (1) a surface plume dispersing away from the vessel (i.e., TSHD); (2) a dynamic plume, representing the coarser part of the initial plume, and descending in the near field; and (3) a passive plume, bringing together the finest fractions from the surface and dynamic plumes, and from a near-bed plume caused by the draghead. The dispersion of the passive plume can easily extend several km from the vessel (e.g., Newell et al., 1999; Hitchcock, 2004). In the study area of the Hinder Banks, first observations of such plumes were made in 2013 using the unmanned surface vehicle Wave Glider and have been submitted for publication (Van Lancker & Baeye, submitted). In 2014, measurements were carried out to quantify the extent and impact of such plumes.

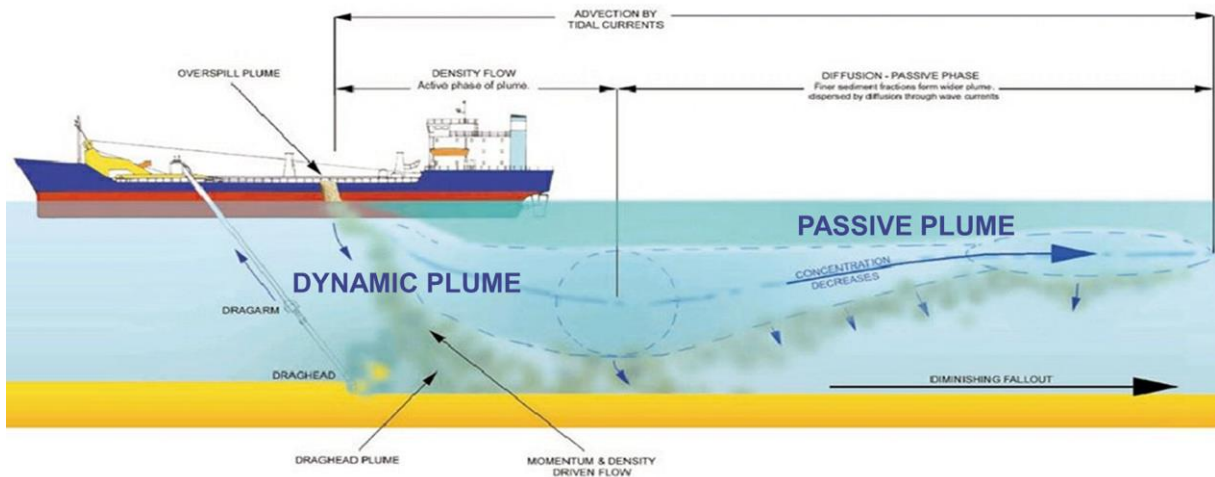


Figure 31. Dynamic and passive plumes, as a consequence of the overflow of a trailing hopper suction dredger (TSHD) (Spearman et al., 2011).

4.2.2. Extraction practices

For the first time intensive marine aggregate extraction took place in the Hinder Banks region using small (2,500 m³), medium (4,500 m³) and large (> 10,000 m³) TSHDs. Extractions were most intensive in autumn, winter and spring of 2013-2014, with simultaneous extractions in spring 2014 (Figure 32). From the analyses of the EMS and hydro-meteo database, it was evidenced that the large and small TSHD extracted exclusively during the ebbing phase of the tide, respectively in 100 % and 91 % of their operations (see also Figure 37). In Annex D details on the different TSHDs are given.

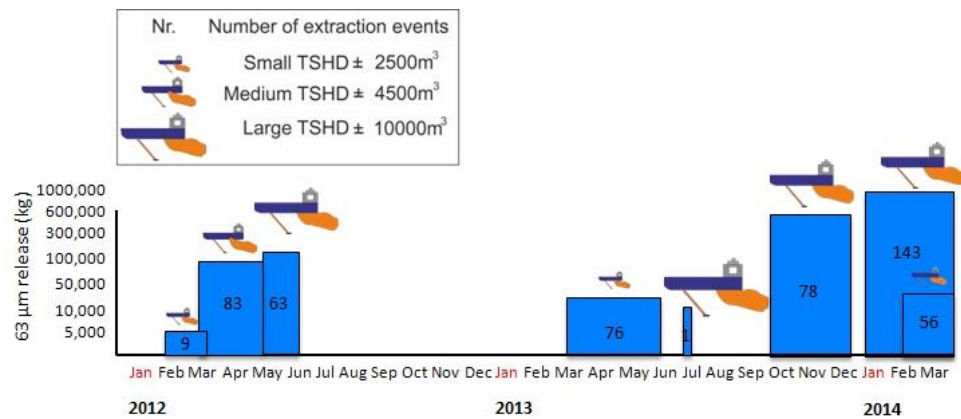


Figure 32. Extraction practices in the period 2012-2014. Periods of extraction with number of extraction events of small, medium and large TSHDs. Y-axis represents the estimated amount of release of fines (63 µm in kg) over the consecutive years.

4.2.3. Near-field impacts

(i) Sediment plumes observations

ADCP backscatter (RV Belgica, ST1407) showed well-delineated sediment plumes resulting from marine aggregate extraction activities. The dynamic plume (Figure 33) deposited close to the dredge track. Previously, deposition of the passive plume was reported (Van Lancker et al., 2014; Van Lancker & Baeye, submitted), around 8 km off the last dredging activity, in the direction of the ebb current. This observation was rather unique and was captured by an autonomous surface vehicle (WaveGlider@Liquid Robotics) (Van Lancker & Baeye, submitted).

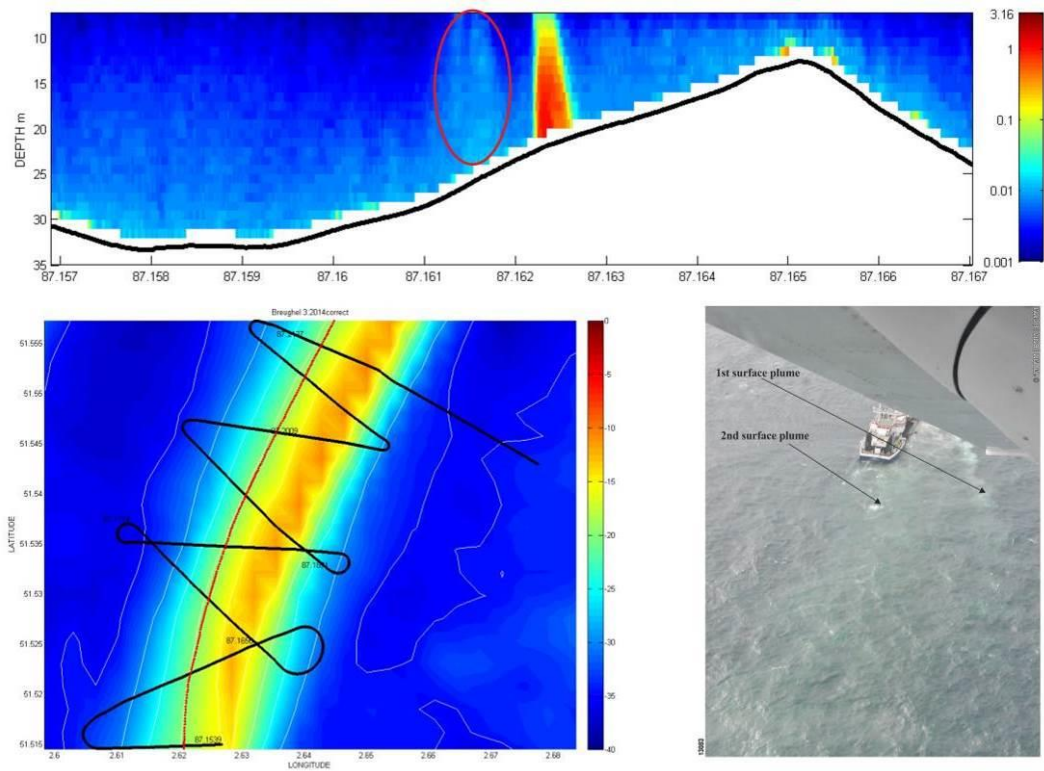


Figure 33. Dynamic plume (50-m wide) descent generated from a small-sized TSHD, as observed from ADCP data (RV Belgica March 27, 2014). Bottom left: TSHD extraction pathway (red line), together with the zig-zag track line of RV Belgica (black). Bottom right: Aerial Photo of the small-sized TSHD extracting in Sector 4c, Oosthinder sandbank (RBINS OD-Nature, Belgian Flight report of Observation at Sea, 25/03/14). Arrows indicate the surface plumes; both were also visible on the ADCP data (left of the main dynamic plume).

(ii) Sediment plume characteristics

At several occasions, it was attempted to sample in the surface sediment plume, as released by a TSHD. Only the water samples taken during campaign ST1406 (March 12-13) showed higher than background values in SPM concentrations (0.423 g l^{-1}). In Figure 34, particle-size distribution curves are shown from a bucket of water taken directly in the overflow of a TSHD, together with PSDs from samples extracted by the centrifuge purifier during the nights that RV Belgica measured, whilst TSHDs were extracting, and when no extraction took place.

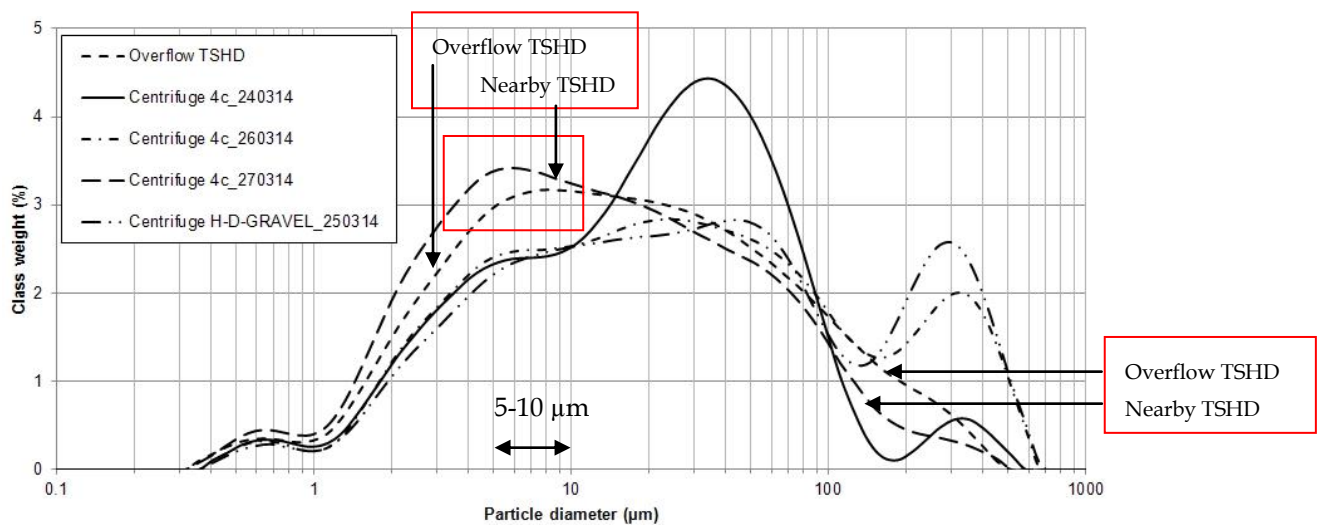


Figure 34. Particle-size distribution curves (PSD) of the water samples. RV Belgica March 2014. Note that the PSD of the sample taken in the overflow of the TSHD and the one taken during the period of active extractions differed from the PSDs taken during non-extraction periods and in the gravel area. The ones influenced by the extractions have higher weight percentages in the 5-10 μm range, and lower weight percentages in the 100-600 μm range.

It needs emphasis that it is utmost difficult to sample within a plume that is limited in extent and time. Hence, the SPM concentrations and particle sizes only partially represent the characteristics of a sediment plume.

(iii) Changing sediment characteristics in the near field

Near the dredge tracks, detailed core analyses showed that sediments were more heterogeneous than outside of the dredging zone. Additionally, some fining trend was observed in the top surface of the seabed (Figure 35). Most importantly, it was evidenced that some of the in-situ sediments do contain mud fractions, especially near the western edge of Sector 4c. At one location, 25.3 % mud content was measured (Position 7, Figure 35; detail in Figure 36).

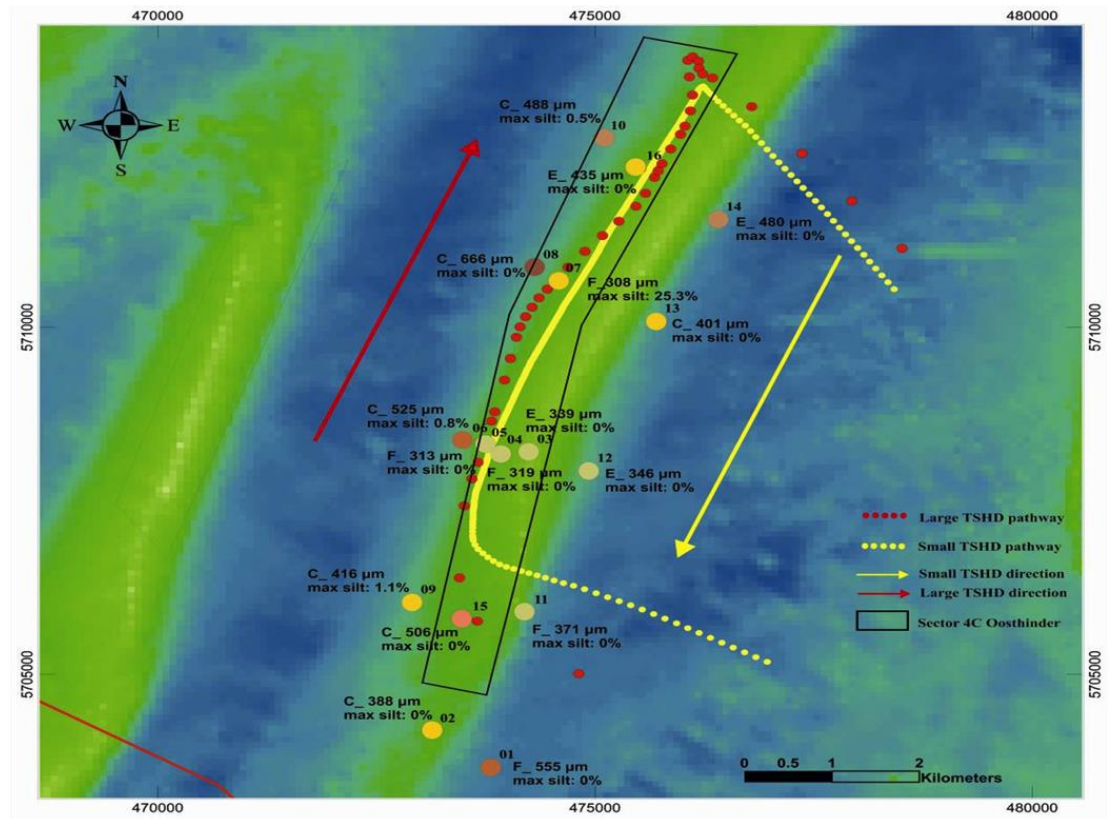


Figure 35. Sediment characteristics along Sector 4c, Oosthinder sandbank, based on shallow cores (up to ± 15 cm). Particle sizes refer to the top cm of the core; darker colours are coarser. F: indicates sediment fining in the top layers; C: indicates coarsening; and E indicates no difference. The maximum silt % in the entire core is also indicated, as also the main extraction pathways of the TSHDs (Evangelinos, 2014).

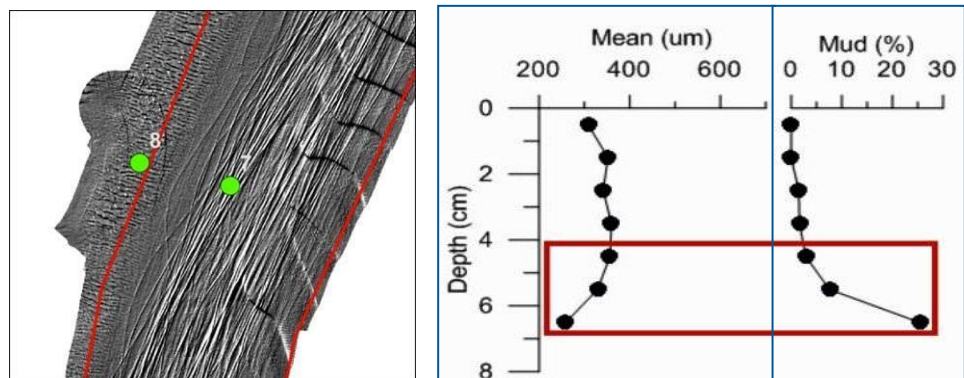


Figure 36. Zoom on Reineck boxcore sampling position 7 (Left), where high percentages of mud were measured below 5 cm of the top seabed surface (Right). Background of the left image is a shaded relief map of very-high resolution depth imagery, showing the intensity of the dredge tracks in the area (FPS Economy, RV Belgica ST1406 (March 2014)).

(iv) Changing sediment transport in the near field

During the 186-days ADCP deployment along the steep slope of the Oosthinder sandbank (13/10/2013 to 17/04/2014), multiple marine aggregate extraction events took place. In Figure 37 all of the events are plotted on the tidal ellipse. Clearly, the extraction took place primarily in the window of slack tide after high water (~flood) and the subsequent maximal ebb current. Note the position of the ADCP relative to the TSHD tracks in Figure 38. Minimum distance was 500 m, the area in which deposition of plumes may occur (Van Lancker & Baeye, submitted).

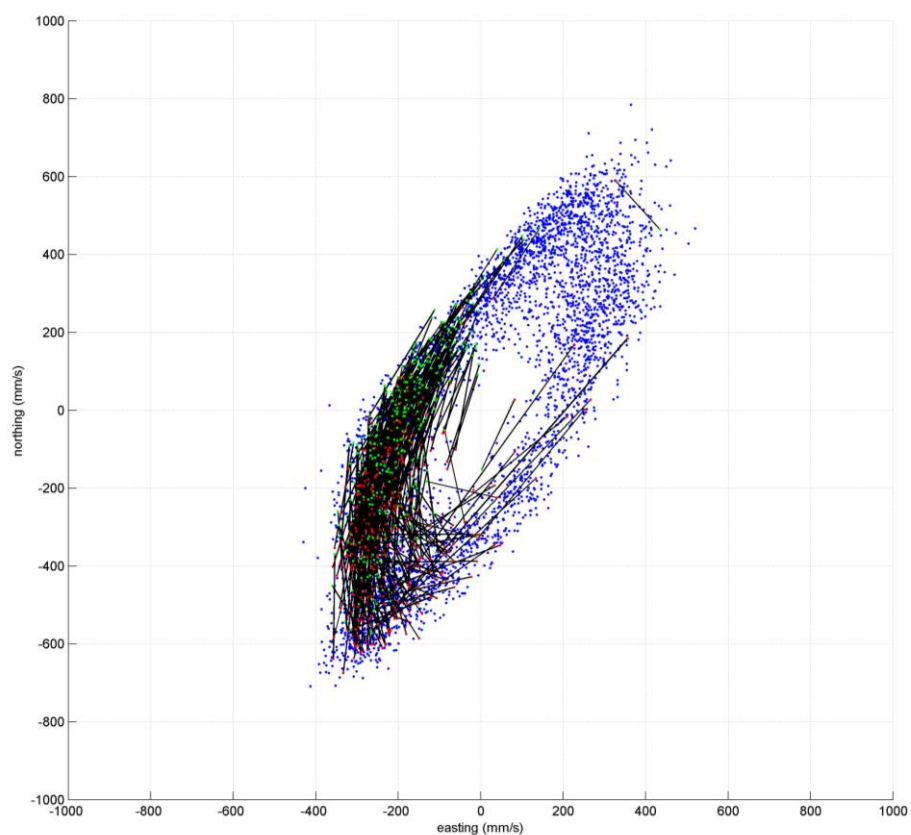


Figure 37. Tidal ellipse superimposed with TSHD extraction events (black lines; green and red dot: start and end position, respectively). Clearly, the extraction took place primarily in the window of slack tide after high water (~flood) and the subsequent maximal ebb current, being higher in directionality than the flood current. Sediment plumes arising from the TSHDs were transported to the SW, and may have reached the position of the ADCP also.

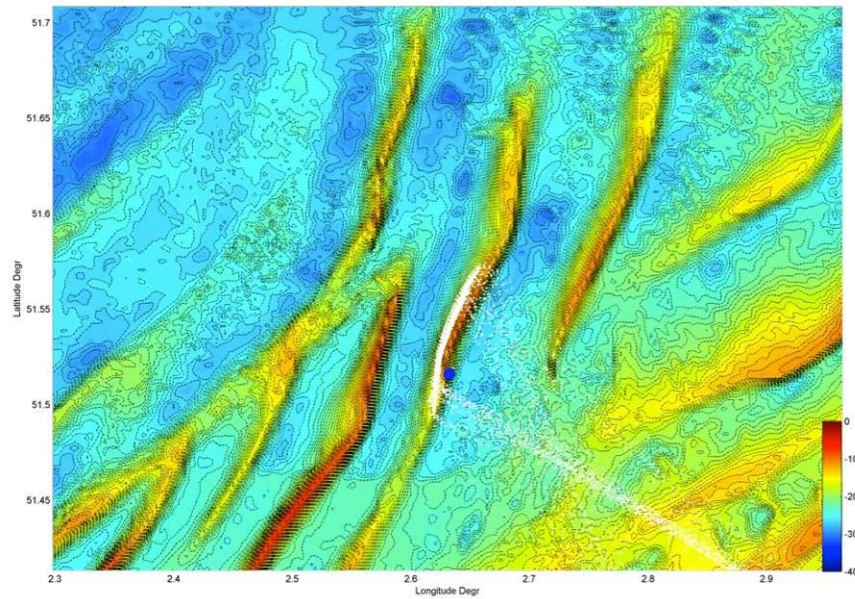


Figure 38. Track plot (in white) of the TSHDs in the period of the long-term BM-ADCP (blue dot) deployment. Minimum distance between extraction operations and location of the ADCP was 500 m.

Preliminary analyses of currents, SPM concentration values and bottom shear stresses against aggregate extraction data did not reveal significant relationships. Particular attention was devoted to the deposition events that were derived from the percentage 'Good' of one of the ADCP beams (see Material and Methods) (Figure 39). However, here also, no direct relationship could be found between the derived deposition periods and the extraction events. The onset of the first deposition event was likely related to a certain required burial percentage of the entire trawling resistant frame. From then onwards, the ADCP instrument was more vulnerable to deposition causing attenuation of its acoustic beams. This happened around DoY2013 323. Deposition was derived both under natural and human-perturbed periods. Major deposition took place around DoY 342 and DoY 358, 2013. During this period no extraction took place, but a storm occurred on DoY2013 340 ('Sinterklaasstorm'). This storm may have caused important scouring of the sandbank, with a subsequent re-establishment of its equilibrium through reorganization of the available sediments (e.g., Baeye et al., 2012; Papili et al., 2014). In the following period, with active extractions, sporadic events of deposition took place, though no systematic cause has hitherto been found (combination of the closeness of the TSHD, hydro-meteorological conditions; and the cross-bank component at the time of slack water). At the end of the deployment period (from DoY2014 90 onwards), another major deposition period was derived. In this period, more NE wind conditions were encountered, reversing the along-bank velocity component, though this pattern alone could not explain the deposition events over the entire time series. More in-depth research is needed to clarify the origin of the events.

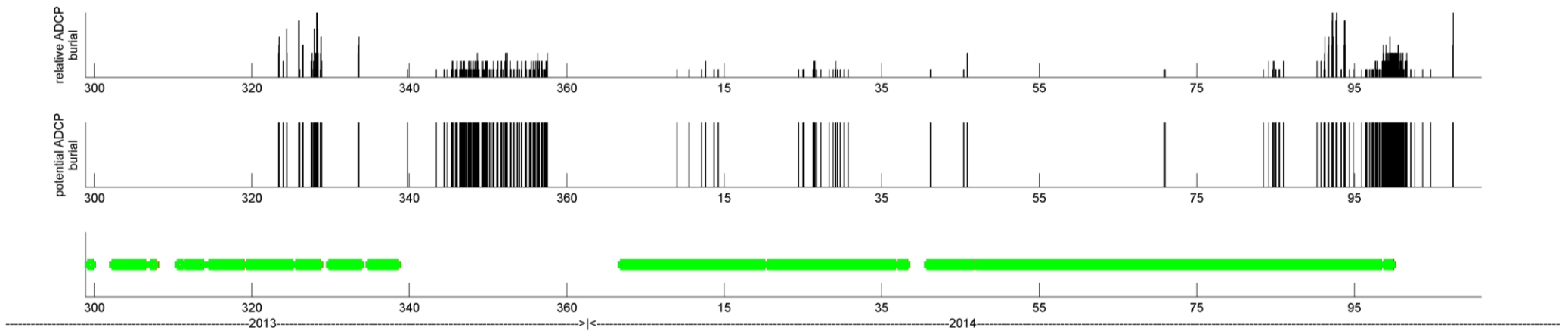


Figure 39. Burial events as derived from the long-term BM-ADCP. Subplot 1 is the relative ADCP burial; subplot 2 is the potential ADCP burial based on the percentage ‘good’ of beam 3 (PG3 parameter), when lower than 90 %. These events corresponded to the unusual low echo intensities as seen in Figure 24. The third subplot gives the extraction phases. There is no direct relation between extraction and burial events. E.g., between DoY2013 340 and 360, no extraction took place, though there were several periods of burial. From the time series, it could be observed that short phases of burial occurred during slack tides. E.g., around DoY2013 320, burial happened after slack tide after low water (~ebb). The cross-bank current component was then directed to the SE, and could transport sediment towards the steep side of the sandbank. Between DoY2014 90 and 95, the opposite happened: burial during slack tide after high water (~flood). At DoY2013 340 a major storm passed the area (“Sinterklaasstorm”). This storm likely provoked erosion and triggered subsequently a redistribution of sediments. More research is needed to clarify the events.

4.2.4. Far-field impacts

(i) Mud enrichment in the Habitat Directive area

Pre-extraction observations

The northern extension of the Habitat Directive area was defined based on the presence of ecologically valuable gravel beds, discovered by Gilson (1900), and later re-investigated by Houziaux et al. (2008). The rich biodiversity was demonstrated based on samples taken with a Gilson dredge (track sampling over ± 500 m), and with a Hamon grab. At some locations divers made visual observations in the period 2006-2008 (Figure 40). Based on all data, two refugia areas were defined where epifauna was most abundant. These occurred at the foot of the steep (lee) side of morphologically distinct barchan dunes, present at the western extremity of the Oosthinder sandbank. Barchan dunes are steep dunes, composed of coarse sands, and occur typically where high currents prevail over hard substrates (Belderson et al., 1982). Since the rich gravel beds occurred near the lee side of the barchans, Houziaux et al. (2008) hypothesized that fishing nets would jump over these biodiversity hotspots, hence they were called refugia (Figure 40).



Figure 40. Stills and video imagery taken on 13/6/2007 en 12/9/2008 (Houziaux et al. 2008). Measured sand thicknesses were 0 cm. Note the presence of soft corals and an abundance of small-sized anemones, popping-out above the sandy gravels. Scientific diving team @Alain Norro, RBINS-OD Nature.

After the 2008 samples, Ghent University re-investigated the main gravel areas of Houziaux et al. (2008) in the framework of an Msc thesis (Gogo, 2008), and used also a Hamon grab. These results, together with mud percentages prior to 2012 are shown in Figure 41.

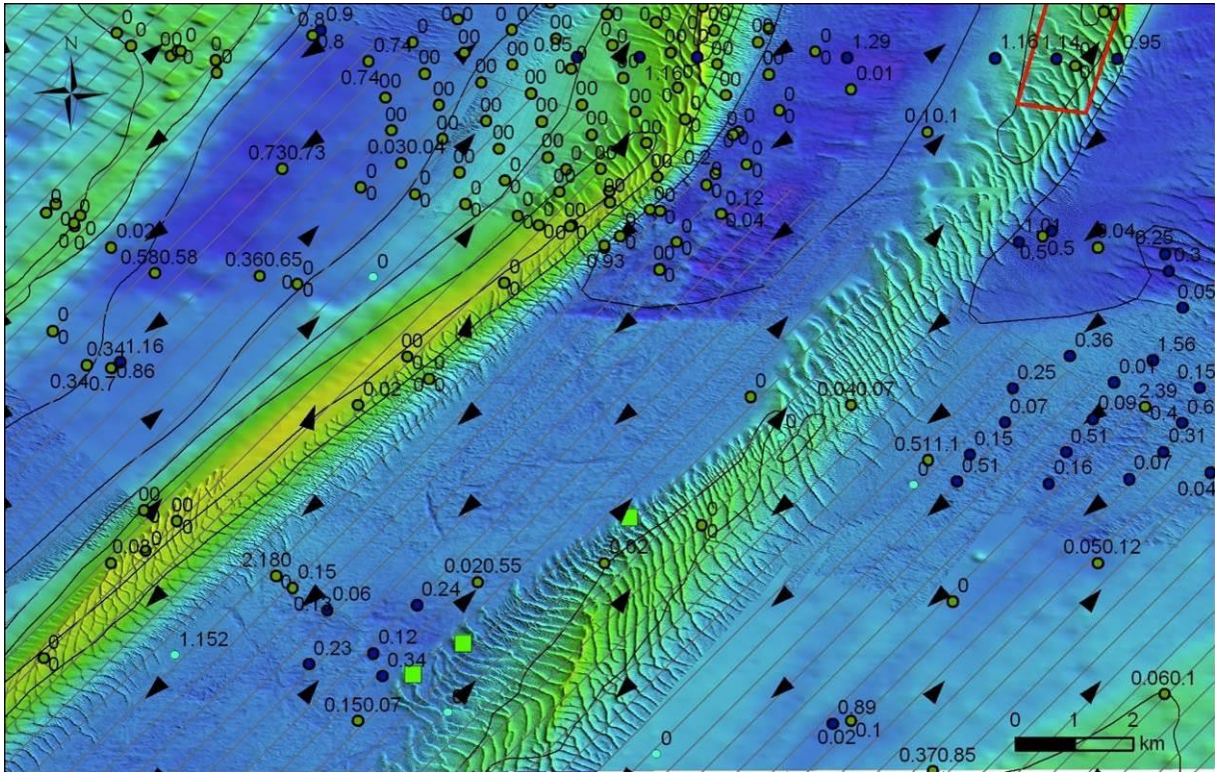


Figure 41. Mud percentages in the sandbank area of the Westhinder (left sandbank) and Oosthinder (right sandbank). Period 1976-2010. Arrows indicate direction of maximum current. Green squares represent the locations where rich biodiversity occurs. Note that the maximum known mud percentage sampled in the period 1976-2010 is 2.18 %, near the eastern slope of the Westhinder sandbank. Dark blue dots are the samples analysed by Gogo (2008); the green dots come from the SediCURVE database (Van Lancker, 2009).

Observations since the start of extraction in 2012

Since the first seabed sampling in July 2012 mud enrichment was observed in the area where previously the most rich gravel beds were observed (see above). Similar observations were made in July 2013, July 2014, and March 2014. In March 2014, up to 22 % mud was measured (Figure 42, Figure 43).



Figure 42. Mud enrichment in the gravel rich area of the barchan dunes, west of the Oosthinder sandbank, Habitat Directive area. Hamon grabs were taken during RV Belgica ST1407, for positions, see Figure 16.

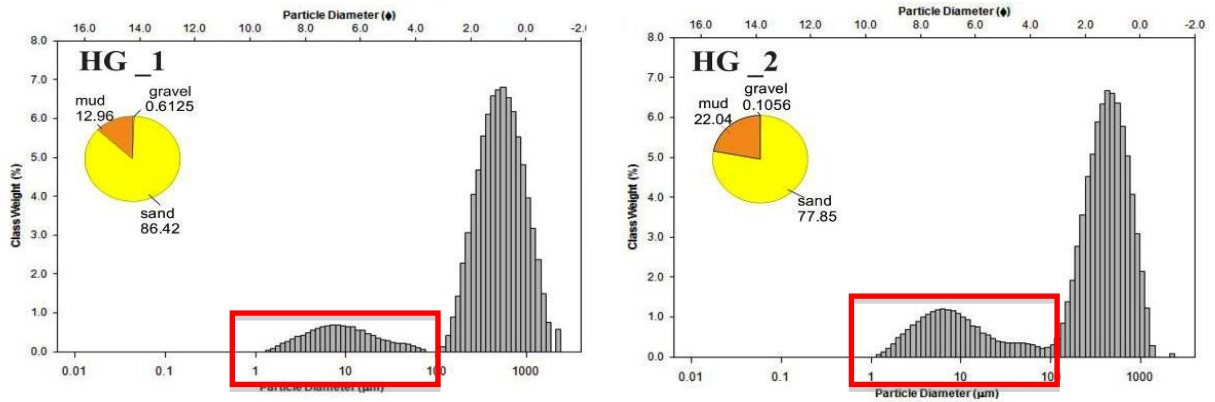


Figure 43. Seabed characteristics of the gravel-rich area. Grain-size analysis of the soft sediment in-between the gravel showed coarse-grained sands (median grain-size around 400-500 µm), however with an admixture of fines. Left: ± 13 % mud, fine mode around 8 µm; Right: ± 22 % mud, fine mode around 8 µm (ST1407).

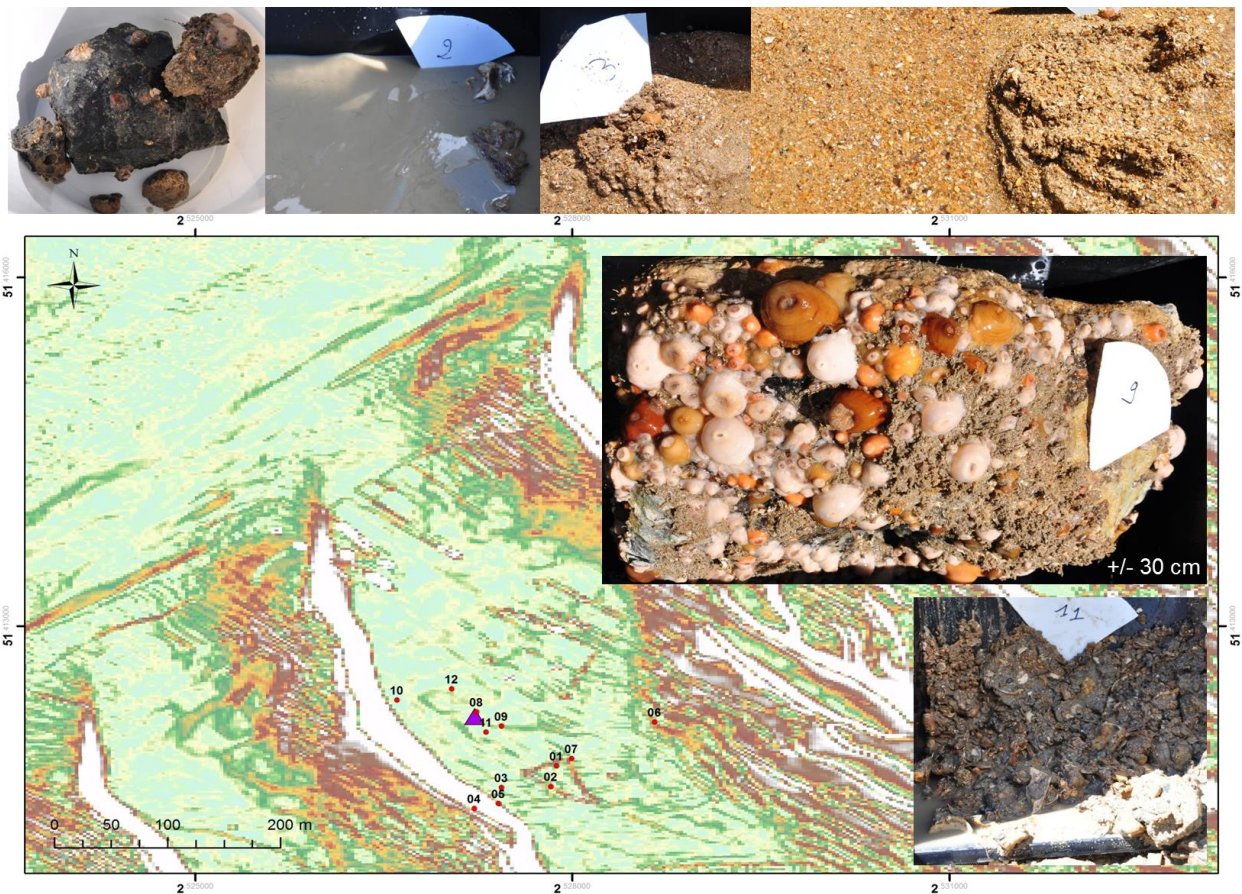


Figure 44. Variability in sediment composition in the barchan dune area, as sampled with a Hamon grab during ST1417. Note that the top and slope of the dune were composed of coarse sands solely; in the through gravel blocks were present, sometimes completely overgrown with anemones, sample 9). Samples 2 and 11 were clearly enriched with mud. Background is a slope map, based on multibeam bathymetry acquired in 2013. The position of the refugium, as defined by Houziaux et al. (2008) is indicated also (purple triangle).

However, video observations in July and December 2014 did not show surficial smothering of the seabed, but only some limited mud patches in the barchan dune area. Though, video from divers showed abundant release of fines when stirring the sediments (Figure 45). This confirms that fines are trapped, but above all that they are buffered in the parent bed, which is primarily composed of coarse sands and shell hash (Figure 45). In literature such buffering mechanisms are described (e.g., Santos et al., 2012) and are typical in coarse permeable beds. Especially in areas with bedform migration (as is the case), obstruction and acceleration of flow over topography causes horizontal pressure gradients causing fluid transport across the sediment-water interface, transporting fluid and small particles into the bed in zones of high pressure (troughs) (Huettel et al., 1996). In permeable sediments this is a normal mechanism and ensures remineralization of the seabed, playing a major role in the functioning of the ecosystem (Precht and Huettel, 2003). If the pore waters, or interstitial spaces between substrate particles, are now being clogged by excessive fines, this smothering may induce a reduction in ecosystem efficiency (e.g., Blettler et al., 2014). Further monitoring and research is vital to validate this hypothesis.



Figure 45. Video fragment showing a coarse top surface enriched with shell hash, and a release of the fine fraction after sediment stirring (ST1417, July 2014). Distance between laser lines (red lines) is ± 8 cm. Video fragment @Alain Norro, Scientific Diving, RBINS-OD Nature.

Another observation was an increasing sand thickness, compared to the situation 2006-2008. In that period, measured sand thicknesses by divers using a steel rod were 0 cm (Figure 40). There was an overall presence of soft corals and an abundance of small-sized anemones, popping-out above the sandy gravels. Now, video imagery showed an abundance of sand and most of the gravel blocks were partially buried in the sand. Analyses and sediment volume difference maps of multibeam data from 2012-2014 against 2006-2008 will shed light on changing sand volumes. Also, the ROV imagery (4/12/2014) showed an abundance of sand in the barchan dune troughs. Only, near the steep side of the dunes the sand thickness was minimal, but still more than observed on the records of 2006-2008. More fine material seems to be present (Figure 46).



Figure 46. Video fragment showing the status of the gravel beds near the foot of the steep slope of a barchan dune, where the richest biodiversity is expected. ROV GENESIS (@VLIZ), 4/12/2014. Compare with Figure 40.

First analyses of the epifauna (RBINS-OD Nature, MARECO), showed that the samples collected in 2013, had unexpectedly a decrease in numbers of long-living species. Species that need long periods without disturbance to establish and grow, such as members of the Porifera, were largely lacking (Verfaillie, 2014). However, the area was still species-rich, with a high potential for recovery. Comparison with samples collected in 2006-2007 will reveal whether shifts in functional groups are occurring. Although, the 2014 video material did not show traces of beam trawling, recent fishing-intensity maps did show more disturbances in the area (ILVO Visserij, 2014), which may be the cause of the decrease in long-living species. Still, the cumulative influence of the intensive extraction activities cannot be excluded. Further follow-up of their evolution is needed, requiring integrated approaches, combining sampling and visual observations, together with continuous time series of currents and turbidity.

4.3. Modelling of changing hydrographic conditions

4.3.1. Validation of advection-diffusion sediment transport models

To assess the probability of deposition in the Habitat Directive area, some particle tracking simulations were done first. Simplified pathways of sediment particles of 63 μm , released during extraction in Sector 4c are shown in Figure 47. Black dots indicate the possible deposition locations, where the particle reached the depth of the bottom. The simulation was done when extraction coincided with the ebbing phase of the tide. Under these conditions, the Habitat Directive area is clearly within the tidal stream axis of particles released in Sector 4c and fines from the overflow can deposit there.

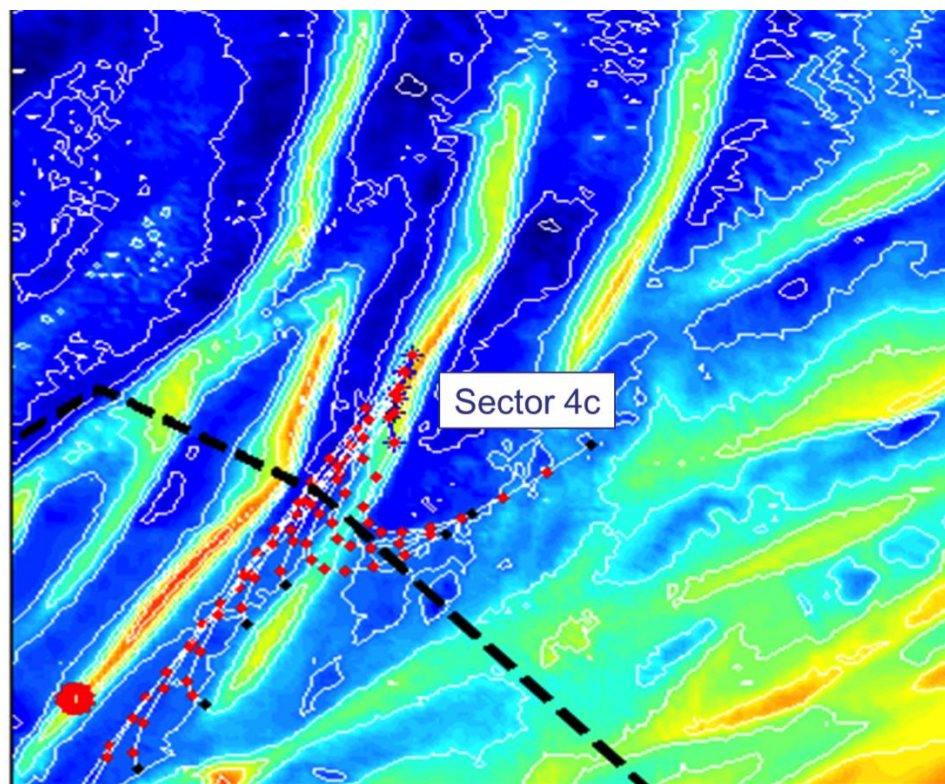


Figure 47. Example of simplified particle pathways (63 μm ; red dots) when fines are released during extraction in Sector 4c under the ebbing phase of the tide. Black dots indicate potential deposition areas. Hatched line represents the delineation of the Habitat Directive area. Red pentagon (left of the figure) is the MOW7 measuring pile on the Westhinder, from which current data were used for the predictions.

Next, sediment plume modelling was conducted, based on the modified MU-STM model and the coupling with the TASS results. For both small and large TSHDs, deposition of fines in the Habitat Directive area was confirmed (Figure 48), though the models did predict that, under agitated conditions, these fines would be resuspended and washed away. For large TSHDs only, the fines would ultimately deposit to the northeast, given the longer duration of the flood current (Figure 49; Figure 50).

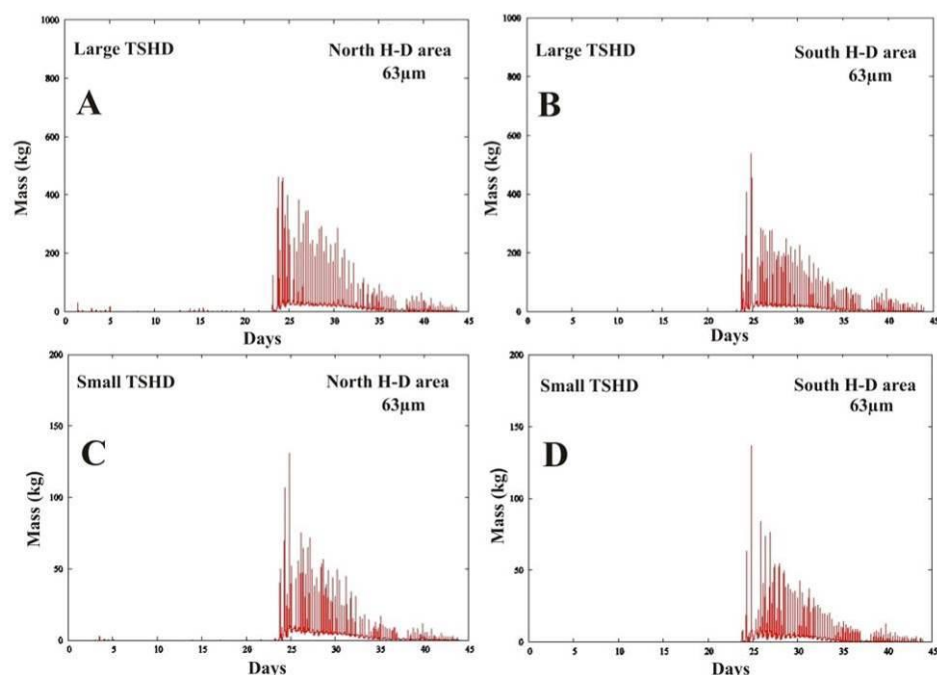


Figure 48. Simulation of the evolution in mass concentration (kg) of very fine sands ($63\ \mu\text{m}$) for the period 15/02/2014 - 22/03/2014 (45 days). (A) Deposition of $63\ \mu\text{m}$ particles along a northern location in the Habitat Directive area, arising from a large TSHD. (B) Similar, but along a southern location. (C) Deposition of $63\ \mu\text{m}$ particles in the northern area, arising from a small TSHD. (D) Similarly, in a southern area. Coupling with hydro-meteorological data showed the occurrence of 2 spring-neap cycles with spring tidal conditions around day 15 and day 30. Spring tide and high wave conditions (up to 3 m) in the first 24 days inhibited deposition of fines; afterwards, settling of fines started under neap tide and low wave conditions. However, fines were resuspended and washed away when tidal level increased. At least temporarily, the gravel beds were subdued to higher than usual SPM levels.

First ground validation of the model results was performed in October 2014 (ST1425). Hamon grabs were taken in the Bligh Bank region (near Belgian-Dutch border as shown in Figure 50), where highest deposition of fines was predicted (Figure 50). Indeed in the predicted location comparable mud enrichment as in the Habitat Directive area was found. Samples will be analysed for grain-size, as well as organic enrichment.

Although the simulations predict resuspension of the fines, it needs emphasis that a buffering of fines in the sand matrix is not accounted for (armouring process). This would limit resuspension to higher bottom shear stresses only (e.g., storms) and likely simulations could show more permanent deposition in the Habitat Directive area. In any case simulations are also needed during periods of low energetic conditions.

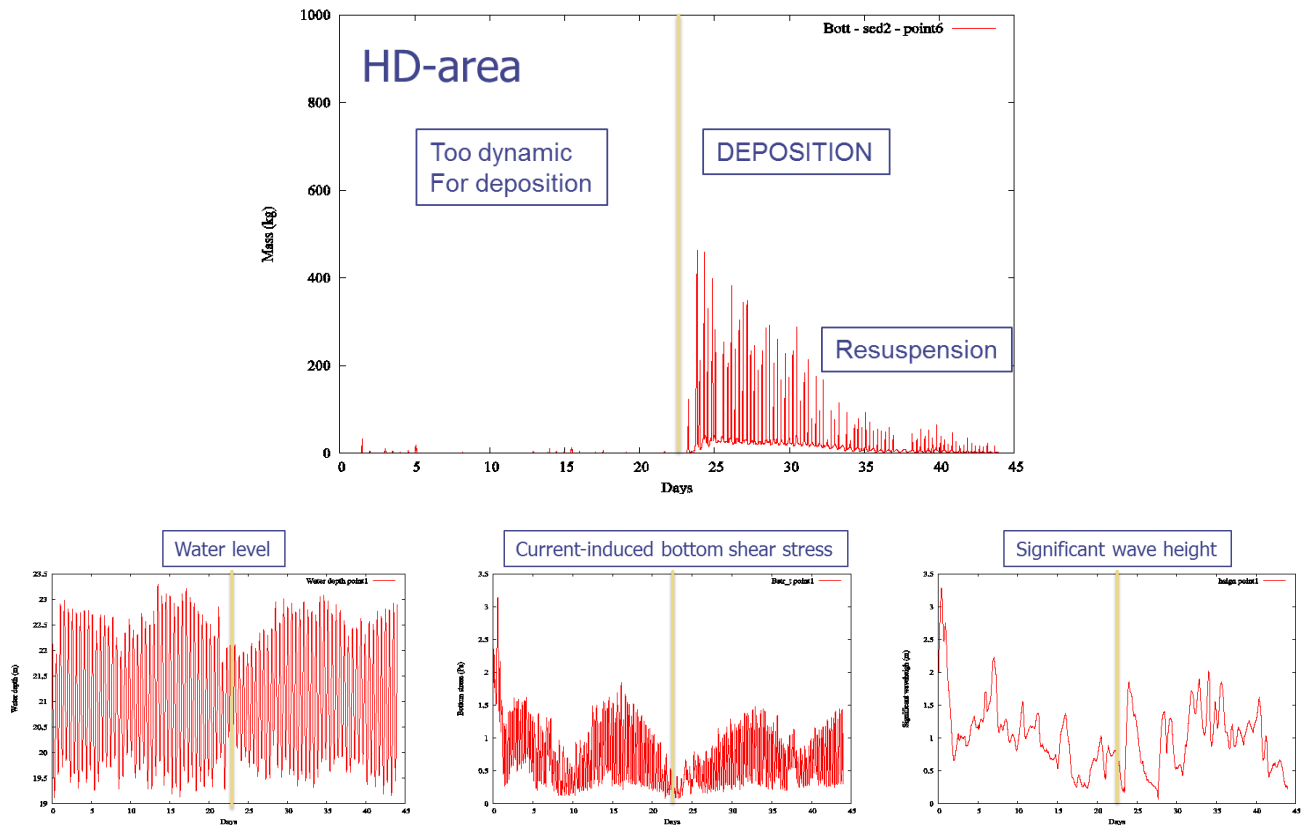


Figure 49. Model results confirmed that the fine fraction can deposit in the Habitat Directive area (HD), though only under neap tide conditions, hence low current-induced bottom shear stresses and low wave activity. Resuspension is predicted under more agitated conditions.

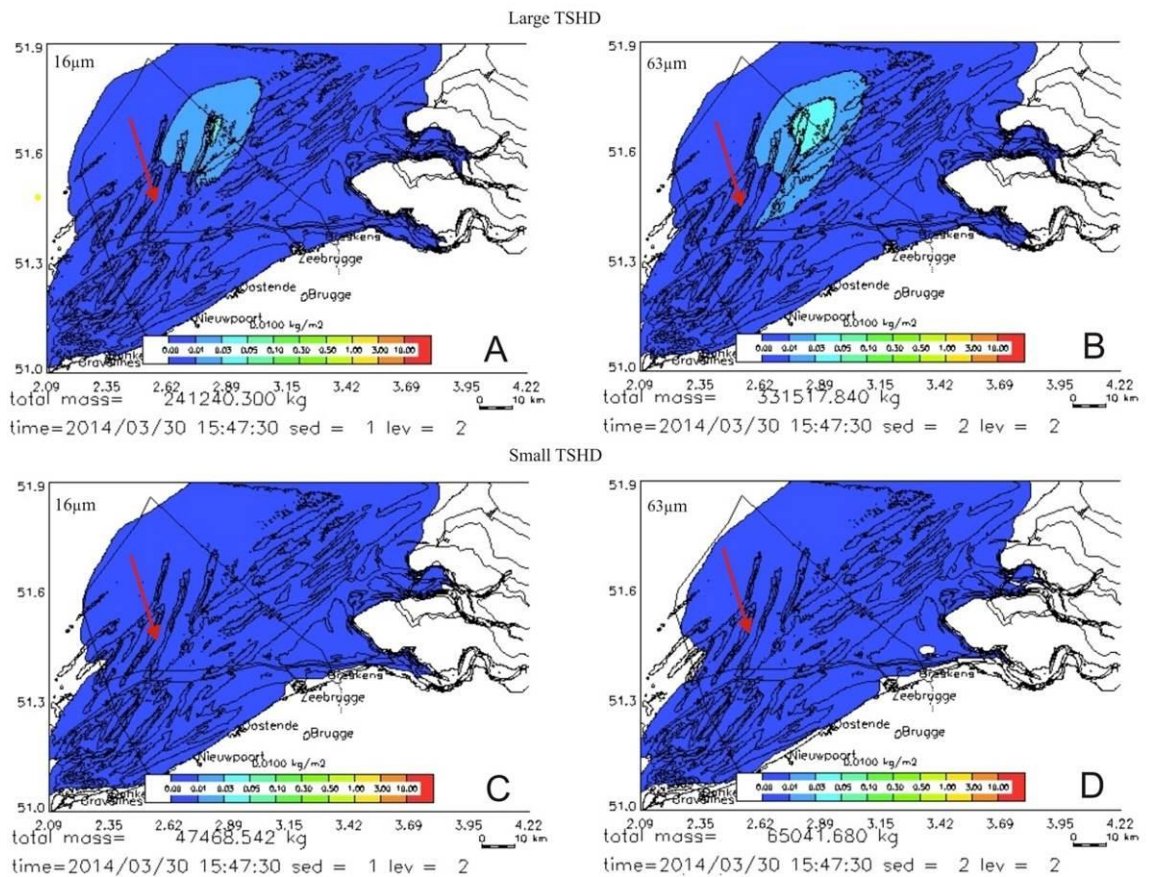


Figure 50. Results of plume modelling illustrating the dispersion of fine sediment fractions from a large and small TSHD, as well as the total mass dispersed (kgm^{-2}). Period: 15/02/2014 - 30/03/2014; end result is presented. (A) and (B) represent the fine silt particles released from a large TSHD. (A): 16 μm fraction and (B): 63 μm . (C) and (D) illustrate the sediment fractions released from a small TSHD: (C) 16 μm ; (D) 63 μm . Red arrow indicates the location of the gravel beds. Simulations showed significant deposition for the large TSHD only, with the depocentre near the Belgian-Dutch border. Model simulations did not account for buffering of fines.

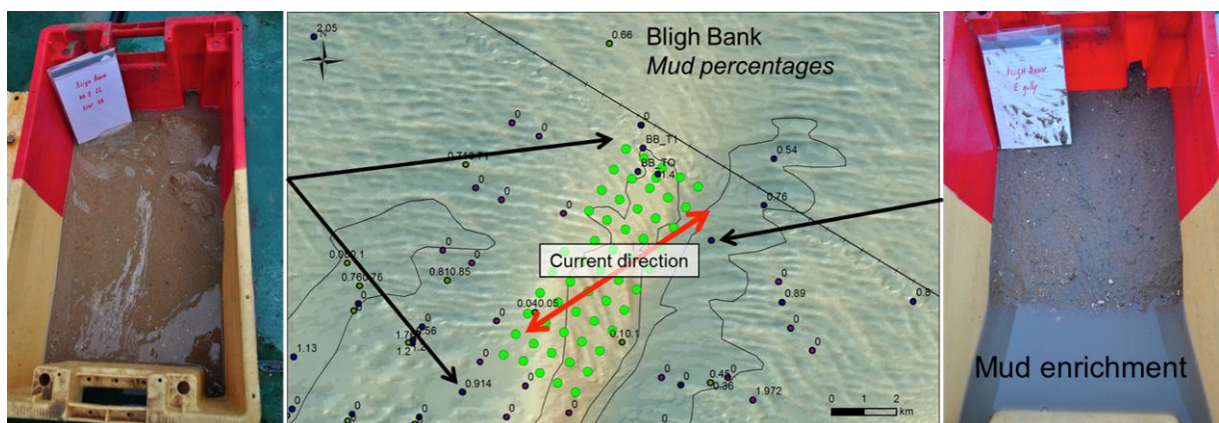


Figure 51. Mud percentages in the vicinity of the Bligh Bank wind farm (green dots) (UGent samples). For validation of the mud enrichment as predicted by the model (see above), Hamon grab samples were taken west, south and east of the Bligh Bank (RV Belgica ST1425). Only east of the Bligh Bank in the deeper part of the gully, coarse sands were clearly enriched with muds. This is the location where the model predicted deposition of fine material from the overflow of the dredging activities (Figure 50).

4.3.2. Validation of sand transport models

The bottom shear stress is an important parameter for the calculation of sediment transport as it determines erosion and deposition of the material. Since the Belgian State stipulated bottom shear stress as an indicator of the descriptor hydrographic conditions within the context of the Marine Strategy Framework Directive (Belgische Staat, 2012), it is important to have validated mathematical models for future assessments of changing bottom shear stresses. Following, the main conclusions of the model validation are reported. *See Annex C for a full reporting of the results.*

For the validation, measurements have been compiled when the current profile and high frequency velocities near the bottom were available, since these allow calculation of bottom shear stresses. A series of 70 deployments (2005-2013, various locations) was analysed, using three different techniques to determine bottom shear stress: (1) A first method used the measured current profile near the bottom, assumed to be logarithmic, and governed by the bottom shear stress and the bottom roughness length. (2) The turbulent kinetic energy (TKE) method. The TKE can be derived from the high frequency variations of the currents, and is assumed to be linearly related to the bottom shear stress. (3) The inertial dissipation method using the velocity spectrum. The high frequency part of the spectrum shows a decay with the wave number, following a characteristic $-5/3$ power, which is related to the turbulent kinetic energy dissipation and subsequently the bottom shear stress.

To model the bottom shear stress, four different models were implemented and tested. Normally, a constant bottom roughness length is applied. However, the bottom roughness length can also be modelled as a function of currents and waves. In the framework of this report, a series of new models were implemented for the calculation of the bottom roughness length, under the influence of the bed load and two models for the calculation of the bottom roughness length, as a function of the bottom ripples. To validate the model outcome, results were compared with the calculated bottom shear stresses from the measurements.

When comparing the calculated bottom shear stresses from the measurements, it was clear that no correlation existed between the different calculation methods. Furthermore, it was clear that the bottom shear stress, calculated from the current profile, was highly dependent on the number of current measurements that was accounted for. Since the method outcome were not correlating with sometimes large differences in their values, it was not clear which method gave the best approximation of reality and should be used to validate the model results. However, the fact that the bottom shear stress, derived from the turbulent kinetic energy, was influenced clearly by the wave height, while the other bottom shear stresses had no correlation with the significant wave height, it was found that this technique gave the best results and should be used to validate the model results. Furthermore, it was shown that the burst length of current measurements may not be

too short for adequate calculations of bottom shear stresses. Good acquisition settings were only available since September 2010.

The validation of the model results was first executed in more detail for two specific deployments, i.e. deployment 025, on the Gootebank in a water depth of 23 m, over a period with low wave activity, and deployment 078, near the station MOW1 in a water depth of about 10 m and during a period of high wave activity, with waves with a significant wave height up to 3 m.

It was first shown that the hydrodynamic and the wave models gave good results for the two deployment periods. For deployment 025, a large difference was found between the bottom shear stress, derived from the current profile between 0.01 m and 2.2 m, and the bottom shear stress, derived from the turbulent kinetic energy or derived from the current profile between 0.15 and 2.2 m. A quite low constant bottom roughness length of 0.004 m was used to have a good agreement between the model results and the bottom shear stress, derived from the current profile between 0.01 and 2.2 m. In the other case, a very high bottom roughness length of 0.6 m had to be used to give a good agreement between the model results and the measured bottom shear stress. When the bottom roughness was calculated in the model itself, it was observed that the calculated bottom roughness length was a factor 10 too high, to give good agreement with the bottom shear stress, derived from the current profile between 0.01 and 2.2 m. For the deployment 078, clearly the best results were obtained when comparing the model results with the bottom shear stress, derived from the turbulent kinetic energy. When using the Soulsby-Clarke model and a constant bottom roughness length of 0.01 m, a small bias was found of -0.22 Pa, and a correlation coefficient of 0.93. When using the bottom roughness, calculated in the model, good results were obtained when the total bottom roughness length was again multiplied by a factor 0.1. In this case the results were better than the results with a constant bottom roughness length.

When looking at the best agreement between the model results and the measured bottom shear stress for all deployments, more or less the same conclusions were made. Best results are obtained when comparing the model results with the bottom shear stress, derived from the turbulent kinetic energy. Furthermore, the Soulsby model gave overall the best results, when using a constant bottom roughness length of 0.01 m. When using the bottom roughness, calculated by the model, a scaling factor of 0.1 should be used to lower the calculated bottom roughness. The Soulsby or the Soulsby-Clarke model gave the best results, when the Soulsby-Whitehouse formulation was used to calculate the bottom roughness length, due to bottom ripples. Remark that the model results with the calculation of the bottom roughness in the model did not give necessarily better results than using a constant total bottom roughness. It is, for now, therefore recommended to use in the sediment transport model a constant bottom roughness length.

Overall, one can conclude that using the above parameters, good results can

be obtained, modelling the bottom shear stress, for most of the deployments. However, one has to take into account that the fact that the measured bottom shear stress, using different techniques did not show any correlation, hence rendering the results of this study uncertain. It is clear that more research has to be done to evaluate the measurements and to obtain in the future high quality measurements of the bottom shear stress. Only in this way, a solid validation of the model results can be achieved.

In the future, the results of the different deployments will be analysed in more detail. Furthermore, an analysis will be made on the dependency of the best bottom roughness length on the water depth, the maximum current or the significant wave height. Unfortunately, all measurements since September 2010 were executed in shallow, near shore waters (MOW1 and WZ-buoy). Hence, it is critical to obtain new, high-quality measurements in deeper waters. Finally, one must remark that so far only data from an Acoustic Doppler Velocimeter (ADV) and Acoustic Doppler current Profiler (ADP/Nortek) were used, as mounted on a tripod. Data from bottom-mounted ADCPs (RDI), as a.o. obtained in the Hinder Banks region, have not been analysed yet.

5. Conclusions

5.1. General conclusions

Since 2011, integrated monitoring of sediment processes is in place allowing quantification of the impacts of marine aggregate extraction in the Hinder Banks region and evaluating the compliancy of the activities with what is stipulated in European Directives. One of the issues is to assess Good Environmental Status, and therefore a number of indicators needs evaluation. These indicators relate to seafloor integrity (e.g., sediment changes), and hydrographic conditions (e.g., changes in current regime).

First of all it needs emphasis that the monitoring series is only 3 years long, implying that most of the impact hypotheses can yet not be tested. A first integrated assessment is foreseen in 2015, when all of the monitoring in the Hinder Banks region will be combined (e.g., with results of FPS Economy, SMEs, Self-Employed and Energy, and ILVO, respectively on the geomorphological and biological follow-up). Nonetheless, the monitoring provided at least three major results:

1. Comprehensive database and knowledge on the natural variability of the Hinder Banks region, hitherto only poorly known;
2. First data-modelling approaches that quantify the impact of differences in extraction practices, particularly related to the use of small (2,500 m³), medium (4,500 m³) and large (> 10,000 m³) TSHDs. The extent and mass concentrations of sediment plumes were modelled. In the near field, the main part of the overflow of TSHDs deposits. Minor changes in the seabed nature were shown. For the far field, model results showed that fine material from the overflow reached easily the Habitat Directive area, but under agitated conditions the fine material would be resuspended.
3. In the far field, in the axis of the tidal stream, seabed samples and video observations did show fining of the seabed. Concerns are raised on changes in seafloor integrity, potentially due to morphology-induced trapping and deposition of the fine material in permeable coarse sands. This could lead to changes in ecosystem efficiency of which the mechanism, impact and significance requires further research.

Mathematical models, to be used in future impact assessments, were further refined and validated. A new approach for sediment plume modelling was developed coupling technical specifications of a series of TSHDs and data on extraction activities to an advection-diffusion model that predicts the extent and total mass / concentration of sediment fractions released from the TSHDs. Furthermore, the calculations of bottom shear stress from measurements was revisited and used for the validation of bottom shear stress models. The modelling approaches were revisited also and first recommendations were provided on how

to proceed. This is important since the Belgian State put forward bottom shear stress as an indicator of hydrographic conditions, a key descriptor in the definition of 'Good Environmental Status', within Europe's Marine Strategy Framework Directive.

5.2. *Recommendations for future measurements*

Since the start of the monitoring in 2011, a series of instrumentation and approaches have been used to study both naturally- and human-induced variability in sediment processes. Data prior to this period was scarce, and little was known on the sandbank dynamics, as well as of the water properties in the region. In 2011-2013 emphasis was put on the spatial variability in zone 4 and measurements were made along transects over the sandbanks in all sectors, albeit in combination with measurements on fixed locations. The spatial approach was important to characterise the T_0 situation. In 2014, more stationary measurements were conducted, focussing on Sector 4c and on the gravel beds in the Habitat Directive area. Experience has shown that results from measurements along transects or on drift complicate largely the interpretation and quantitative correlative analyses of the data, since in a sandbank area, sediment resuspension and advection vary strongly with morphological position. The spatial measurements did allow capturing unexpected turbidity increases in the water column and evidenced important lag effects between such increases and the drivers, naturally- or human-induced.

To study cause-effect relationships in detail, it is recommended to opt, at key locations, for longer-term fixed deployments of instrumentation (e.g., with benthic landers). This strategy would provide less biased data on natural variability over spring-tidal cycles, and these datasets can then be analysed statistically against external data, e.g., on aggregate extraction. Such landers would also allow measurements up to the bottom which is needed for adequate calculations of bottom shear stresses. Hitherto, such data are hardly available in the offshore area. However, in open sea, such as in zone 4 of the Hinder Banks region, there is no protection for the landers (e.g., measuring pole) and creative solutions need to be sought for safe deployments.

A prerequisite remains that the fixed locations are chosen well. This should be based on a regional assessment of currents and sediment transport, from models and process knowledge; the latter ideally based on measurements.

Regarding process knowledge, there is a need to better understand the composition and behaviour of particles in the overflow, which determines the settling velocity and dispersal. Therefore, samples need to be taken in the weir and when entering the surrounding water mass. From a modelling perspective, these new input data can further refine the outcome of the sediment plume models. An important development will be the use of a 3D advection-diffusion model, instead of a 2D depth-averaged model as used now. This would allow accounting for the difference between overflow at the surface (small TSHD) and below the hull of a

vessel (large TSHD). Following, a regional probability assessment of deposition of fine material from TSHD overflow would be useful and would steer validation at most critical locations. From the experience so far, it is important to understand morphological trapping of fines and to determine criteria on where this is most likely to occur on the BPNS. In a next phase the study of cumulative effects becomes important, accounting for all extraction activities on the BPNS, as well as other activities that bring or remobilize fine material in the marine environment (e.g., dredging and disposal; fishing activities; windmill farms; trenching for cables and pipelines). The quest remains whether or not, per location, the origin of the fine material can be traced. In any case the impact on the benthic ecosystem and on biogeochemical fluxes need assessment, and its relevance framed in the larger North Sea ecosystem.

5.3. *Outreach*

Results have been presented at various national and international conferences and events. See Annex E. A publication was submitted to an A1 journal on the results of the Wave Glider experiment, conducted in 2013.

6. Acknowledgments

Flemish Authorities, Agency Maritime Services and Coast, Coast, are acknowledged for financially contributing to the monitoring activities (MOZ4). Full support is provided by the continuous monitoring programme ZAGRI, paid from the revenues of extraction activities.

RV Belgica shiptime was provided by RBINS OD-Nature and Belgian Science Policy (BELSPO). The commander and crew are acknowledged for their support during the measuring campaigns. Lieven Naudts, and other team members of the Measuring Service Ostend (MSO) (OD Nature) are thanked for their logistical support, especially during the deployment of the bottom-mounted ADCP. Belgian Navy is thanked warmly for relocating the lost ADCP. Special thanks goes to Reinhilde Van den Branden for her continuous support throughout all measurements, and for providing, together with Gregory De Schepper, processed data on the dredging activities.

Flanders Marine Institute, VLIZ, is thanked for the use of its LISST instrument and the Hamon grab for gravel sampling. Additionally, a video frame was provided for visual observations, and their Remote Operated Vehicle, GENESIS, was tested in the Habitat Directive area. RV Simon Stevin was used as base ship.

Ghent University, Renard Centre of Marine Geology, is acknowledged for providing laboratory facilities. Particularly, Sébastien Bertrand is thanked for his assistance during the sediment analyses. The Biology and Soil Sciences lab of UGent are thanked for, respectively, logistic and laboratory support.

Furthermore several OD Nature teams are acknowledged for their contributions: ECOCHEM for the analyses of the filtrations of the water samples; MFC, Sébastien Legrand, for modelled hydro-meteorological data; MARECO, and in particular Francis Kerckhof/An Verfaillie and Ilse De Mesel, for the analyses of the epifauna. The scientific diving team, led by Alain Norro, and comprising Frederic Francken and Daniel Marsham are thanked for the video imagery and seabed samples. Nathan Terseleer for carefully reviewing the report.

Turbidity Assessment Software (TASS) was provided through EcoShape/Boskalis. Ingrid Das is acknowledged for technical support.

Measurements of hydro-meteorological data were acquired from IVA MDK - afdeling Kust - 'Meetnet Vlaamse Banken'.

Continental Shelf Department (COPCO), FPS Economy, Self-Employed, SMEs and Energy are thanked for assistance with multibeam data processing, and active cooperation in general.

Last, but not least, numerous students (Msc Oceans & Lakes) are thanked for assisting in the measurements at sea. Ann Verfaillie (KULAK) is acknowledged for the first analyses on the epifauna of the gravel beds, as well as Anthony Dubourg (Oceans and Lakes) for assisting in the July campaign.

This work contributes to the Brain-be project TILES (Transnational and Integrated Long-term marine Exploitation Strategies), funded by BELSPO under contract BR/121/A2/TILES.

7. References

- Baeye, M., Fettweis, M., Legrand, S., Dupont, Y. & Van Lancker, V. (2012). Mine burial in the seabed of high-turbidity area – Findings of a first experiment. *Continental Shelf Research* 43, 107-119.
- Belgische Staat, 2012. Determination of Good Environmental Status and establishment of environmental Targets for the Belgian marine waters. Art. 9 & 10: 33 pp. Brussels: Federal Public Service Health Food Chain Safety and Environment.
- Belderson, R.H., Johnson, M.A., Kenyon, N.H. (1982) Bedforms. In: Stride A.H. (ed.) *Offshore tidal sands: processes and deposits*. Chapman & Hall, London.
- Bergeron, N.E. and Abrahams, A.D. (1992). Estimating shear velocity and roughness length from velocity profiles. *Water Resources Research* 28, 2155-2158.
- Blettler, M., Amsler, M.L., Ezcurra de Drago, I., Espinola, L.A., Eberle, E., Paira, A., Best, J.L., Parsons, D.R. and Drago, E.E. (2014). The impact of significant input of fine sediment on benthic fauna at tributary junctions: a case study of the Bermejo-Paraguay River confluence, Argentina." *Ecohydrology* DOI: 10.1002/eco.1511
- EcoShape (2013) TASS Software – Trailer suction hopper dredger, User guide for TASS version 4.0 Report prepared by HR Wallingford for the EcoShape Project, HR Wallingford Report DDR4882-RT002, March 2013.
- Evangelinos, D., 2014. Dispersion and deposition of sediment plumes, resulting from intensive marine aggregate extraction. Ocean and Lakes Programme VUB-UGent-UA, Royal Belgian Institute of Natural Sciences, Unpublished Msc thesis, 42 pp.
- Evangelinos, D., Baeye, M., Bertrand, S., Van den Eynde, D. & Van Lancker, V., in prep.. Dispersion and deposition of sediment plumes, resulting from intensive marine aggregate extraction.
- Fettweis, M. & Van den Eynde, D. 2003. The mud deposits and the high turbidity in the Belgian Dutch coastal zone, Southern bight of the North Sea. *Continental Shelf Research* 23: 669-691.
- Gogo, S. (2008). A first evaluation of the biodiversity of a possible Marine Protected Area on the Belgian Part of the North Sea. Unpublished Msc thesis Ghent University, Marine Biology Department.
- Hitchcock DR, Bell S (2004) Physical Impacts of Marine Aggregate Dredging on Seabed Resources in Coastal Deposits. *Journal of Coastal Research*: 101-114. doi:10.2112/1551-5036(2004)20[101:PIOMAD]2.0.CO;2
- Houziaux, J.-S., Kerckhof, F., Degrendele, K., Roche, M.F. & Norro, A. 2008. The Hinder banks: yet an important area for the Belgian marine biodiversity?: 248 pp. Brussels: Belgian Science Policy.
- Huettel, M., Ziebis, W., Forster, S. 1996. Flow-induced uptake of particulate matter in permeable sediments. *Limnology and Oceanography* 41, 309-322.
- Luyten, P. J., J.E. Jones, R. Proctor and MUMM, 2011. COHERENS - A coupled hydrodynamical-ecological model for regional and shelf seas: User Documentation. MUMM Report, Management Unit of the Mathematical Models of the North Sea, version 2, RBINS-MUMM report, Royal Belgian Institute of Natural Sciences. 1177 pp.
- Miedema, S.A. and van Rhee, C. (2007). A sensitivity analysis on the effects of dimensions and geometry of trailing suction hopper dredges. Orlando (USA) WODCON Conference, 22 p.
- Newell RC, Hitchcock DR, Seiderer LJ (1999) Organic Enrichment Associated with Outwash from Marine Aggregates Dredging: A Probable Explanation for Surface Sheens and Enhanced Benthic Production in the Vicinity of Dredging Operations. *Marine Pollution Bulletin* 38: 809-818. doi:10.1016/S0025-326X(99)00045-4.
- Omidyeganeh, M., Piomelli U., Christensen K. T. & Best J.L. (2013) Large eddy simulation of interact-

- ing barchan dunes in a steady, unidirectional flow . *Journal of Geophysical Research-Earth Surface* 118(4), 2089-2104.
- Papili, S, Wever, T, Dupont, Y & Van Lancker, V 2014. Storm influence on the burial of objects in a shallow sandy shelf environment. *Marine Geology* 349, 61-72.
- Precht, E. And Huettel, M. 2003. Advective pore-water exchange driven by surface gravity waves and its ecological implications. *Limnology and Oceanography* 48(4); 1674-1684.
- Santos, I., Eyre, B., & Huettel, M., 2012. The driving forces of porewater and groundwater flow in permeable coastal sediments: a review. *Estuarine, Coastal and Shelf Science* 98, 1-15.
- Sequoia Scientific, 2008. <http://www.sequoiasci.com/article/processing-lisst-100-and-lisst-100x-data-in-matlab/>
- Spearman, J., De Heer, A., Aarninkhof, S.G.J. & van Koningsveld, M., 2011. Validation of the TASS System for predicting the environmental effects of trailing suction hopper dredging. *Terra et Aqua* 125, 14.
- Van den Branden, R., De Schepper, G. & Naudts, L. (2012). Automatische registreersystemen geïnstalleerd aan boord van de zandwinningschepen: overzicht van de verwerkte data van het jaar 2011. Brussel, KBIN-OD Natuur.
- Van den Branden, R., De Schepper, G. & Naudts, L. (2013). Automatische registreersystemen geïnstalleerd aan boord van de zandwinningschepen: overzicht van de verwerkte data van het jaar 2012. Brussel, KBIN-OD Natuur.
- Van den Branden, R., De Schepper, G. & Naudts, L. (2014) Zand- en grindwinning op het Belgisch deel van de Noordzee. Electronic Monitoring System (EMS) voor de monitoring van de aggregaatextractie: overzicht van de verwerkte data van het jaar 2013. RBINS-OD Nature-MSO. Report MDO/2014-21/ZAGRI, 36 pp.
- Van den Eynde, D. (2004). Interpretation of tracer experiments with fine-grained dredging material at the Belgian Continental Shelf by the use of numerical models. *Journal of Marine Systems* 48: 171-189.
- Van den Eynde, D., Giardino, A., Portilla, J., Fettweis, M., Francken, F. & Monbaliu, J. (2010). Modelling The Effects Of Sand Extraction On The Sediment Transport Due To Tides On The Kwinte Bank. *Journal of Coastal Research*, SI 51: 106-116.
- Van Lancker, V. (2009). SediCURVE@SEA: a multiparameter sediment database, in support of environmental assessments at sea. In: Van Lancker, V. et al. QUantification of Erosion/Sedimentation patterns to Trace the natural versus anthropogenic sediment dynamics (QUEST4D). Final Report Phase 1. Science for Sustainable Development. Brussels: Belgian Science Policy 2009 – 63p + Annexes.
- Van Lancker, V. & Baeye, M. (submitted). Wave Glider monitoring of sediment transport and dredge plumes in a shallow marine sandbank environment. *Plos ONE*.
- Van Lancker, V., Baeye, M., Fettweis, M., Francken, F., & Van den Eynde, D. (2014). Monitoring of the impact of the extraction of marine aggregates, in casu sand, in the zone of the Hinder Banks. Scientific Report 1 - January - December 2013. RBINS OD Nature report MOZ4-ZAGRI/X/VVL/201401/EN/SR01.
- Van Lancker, V, Du Four, I, Verfaillie, E, Deleu, S, Schelfaut, K, Fettweis, M, Van den Eynde, D, Francken, F, Monbaliu, J, Giardino, A, Portilla, J, Lanckneus, J, Moerkerke, G. & Degraer, S (2007). Management, research and budgetting of aggregates in shelf seas related to end-users (Marebasse). Brussel (B), Belgian Science Policy (D/2007/1191/49), 139 pp. + DVD GIS@SEA.
- Van Lancker, V.R.M., Bonne, W., Bellec, V., Degrendele, K., Garel, E., Brière, C., Van den Eynde, D., Collins, M.B. & Velegarakis, A.F. (2010). Recommendations for the sustainable exploitation of tidal

sandbanks. *Journal of Coastal Research* SI51: 151-161.

Verfaillie, A. (2014). Macrobenthos op natuurlijke en artificiële harde substraten in het Belgisch deel van de Noordzee. Eindrapport Bachelor Stage Biologie. Kortrijk, KULAK. 15 pp.

Vlaamse Hydrografie (2011). Overzicht van de tijwaarnemingen langs de Belgische kust. Periode 2001-2010 voor Nieuwpoort, Oostende en Zeebrugge. Oostende, Ministerie van de Vlaamse Gemeenschap Agentschap Maritieme Dienstverlening en Kust, Afdeling Kust, Vlaamse Hydrografie, 41 p.

8. Annexes

Annex A. RV Belgica Campaign Reports

Annex B. Sediment sample analyses

Annex C. Validation of modelled bottom shear stresses

Annex D. Technical specifications of the TSHDs

Annex E. Publications

COLOPHON

This report was issued in February 2015

Its reference code is MOD code.

Status draft
 final version
 revised version of document
 confidential

Available in English
 Dutch
 French

If you have any questions or wish to receive additional copies of this document, please send an e-mail to vera.vanlancker@mumm.ac.be, quoting the reference, or write to:

OD NATURE
100 Gulledelle
B-1200 Brussels
Belgium
Phone: +32 2 773 2111
Fax: +32 2 770 6972
<http://www.mumm.ac.be/>

ROYAL BELGIAN INSTITUTE
OF NATURAL SCIENCES
OD NATURE



The typefaces used in this document are Gudrun Zapf-von Hesse's *Carmina Medium* at 10/14 for body text, and Frederic Goudy's *Goudy Sans Medium* for headings and captions.

Annex A

Cruise reports RV Belgica 2014

ST1407-ST1417-ST1425

This Annex forms part of the report:

Van Lancker, V., Baeye, M., Evangelinos, D. & Van den Eynde, D. (2015). Monitoring of the impact of the extraction of marine aggregates, in casu sand, in the zone of the Hinder Banks. Period 1/1 - 31/12 2014. Brussels, RBINS-OD Nature. Report <MOZ4-ZAGRI/I/VVL/201502/EN/SR01>, 74 pp. (+5 Annexes).

RV BELGICA 2014/07 - CRUISE REPORT

Subscribers:	Prof. Dr. Vera Van Lancker ¹ / Prof. Dr. Ann Vanreusel ² (Jelle Van Campenhout ²) Dr. Michael Fettweis ¹ ; Dr. Jan Reubens ² (Yana De Schutter)
Institutes:	¹ Operational Directorate Natural Environment (OD Nature) ² Ghent University, Section Marine Biology (UGent-SMB)
Addresses:	¹ OD Nature-BRU: Gulledelle 100, B-1200 Brussels ² UGent-SMB: Krijgslaan 281, B-9000 Ghent
Telephones:	+32(0)2 773 21 29 (VVL); +32(0)9 264 85 21 (AVR); + 32(0)9 264 85 24 (JVC) +32(0)2 773 21 32 (MF); +32(0)9 264 85 17 (JR)
E-mails:	v.vanlancker@mumm.ac.be , ann.vanreusel@ugent.be , jelle.vancampenhout@ugent.be , m.fettweis@mumm.ac.be , jan.reubens@ugent.be , yana.deschutter@ugent.be

Monitoring/Geology/Education: 24/03/2014 - 28/03/2014

1. Cruise details
2. List of participants
3. Scientific objectives
4. Operational course
5. Track plot
6. Measurements and sampling
7. Remarks
8. Data storage



Reference to this report:

Van Lancker, V., Baeye, M., De Schutter Yana, Francken, F., Norro, A., Hendriks, P., Hindryckx, K., Marsham, D., Reubens, J., Van den Branden, R., Van Campenhout, J. and students party (2014). *Cruise report RV Belgica ST1407, 24-28/3/2014*. Royal Belgian Institute of Natural Sciences, Operational Directorate Natural Environment, 16p.

1. CRUISE DETAILS

1.	Cruise number	2014/07
2.	Date/time	Harbour TD: 24/03/2014 : 10h36 Touch and Go Zeebrugge : 25/03/2014: 8h25-9h46 Touch and Go Zeebrugge : 26/03/2014: 17h-18h30 Touch and Go Zeebrugge : 27/03/2014: 9h45-11h22 Touch and Go Zeebrugge: 27/03/2014: 15h05-15h30 (disembarkation Belgian Navy divers after tripod operations) Harbour TA: 28/03/2014: 09h14
3.	Chief Scientist Participating institutes	Prof. Dr. Vera Van Lancker OD Nature / UGent-SMB
4.	Area of interest	Belgian part of the North Sea

2. LIST OF PARTICIPANTS

Institute	NAME	G	24-25	25-26	26-27	27-28
OD Nature	VAN LANCKER Vera	F	X	X	X	X
	VAN DEN BRANDEN Reinhilde	F	X			
	FRANCKEN Frederic	M		X	X	
	BAEYE Matthias	M				X
	HINDRYCKX Kevin	M				X
	NORRO Alain	M	X	X	Disembarkation	
UG-SMB	VAN CAMPENHOUT Jelle	M	X	X	X	X
	REUBENS Jan	M	X	X	X	
	DE SCHUTTER Yana	F	X	X	X	X
Extra Scientific divers	HENDRIKS Patrick	M	X	X	Disembarkation	
	MARSHAM Daniel	M	X	X	Disembarkation	
Oceans & Lakes Students	AFROSE Sania	F	X			
	ALVAREZ PENA Selene	F	X			
	AMISI Joel Mokenye	M	X			
	BOULLARD Roxane	F	X			
	CANNAERTS Sarah	F				X
	DE BORGER Emil	M	X			
	DIANA Alex	M	X			
	DUBOURG Anthony	M	X			
	ENOW AJEBE Lovet	M		X		
	IGNOUL ANN	F				X
	FONTAN ALENDE Elena	F			X	
	GADO Vincent Jay	M		X		
	GARCIA MAYORAL Elsa	F		X		
	JAPAY Jan harold	M		X		
	KINGUNGE Pili Kassim	F			X	
	KOKUHENNADIGE Hashan Niroshana	M				X
	KORDAS Anna	F			X	
KWARA Clement Babong	M				X	
LEEMANS Kimio	M			X		

MACAMAY Greta	F		X		
NANKABIRWA Angela	F			X	
NELSON Marcus	M			X	
NKWOMBOH Sulliz	F				X
NYAMORA Jane Moraa	F				X
PANAGIOTOU Marika	F				X
PAPASTERGIOU Angelos	M				X
PHAM Thi Tuyet	F			X	
RENQUET Rainer	M			X	
ROTTIERS Thomas	M			X	
SHAH ESLAEILI Yasmina	F		X		
STEMPELS Sara	F		X		
STORMS Simon	M			X	
VERSTEEG Erik Pieter	M			X	
TOTAL		14	14	14	14

3. SCIENTIFIC OBJECTIVES

OD NATURE-VVL/UG-SMB - STUDENTS

Students are trained in the framework of the MSc program Oceans and Lakes, course “In-situ and remote sensing tools in Aquatic Sciences”. They learn to: (1) conduct most of the stages of a scientific expedition at sea (from sample collection to reporting); (2) apply a multidisciplinary approach in marine research; (3) get acquainted with different techniques of data and sample collection at sea; (4) collaborate in a scientific team including the vessel crew in order to achieve common objectives; and (5) gain insight in some important patterns of temporal variation and spatial gradients present on the Belgian Part of the North Sea (BPNS). Measurements and observations are performed in function of scientific projects (ZAGRI/MOZ4-UG-SMB-JR, *see below*).

OD NATURE-VVL-ZAGRI/MOZ4

ZAGRI is a continuous research program on the evaluation of the effects of the exploitation of non-living resources of the territorial sea and the continental shelf. MOZ4 focuses on the monitoring of hydrodynamics and sediment transport in relation to marine aggregate extraction in a far offshore zone. Overall aim is to increase process and system knowledge of this area, with a particular focus on the compliancy of the extraction activities with respect to the European Marine Strategy Framework Directive. More specifically changes in seafloor integrity and hydrographic conditions will be assessed. An important parameter is the bottom shear stress, with knowledge needed on both natural and anthropogenically-induced variability. Results will be used for the validation of mathematical models, necessary for impact quantification. ZAGRI is funded from the revenues of marine aggregate extraction activities. Flemish Authorities, Agency Maritime Services and Coast, Coast financially support the MOZ4 project (contract 211.177).

UG-SMB-JR – REEFS

Natural and artificial reefs are studied aiming at analyzing the mechanisms providing food web resilience against stressors and perturbations. Food webs of reefs within the Belgian part of the North Sea with a different maturity and complexity will be defined and the underlying structures of these food webs will be examined. In order to achieve this as many different species as possible have to be gathered from each reef, together with environmental data, sediment particulate organic matter and water particulate organic matter. Therefore, several sampling techniques will be used. During this sampling campaign, priority will lie in the gathering of as many organisms possible associated with the John Mahn shipwreck and at a natural gravel bed. Sampling at the wreck will be conducted by divers. At the gravel bed, most samples can be taken from RV Belgica.

OD NATURE-MF - MOMO

The project "MOMO" is part of the general and permanent duties of monitoring and evaluation of the effects of all human activities on the marine ecosystem to which Belgium is committed following the OSPAR-convention (1992). The goal of the project is to study the cohesive sediments on the Belgian continental shelf 'BCS' using numerical

models as well as by carrying out of measurements. Through this, data will be provided on the transport processes which are essential in order to answer questions on the composition, origin and residence of these sediments on the BCS, the alterations of sediment characteristics due to dredging and dumping operations, the effects of the natural variability, the impact on the marine ecosystem, the estimation of the net input of hazardous substances and the possibilities to decrease this impact as well as this in-put.

OD NATURE-LN (AUMS)

The AUMS (Autonomous Underway Measurement System) project is inspired by the success of similar systems deployed on various ships of opportunity in the framework of the European Union FerryBox project (www.ferrybox.org). The instrumentation will greatly enhance the continuous oceanographic measurements made by RV Belgica by taking advantage of the significant technological improvements since the design of the existing (salinity, temperature, fluorescence) systems. In particular, many new parameters can now be measured continuously including important ecosystem parameters such as nitrate, ammonia, silicate, dissolved oxygen and CO₂, turbidity, alkalinity and phytoplankton pigments. In addition, the new equipment allows automatic acquisition and preservation of water samples, rendering RV Belgica operations significantly more efficient by reducing onboard human resources. Data will be available in near real-time via OD NATURE's public web site and following quality control, from the Belgian Marine Data Centre.

ESA-MC (GNSS)

For the European Space Agency continuous GNSS (Global Navigation Satellite system) data is autonomously acquired in the maritime environment for performance evaluation under different conditions.

4. OPERATIONAL COURSE

All times are given in local time (UTC+1). All coordinates in WGS84. Throughout the campaign, measurements were made with the AUMS system. Unfortunately the AUMS system malfunctioned.

Monday 24/03/2014

*HW 06h39 & 19h15
Sunrise: 6h37, sunset: 19h02*

09h00-10h30 Embarkation of instruments and personnel

10h36 Sail off from Zeebrugge

Transit to wreck John Mahn

12h18-14h15 Multibeam recordings John Mahn, first line at 75°/20°-75°/20° opening angle (HDEQUIDISTANT); subsequent lines at 60°/20°-60°/20° opening angle. Until 14h20 ADCP was still on.

14h23-14h38 Beam trawl track, west of the wreck John Mahn
15h17-15h46 Seabed sampling (4 Hamon grabs), N-S-W-E of the wreck

16h58-18h16 Start diving operations (Alain Norro en Jan Reubens; Patrick Hendriks (safety))
Diving at John Mahn

Transit to Oosthinder

18h41-22h51 Full-coverage multibeam Oosthinder sandbank. Continuation of the profiles sailed during ST1406 in a western direction.

22h53-06h05 Multibeam (depth, backscatter, water column) and ADCP measurements (1m bin) Oosthinder sandbank (south of Sector 4c) (SW currents: ±23h – 05h00). RV Belgica followed the trailing hopper suction dredger RIO. Vertical profiles and water samples were taken when the vessel was close to the RIO. When the RIO left the area, across bank transects were sailed (W->E). On the E to W profile a vertical profile and water sample was taken with the Seacat (topzone sandbank). Sampling depth

was highly variable as the Seacat had no depth reading. Use of centrifuge purifier from 18h41 until 06h.

Tuesday 25/03/2014

HW 07h58 & 20h43
Sunrise: 6h35, sunset: 19h04

-06h05 End of measurements

Transit to Zeebrugge.

08h25-09h46 Touch & Go Zeebrugge
Disembarkation: students group 1, OD Nature Reinhilde Van den Branden
Embarkation: students group 2, OD Nature Frederic Francken

Transit to wreck John Mahn

12h06 – 12h54 Start diving operations.
Diving at wreck John Mahn. Team 1 (Jan Reubens en Patrick Hendriks; Daniel Marsham (safety))
13h20-13h52 Diving at wreck John Mahn. Team 2 (Alain Norro en Fritz Francken, Daniel Marsham (safety))
14h24-15h43 Multibeam recordings wreck John Mahn (*dynamic colors: CUT to no longer display previously sailed track lines*)
16h28-16h50 Trackline with hyperbenthic sledge near wreck John Mahn

Transit to Oosthinder sandbank, natural reefs area

18h46 Anchoring at location 51°24.679; 002°31.619. 13-hrs water column characterization using the Seacat with CTD, OBS, LISST100 instrumentation and a 10l Niskin bottle for water sampling (every 30' filtration SPM; every 1h POC and salinity). To overcome the failure of depth readings at the winch and in the computer room, a cord was attached to the frame and a label was placed at -25 m. During the profiling the Seacat was lowered until the label was just above the water surface. As such a +/- constant water sampling at -26m from the water surface was obtained. First water sample was taken at 20h09 only, because of the delay with the frame deployment.
Use of centrifuge purifier throughout the measurements (18h46-08h).

Wednesday 26/03/2014

HW 09h26 & 22h04
Sunrise: 6h32, sunset: 19h05

08h00 End of 13-hrs measurements

08h39-09h13 Seabed sampling (Hamon grab, 4) in natural reef area

Weather conditions deteriorated as the wind started blowing and waves formed. It was decided to postpone the GO/NO GO for diving till around 11h. Meanwhile, it was decided to sail to the Oostdijck sandbank to attach and safety clothing to a POD with a zodiac. However, after 0.5h, the ship sailed back to the natural reef area, since the weather conditions would not have allowed safe zodiac operations. At 11h the diving operations were cancelled.

MBES was logged from 09h39 until 11h54.

10h30-12h03 Line fishing in natural reef area (trough barchan dune)

12h22-13h57 Full coverage multibeam recordings natural reefs area (<ST1407_OHGRAVEL>) (HD EQUIDST; 70°/22°; +/- 5 kt; ADCP OFF)

Transit to Zeebrugge

17h-18h30 Touch & Go Zeebrugge
Disembarkation students group 2 and divers Alain Norro, Patrick Hendriks, Daniel Marsham
Embarkation students group 3

Transit to Akkaert Bank, southern gully

19h35-20h Beam trawling gully south of Akkaert Bank

Transit to Oosthinder

21h23-23h33 Reineck boxcoring around Sector4c, Oosthinder sandbank. Onboard slicing of subcores.

23h56-07h30 Multibeam (depth, backscatter, water column) and ADCP measurements (1m bin) Oosthinder sandbank (south of Sector 4c) (SW currents: 1h30-7h36). Sailing along a cross bank transect (W<->E). On the E to W profile a vertical profile (CTD, OBS, but NO LISST) and water sample was taken with the Seacat (SPM topzone sandbank). When the trailing suction hopper dredger entered Sector 4c, transecting continued until ship passed. 3 times vertical profiles and **surface** water samples were taken, RV Belgica followed the cross bank transect to the W, and consecutively sailed to the SPM topzone location to take again a vertical profile and water sample (at +/- 2 m above bottom). Afterwards, the W<->E transecting continued and a vertical profile and water sample (at +/- 2 m above bottom) was taken at the SPM topzone location.
Use of centrifuge purifier from 21h15 until 07h30.

Thursday 27/03/2014

HW 10h40 & 23h09
Sunrise: 6h30, sunset: 19h07

-07h30 End of measurements

Transit to Zeebrugge

09h45-11h22 Touch & Go Zeebrugge
Disembarkation: students group 3, OD Nature Frederic Francken
Embarkation: students group 4
Embarkation: OD Nature Matthias Baeye, Kevin Hindryckx
Embarkation: Belgian Navy (DOVO) divers for recovery tripods
Disembarkation: hyperbenthic sledge
Embarkation: tripod.

Transit to WZ buoy

11h47-12h20 Attempt to localize tripod with MBES (line 51°22.7465', 003°10.8129'-51°22.685', 003°10.775')
12h25-12h50 Divers in the water for relocalization of tripod and re-attachment buoy.

Transit to MOW1

13h30-13h38 Divers in the water for re-attachment of a strong cord to tripod enabling safe recovery
13h56 Tripod recovered
14h23 Deployment tripod at position 51°21.632', 003°06.833'

Transit to Zeebrugge

15h05-15h30 Touch & Go Zeebrugge for disembarkation Belgian Navy divers and their equipment

Transit to Oosthinder sandbank

18h00-20h02 Reineck boxcoring Oosthinder sandbank. Onboard slicing of the subcores.

20h27- Full-coverage multibeam along the Oosthinder sandbank (topzone and to the east of Sector 4c).

Friday 28/03/2014

HW 11h39
Sunrise: 6h28, sunset: 19h08

-04h40 End of full-coverage multibeam

04h40-06h15 Multibeam (depth, backscatter, water column) and ADCP measurements (1m bin) Oosthinder sandbank (south of Sector 4c) (SW currents: 2h30-8h36). RV Belgica sailed along a ZIGZAG pattern behind the trailing hopper suction dredger RIO until the extraction ended. Most nearby distance was +/- 100m.
Use of centrifuge purifier from +/- 23h until 07h45.

Transit to Zeebrugge

08h15-08h40 Recovery aMT-tripod at WZ-buoy

MBES and sampling in the Vlakte van de Raan area were cancelled. This was purely for demonstration purposes for the students, but all students had already performed MBES the day before and had already assisted in the boxcoring.

Transit to Zeebrugge

09h14 Zeebrugge Harbor

End of campaign

5. TRACK PLOT

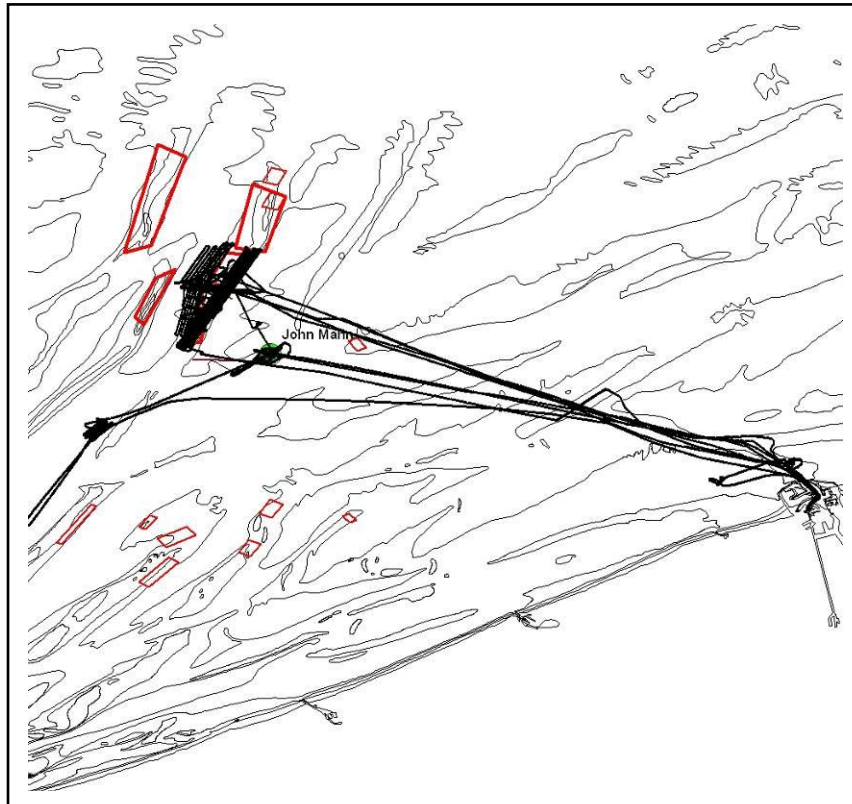


Figure 1: Track plot ST1407.

6. MEASUREMENTS AND SAMPLING

6.1. OD Nature-VVL-ZAGRI/MOZ4-STUDENTS

Hydrodynamic and sediment transport related measurements and observations in marine aggregate concession zone 4, Hinder Banks region and adjacent Habitat Directive Area 'Flemish Banks'.

Measurements and observations:

- a. **13-hrs water column characterization** (every 30') using the Seacat with CTD, OBS, LISST100 (OD NATURE) instrumentation and a 10l Niskin bottle for water sampling (filtration SPM, POC, salinity). Location: 51°24.674; 002°31.625 (trough barchan dune).
- b. **Full-coverage multibeam echosounding** (Kongsberg-Simrad 300 kHz). West and East of Sector 4c, Oosthinder sandbank.
- c. **Hamon Grab**, for sampling of soft sediment in patches of coarse sands and gravel. Habitat Directive Area (Table 2).
- d. **Centrifuge purifier sampling** to obtain suspended particulate matter (nights of 24-25/3; 25-26/3; 26-27/3; 27-28/3).
- e. **AUMS** registrations (malfunctioning)
- f. **Multibeam wreck John Mahn** (see 6.2)

During three nights, a trailer hopper suction dredger (TSHD) (Sector 4c) was followed to quantify dredging-induced sediment plumes. During these passages the following actions were undertaken:

- g. **Transects and in-situ sampling and profiling** (Hull-mounted ADCP RDI 300 kHz, 1m bin size), together with **MBES** recordings (Kongsberg-Simrad 300 kHz; depth, backscatter and water column data), together with vertical profiling of oceanographic parameters and water sampling. Three approaches were tested:
 - i. 24-25/3: RV Belgica followed the TSHD RIO. Vertical profiles and water samples were taken when the vessel was close to the RIO. When the RIO left the area, across bank transects were sailed (W<->E). On the E to W profile a vertical profile (CTD, OBS, LISST100) and water sample was taken with the Seacat (topzone sandbank). Sampling depth was highly variable as the Seacat had no depth reading.
 - ii. 26-27/3: Sailing along a cross bank transect (W<->E). On the E to W profile a vertical profile and water sample was taken with the Seacat (SPM topzone sandbank). When the TSHD entered Sector 4c, transecting continued until ship passed. 3 times vertical profiles (CTD, OBS, but NO LISST) and **surface** water samples were taken, RV Belgica followed the cross bank transect to the W, and consecutively sailed to the SPM topzone location to take again a vertical profile and water sample (at +/- 2 m above bottom). Afterwards, the W<->E transecting continued and a vertical profile and water sample (at +/- 2 m above bottom) was taken at the SPM topzone location.
 - iii. 27-28/3: RV Belgica sailed along a ZIGZAG pattern behind the TSHD RIO until the extraction ended. Most nearby distance was +/- 100m. No vertical profiles, nor water samples were taken.

Table 1: Cross bank transect over Sector 4c along which MBES (depth, backscatter, water column) and ADCP (1m bin) data were acquired before and after the TSHD RIO passed the sector.

Track				
X-Y	51°32.609'	002°36.798'	51°32.356'	002°40.435'

Table 2: Location topzone Oosthinder sandbank where vertical profiling and a water sample was taken (location on the transect specified above)

Sample id	WGS84_NB	WGS84_OL
SPM_topzone	51°32.480'	002°38.440'

Table 3: Positions of the Hamon grabs in the trough of the barchan dune, west of the Oosthinder sandbank. UTM positions corrected for the sampler position. See also Fig. 2.

id	Timestamp (UTC)	wgs84_lat	wgs84_long	wg84_x_corr	wg84_y_corr	eadepth210	eabscat33
HG1	2014-03-26 07:39:21	51,412578	2,528201	467214	5695793	-36,22	-16
HG2	2014-03-26 07:57:01	51,412330	2,528524	467240	5695772	-35,65	-13
HG3	2014-03-26 08:08:54	51,412052	2,527651	467119	5695761	-36,00	-18
HG4	2014-03-26 08:13:07	51,412160	2,527769	467170	5695736	-36,31	-13

Table 4: Centrifuge samples

id	Timestamp1 (UTC)	Timestamp2 (UTC)	Time residual (h)	Start volume (l)	End volume (l)	Discharge (ls-1)	Remark
C1	2014-03-24 17:41	2014-03-25 05:00	11,32	2712307	2714828	0,06	Too low discharge; no representative sample
C2	2014-03-25 17:46	2014-03-26 07:00	13,23	2714828	2716829	0,04	Too low discharge; no representative sample
C3	2014-03-25 20:15	2014-03-26 06:30	10,25	2716829	2727708	0,29	Discharge of +/- 0.33 ls-1 is ideal
C4	2014-03-27 22:00	2014-03-28 06:45	8,75	2727708	2735184	0,24	Centrifuge was not stopped at the end of the Oosthinder measurements

Table 5: Positions of the Reineck boxcores along Sector 4c, Oosthinder sandbank. UTM positions corrected for the sampler position. See also Fig. 3.

id_short	Timestamp (UTC)	wgs84_lat	wgs84_long	eadepth210	eabscat33	wg84_y_corr	wg84_x_corr
OH_4c_RC01	2014-03-26 20:23:00	51,483590	2,622740	-38,11	0	473816	5703665
OH_4c_RC02	2014-03-26 20:34:57	51,488219	2,612934	-29,41	-15	473139	5704186
OH_4c_RC03	2014-03-27 18:14:41	51,524505	2,628926	-15,33	-13	474249	5708208
OH_4c_RC04	2014-03-27 18:24:12	51,524281	2,623669	-21,54	-20	473905	5708200
OH_4c_RC05	2014-03-27 17:55:02	51,525344	2,621758	-23,09	-18	473763	5708302
OH_4c_RC06	2014-03-26 21:20:48	51,525846	2,617940	-30,49	-14	473508	5708367
OH_4c_RC07	2014-03-26 21:50:05	51,546683	2,633294	-26,69	-43	474577	5710672
OH_4c_RC08	2014-03-26 22:00:15	51,548331	2,629435	-32,32	-20	474319	5710867
OH_4c_RC09	2014-03-26 20:57:19	51,504851	2,609590	-30,91	-12	472917	5706041
OH_4c_RC10	2014-03-26 22:33:11	51,565116	2,640420	-33,37	-12	475088	5712725
OH_4c_RC11	2014-03-27 19:02:27	51,503728	2,628377	-24,27	-20	474214	5705897
OH_4c_RC12	2014-03-27 17:43:02	51,522108	2,638791	-30,56	-14	474937	5707936
OH_4c_RC13	2014-03-27 17:27:11	51,541422	2,649888	-34,74	-9	475706	5710092
OH_4c_RC14	2014-03-27 17:11:21	51,554724	2,659734	-32,14	-17	476410	5711556
OH_4c_RC15	2014-03-27 18:41:01	51,502805	2,618186	-22,28	-11	473508	5705800
OH_4c_RC16	2014-03-26 22:20:14	51,561266	2,646356	-24,45	-14	475496	5712293

Table 6: Timestamps water samples (SBE19-L-10). UTM positions corrected for the sampler position. See also Fig. 2, 3, 4.

id	Timestamp (UTC)	Depth < surface	wg84_x_corr	wg84_y_corr	Eadepth 210 kHz	wgs84 lat	wgs84 long
OH_4c_RIO_D1W01_Surface	2014-03-24 23:26:00	NA	473767	5708733	-23,61	51,529205	2,621923
OH_4c_RIO_D1W02_Surface	2014-03-25 00:03:12	NA	474224	5710639	-30,34	51,546385	2,628278
OH_4c_RIO_D1W03_Surface	2014-03-25 00:26:46	NA	475003	5711388	-22,75	51,553132	2,639564
OH_4c_RIO_D1W04_Bottom	2014-03-25 02:08:48	NA	475031	5710128	-13,04	51,541806	2,640053
OH_4c_RIO_D1W05_Bottom	2014-03-25 03:08:43	NA	474970	5710067	-15,45	51,541232	2,639228
OH_4c_RIO_D1W06_Bottom	2014-03-25 04:02:32	NA	475190	5710222	-14,94	51,542679	2,642228
OH_4c_RIO_D1W07_Bottom	2014-03-25 04:49:17	NA	475247	5710215	-13,94	51,542617	2,643068
OH_GRAVEL_W01	2014-03-25 19:09:06	-26	467150	5695767	-35,83	51,412177	2,527445
OH_GRAVEL_W02	2014-03-25 21:05:06	-26	467233	5695730	-34,81	51,411767	2,529004
OH_GRAVEL_W03	2014-03-25 21:35:47	-26	467237	5695762	-33,76	51,412066	2,529075
OH_GRAVEL_W04	2014-03-25 22:05:26	-26	467170	5695713	-34,94	51,411648	2,528134
OH_GRAVEL_W05	2014-03-25 22:33:26	-26	467110	5695665	-30,70	51,411307	2,527261
OH_GRAVEL_W06	2014-03-25 23:08:05	-26	467021	5695608	-33,11	51,410796	2,525989
OH_GRAVEL_W07	2014-03-25 23:34:24	-26	467027	5695592	-32,66	51,410695	2,526012
OH_GRAVEL_W08	2014-03-26 00:04:34	-26	467023	5695588	-32,09	51,410658	2,525941

OH_GRAVEL_W09	2014-03-26 00:33:28	-26	467023	5695581	-32,00	51,410607	2,525911
OH_GRAVEL_W10	2014-03-26 01:03:51	-26	467024	5695583	-31,92	51,410618	2,525940
OH_GRAVEL_W11	2014-03-26 01:33:34	-26	467005	5695609	-32,95	51,410839	2,525693
OH_GRAVEL_W12	2014-03-26 02:04:18	-26	467007	5695605	-32,65	51,410813	2,525715
OH_GRAVEL_W13	2014-03-26 02:32:54	-26	467015	5695599	-32,71	51,410766	2,525787
OH_GRAVEL_W14	2014-03-26 03:09:41	-26	467025	5695590	-32,40	51,410689	2,525923
OH_GRAVEL_W15	2014-03-26 03:36:12	-26	467021	5695586	-32,57	51,410638	2,525915
OH_GRAVEL_W16	2014-03-26 04:05:39	-26	467025	5695584	-32,67	51,410633	2,525939
OH_GRAVEL_W17	2014-03-26 04:36:32	-26	467037	5695581	-34,05	51,410614	2,526067
OH_GRAVEL_W18	2014-03-26 05:08:07	-26	467048	5695573	-35,09	51,410538	2,526213
OH_GRAVEL_W19	2014-03-26 05:35:55	-26	467047	5695570	-35,5	51,410516	2,526233
OH_GRAVEL_W20	2014-03-26 06:04:24	-26	467094	5695566	-34,85	51,410467	2,526785
OH_GRAVEL_W21	2014-03-26 06:30:51	-26	467099	5695572	-35,62	51,410457	2,526748
OH_GRAVEL_W22	2014-03-26 06:50:33	-26	467097	5695597	-35,13	51,410643	2,526703
OH_4c_RIO_D3W01_Bottom	2014-03-26 23:14:11	-12,86	475114	5710058	-14,46	51,540946	2,641148
OH_4c_RIO_D3W02_Bottom	2014-03-27 00:25:41	-13,09	474960	5710039	-16,06	51,540785	2,639031
OH_4c_RIO_D3W03_Bottom	2014-03-27 01:31:21	-12,74	474980	5710082	-15,3	51,541166	2,639288
OH_4c_RIO_D3W04_Bottom	2014-03-27 02:28:00	-10,03	475053	5710012	-11,72	51,540667	2,640478
OH_4c_RIO_D3W05_Bottom	2014-03-27 03:29:34	-6,68	474943	5710107	-15,36	51,541587	2,638835
OH_4c_RIO_D3W06_Surface	2014-03-27 04:37:42	-3,42	474520	5710151	-21,41	51,542005	2,632614
OH_4c_RIO_D3W07_Surface	2014-03-27 04:43:59	-3,56	474532	5710193	-21,36	51,542372	2,632830
OH_4c_RIO_D3W08_Surface	2014-03-27 04:49:28	-3,57	474557	5710214	-21,75	51,542561	2,633213
OH_4c_RIO_D3W09_Surface	2014-03-27 05:17:11	-3,44	474993	5710043	-14,37	51,541036	2,639528
OH_4c_RIO_D3W10_Bottom	2014-03-27 06:08:16	-10,07	475161	5710092	-12,89	51,541499	2,641892

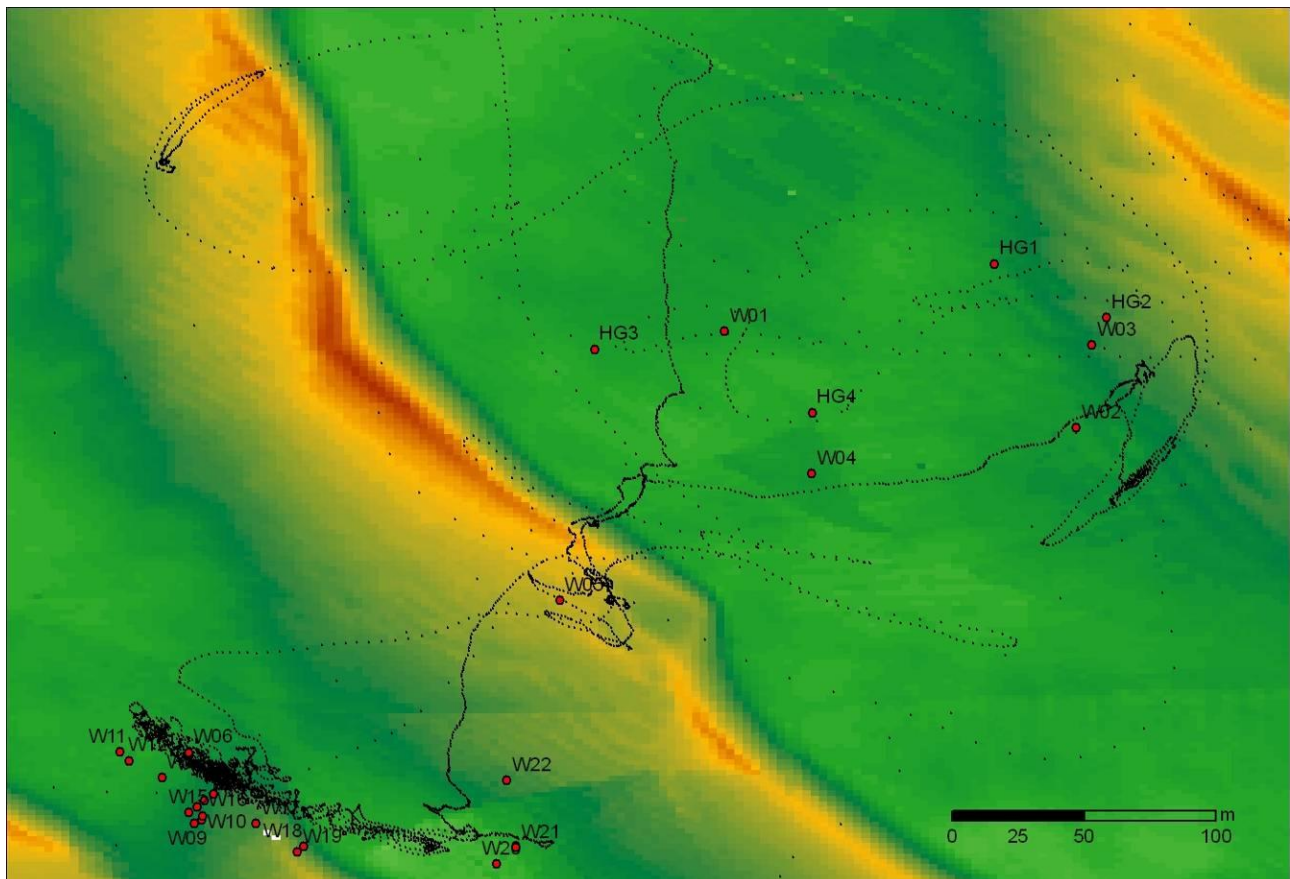


Figure 2: Trajectory along the barchan dune, west of the Oosthinder sandbank. Four Hamon Grabs were taken (HG1 to HG4). On March 25, RV Belgica anchored at position 51°24.679; 002°31.619 (W05) for a 13-hrs water sampling cycle (W01 to W22). Note the strong drift of the ship with the tide.

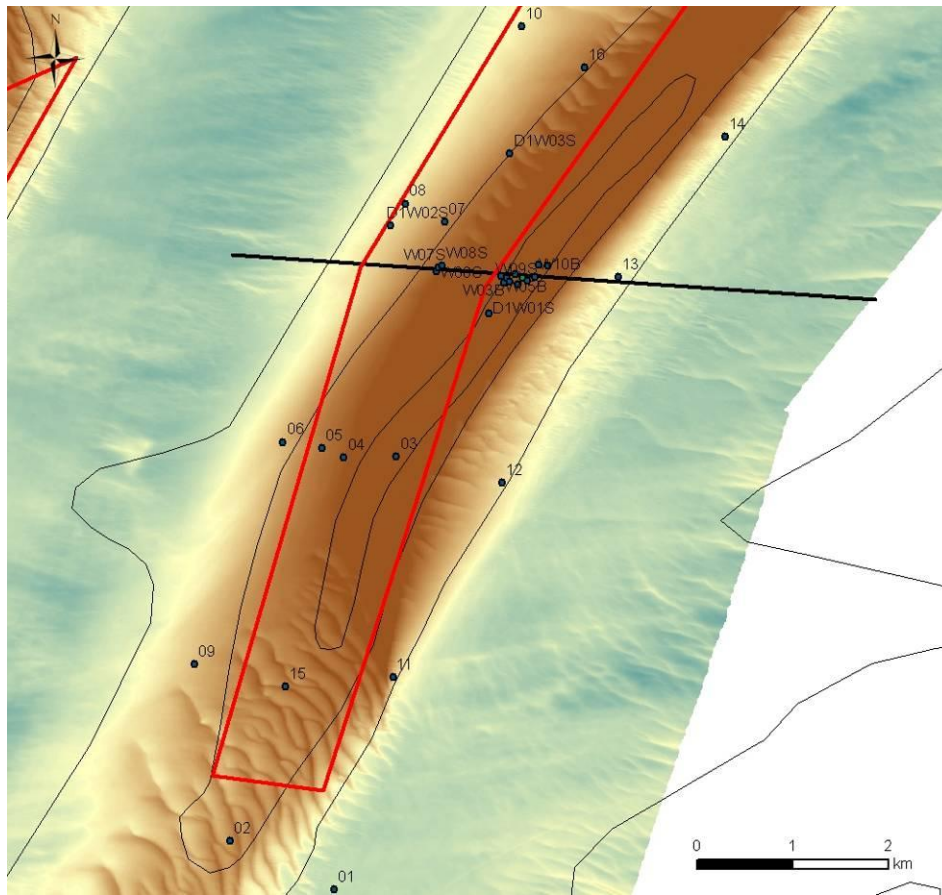


Figure 3: Reineck boxcoring (1 to 16) along Sector 4c (red polygon), Oosthinder sandbank. Positions of water sampling are also indicated (prefix D1 are the samples from 24-25/3/2014). Along the middle transect multibeam (depth, backscatter, water column) and ADCP measurements were conducted during the dredging period of the TSHD RIO.

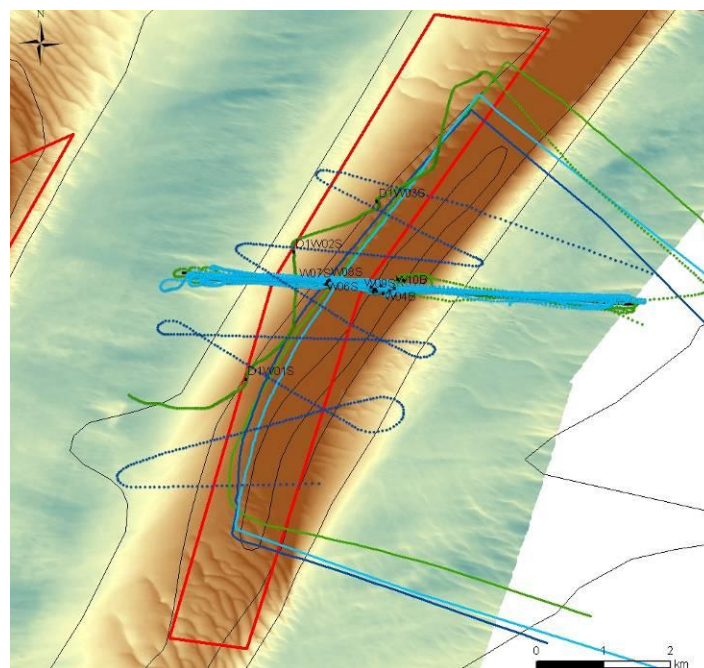


Figure 4: Follow-up dredging-induced sediment plumes along Sector 4c, Oosthinder sandbank. 24-25/3: green trajectory with polyline representing the track of the TSHD RIO and the dots RV Belgica's track (follow and transect approach); 26-27/3: cyan trajectory with polyline representing the track of the vessel RIO and the dots RV Belgica's track (transect approach); 27-28/3: blue trajectory with polyline representing the track of the TSHD RIO and the dots RV Belgica's track (zig-zag approach). The RIO sailed from south to north. Multibeam (depth, backscatter, water column) and ADCP measurements were conducted during the dredging period of the TSHD RIO. The first 2 approaches were combined with water sampling and vertical profiling of oceanographic parameters and in-situ particle sizes.

4.2. SMB-JR

(1) Samples at the John Mahn Schipwreck (overall coordinates: N 51°28',930 E 02°41',350):

Dive samples

Scraping
Airlift samples water
Airlift samples sediment
Sediment cores
Bottle traps

Other

Water sampling collected by divers

Table 7: Startline multibeam echosounding John Mahn (RBINS-OD NATURE)

id	WGS84_NB (from)	WGS84_OL (from)	WGS84_NB (to)	WGS84_OL (to)
1	51°28.93'	002°41.369'	51°28.940'	002°41.319'

Table 8. Beam trawling near John Mahn. UTM positions corrected for the sampler position.

Timestamp (UTC) from	Timestamp (UTC) to	wg84_x_corr_from	wg84_y_corr_from	wg84_x_corr_to	wg84_y_corr_to	Eadepth 210
2014-03-24 13:23:06	2014-03-24 13:38:20	477927	5703102	479214	5704482	-33,49

Table 9. Positions of the Hamon grabs near John Mahn (N-S-W-E of the wreck). UTM positions corrected for the sampler position.

id	Timestamp (UTC)	wgs84_lat	wgs84_lon	wg84_x_corr	wg84_y_corr	eadepth210	eabscat33
HG1_S	2014-03-24 14:17:46	51,481573	2,688358	478382	5703449	-32,46	-16
HG2_E	2014-03-24 14:25:30	51,482051	2,690152	478486	5703510	-31,69	-13
HG3_W	2014-03-24 14:36:52	51,482413	2,687798	478351	5703529	-31,30	-18
HG4_N	2014-03-24 14:46:20	51,483183	2,688751	478396	5703636	-31,48	-13

Table 10. Hyperbenthic sledge near John Mahn. UTM positions corrected for the sampler position.

Timestamp (UTC) from	Timestamp (UTC) to	wg84_x_corr_from	wg84_y_corr_from	wg84_x_corr_to	wg84_y_corr_to	Eadepth 210
2014-03-25 15:28:59	2014-03-25 15:43:38	478261	5703457	478853	5704080	-33,91

(2) Samples at a natural gravel bed (overall coordinates: N 51°24.44' E 02°31.38')

Start position dive (foot of the gentle slope of the barchan dune, west of the trough): 51°24.709'; 002°31.559'

Dive samples (not performed due to unfavourable weather conditions)

Scraping/collection of small stones
Airlift samples water
Photos

Other

Hamon grab (4x)
Niskin bottle
Line fishing

Table 11. Positions of the Hamon grabs in the trough of the barchan dune, west of the Oosthinder sandbank. UTM positions corrected for the sampler position. See also Fig. 2.

id	Timestamp (UTC)	wgs84_lat	wgs84_long	wg84_x_corr	wg84_y_corr	eadepth210	eabscat33
HG1	2014-03-26 07:39:21	51,412578	2,528201	467214	5695793	-36,22	-16
HG2	2014-03-26 07:57:01	51,412330	2,528524	467240	5695772	-35,65	-13
HG3	2014-03-26 08:08:54	51,412052	2,527651	467119	5695761	-36,00	-18
HG4	2014-03-26 08:13:07	51,412160	2,527769	467170	5695736	-36,31	-13

(3) Beam trawling gully Akkaert Bank

Table 12. Beam trawling gully south of Akkaert Bank. UTM positions corrected for the sampler position.

Timestamp_from	Timestamp_to	wg84_x_f	wg84_y_f	wg84_x_t	wg84_y_t	eadept210
2014-03-26 18:35:00	2014-03-26 18:49:32	499528	5698857	498300	5697565	-25,92

4.3. OD NATURE-MF (MOMO)

Recovering and deployment of tripods

The tripod deployed at MOW1 (51°N 21.595', 3°E 6.850') was recovered on 27/03, after attaching an additional cord to the tripod by diving. Another tripod was deployed at the same location, see table 1 and figure 1. The TP_aMT tripod (WZ-buoy) first had to be relocalized by divers. A buoy was attached on 27/3. The tripod was recovered on 28/3.

Table 13: Position and time of tripod recovery/ deployment.

ID	Instrument	Date (local time)	Lat_wgs84	Lon_wgs84
MOW1	Tripod recovery+deployment	27/03 13h56-14h23	51°21.632'	003°06.833'
TP_aMT	Tripod recovery	28/03 08h15-08h40		

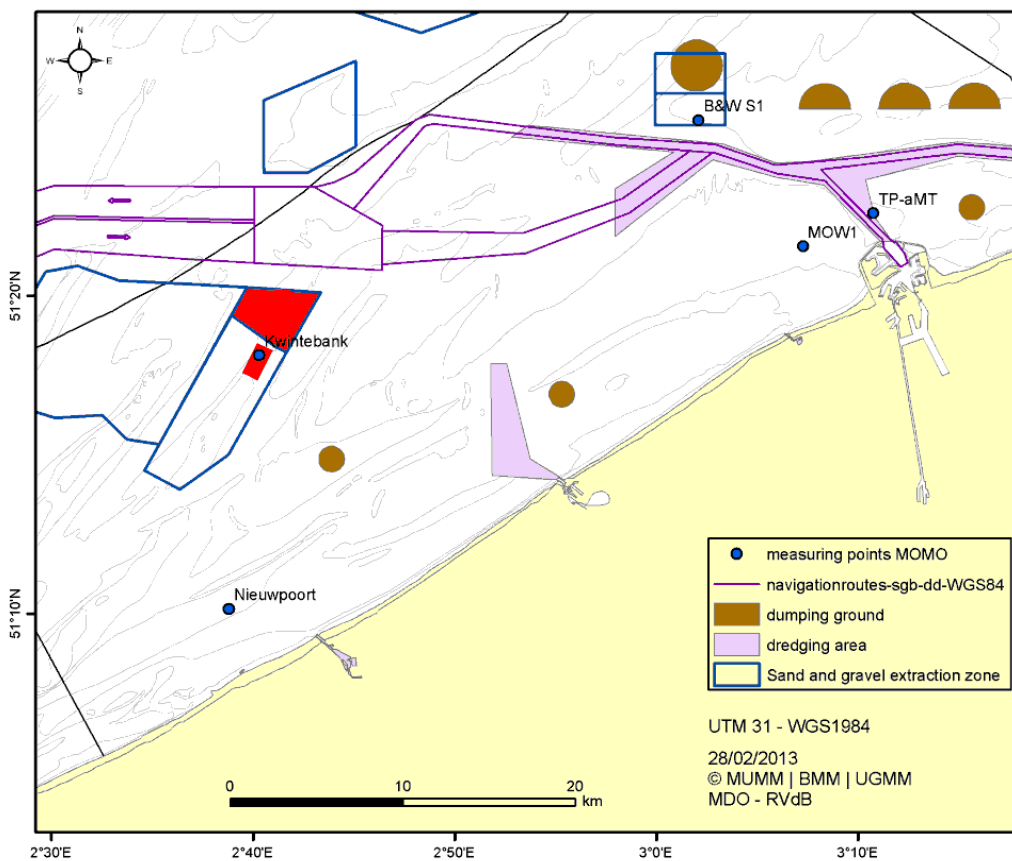


Figure 5: Location of MOMO tripod locations MOW1 and TP-aMT.

7. REMARKS

- Officers and crew are thanked warmly for the skillful handling of the operations and student assistance.
- We are grateful to the Belgian Navy for the relocalization of the tripods, and the preparations needed for their safe recovery.
- Favourable weather conditions

8. DATA STORAGE

OD NATURE

- Multibeam echosounding: on hard disk OD NATURE-BRU; copy will be provided to BMDC. Contact person: Vera Van Lancker (213 nm). Water column data: 76 nm.
- ADCP: on hard disk MUMM-BRU; copy OD NATURE -OST. Contact person: Vera Van Lancker (76 nm)
- Water samples: Integration BMDC via MARCHEM (39 samples)
- Seabed samples; integration into BMDC. Contact person: Vera Van Lancker (20 samples)
- Tripod data. Contact person: Michael Fettweis

UG-SMB

- Seabed samples. Contact person: Yana De Schutter (8 samples)
- Divers' samples. Contact person: Yana De Schutter
- Beam trawling results. Contact person: Yana De Schutter (2 tracks)
- Hyperbenthic sledge results. Contact person: Yana De Schutter (1 track)

Annex – Pictures

Table A1: Oosthinder gravel area. Hamon grabs.

	
HG01	HG04
	
HG02	HG02
	
HG03	HG03

Table A2. Oosthinder gravel area. Centrifuge sample.



Table A3. Oosthinder Sector 4c. Centrifuge sample.



RV BELGICA CRUISE 2014/17 - REPORT

Subscribers:	Dr. Vera Van Lancker ^{1a} ; Dr. Michael Fettweis ^{1a} ; Koen Degrendele ² (KD); Jan Haelters ^{1b} (JH)
Institutes:	¹ Operational Directorate Natural Environment (OD Nature) ² FPS Economy, SMEs, self-employed and Energy, Continental Shelf Department (FPS-CSD)
Addresses:	^{1a} OD Nature-BRU: Gulledele 100, B-1200 Brussels ^{1b} OD Nature-OST: 3de en 23ste Linierregimentsplein, B-8400 Ostend ² FPS-CSD: NGII - Koning Albert II Laan 16 , B-1000 Brussels
Telephones:	+32(0)2 773 21 29 (VVL); +32(0)2 773 21 32 (MF); +32(0)2 2778411 (KD); +32(0)59 24 20 55 (JH)
E-mails:	v.vanlancker@mumm.ac.be , m.fettweis@mumm.ac.be , koen.degrendele@economie.fgov.be , jan.haelters@mumm.ac.be

Monitoring/Geology: 30/06/2014 - 04/07/2014

1. Cruise details
2. List of participants
3. Scientific objectives
4. Operational course
5. Track plot
6. Measurements and sampling
7. Remarks
8. Data storage



Reference to this report:

Van Lancker, V., Degrendele, K., De Clercq, M., De Mol, L., De Rycker, K., Dubourg, A., Francken, F., Kerckhof, F., Norro, A., Hindryckx, K., Marsham, D., Van den Branden, R., Verfaillie, A. (2014). *Cruise report RV Belgica ST1417, 30/6-04/07/2014*. Royal Belgian Institute of Natural Sciences, Operational Directorate Natural Environment, 17p.

1. CRUISE DETAILS

1.	Cruise number	2014/17
2.	Date/time	Harbour TD: 30/06: 13h10 (delayed) Touch and Go Zeebrugge : 04/07: 06h36-07h08 RHIB transfer Harbour TA: 04/07: 10h
3.	Chief Scientist Participating institutes	Dr. Vera Van Lancker OD Nature / CSD / UG-RCMG
4.	Area of interest	Belgian part of the North Sea

2. LIST OF PARTICIPANTS

Institute	NAME	30/06 – 04/07	04/07 extra
OD NATURE	VAN LANCKER Vera	X	
	VAN DEN BRANDEN Reinhilde	X	
	FRANCKEN Frederic (diver)	X	
	NORRO Alain (diver)	X	
	KERCKHOF Francis	X	
	VERFAILLIE An ¹ (student)	X	
	DUBOURG Anthony ¹ (student)	X	
	HINDRYCKX Kevin		X
	VANHAVERBEKE Wim		X
	MARSHAM Daniel	X	
CSD	DEGRENDELE Koen	X	
	DE MOL Lies	X	
UG- RCMG	DE RYCKER Koen	X	
	DE CLERCQ Maikel	X	
		12	2

3. SCIENTIFIC OBJECTIVES

OD NATURE-VVL - ZAGRI/MOZ4

ZAGRI is a continuous research program on the evaluation of the effects of the exploitation of non-living resources of the territorial sea and the continental shelf. MOZ4 focuses on the monitoring of hydrodynamics and sediment transport in relation to marine aggregate extraction in a far offshore zone. Overall aim is to increase process and system knowledge of this area, with a particular focus on the compliancy of the extraction activities with respect to the European Marine Strategy Framework Directive. More specifically changes in seafloor integrity and hydrographic conditions will be assessed. An important parameter is the bottom shear stress, with knowledge needed on both natural and anthropogenically-induced variability. Results will be used for the validation of mathematical models, necessary for impact quantification.

CSD-KD

Implementation of the continuous investigation laid down in section 3, §2, subsection 3, of the law of June 13th 1969, concerning the exploration and exploitation of non-living resources on the Belgian Continental Shelf, and the concession decisions. The follow up of the repercussions of the sand extraction on the stability of the sand banks en surrounding area in the exploitation zones, in order to formulate policies concerning the exploitation in the concession zones on a scientific base. The sediments of the Belgian continental shelf will be investigated in order to:

1. Establish the impact of sand extraction on the sand budget and seabed sediments.
2. Survey the sand winning sites to detect significant changes of the seabed sediments and the morphology of the seabed and sand banks in order to guarantee the availability of sand to extract in the future.

OD Nature-MOMO (MF)

The project "MOMO" is part of the general and permanent duties of monitoring and evaluation of the effects of all human activities on the marine ecosystem to which Belgium is committed following the OSPAR-convention (1992). The goal of the project is to study the cohesive sediments on the Belgian continental shelf 'BCS' using numerical models as well as by carrying out of measurements. Through this, data will be provided on the transport processes which are essential in order to answer questions on the composition, origin and residence of these sediments on the BCS, the alterations of sediment characteristics due to dredging and dumping operations, the effects of the natural variability, the impact on the marine ecosystem, the estimation of the net input of hazardous substances and the possibilities to decrease this impact as well as this in-put.

OD NATURE-JH - Monitoring of offshore windfarms: mooring of PODs

In the framework of the assessments of the effects of the construction and operation of offshore windfarms on small cetaceans, MUMM uses Passive Acoustic Monitoring Devices: porpoise detectors (C-PODs). A C-POD consists of a hydrophone, a processor, batteries and a digital timing and logging system, and has an autonomy of up to four months (www.chelonia.co.uk). Data obtained provide an indication of the (relative) abundance of harbor porpoises in the vicinity of the device, up to a distance of approximately 300m. Data obtained from one POD can give an indication of presence/absence of porpoises, and can be compared to data obtained from PODs moored at other locations. For mooring PODs at MOW1, a tripod is used; the POD is attached vertically to the central column. PODs moored at Gootebank, at the Oostdyck Bank and at other locations are attached to cardinal buoys.

OD NATURE VISUALS

Adaptive management of human activities at sea requires a good and up to date scientific knowledge base, underpinned by remote observations and ground-truthing. Focusing on the benthal, samples are mostly used, though the results are often biased by the way the samples have been taken and unequivocal interpretation is hampered by the partial view on the seabed. OD Nature explores visual techniques and evaluates their added value in the assessment of ecological status and the quantification of human impacts. Cases are related to finding new ways to quantify smothering related to aggregate extraction, damage from fisheries activities, as also growth and decay of hard substrata fauna in offshore wind farms and in natural gravel beds. Techniques of interest are remotely operated vehicles, video frames and sledges, sediment profile imagery, as also hand-held devices by scientific divers.

OD NATURE-MB (JERICO)

OD Nature's commitment to the European framework programme JERICO (www.jerico-fp7.eu/about) is WP 10.6, viz. inter-comparison study between SPM concentrations derived from different platforms and sensors (i.e. surface buoys, benthic frames, satellites). The sensor used for this study is the Campbell Sc. OBS-5+, an optical backscatter point sensor measuring turbidity. It is stand-alone, equipped with an anti-biofouling wiper and installed in a stainless steel frame hanging at about 1.5 m under sea surface. It is a valuable tool towards better understanding SPM dynamics in the high-turbidity area in front of the Belgian coast. Continuous time-series of SPM concentration covers a wide range of hydro-meteo conditions. The AW buoy (51°22.42'N 3°7.05'E) is located at about 6 km off Zeebrugge harbor, in water depth of 10 m LAT and in the direct proximity of the benthic tripod frame with location MOW1.

OD NATURE-LN (AUMS)

The AUMS (Autonomous Underway Measurement System) project is inspired by the success of similar systems deployed on various ships of opportunity in the framework of the European Union FerryBox project (www.ferrybox.org). The instrumentation will greatly enhance the continuous oceanographic measurements made by RV Belgica by taking advantage of the significant technological improvements since the design of the existing (salinity, temperature, fluorescence) systems. In particular, many new parameters can now be measured continuously including important ecosystem parameters such as nitrate, ammonia, silicate, dissolved oxygen and CO₂, turbidity, alkalinity and phytoplankton pigments. In addition, the new equipment allows automatic acquisition and preservation of water samples, rendering RV Belgica operations significantly more efficient by reducing onboard human resources. Data will be available in near real-time via OD NATURE's public web site and following quality control, from the Belgian Marine Data Centre.

ESA-MC (GNSS)

For the European Space Agency continuous GNSS (Global Navigation Satellite system) data is autonomously acquired in the maritime environment for performance evaluation under different conditions.

4. OPERATIONAL COURSE

All times are given in local time (**UTC+2**). All coordinates in WGS84. Throughout the campaign, measurements were made with the AUMS system.

Monday 30/06/2014

HW OSTEND 03h50 & 16h06

LW: 10h14 & 22h39

Sunrise: 5h33, sunset: 22h00

09h00-13h10 Embarkation of instruments and personnel
Delay of departure was due to the need to secure the container emergency generator.

Since the favourable tidal window for the recovery/deployment operations of the tripod could be met, these operations were postponed to 4/7.

Transit to Gootebank for POD replacement

14h40-15h00 POD replacement (OD Nature-JH)

Transit to Oosthinder sandbank, trough barchan dune.

18h48-19h43 Testing of video frame Area 2

20h29 Deployment of ADCP (OD Nature-VVL MOZ4) at position 51°24.779; 002°31.608, trough of a barchan dune, where rich epifauna occurs (flatter area chosen for safe deployment/recovery).

Transit to zone 2, Oostdyck area, for seismic recordings (CSD)

21h30- Seismic investigations zone 2, in combination with multibeam

Tuesday 01/07/2014

HW OSTEND 04h23 & 16h37

LW: 10h43 & 23h11

Sunrise: 5h33, sunset: 21h59

-06h01 End of seismics and multibeam

Transit to Oosthinder sandbank, area 4 (OD Nature-VVL MOZ4)

07h55-09h00 Scientific diving (seabed/water column sampling, sand thickness estimation, video/photo). Area 4
Similar track as in 2006.

09h07-10h20 Video frame. Area 4

10h41-18h29 Multibeam calibration and start surveying barchan dune area (130 km) (OD Nature-VVL MOZ4)

19h05 13-hrs water column characterization (every 30') using the Seacat with CTD, OBS, LISST100 instrumentation and a 10l Niskin bottle for water sampling (filtration SPM, POC, salinity).
Location: 51°24.674; 002°31.625 (trough barchan dune).

Wednesday 02/07/2014

HW OSTEND 04h56 & 17h08

LW: 11h15 & 23h47

Sunrise: 5h34, sunset: 21h59

-08h End 13-hrs cycle

08h15-08h57 Scientific diving (sand thickness estimation, video/photo). Area 2

09h20-10h30 Video frame deployment. Area 2

10h44-10h55 Targeted seabed sampling (5 Hamon Grabs). Area 2.

Transit to zone 2, for seismic recordings (CSD)

11h39- Seismic investigations zone 2, in combination with multibeam

Thursday 03/07/2014

HW OSTEND 05h30 & 17h44

LW: 11h52

Sunrise: 5h35, sunset: 21h59

-08h00 End of seismics

Transit to Oosthinder sandbank, trough barchan dune, Area 3 (OD Nature-VVL MOZ4)

09h27-10h02 Scientific diving (seabed/water column sampling, sand thickness estimation, video/photo). Area 1

10h20-11h00 Video frame Area 3

BBQ!

14h16-14h54 Targeted seabed sampling (5 Hamon Grabs). Area 2.

15h15-15h52 Recovery bottom-mounted ADCP

Transit to zone 2, for seismic recordings (CSD)

16h48-19h52 Seismic investigations zone 2

Transit to Oosthinder sandbank, trough barchan dune NORTH AREA (OD Nature-VVL MOZ4)

20h58-22h17 Video frame Area 1

Transit to zone 2, for seismic recordings (CSD)

23h Seismic investigations zone 2

Friday 04/07/2014

HW OSTEND 06h11 & 18h28

LW: 00h28 & 12h37

Sunrise: 5h35, sunset: 21h58

02h05 End of seismics

Transit to Zeebrugge

06h36-07h08 Pax transfer Rhib ZB.
Embarkment MOMO team

08h15-08h30 Recuperatie OBS5

08h47 Recuperation and deployment of tripod at MOW1 (51°N 21.597, 3°E 6.997');

Transit to Zeebrugge

10h00 Zeebrugge Harbour

End of campaign

5. TRACK PLOT

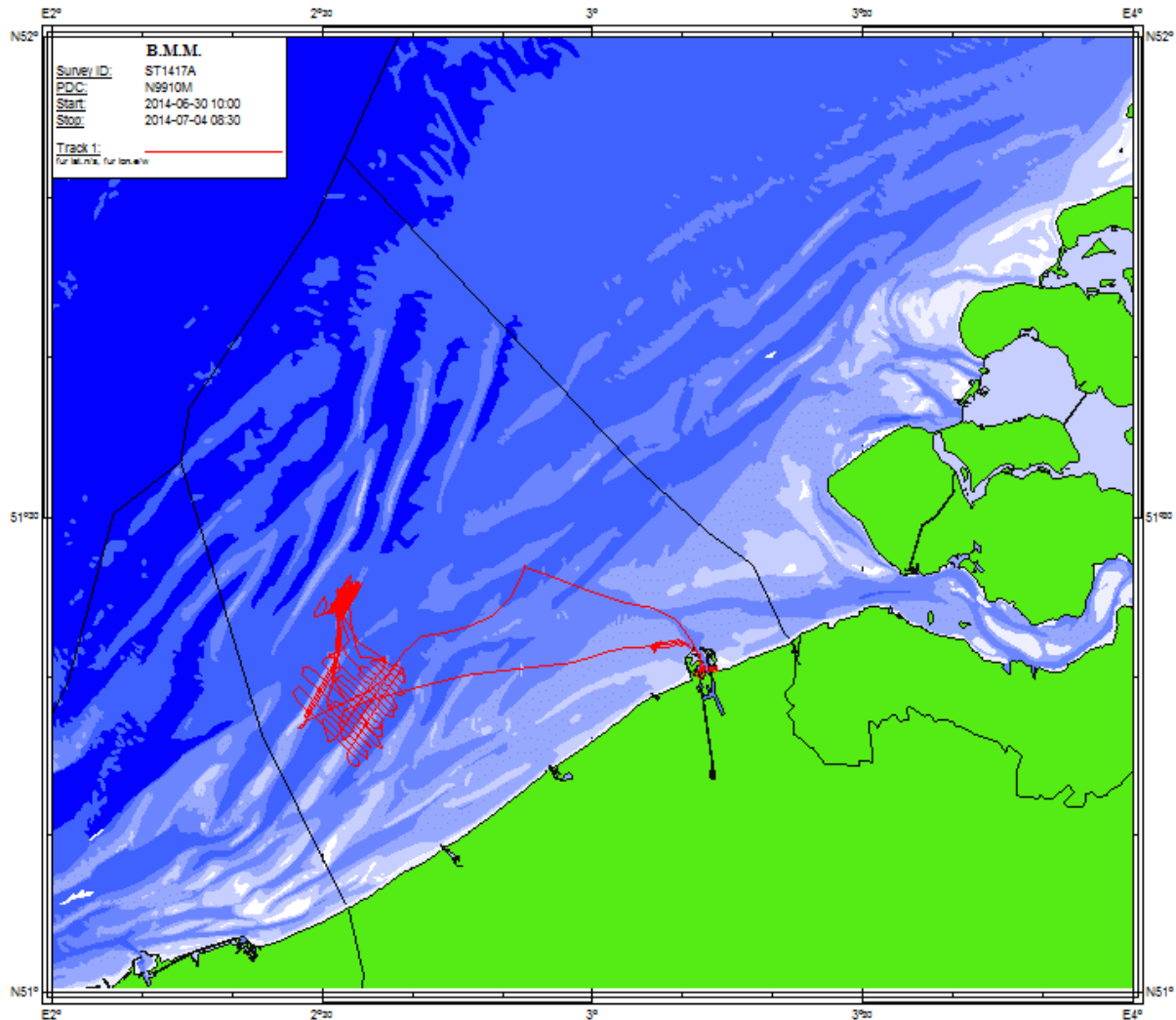


Figure 1: Track plot ST1417.

6. MEASUREMENTS AND SAMPLING

6.1. OD Nature-VVL-ZAGRI/MOZ4/VISUALS

Hydrodynamic and sediment transport related measurements and observations in marine aggregate concession zone 4, Hinder Banks region and adjacent Habitat Directive Area 'Flemish Banks'. Previous sampling campaign in the Habitat Directive Area showed enrichment of silt in the area of ecologically valuable gravel beds (in trough barchan dunes). During this campaign, visual observations were done to confirm this siltation. In the barchan dune region, 4 subareas were identified to verify sediment texture and composition. During and after the visual observations in area 2, samples for biological analyses were taken.

Measurements and observations:

- Deployment and recovery of an **ADCP Deployment** at position 51°24.779; 002°31.608, trough of a barchan dune, where rich epifauna occurs (flatter area chosen for safe deployment/recovery)
- Full-coverage multibeam echosounding** (Kongsberg-Simrad 300 kHz) barchan dune area (130 km).

- c. **13-hrs water column characterization** (every 30') using the Seacat with CTD, OBS, LISST100 instrumentation and a 10l Niskin bottle for water sampling (filtration SPM, POC, salinity). Location: 51°24.674; 002°31.625 (trough barchan dune).
- d. **Scientific diving**: along transects that crossed the sand dune from its gentle slope over the top to the steep slope. This was to ensure that the diver hit the refugium, being closely situated to the steep slope. Area 2, 3, 4. 3 seabed samples were taken in area2; 3 in area 3. In total, 6 samples.
- e. **Video frame observations (VLIZ)**. Area 1, 2, 3, and 4.
- f. **Hamon Grab**, for sampling of biological and sediment data in patches of coarse sands and gravel. Trough barchan dunes, Habitat Directive Area (see Table x). Only in Area 2 biological sampling was conducted.
- g. **AUMS** registrations (continuous)

Table 1: Position and time of ADCP deployment and recovery, trough barchan dune, Area2.

ID	Operation	Timestamp UTC	Lat_WGS84	Lon_WGS84
ADCP-GRAVEL	ADCP deployment	2014-06-30 18:29	51°24.779	002°31.608
	ADCP recovery	2014-07-03 13:30	id	id

Table 2: Locations for visual observations (four different areas, all in the trough of barchans dunes)

Sample id	WGS84_NB	WGS84_OL	Remar5
Area 1_Refugium North	51°25.8833'	2°33.1500'	Location refugium
Area 2_Refugium South	51°24.7333'	2°31.6333'	Location refugium
Area 3_Limit barchans dunes	51°24.4501'	2°31.1762'	Similar location refugium
Area 4_Previous dive 2007	51°24.8322'	2°31.6590'	Start position dive

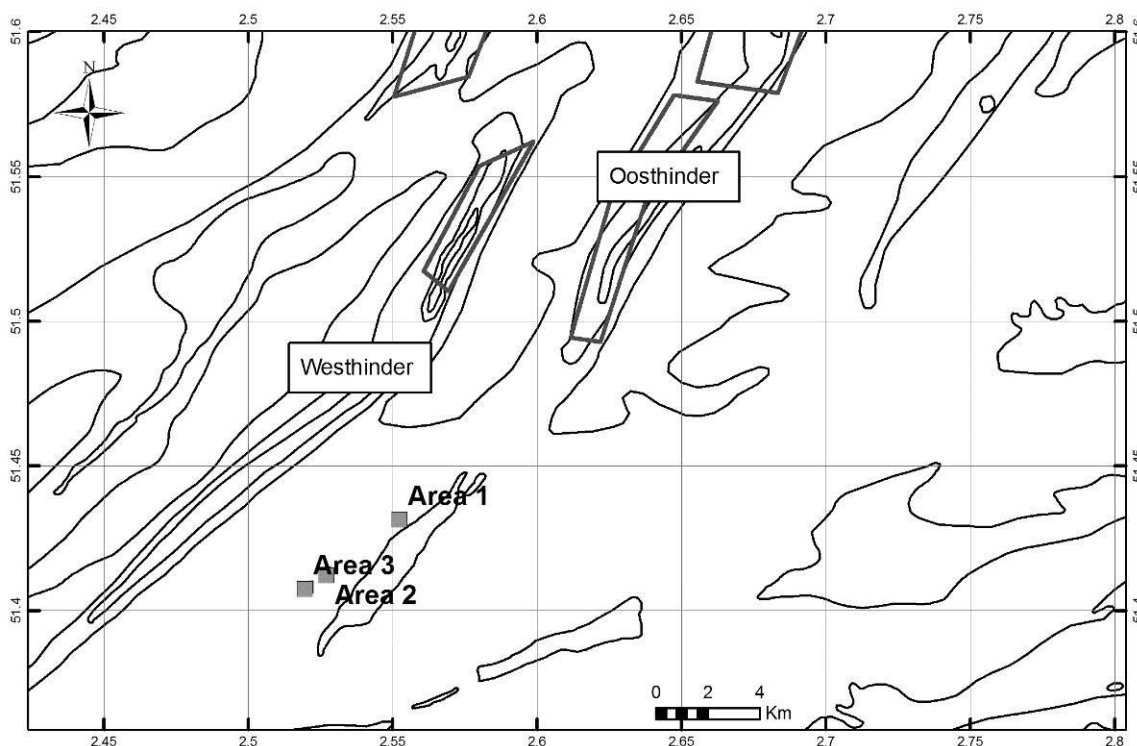


Figure 2. Location of the areas of interest for visual observations. For details, as well as location of Area 4, see Figure 3.

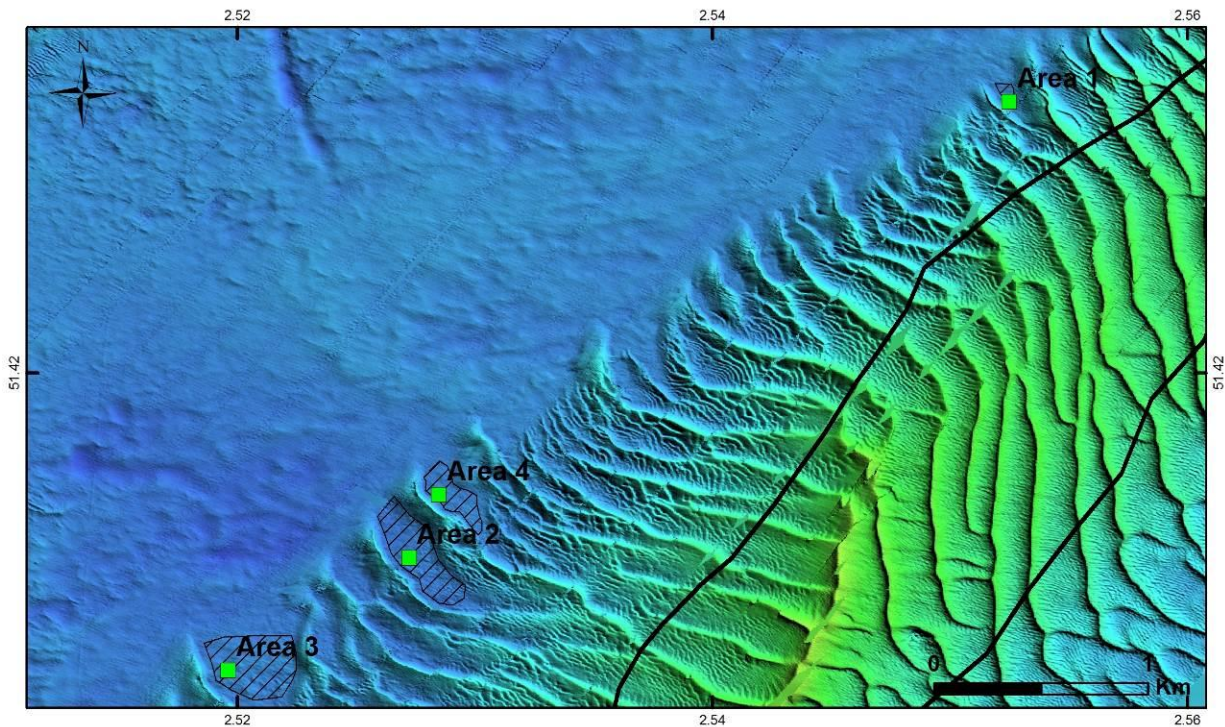


Figure 3. South part of the Oosthinder sandbank where a series of barchan dunes are attached to the main sandbank. In their trough position gravel beds were found and previously 2 refugia were identified (Area 1 and Area 2; Houziaux et al., 2008), which were exceptionally rich in biodiversity. Area 3 was taken as a test area to verify biodiversity at the extremity of the barchan dune field and furthest away from the extraction activities. The four areas were video-imaged, and dives were performed in Area 2, 3 and 4.

Table 2. Hamon grabs taken in the trough of a barchan dune, Area 2. Pictures are given in Annex. Positions corrected for an antenna layback of 32 m.

id	Timestamp	Eadepth 33 kHz	Eadepth 38 kHz	Eadepth 210 kHz	Eabscat 33 kHz	wgs84_nbd	wgs84_old	sept_taw
1	2014-07-02 08:41:00	-32.76	-32.79	NA	-11	51.41179618	2.52787298	-2.56
2	2014-07-02 08:45:38	-32.68	-32.63	NA	-5	51.41161982	2.52782313	-2.31
3	2014-07-02 08:48:14	-32.60	-32.68	NA	-7	51.41161322	2.52744268	-1.44
4	2014-07-02 08:50:54	-29.73	-30.88	NA	-29	51.41143150	2.52721938	-1.40
5	2014-07-02 08:54:12	NA	-32.45	NA	0	51.41147053	2.52740682	-2.41
6	2014-07-03 12:17:12	-33.12	-33.05	-33.12	-7	51.41218020	2.52864355	-1.13
7	2014-07-03 12:28:24	-34.21	-34.11	-33.91	-15	51.41187693	2.52799962	-1.04
8	2014-07-03 12:34:45	-34.00	-33.87	-33.90	-9	51.41227405	2.52720592	-0.80
9	2014-07-03 12:38:40	-34.07	-34.12	-33.99	-7	51.41213938	2.52743428	-0.85
10	2014-07-03 12:43:35	-34.29	-34.40	-34.37	-9	51.41237703	2.52655995	-0.95
11	2014-07-03 12:47:34	-34.11	-34.05	-34.02	-6	51.41211485	2.52731527	0.61
12	2014-07-03 12:53:24	-34.36	-34.31	-34.27	-13	51.41245078	2.52704543	0.15

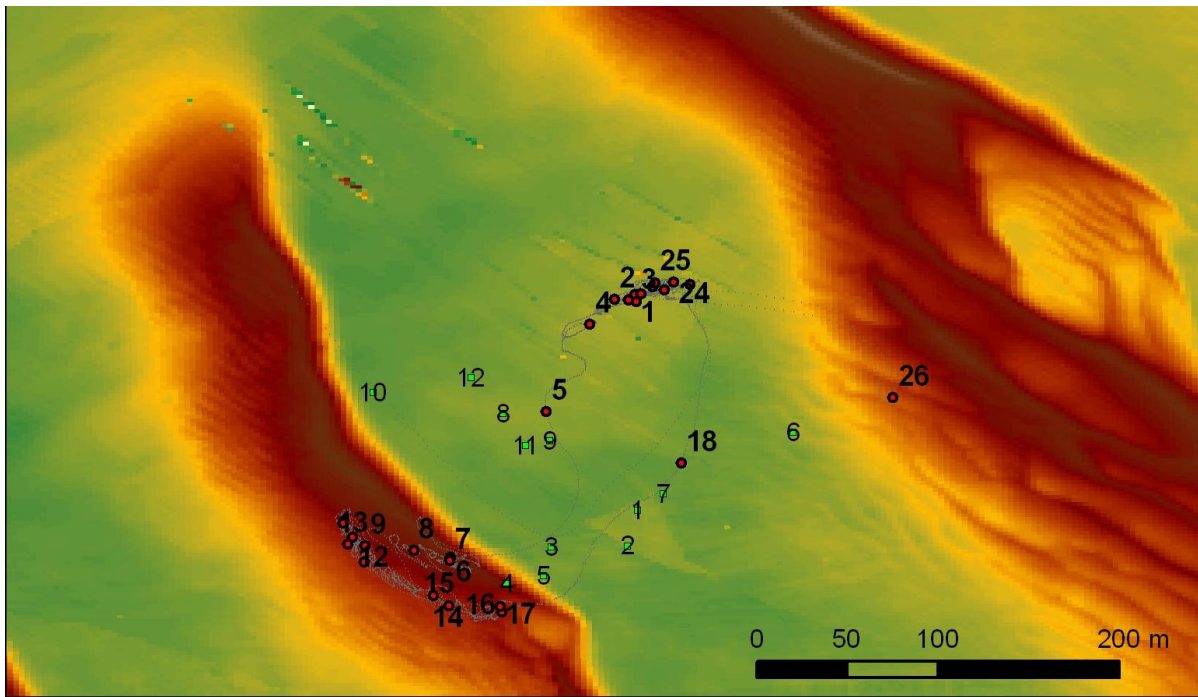


Figure 4. Position of the Hamon grabs (green dot) and water samples (red dot and bold).

Table 3. Water samples taken with the Seacat SBE19-10I. Seacat was mounted with a LISST. Meanwhile ADCP data were acquired. Positions corrected for an antenna layback of 12 m and an offset of 7 m.

id	Timestamp	Eadepth 33 kHz	Eadepth 38 kHz	Eadepth 210 kHz	Eabscat 33 kHz	wgs84_nbd	wgs84_old	sept_taw
1	2014-07-01 17:11:00	-34.50	-34.41	-34.44	-9	51.41286227	2.52785797	1.67
2	2014-07-01 17:31:20	-34.26	-34.18	-34.11	-12	51.41283875	2.52775523	-0.36
3	2014-07-01 18:01:40	-33.77	-33.69	-33.64	-18	51.41282807	2.52786332	-0.48
4	2014-07-01 18:31:20	0.00	-33.38	-33.36	0	51.41271528	2.52763317	-1.21
5	2014-07-01 19:00:00	-33.24	-33.21	-33.20	-7	51.41228243	2.52741597	-1.89
6	2014-07-01 19:30:00	-27.88	-29.24	-27.69	-27	51.41156082	2.52694320	-1.66
7	2014-07-01 20:02:10	-27.41	-27.45	NA	-25	51.41154403	2.52693837	-1.97
8	2014-07-01 20:32:00	-27.77	-27.86	NA	-13	51.41159402	2.52675883	-2.01
9	2014-07-01 21:07:10	-28.17	-28.02	NA	-5	51.41161767	2.52651672	-2.52
10	2014-07-01 21:31:50	-28.37	-28.32	NA	-18	51.41153628	2.52651520	-2.33
11	2014-07-01 22:00:10	-27.93	-27.76	NA	-9	51.41172855	2.52640863	-1.19
12	2014-07-01 22:30:10	-28.33	-28.20	NA	-14	51.41166013	2.52645595	-1.49
13	2014-07-01 23:00:40	-28.87	-28.68	NA	-12	51.41162643	2.52643433	-1.76
14	2014-07-01 23:31:00	-29.24	-29.42	NA	-17	51.41136997	2.52685522	-1.75
15	2014-07-02 00:00:10	-29.72	-29.68	NA	-21	51.41132317	2.52693608	-0.92
16	2014-07-02 00:30:40	-30.58	-30.57	NA	-10	51.41128858	2.52719777	-1.92
17	2014-07-02 01:02:00	-30.90	-31.12	NA	-14	51.41131745	2.52719015	-0.93
18	2014-07-02 01:30:40	NA	-35.51	-35.26	NA	51.41202635	2.52808737	1.26
19	2014-07-02 02:01:40	NA	-35.39	-35.35	NA	51.41283328	2.52782390	1.17
20	2014-07-02 02:30:00	-35.79	-35.71	-35.69	-6	51.41286595	2.52788773	1.19
21	2014-07-02 03:00:50	-35.89	-35.67	-35.62	-10	51.41288618	2.52800420	1.14
22	2014-07-02 03:31:00	-35.83	-35.69	-35.64	-15	51.41290130	2.52794393	1.13
23	2014-07-02 03:59:50	-35.55	-35.38	-35.35	-16	51.41291047	2.52812932	0.62
24	2014-07-02 04:31:40	-35.21	-35.19	-35.08	-7	51.41292190	2.52805023	1.10
25	2014-07-02 05:00:00	-35.02	-34.98	-34.87	-12	51.41292025	2.52795613	0.22
26	2014-07-02 05:30:10	-33.10	-33.18	-32.93	-10	51.41235022	2.52913945	0.11

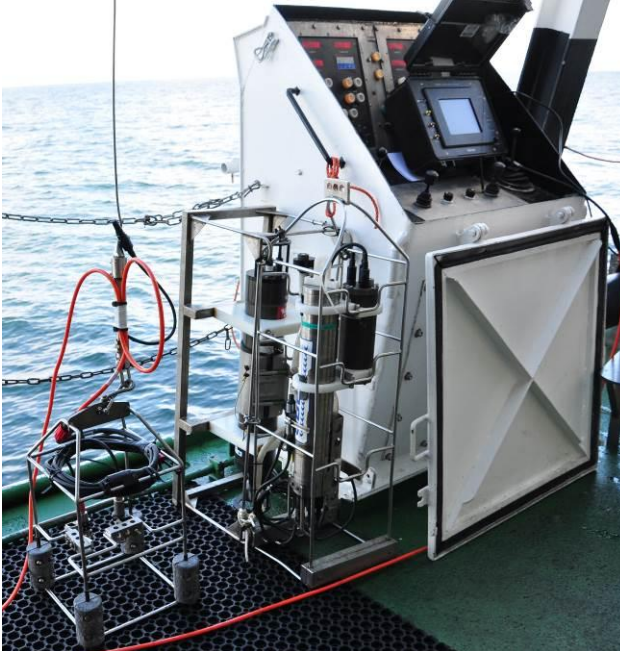
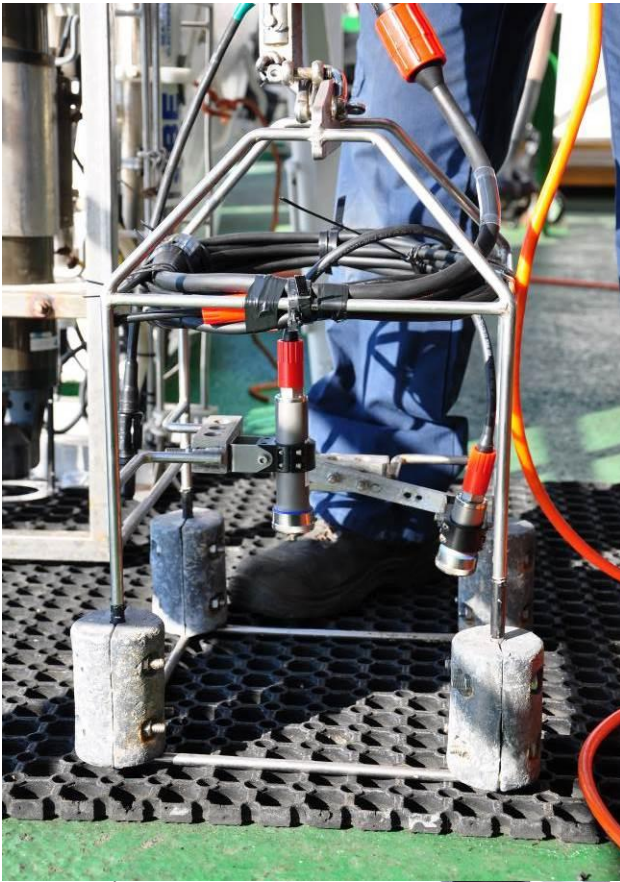


Figure 5. Visual observations: small video frame with real-time data visualisation (@VLIZ) and hand-held video imaging by divers (Scientific diving team RBINS OD Nature).

4.2. CSD-KD

- Cartography and 3D modeling of the sand reserves inside the extraction areas (collaboration with UGent): seismic profiles in extraction area 2 (Vlaamse Banken). Profiles will be recorded along decca (and parallel) lines.**

Equipment and seismic characteristics

Two seismic sources were used during the campaign: the Centipede and the SIG sparker 1200 (see Table 1). During the campaign only the latter was used due to a malfunctioning of the Centipede sparker.

Table 4. Characteristics of the equipment used during the survey.

Equipment	Frequency range	Vertical resolution	Penetration
Centipede sparker	1.1 – 1.2 kHz	> 35 cm	sandy sea bottom, up to 50 m
SIG sparker 1200	800 - 900 Hz	> 50 cm	sandy sea bottom, up to 100 m

Recorded network

The final recorded seismic network is over 160 km in total length. The weather conditions were very good during the recording and varied only slightly in wind velocity. The data quality is very high and has a very good resolution. The data covers two specific tidal sandbanks that cross the Belgian-French borderline, namely the Oostdyck and the Buiten Ratel (see figure 6). Of the seismic network four lines cover the longitudinal axis of the sandbank whilst all the majority of line (17) cover the transverse axis of the sand banks. This way an optimal coverage of the internal structure of the sand banks was achieved.

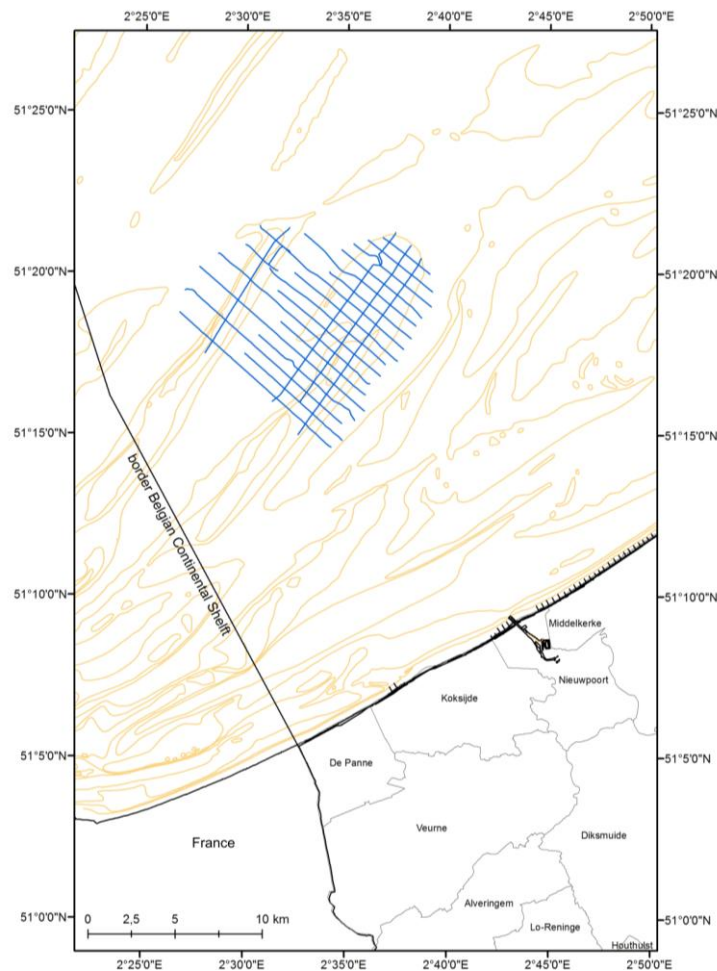


Figure 6. Seismic network on top of the sandbanks Oostdyck (left) and Buiten Ratel (right).

Table 5. Details on the seismic survey lines.

Time UTC	Shot nr	Latitude	Longitude	Water depth (m)	Vessel		Remarks
					Velocity (knots)	Heading (degrees)	
30/06/2014 - 01/07/2014							
19:41	777	51°20'57.18"	2°33'21.86"	29	3,6	130	SOL RG21_SIG
20:46	8560	51°18'19.07"	2°38'23.57"	25	4	130	EOL RG21_SIG
20:57	0	51°17'39.82"	2°37'42.48"	25,7	4	310	SOL RG20
22:25	0	51°20'08.02"	2°31'12.14"	21,42	3,8	145	EOL RG20_SIG SOL RG19_SIG
23:41	9080	51°07'09.23"	2°36'51.47"	26	3,7	145	EOLRG19_SIG
23:53	0	51°16'34.71"	2°36'01.31"	27	2,5	300	SOLRG18_SIG
1:59	15200	51°20'25,99"	2°28'33,65"	31,52	3,9	300	EOLRG18_SIG
2:19	0	51°20'09,98"	2°27'46,16"	31,13	4,32	130	SOLRG17_SIG
3:57	11700	51°15'43,56"	2°35'52,64"	28,77	4,17	130	EOLRG17_SIG

02/07/2014 - 03/07/2014							
							SOLRG23_CENT
							problems with centipeed, switch to SIG and CSP500, 300J
10:12	0	51°21'04.97"	2°36'48.62"	21,97	3,9	123	SOL RG23_SIG
10:39	3200	51°19'58.59"	2°39'06.72"	24	4,1	123	EOL RG23_SIG
10:52	0	51°20'24.48	2°38'35.19	23,4	5,2	198	SOL RL03_SIG
12:41	13100	51°14'55.49	2°32'34.08	11,28	3,19	200	EOL_RL03_SIG
12:00	0	51°14'36.91"	2°34'12.01"	26,37	3,78	295	SOL RG15_SIG
14:45	11800	51°18'45.20"	2°26'43.66"	32,45	4	295	EOL RG15_SIG
14:56	0	51°19'28.37"	2°27'05.39"	31,95	3,73	100	SOL RG16_SIG
16:47	12200	51°15'17.08"	2°34'53.45"	28	3,7	100	EOL RG16_SIG
16:52	0	51°14'54.17"	2°34'37.01"	27,16	4,43	305	SOL RG15_5_SIG
17:50	7200	51°17'29.32"	2°29'50.28"	30	4	305	EOL RG15_5_SIG
18:28	0	51°16'02.86"	2°31'23.40"	27	4	48	SOL RL05_SIG
							uitwijken voor schip voor anker
19:05	12900	51°21'16.70"	2°37'20.03"	24	4	48	EOL RL05_SIG
							cutting of sparker
20:39	0	51°20'52.18"	2°35'22.85"	24,8	3	126	SOL RG22_SIG
							uitwijken voor schip voor anker
21:29	6000	51°18'55.81"	2°39'10.29"	25,08	4	126	EOL RG22_SIG
21:36	0	51°18'37.40"	2°38'37.29"	24,99	4	320	SOL RG21_5_SIG
22:25	5800	51°20'43.99"	2°34'39.94"	30,46	4,1	330	EOL RG21_5_SIG
22:41	0	51°20'01.22"	2°34'07.96"	27,78	2,27	142	SOL RG20_5_SIG
23:40	7200	51°17'59.62"	2°38'08.11"	26,06	3,24	129	EOL RG20_5_SIG
23:53	0	51°17'17.37"	2°37'25.91"	26,28	4,59	308	SOL RG19_5_SIG
0:58	7730	51°20'03.55"	2°32'10.25"	30,69	3,24	300	EOL RG19_5_SIG
1:19	0	51°19'21.00"	2°31'49.00"	30,86	3,73	127	SOL RG18_5_SIG
2:20	7320	51°16'43.00"	2°36'41.00"	28,75	3,2	175	EOL RG18_5_SIG
2:38	0	51°16'15.00"	2°35'51.00"	28,4	4,2	305	SOL RG17_5_SIG
3:35	6970	51°18'29.00"	2°31'42.00"	32,3	1,9	308	EOL RG17_5_SIG
3:58	0	51°17'49.00"	2°31'07.00"	31,11	4,3	130	SOL RG16_5_SIG
							recording stopped at ping 171, redo line in other direction
5:00	0	51°15'24.00"	2°35'30.00"	27,01	4,3	330	SOL RG16_5_1SIG

6:00	7600	51°18'15.00"	2°30'22.00"	31,26	3,8	330	EOL RG16_5_1SIG
------	------	--------------	-------------	-------	-----	-----	-----------------

03/07/2014 - 04/07/2014							
15:09	0	51°20'51.30"	02°30'01.74"	31	4,05	120	SOL RG19_1
15:27	1400	51°20'04.07"	02°31'34.86"	31,9	4,4	140	EOL RG19_1
15:35	0	51°20'37.67"	02°32'08.86"	32,7	2,2	340	SOL RG20_1
16:02	2144	51°21'28.58"	02°30'40.69"	29,95	3,5	340	EOL RG20_1
16:14	0	51°21'23.68"	02°32'07.32"	19,12	1,84	215	SOL RL06
17:51	7700	51°17'29.00"	02°27'57.00"	10,92	3,5	213	EOL RL06
21:15	0	51°21'00.00"	02°36'03.51"	26	4,43	125	SOL RL22.5 300joule
21:54	4600	51°19'24.00"	02°39'17.00"	28,45	3,19	125	EOL RL22.5
22:19	0	51°20'50.08"	02°38'04.82"	22,7	4,6	215	SOL RL04
23:54	11400	51°15'58.82"	02°32'35.80"	12,98	3,6	215	EOL RL04

2. Multibeam surveying of monitoring areas on the Flemish Banks and Hinderbanken: BRMA, BRMC, HBMC (under reserve).

This subprogramme was not executed.

4.3. OD NATURE-MF (MOMO)

1) Recovering and deployment of tripod

The tripod deployed at MOW1 (51°N 21.595', 3°E 6.850') was recovered 04/07 and another one was deployed at the same location.

Table 6: Position and time of tripod recuperation/ deployment

ID	Instrument	Date (local time)	Lat_WGS84	Lon_WGS84
MOW1	Tripod recuperation	04/07 08h47	51°N 21.595'	3°E 6.850'
	Tripod +deployment		51°N 21.595'	3°E 6.850'

Before the recovery of the tripod: recuperation of an OBS5 frame at AW buoy (51°22.42'N 3°7.05'E) (OD Nature-MB) (4/7 08h15-08h30, local time) was conducted.

4.4. OD NATURE-JH (MONIWIND)

Replacement of a POD (Passive Acoustic Monitoring Devices) at the cardinal buoy of the following location:

Table 7: Position and time of POD recuperation/ deployment

ID	Instrument	Date (local time)	Lat_wgs84	Lon_wgs84
Gootebank	POD replacement	2014-06-30	51°N 26.953'	002°E 52.723'

7. REMARKS

- Officers and crew are thanked warmly for the skillful handling of the operations.
- Favourable weather conditions

8. DATA STORAGE

OD NATURE

- Multibeam echosounding: on hard disk OD NATURE-BRU; copy will be provided to BMDC. Contact person: Vera Van Lancker (130 km).
- ADCP: on hard disk MUMM-BRU; copy OD NATURE -OST. Contact person: Vera Van Lancker
- Water samples: Integration BMDC via MARCHEM (26 locations)
- Seabed samples; integration into BMDC. Contact person: Vera Van Lancker (12 Hamon grab samples; 6 diver samples)
- Tripod data. Contact person: Michael Fettweis

CSD/UG-RCMG

- Multibeam recordings (160 km): COPCO. Contact person: Koen Degrendele
- Seismics (160 km): UG-RCMG. Contact person: Tine Missiaen

Table A1: Oosthinder gravel area. Hamon grabs.

	
HG01. Gravel field near steep slope barchans dune	HG01 Gravel field near steep slope barchans dune
	
HG02 Gravel field near steep slope barchans dune	HG03 Steep slope barchan dune
	
HG04 Steep slope barchan dune	HG05 Steep slope barchan dune



HG07 Gravel field near steep slope barchan dune



HG07 Gravel field near steep slope barchan dune



HG08 Gravel field near steep slope barchan dune



HG08 Gravel field near steep slope barchan dune



HG09 Gravel field near steep slope barchan dune



HG10 Gravel field near steep slope barchan dune



HG11 Gravel field near steep slope barchan dune



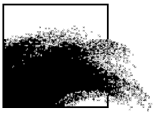
HG11 Gravel field near steep slope barchan dune



HG11 Gravel field near steep slope barchan dune



HG12 Gravel field near steep slope barchan dune



RV BELGICA CRUISE 2014/25

Subscriber:	Dr. Jan Vanaverbeke ¹ , Dr. Vera Van Lancker ²
Institute:	¹ Ghent University ² RBINS OD Nature
Address:	¹ UGent-SMB: Krijgslaan 281 S8, B-9000 Gent ² RBINS OD Nature: Gulledelle 100, B-1200 Brussels
Telephone:	+32 (0) 9 264 85 30 (JV); +32(0)2 7732129 (VVL)
E-mail:	jan.vanaverbeke@UGent.be ; v.vanlancker@mumm.ac.be ;

Ecosystems: 13-17/10/2014

1. Cruise details
2. List of participants
3. Scientific objectives
4. Operational course
5. Track plot
6. Measurements and sampling
7. Remarks
8. Data storage

Reference to this report:

Vanaverbeke, J. and Van Lancker, V. (2014). *Cruise report RV Belgica ST1425, 13-17/10/2014*. Ghent University, Marine Biology Research Group and Royal Belgian Institute of Natural Sciences, Management Unit of the North Sea Mathematical Models, 13p.

1. CRUISE DETAILS

1.	Cruise number	2014/25
2.	Date/time	Zeebrugge TD: 13/10/2014 at 10h45 Zeebrugge TA: 17/10/2014 at 13h22
3.	Chief Scientist Participating institutes	Dr. Jan Vanaverbeke UGent-SMB / MUMM
4.	Area of interest	Belgian part of the North Sea

2. LIST OF PARTICIPANTS

Institute	Participant	13/10-17/10	17/10
UGent	Jan VANAUVERBEKE (chief scientist)	X	X
	Guy DESMET	X	X
	Bart BEUSELINCK	X	X
	Niels VIAENE	X	X
	Liesbet COLSON	X	X
	REUBENS Jan	X	X
	Sebastiaan MESTDAGH	X	X
	Mohammed ALSEBAI	X	X
	Katherine BROWNLIE	X	X
			X
MUMM	Vera VAN LANCKER	X	
	Reinhilde VAN DEN BRANDEN	X	X
	TERSELEER LILLO Nathan		X
	Kevin HINDRYCKX		X
	Total	12	13

3. SCIENTIFIC OBJECTIVES

This cruise was made for the purpose of the Marine Biology Research Group of Ghent University and RBINS OD NATURE. The cruise collected samples to be used in UGent's FWO project "The functional role of marine macrobenthos for the functioning of the sea floor", the Fish Telemetry project, and the MONWIND project. The latter project aims at monitoring the effects of the installation of offshore windmill farms on the marine ecosystem. During this cruise, data were collected for the monitoring of the macrobenthos inhabiting soft sediments. MUMM's main activities related to the project ZAGRI and MOZ4. ZAGRI aims on the evaluation of the effects of the exploitation of non-living resources of the territorial sea and the continental shelf. MOZ4 focuses on the monitoring of hydrodynamics and sediment transport in a marine aggregate extraction zone, far offshore, and its impact on an adjacent Habitat Directive Area. Overall aim is to increase process and system knowledge of both areas, with particular focus on the compliancy of the extraction activities with respect to the European Marine Strategy Framework Directive

UGENT/SMB-JV: The functional role of marine macrobenthos for the functioning of the sea floor
Research within this project aims at (1) investigating the effect of soft sediment inhabiting key organisms on the functioning of the seafloor and the processes related to the benthic-pelagic coupling and (2) understanding the structural and functional link between the distribution of these key species and the ecological features of the seabed.

UGENT/SMB-JV: MONWIND / Benthos of soft substrates

This part of MONWIND aims at assessing the possible effects of the installation of wind mill farms on the macrobenthos from soft sediments, both at a large scale as on a very detailed scale in the immediate vicinity of a wind mill. During this cruise, samples for the large-scale assessment were collected.

UGENT/SMB-JR: Fish telemetry.

This project collects information on migration routes, spatiotemporal habitat use and fish behaviour by setting up an acoustic telemetry network.

OD NATURE-VVL: ZAGRI/MOZ4

ZAGRI is a continuous research program on the evaluation of the effects of the exploitation of non-living resources of the territorial sea and the continental shelf. MOZ4 focuses on the monitoring of hydrodynamics and sediment transport in relation to marine aggregate extraction in a far offshore zone. Overall aim is to increase process and system knowledge of this area, with a particular focus on the compliancy of the extraction activities with respect to the European Marine Strategy Framework Directive. More specifically changes in seafloor integrity and hydrographic conditions will be assessed. An important parameter is the bottom shear stress, with knowledge needed on both natural and anthropogenically-induced variability. Results will be used for the validation of mathematical models, necessary for impact quantification.

OD-NATURE -AUMS

The AUMS (Autonomous Underway Measurement System) project is inspired by the success of similar systems deployed on various ships of opportunity in the framework of the European Union FerryBox project (www.ferrybox.org). The instrumentation will greatly enhance the continuous oceanographic measurements made by RV Belgica by taking advantage of the significant technological improvements since the design of the existing (salinity, temperature, fluorescence) systems. In particular, many new parameters can now be measured continuously including important ecosystem parameters such as nitrate, ammonia, silicate, dissolved oxygen and CO₂, turbidity, alkalinity and phytoplankton pigments. In addition, the new equipment allows automatic acquisition and preservation of water samples, rendering RV Belgica operations significantly more efficient by reducing onboard human resources. Data will be available in near real-time via MUMM's public web site and following quality control, from the Belgian Marine Data Centre.

4. OPERATIONAL COURSE

All times are given in local time (UTC-2). All coordinates in WGS84.

Monday 13 October

09.00: arrival and boarding of UGent and RBINS OD Nature teams. Jellyfish observation at harbour.

10.45: Departure of RV Belgica

12.00-13.50: **Gootebank**: Samples (3 replicate Van Veen samples) were collected at 4 stations. Jellyfish observation

16.15-18.15: **Station 115**. CTD, Van Veen sampling (5 replicates), Reineck boxcorer (3 replicates), beam trawl, hyperbenthic sledge. Meanwhile, receiver locations "Golfmeter Nieuwpoort" and "D1" were visited by RHIB for collection of telemetry data.

19h10-19.50: **Station 120**. Van Veen sampling (5 replicates), Reineck boxcorer (3 replicates)

21.15-21.45: **Station 790**. Van Veen sampling (5 replicates), Reineck boxcorer (3 replicates)

23.45-00.03: **Station 701**. Van Veen sampling (5 replicates), Reineck boxcorer (3 replicates)

Transit to Vlakte van de Raan for ADCP profiling (ODN-VVL)

Tuesday 14 October

01.35-07.37: **ADCP profiling** (1m bin size) up-and-down the deltafront of the Vlakte van de Raan. Every 30' a water sample was taken from the seawater pump and filtered for suspended particulate matter (SPM).

08.05-08.15: **Station 780** CTD sampling. Further sampling at this location was postponed due to heavy weather. Belgica returned to more nearshore locations in order to complete sampling on coastal stations.

09.15-10.15: **Station 701**. CTD, hyperbenthic sledge, beam trawl. Due to the presence of a large object on the sea floor, the beam trawl was destroyed and needed to be replaced.

12.25-13.27: **Station 790**. CTD, hyperbenthic sledge, beam trawl.

15.10-16.30: **Station 215**. . CTD, Van Veen sampling (5 replicates), Reineck boxcorer (3 replicates), beam trawl, hyperbenthic sledge.

Transit to Oosthinder sandbank, eastern slope, for a 13-hrs cycle (ODN-VVL)

18.14- : Anchoring near 51°30,577'; 002° 37,800'E (ADCP-Impact), eastern slope of the Oosthinder sandbank. **13-hrs water column characterization** using the Seacat with CTD, OBS (Seapoint), LISST100 instrumentation and a 10l Niskin bottle for water sampling (every 30' filtration SPM; every 1h POC and salinity). Sampling depth: ±3-4 m above the bottom. Use of centrifuge purifier throughout the measurements (18h30-07h30).

Wednesday 15 October

-07.51: End of 13-hrs cycle

Transit to Thornton Bank (UG-JV)

08.40-16.23: **Thornton Bank**. Van Veen sampling at 20 locations (3 Van Veen's per station)

18.00-19.00: RHIB transport to receiver location 'Birkenfels'

Transit to Oosthinder sandbank, western slope, for a 13-hrs cycle (ODN-VVL)

19.15- : Anchoring near position 51°32.801'N, 002°37.998'E (Core 7, ST1407), western slope of the Oosthinder sandbank. **13-hrs water column characterization** using the Seacat with CTD, OBS (Seapoint), LISST100 instrumentation and a 10l Niskin bottle for water sampling (every 30' filtration SPM; every 1h POC and salinity). Sampling depth: ±2-3 m above the bottom. Use of centrifuge purifier throughout the measurements (19h15-09h00).

Thursday 16 October

-08.53: End of 13-hrs cycle

Transit to Bligh Bank (UG-JV)

10.05-18.40: **Bligh Bank**. Van Veen sampling at 23 locations (3 Van Veens per station). Addition Hamon Grab samples were collected at station BB22, BBC07, BBI33 and a new location at the eastern side of the sandbank.

20.20-21.15: **Station 330**. Van Veen (5 replicates), Reineck boxcorer (3 replicates)

Transit to south Oosthinder sandbank (Habitat Directive Area) for multibeam mapping (ODN-VVL)

22.11: Start full-coverage **multibeam echosounding** (depth and backscatter) along the barchan dune area of the Oosthinder sandbank (Kongsberg-Simrad EM3002; (HD EQUIDST; 75°/25°; +/- 8 kt; ADCP OFF)).

Friday 17 October

-05.20: End of multibeam echosounding.

Transit to Vlakte van de Raan (UG-JV)

07.15-07.45. **Station 780**. Reineck boxcorer (3 replicates), Van Veen sampling (5 replicates).

08.03-08.14: RHIB visit to receiver location 'S4'.

09.35: Touch and Go Zeebrugge. Embarkation of tripod and OD Nature personnel. Disemberkation of Vera Van Lancker.

10.35. Departure Zeebrugge

10.45-11.30: **MOW1**: recovery and deployment tripod.

13.20: arrival Zeebrugge, end of campaign.

5. TRACK PLOT

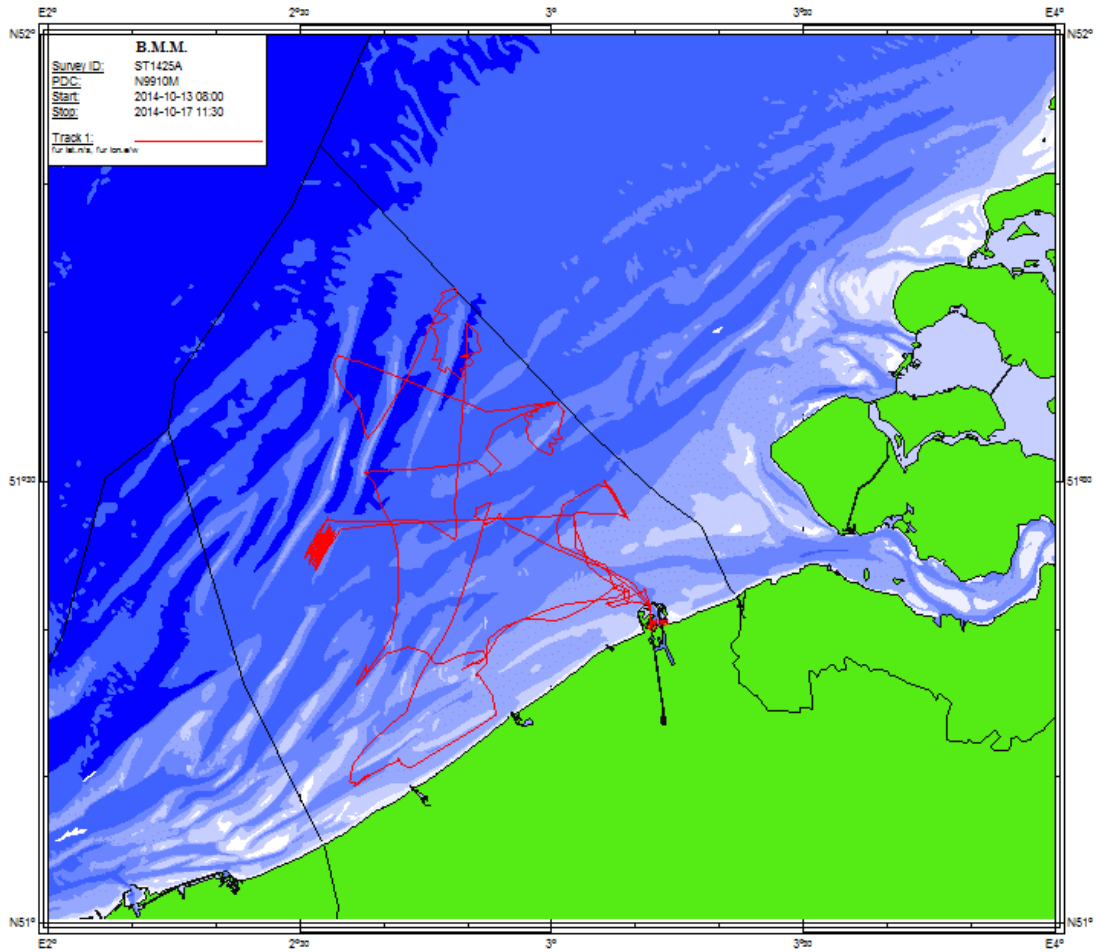


Fig 5.1: Track plot of campaign 2014/25

6. MEASUREMENTS AND SAMPLING

6.1. UGENT-JV: FUNCTIONAL ROLE MACROBENTHOS

Methodology

The operations for the UGent team included sampling of the fixed stations mentioned above and collecting macrobenthos samples at the monitoring stations. All fixed stations on the Belgian Part of the North Sea were sampled for meiobenthos, macrobenthos, hyperbenthos and epibenthos.

Meiobenthos was sampled by means of a Reineck boxcorer.

Every time, the corer was deployed three times in order to get true replicates. At all stations, two perspex cores (10 cm²) were used to subsample the Reineck boxcorer. One core was fixed in a 4% formaldehyde tap water solution and will be used for meiobenthic studies. The sediment from the other core was dried in the oven and will serve to establish sediment characteristics.

Macrobenthos was sampled using a Van Veen grab. Out of each grab, some sediment was collected for sediment characterisation. On all stations, five replicates were taken. The sediment was sieved on board of the Belgica over a 1-mm sieve. At St. 330, extra Van Veen grabs served a planned experiment in which seawater exchange between the water column and the permeable sediments will be measured over a mimicked tidal cycle.

Epibenthos was sampled with a three-meter beam trawl with a mesh size of 5 mm (10 mm stretched) in the cod end. All tows were made over a distance of 1000 m in the direction of the current with a towing speed of 1.5 knots per hour.

Hyperbenthos was sampled with a hyperbenthic sledge containing four nets: two nets with 0.5-mm mesh and two with 1.0-mm mesh. The lower nets sample the lower 0.5 m of the water column while the upper nets sample the water column between 0.5 and 1 m above the bottom. All tows were made against the current at a speed of 1.5 knot per hour.

Monitoring stations for soft sediment macrobenthos were only sampled with the Van Veen Grab. Again, 5 replicates per station were collected, and sediment was sieved on board over a 1 mm-sieve

Stations

Samples for the FWO project were planned to be collected at fixed locations on the Belgian Part of the North Sea.

Sampled locations include:

Table 6.1.1 Location of sampled stations.

780	51° 27.70	03° 02.60
790	51° 16.87	02° 51.13
115	51° 09.350	02° 36.350
215	51° 16.20	02° 36.76
330	51° 26.037	02° 48.486
120	51° 11.10	02° 42.07

6.2. UGENT-JV: MONWIND

Methodology

See 6.1

Stations

Samples for the MONWIND project were collected at the Gootebank, Thornton Bank and Bligh Bank.

Table 6.2.2 Sampling locations at Bligh Bank

Bligh Bank - Belwind									
	Samples	Latitude	Longitude	North WGS	East WGS		Latitude	Longitude	
1	BBI02	51.655106	2.7730616	5722703.67	484301.12		51° 39.306	2° 46.384	5xVV
2	BBI05	51.684861	2.791611	5726009.1	485593.75		51° 41.092	2° 47.497	5xVV
3	BBI26	51.639578	2.8187704	5720967.85	487458.83		51° 38.374	2° 49.126	5xVV
4	BBI33	51.666024	2.8512395	5723903.97	489711.69		51° 39.961	2° 51.074	5xVV
5	BBE09	51.653214	2.8545808	5722478.82	489939.94		51° 39.193	2° 51.275	5xVV
6	BBE06	51.639543	2.8371367	5720960.98	488729.77		51° 38.373	2° 50.228	5xVV
7	BBE05	51.625775	2.8180737	5719432.88	487406.79		51° 37.547	2° 49.084	5xVV
8	BBE14	51.706222	2.784802	5728386.07	485130.04		51° 42.373	2° 47.088	5xVV
9	BBE12	51.68862	2.7744012	5726430.67	484405.3		51° 41.317	2° 46.464	5xVV
10	BBE16	51.671145	2.7661829	5724488.92	483830.99		51° 40.269	2° 45.971	5xVV
11	BBC01	51.674729	2.758216	5724889.33	483281.38		51° 40.484	2° 45.493	5xVV
12	BBC02	51.69194	2.767305	5726801.43	483915.95		51° 41.516	2° 46.038	5xVV
13	BBC03	51.709924	2.777361	5728799.39	484617.13		51° 42.595	2° 46.641	5xVV
14	BBC04	51.61909	2.824985	5718688.2	487883.42		51° 37.145	2° 49.499	5xVV
15	BBC05	51.633346	2.844077	5720270.7	489208.57		51° 38.001	2° 50.645	5xVV
16	BBC06	51.646999	2.860551	5721786.83	490351.64		51° 38.820	2° 51.633	5xVV
17	BBE19	51.643853	2.768525	5721453.11	483983.33		51° 38.631	2° 46.111	5xVV
18	BBE20	51.637251	2.781047	5720716.19	484847.58		51° 38.235	2° 46.863	5xVV
19	BBE21	51.629738	2.793114	5719878.19	485680.29		51° 37.784	2° 47.587	5xVV
20	BBC07	51.635429	2.763744	5720517.28	483649.48		51° 38.126	2° 45.825	5xVV
21	BBC08	51.628599	2.775811	5719755.05	484482.27		51° 37.716	2° 46.549	5xVV
22	BBC09	51.621086	2.786739	5718917.22	485236.24		51° 37.265	2° 47.204	5xVV
23	BBE22	51.709344	2.813136	5728727.95	487088.77		51° 42.561	2° 48.788	5xVV
Total numbers of samples									115

Table 6.2.3 Sampling locations at Thornton Bank

Thorntonbank – C-Power									
	Samples	Latitude	Longitude	North WGS	East WGS		Latitude	Longitude	
1	TBE05	51.5486204	2.9524304	5710837.5	496701.58		51° 32.917	2° 57.146	5xVV
2	TBE14	51.543939	2.959807	5710316.55	497212.78		51° 32.636	2° 57.588	5xVV
3	TBE15	51.5875910	3.0088560	5715170.56	500613.54		51° 35.255	3° 0.531	5xVV
4	TBE16	51.5779660	3.0244030	5714100.37	501690.99		51° 34.678	3° 1.464	5xVV
5	TBE06	51.5435374	2.9930165	5710271.15	499515.72		51° 32.612	2° 59.581	5xVV
6	TBE07	51.5489043	3.0020033	5710868	500138.91		51° 32.934	3° 0.120	5xVV
7	TBE08	51.5537713	3.0121983	5711409.35	500845.72		51° 33.226	3° 0.732	5xVV
8	TBE10	51.5657709	2.9532999	5712744.84	496763.09		51° 33.946	2° 57.198	5xVV
9	TBE11	51.5713212	2.9644317	5713361.68	497534.96		51° 34.279	2° 57.866	5xVV
10	TBE12	51.5772048	2.9706467	5714015.83	497965.95		51° 34.632	2° 58.239	5xVV
11	TBEC01	51.5365510	3.0022860	5709494.14	500158.55		51° 32.193	3° 0.137	5xVV
12	TBEC02	51.5430130	3.0109010	5710212.86	500755.96		51° 32.581	3° 0.654	5xVV
13	TBEC03	51.5478360	3.0199790	5710749.38	501385.34		51° 32.870	3° 1.199	5xVV
14	TBEC04	51.5710110	2.9469410	5713327.92	496322.76		51° 34.261	2° 56.816	5xVV
15	TBEC05	51.5771790	2.9574920	5714013.41	497054.39		51° 34.631	2° 57.450	5xVV

16	TBEC06	51.5838340	2.9647960	5714753.28	497560.88	51° 35.030	2° 57.888	5xVV
17	TBC01	51.5066849	2.8768615	5706179.8	491453.87	51° 30.401	2° 52.612	5xVV
18	TBC06	51.5199189	2.8965500	5707649.49	492822.38	51° 31.195	2° 53.793	5xVV
19	TBC10	51.5228517	2.8503055	5707981.21	489614.49	51° 31.371	2° 51.018	5xVV
20	TBC12	51.5301357	2.8803159	5708787.46	491697.88	51° 31.808	2° 52.819	5xVV
Total numbers of samples								100

Table 6.2.4 Sampling Locations at the Gootebank

Goote Bank – Reference area								
	Samples	Latitude	Longitude	North WGS	East WGS	Latitude	Longitude	
1	GBC06	51.4697949	2.8498133	5702080.66	489568.24	51° 28.188	2° 50.989	5xVV
2	GBC07	51.4754565	2.8698290	5702707.64	490959.62	51° 28.527	2° 52.190	5xVV
3	GBC21	51.4532919	2.8697684	5700242.67	490951.03	51° 27.198	2° 52.186	5xVV
4	GBC24	51.4630499	2.8971875	5701324.85	492857.73	51° 27.783	2° 53.831	5xVV
Total number of samples								20

6.3 OD Nature-JR: Fish telemetry

The Rhib was used to drive to the mooring (i.e. bouys).

Once we were at the bouy, the mooring chain was released. All equipment was taken onboard and processing was done in the Rhib.

The receivers were cleaned, data offloaded and if needed the mooring repaired. When all work was finished, the mooring was re-installed on the buoy. Total workload near the buoy is approx. 10-15min.

Visited locations include:

Table 6.3.1 visited receiver locations

Location	Latitude	Longitude	Coordinates
Golfmeter Nieuwpoort	51.160167	2.691833333	51° 09.61 N 002° 41.51 E
D 1	51.232500	2.643166667	51° 13.95 N 002° 38.59 E
S 4	51.417167	3.0475	51° 25.03 N 003° 02.85 E
Birkenfels	51.649333	2.533833333	51° 29.12 N 002° 17.92 E

6.4 OD Nature-VVL: ZAGRI/MOZ4

1. Hydrodynamic and sediment transport related measurements and observations were made in marine aggregate concession zone 4, Hinder Banks region and adjacent Habitat Directive Area 'Flemish Banks'.
 - a. Two 13-hrs water column characterization (every 30') time series were obtained using the Seacat frame mounted with CTD, OBS (Seapoint), LISST100 instrumentation and a 10l Niskin bottle for water sampling (filtration SPM (filtration 1.5 l), POC (0,250 l), salinity) (Table 6.4.1). Meanwhile the centrifuge purifier was used to collect suspended particulate matter in the water column;
 - b. Full-coverage multibeam echosounding (Kongsberg-Simrad EM3002) was performed in the Habitat Directive Area (Table 6.4.2).
 - c. AUMS registrations (continuous)

Table 6.4.1: Location 13-hrs cycles

East slope Oosthinder sandbank	51°30,577'N	002° 37,800'E
West slope Oosthinder sandbank	51°32.801'N	002°37.998'E

Table 6.4.2: Timestamp and parameters water samples (SBE19-L-10), East slope Oosthinder sandbank.

id	id_short	Timestamp	Volume (l)	POC (250ml)	Salinity	eadepth210	eadepth33	wgs84_nbd	wgs84_old
4c_E_01	1	2014-10-14 16:26:50.00	1.5			-30.59	-30.81	51.510488	2.632090
4c_E_02	2	2014-10-14 17:01:00.00	1.5	X	X	-29.61	-29.72	51.510629	2.631942
4c_E_03	3	2014-10-14 17:28:20.00	1.5			-29.18	-29.34	51.510685	2.631874
4c_E_04	4	2014-10-14 17:58:50.00	1.5	X	X	-29.98	-30.36	51.510596	2.632028
4c_E_05	5	2014-10-14 18:28:50.00	1.5			-29.05	-29.18	51.510603	2.632012
4c_E_06	6	2014-10-14 19:00:10.00	1.5	X	X	-28.58	-28.26	51.510626	2.631969
4c_E_07	7	2014-10-14 19:29:40.00	1.5			-28.47	0.00	51.510569	2.632052
4c_E_08	8	2014-10-14 20:00:10.00	1.5	X	X	-28.88	0.00	51.510391	2.632200
4c_E_09	9	2014-10-14 20:29:30.00	1.5			-28.45	-28.61	51.510377	2.632150
4c_E_10	10	2014-10-14 21:00:30.00	1.5	X	X	-28.37	-28.86	51.510057	2.632285
4c_E_11	11	2014-10-14 21:30:00.00	1.5			-28.48	-28.69	51.510011	2.632210
4c_E_12	12	2014-10-14 22:00:50.00	1.5	X	X	-27.91	-28.09	51.509826	2.631805
4c_E_13	13	2014-10-14 22:29:30.00	1.5			-21.72	-22.03	51.510008	2.629608
4c_E_14	14	2014-10-14 23:00:10.00	1.5	X	X	-20.98	-21.77	51.509904	2.629565
4c_E_15	15	2014-10-14 23:30:30.00	1.5			-20.94	-21.19	51.510013	2.629566
4c_E_16	16	2014-10-15 00:00:10.00	1.5	X	X	-21.61	-21.76	51.509901	2.629544
4c_E_17	17	2014-10-15 00:30:10.00	1.5			-22.40	-22.56	51.509801	2.629580
4c_E_18	18	2014-10-15 01:00:00.00	1.5	X	X	-22.58	0.00	51.509813	2.629588
4c_E_19	19	2014-10-15 01:30:00.00	1.5			-23.44	-23.54	51.509737	2.629655
4c_E_20	20	2014-10-15 01:59:50.00	1.5	X	X	-24.15	-24.29	51.509733	2.629748
4c_E_21	21	2014-10-15 02:29:10.00	1.5			-26.19	0.00	51.509484	2.630425
4c_E_22	22	2014-10-15 02:59:20.00	1.5	X	X	-28.21	0.00	51.509728	2.631134
4c_E_23	23	2014-10-15 03:31:50.00	1.5			0.00	0.00	51.510137	2.631541
4c_E_24	24	2014-10-15 03:59:40.00	1.5	X	X	-29.22	-29.95	51.510363	2.631536
4c_E_25	25	2014-10-15 04:29:20.00	1.5			-28.67	-28.66	51.510540	2.631515
4c_E_26	26	2014-10-15 04:59:00.00	1.5	X	X	-29.50	-29.55	51.510541	2.631675
4c_E_27	27	2014-10-15 05:29:00.00	1.5			-28.00	-28.15	51.510596	2.631501

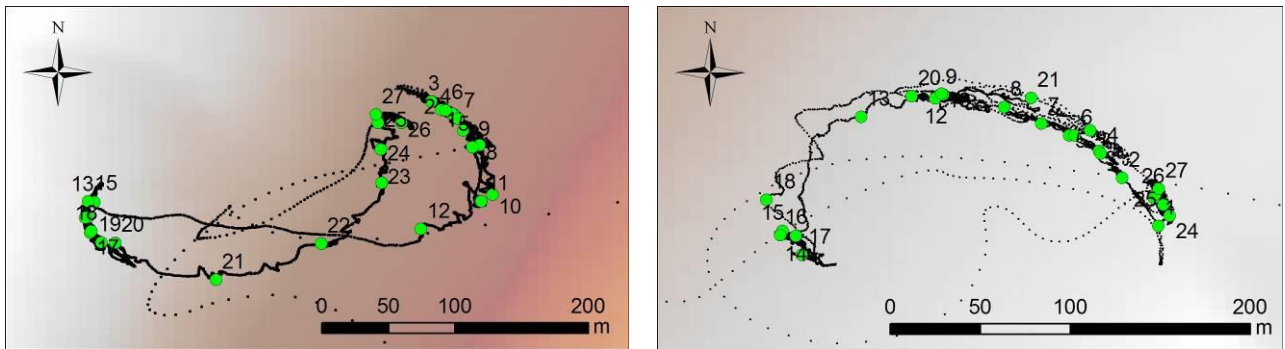


Figure 6.4.1: Left: RV Belgica track during 13-hrs cycle along eastern slope Oosthinder sandbank; Right: along western slope. Positions of the water samples are indicated.

Table 6.4.3: Timestamp and parameters water samples (SBE19-L-10), West slope Oosthinder sandbank.

id	id_short	Timestamp	Volume (l)	POC (250ml)	Salinity	eadepth210	eadepth33	wgs84_nbd	wgs84_old
4c_W_01	1	2014-10-15 17:29:10.00	1.5			-24.43	-24.61	51.547627	2.636352
4c_W_02	2	2014-10-15 17:59:20.00	1.5	X	X	-25.58	-24.90	51.547866	2.636173
4c_W_03	3	2014-10-15 18:29:40.00	1.5			-25.10	-25.27	51.548001	2.636056
4c_W_04	4	2014-10-15 18:59:40.00	1.5	X	X	-24.19	-24.31	51.547988	2.636066
4c_W_05	5	2014-10-15 19:29:50.00	1.5			-24.39	-24.59	51.548078	2.635907
4c_W_06	6	2014-10-15 19:59:00.00	1.5	X	X	-23.46	-23.55	51.548078	2.635936
4c_W_07	7	2014-10-15 20:29:30.00	1.5			-24.12	-24.21	51.548137	2.635770
4c_W_08	8	2014-10-15 20:58:50.00	1.5	X	X	-24.35	-24.07	51.548220	2.635584
4c_W_09	9	2014-10-15 21:30:10.00	1.5			-24.29	-24.33	51.548280	2.635262
4c_W_10	10	2014-10-15 22:00:00.00	1.5	X	X	-23.74	-23.85	51.548280	2.635269
4c_W_11	11	2014-10-15 22:30:30.00	1.5			-23.84	-24.09	51.548283	2.635281
4c_W_12	12	2014-10-15 23:00:20.00	1.5	X	X	-24.11	0.00	51.548263	2.635241
4c_W_13	13	2014-10-15 23:30:00.00	1.5			-23.99	-24.13	51.548170	2.634872
4c_W_14	14	2014-10-16 00:00:00.00	1.5	X	X	-24.08	-24.24	51.547578	2.634547
4c_W_15	15	2014-10-16 00:30:30.00	1.5			-23.90	-24.11	51.547603	2.634479
4c_W_16	16	2014-10-16 01:00:40.00	1.5	X	X	-24.06	-24.27	51.547581	2.634470
4c_W_17	17	2014-10-16 01:30:00.00	1.5			-24.34	-24.50	51.547484	2.634577
4c_W_18	18	2014-10-16 02:02:00.00	1.5	X	X	-25.39	-25.62	51.547758	2.634401
4c_W_19	19	2014-10-16 02:29:30.00	1.5			-25.19	-25.37	51.548286	2.635272
4c_W_20	20	2014-10-16 03:00:20.00	1.5	X	X	-25.58	0.00	51.548274	2.635124
4c_W_21	21	2014-10-16 03:31:50.00	1.5			-25.08	0.00	51.548265	2.635719
4c_W_22	22	2014-10-16 03:59:40.00	1.5	X	X	-24.82	0.00	51.548104	2.636012
4c_W_23	23	2014-10-16 04:30:20.00	1.5			-25.27	-24.90	51.547768	2.636330
4c_W_24	24	2014-10-16 04:59:40.00	1.5	X	X	-24.68		51.547678	2.636409
4c_W_25	25	2014-10-16 05:29:00.00	1.5			-24.54	-24.74	51.547732	2.636377
4c_W_26	26	2014-10-16 06:00:00.00	1.5	X	X	-25.16	-24.99	51.547784	2.636337
4c_W_27	27	2014-10-16 06:29:40.00	1.5			-23.79	-24.35	51.547812	2.636355

Table 6.4.4: Reference location for multibeam registration

Sample id	WGS84_NB	WGS84_OL
Area 2_ Refugium South	51°24.7333'	2°31.6333'

Table 6.4.5: Centrifuge samples

id	Timestamp1 (UTC)	Timestamp2 (UTC)	Time residual (h)	Start volume (l)	End volume (l)	Discharge (ls-1)	Remark
C1	2014-10-14 16:30	2014-10-15 05:30	13	2757840	2771618	0.29	4c, east slope (silt-sand!)
C2	2014-10-15 17:15	2014-10-16 07:00	13,75	2771618	2786312	0.30	4c, west slope (silt only)

2. Because of adverse weather conditions in the offshore area during the first 2 days of the campaign, an alternative research area was chosen for the measurements. In the continuation of previous measurements in the period 2006-2012, ADCP profiling (Hull-mounted ADCP RDI 300 kHz, 1 m bin size) was conducted along the deltafront of the Vlake van de Raan. Water sampling (seawater pump) and filtrations were carried out every 30 min (filtration of 0.5 to 0.750 l) (SPM only) (Table 6.4.6).

Table 6.4.6: ADCP track up and down the deltafront of the Vlake van de Raan. Water samples were taken from the seawater pump every 30' and were filtered for SPM.

ADCP track (+/-7km)			
X-Y	51°33.419 N	002°34.269 E	51°33.037 N 002°40.252 E

Table 6.4.7: Timestamp and parameters water samples (SBE19-L-10) Vlakte van de Raan.

id	id_short	Timestamp	Volume (l)	POC (250ml)	Salinity	eadepth210	eadepth33	wgs84_nbd	wgs84_old
VVR_01	1	2014-10-13 23:48:00.00	0.8			-15.86	-15.36	51.481328	3.125012
VVR_02	2	2014-10-14 00:30:00.00	0.75			-19.63	-19.48	51.492977	3.111499
VVR_03	3	2014-10-14 01:00:00.00	0.5			-12.45	-12.59	51.471139	3.135591
VVR_04	4	2014-10-14 01:30:00.00	0.75			-16.02	-16.19	51.479377	3.126729
VVR_05	5	2014-10-14 02:00:00.00	0.75			-16.63	-16.77	51.479483	3.129249
VVR_06	6	2014-10-14 02:30:00.00	0.75			-13.87	-14.00	51.469837	3.137660
VVR_07	7	2014-10-14 03:00:00.00	1			-19.18	-19.31	51.488799	3.121385
VVR_08	8	2014-10-14 03:30:00.00	0.75			-16.44	-15.33	51.465839	3.141623
VVR_09	9	2014-10-14 04:00:00.00	1			-23.24	-23.05	51.495109	3.111050
VVR_10	10	2014-10-14 04:30:00.00	0.75			-14.17	-14.32	51.457680	3.151201
VVR_11	11	2014-10-14 05:00:00.00	1			-25.56	-25.65	51.500178	3.106779
VVR_12	12	2014-10-14 05:30:00.00	0.75			-14.40	-14.70	51.459370	3.147029

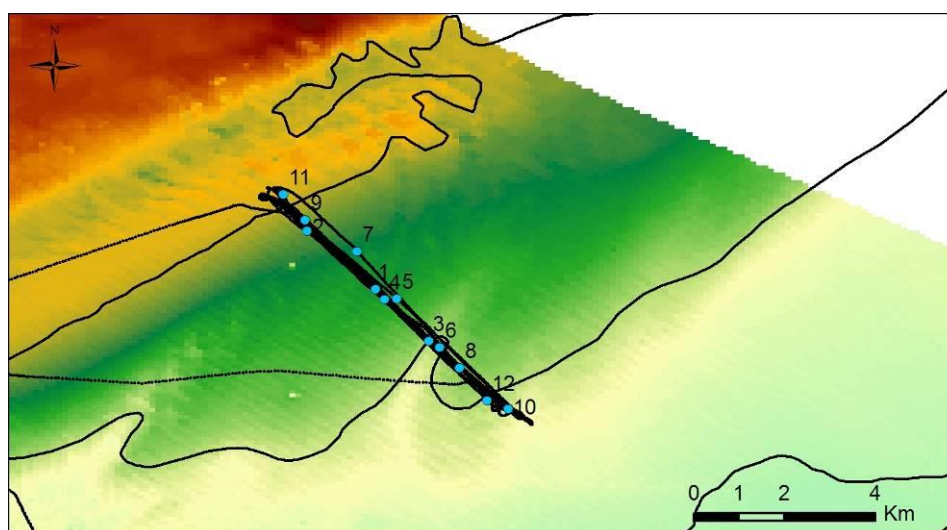


Figure 6.4.2: Left: RV Belgica track during 13-hrs cycle along Vlakte van de Raan. Positions of the water samples are indicated.

- Near the Bligh Bank, 3 hamon grabs were taken to evaluate the presence of mud within the coarse permeable sandy seabed.

Table 6.4.8: Position of the Hamon Grabs near the Bligh Bank (corrected for a lay-back of 32 m)

Sample id	Timestamp	WGS84_NB	WGS84_OL
BBE22	2014-10-16 08:21:40	51°42.545'N	2°48.774'E
BBC07	2014-10-16 12:03:52	51°38.128'N	2°45.756'E
BB_Gully East	2014-10-16 16:37:50	51°40.633'N	2°49.958'E

6.4. MUMM-AUMS

Throughout the campaign measurements were made with the AUMS system. At 2 locations water samples were taken with the in-built AUMS sampler (see above Table 6.4.2; 6.4.5). Water filtrations were carried out for the calibration of the turbidity sensor.

6.4. MUMM-MOMO

Recovering and deployment of tripod

Table 1: Position of the deployed/recovered tripods.

Station		Lat/Lon WGS 84	Deployment (GMT)	Recuperation (GMT)
MOW1	Tripod	51°N 21.640', 3°E 6.820'	09/09/2014 09h27	17/10/2014 10h57
MOW1	Tripod	51°N 21.602', 3°E 6.818'	17/10/2014 10h33	planned during 2014/28

7. REMARKS

We warmly acknowledge the skilful and patient help of the master and crew of the *RV Belgica*.

8. DATA STORAGE

OD NATURE

- Multibeam echosounding: on hard disk OD NATURE-BRU; copy will be provided to BMDC. Contact person: Vera Van Lancker (± 50.4 nm).
- ADCP: 1 data set on Vlakte van de Raan : on hard disk MUMM-BRU; copy OD NATURE -OST. Contact person: Vera Van Lancker (± 32.5 nm)
- Water samples: Integration BMDC via MARCHEM (39 samples)
- Seabed samples; integration into BMDC. Contact person: Vera Van Lancker (3 Hamon grab samples)
- Tripod data. Contact person: Michael Fettweis

UG-SMB

- CTD data: on hard disk UGent SMB (JV)
- Receiver data: on hard disk UGent SMB (JR)
- Biological data will be transferred to BMDC following the WinMon procedures

Annex B

Sediment sample analyses

This Annex forms part of the report:

Van Lancker, V., Baeye, M., Evangelinos, D. & Van den Eynde, D. (2015). Monitoring of the impact of the extraction of marine aggregates, in casu sand, in the zone of the Hinder Banks. Period 1/1 - 31/12 2014. Brussels, RBINS-OD Nature. Report <MOZ4-ZAGRI/I/VVL/201502/EN/SR01>, 74 pp. (+5 Annexes).

Annex B. Sediment sample analyses

Sediment samples from RV Belgica campaign ST1407 were analysed at the sedimentology laboratory at Ghent University, Department of Geology. The Msc student Dimitris Evangelinos performed the analyses under the supervision of Dr. Sébastien Bertrand.

B.1 Organic matter and carbonate content via Loss-On-Ignition (LOI)

All cores were analysed for total organic matter content (TOM %), as well as carbonate content by using the Loss-on-ignition method (Dean, 1974; Heiri et al., 2001). Four (4) grams of sediments from each slice of the ST1407 core samples were put in pre-weighed porcelain crucibles and dried in an oven at 105 °C for 17 h. The samples were subsequently placed in a desiccator for half an hour in order to reach room temperature and were weighed. In the next step, samples were placed in a muffle furnace at 550 °C for 4 h (Heiri et al., 2001). After cooling to room temperature in a desiccator, samples were weighed again. The difference between the weight of samples at 105 °C and 550 °C represents the amount of organic matter. The samples were then returned to the muffle furnace and heated at 1000 °C for 5 h. The weight difference between 550°C and 1000°C represents the amount of CO₂ evolved from carbonate minerals. The actual carbonate content of a sample is calculated as the weight of CO₂ lost between 550 °C and 1000 °C divided by 0.44, representing the mass fraction of CO₂ in calcium carbonate (CaCO₃). Three (3) replicates were taken from core 11, from the top layer (1 cm), to verify the accuracy of the method.

B.2 Particle-size distribution

The 1-cm sliced sediment samples from the ST1407 cores were analysed using a Malvern Mastersizer 3000 laser particle analyser. Prior to analysis, samples were sieved with a 2 mm stainless steel sieve, in order to separate the coarse fraction (>2 mm) of the sediment which cannot be analyzed by laser diffraction. Both the > 2 mm and < 2 mm fractions of the samples were dried in the oven overnight (70 °C). The dry samples were then cooled down and weighted. For each sample, a very small portion of the < 2 mm fraction of each sample was introduced in the Malvern Mastersizer. Sample quantity was adjusted to obtain obscuration values between 12 and 25 %. The results obtained by laser diffraction were then exported to an Excel spreadsheet and combined with the weight of the < 2 mm fraction to calculate the weight of each particle-size class. The weights of the > 2 mm and < 2 mm fractions were then merged and imported to Gradistat version 8.0 (Blott and Pye, 2001; <http://www.kpal.co.uk/gradistat.html>) to calculate the complete particle-size distribution (PSD) of each sample. Three (3) replicates were taken from core 13, from the top layer (1cm) to quantify the precision of the measurements.

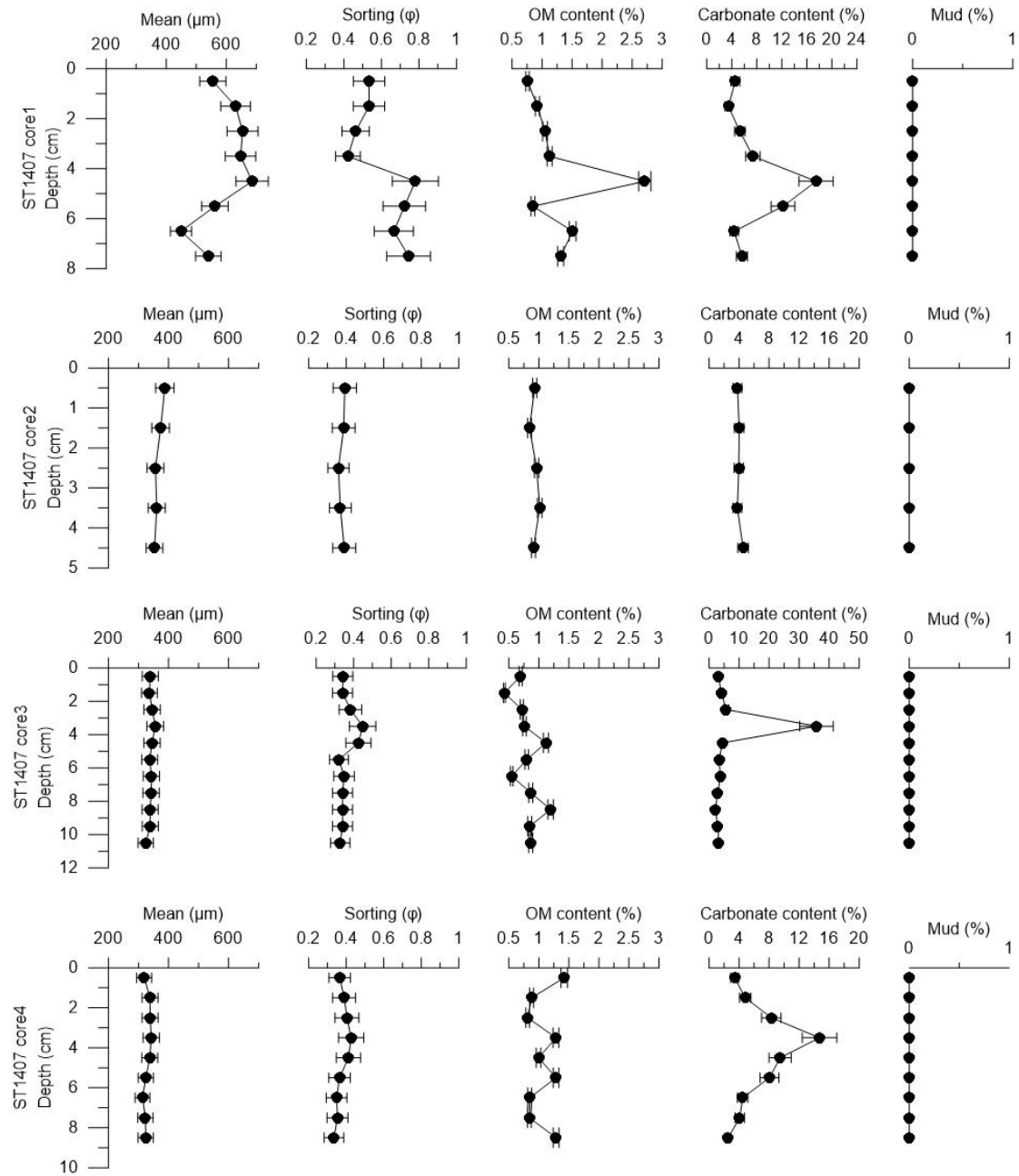
The three (3) Hamon grab samples of ST1407 were prepared following the same procedure, except that the < 2 mm fraction was freeze-dried instead of oven-dried. This method is preferred for samples containing significant amounts of clays and fine silts. Same procedure was followed for the very-fine sediment fractions collected from the bucket of water (7-1). First the sample was subsampled into 5 sets, which were then centrifuged (each time 10 min on 2400 rounds). All retained particles were gathered in one recipient for further particle-size analyses. The > 2 mm fractions of the 3 Hamon grab samples were analysed following the same procedure as for the core samples. An aliquot of each < 2 mm freeze-dried sample was then boiled with Calgon (Na Hexametaphosphate) to allow complete disaggregation of the particles before analysis.

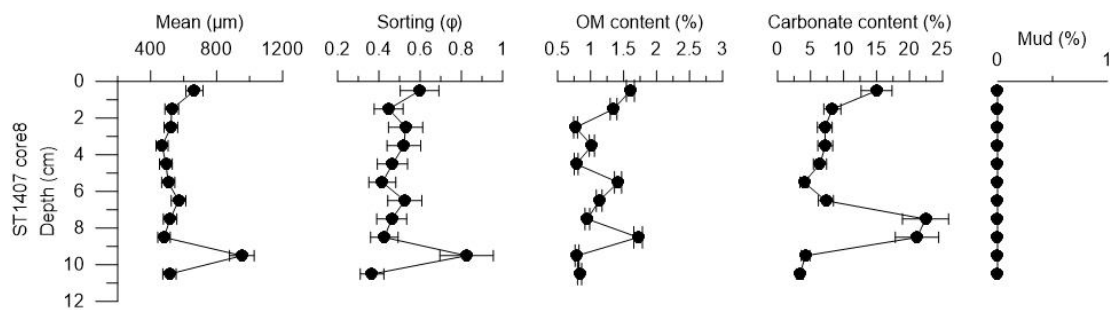
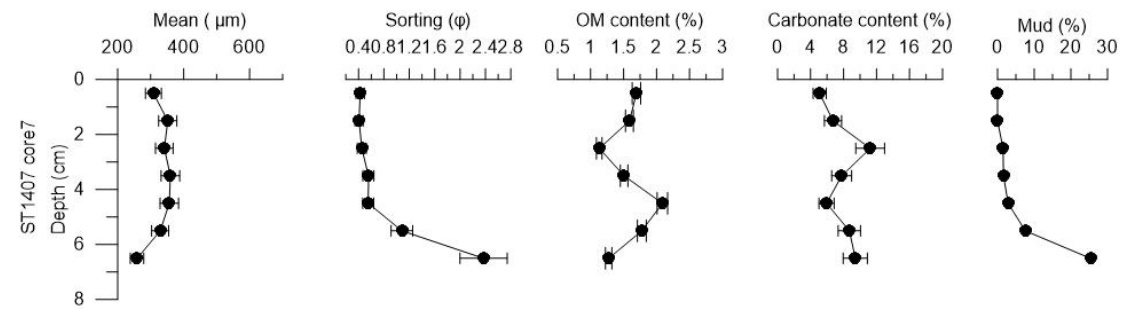
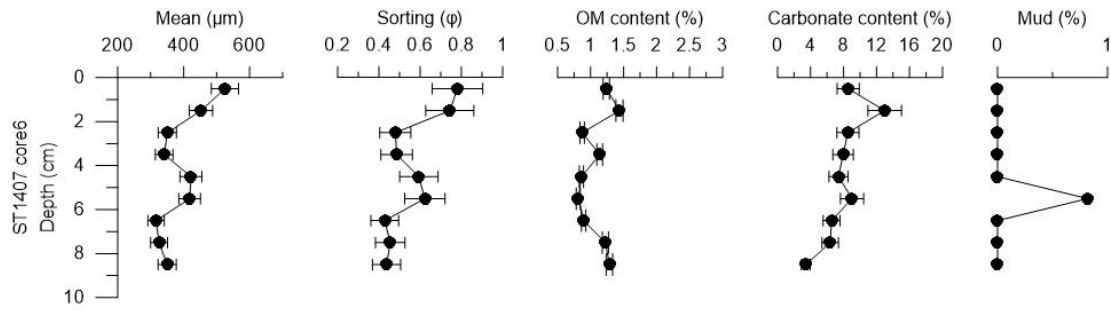
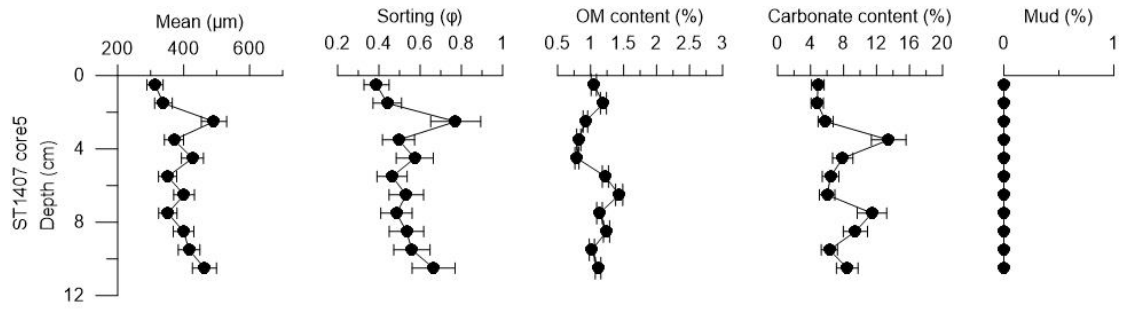
Blott, S.J. and Pye, K. (2001) GRADISTAT: a grain size distribution and statistics package for the analysis of unconsolidated sediments. *Earth Surface Processes and Landforms* 26, 1237-1248..

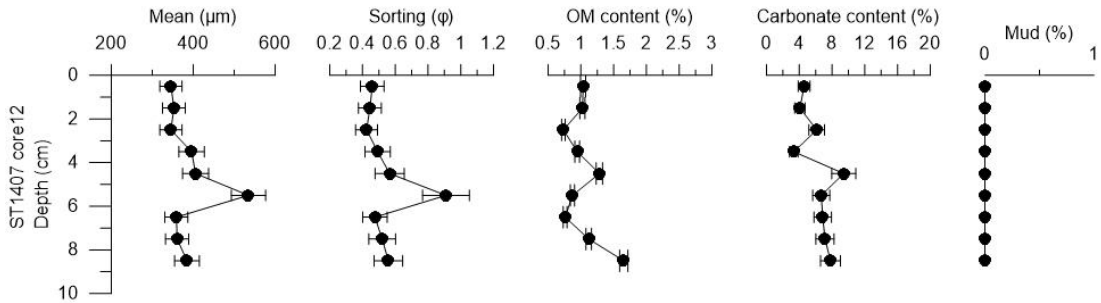
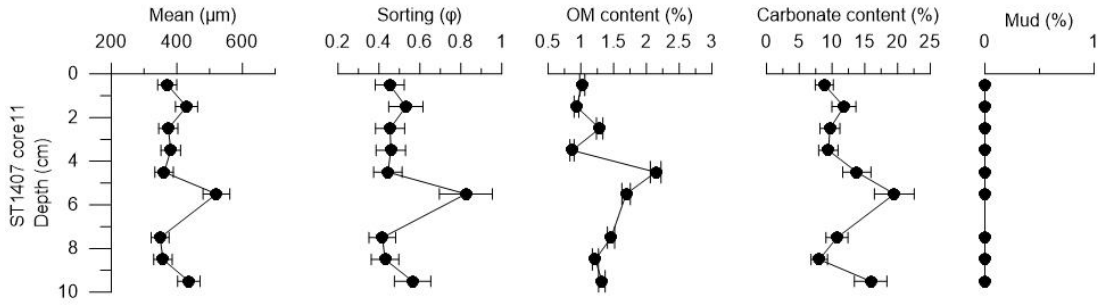
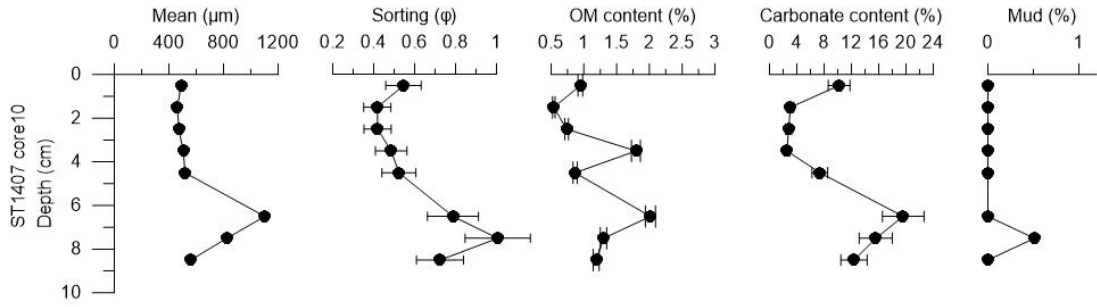
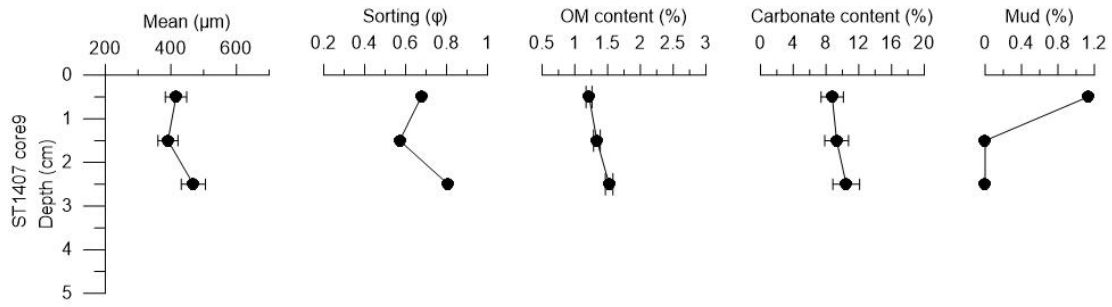
Dean, JR, Walter, E. (1974) Determination of carbonate and organic matter in calcareous sediments and sedimentary rocks by loss on ignition: Comparison with other methods. *Journal of Sedimentary Petrology* 44(1), 242-248.

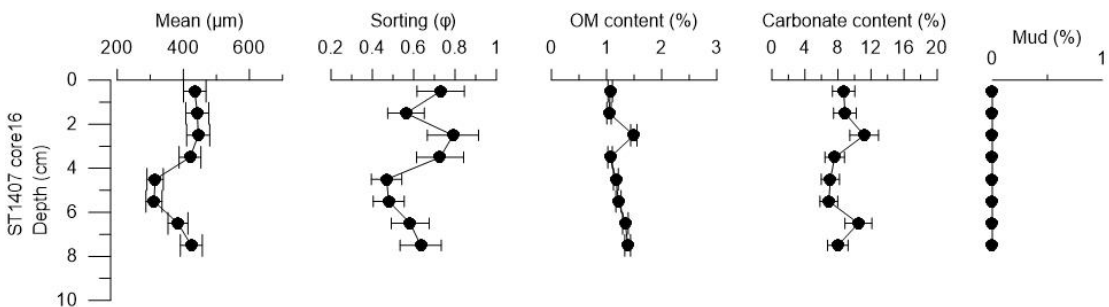
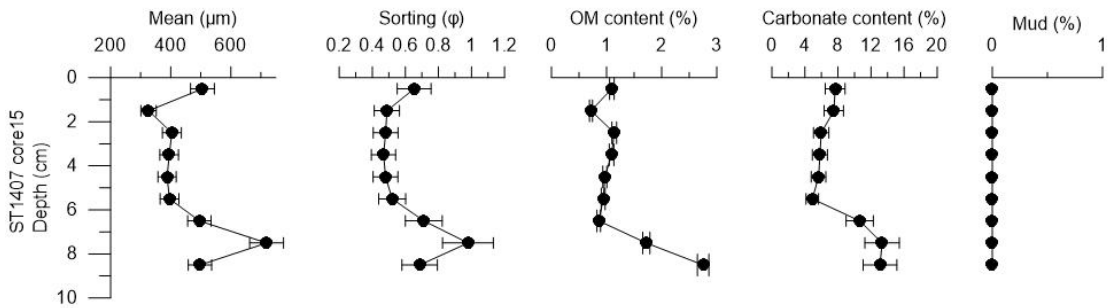
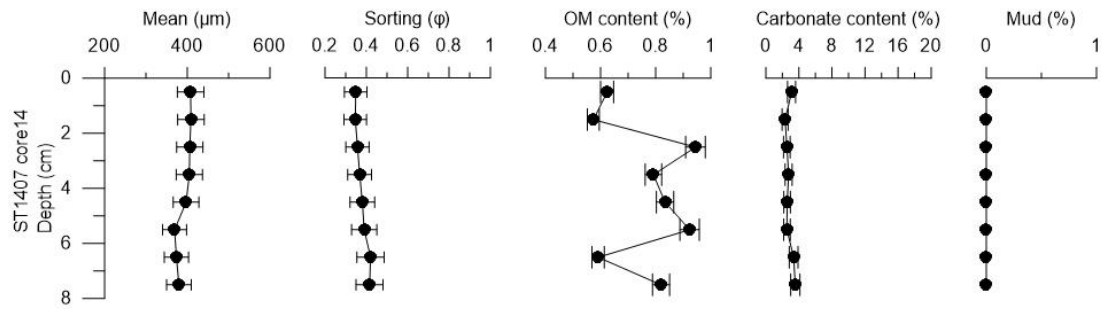
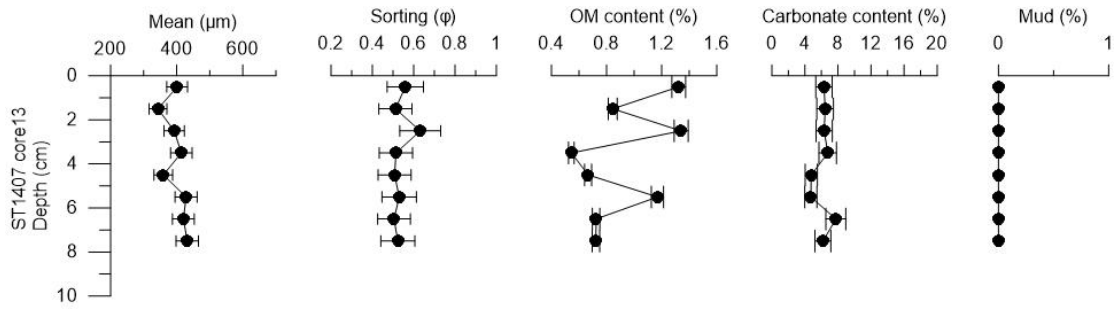
Heiri, O., Lotter, A. F. & Lemcke, G. (2001) Loss on ignition as a method for estimating organic and carbonate content in sediments: reproducibility and comparability of results. *Journal of Paleolimnology* 25: 101-110.

B.3 Particle-size analysis of the Reineck cores









Annex C

Bottom shear stress: calculations and modelling

This Annex forms part of the report:

Van Lancker, V., Baeye, M., Evangelinos, D. & Van den Eynde, D. (2015). Monitoring of the impact of the extraction of marine aggregates, in casu sand, in the zone of the Hinder Banks. Period 1/1 - 31/12 2014. Brussels, RBINS-OD Nature. Report <MOZ4-ZAGRI/I/VVL/201502/EN/SR01>, 74 pp. (+5 Annexes).

ROYAL BELGIAN INSTITUTE FOR NATURAL SCIENCES
OPERATIONAL DIRECTORATE NATURAL ENVIRONMENT

Section Ecosystem Data Analysis and Modelling
Suspended Matter and Sea Bottom Modelling and Monitoring Group



Measuring, using ADV and ADP sensors, and modelling bottom shear stresses in the Belgian coastal waters

Dries Van den Eynde

ZAGRI-MOZ4/1/DVDE/201502/EN/TR02

Prepared for ZAGRI and MOZ4 projects

RBINS-OD Nature
100 Gulledelle
B-1200 Brussels
Belgium

Table of Contents

1.	INTRODUCTION	3
2.	MEASUREMENTS OF THE BOTTOM SHEAR STRESS.....	4
2.1.	MATERIAL	4
2.2.	OVERVIEW OF THE MEASUREMENTS	4
2.3.	MEASUREMENTS OF THE BOTTOM SHEAR STRESS	8
3.	CALCULATION OF THE BOTTOM SHEAR STRESS	10
3.1.	INTRODUCTION	10
3.2.	CALCULATION OF CURRENTS AND WAVES.....	10
3.3.	CALCULATION OF THE BOTTOM SHEAR STRESS.....	10
3.3.1.	<i>Bottom stress under the influence of currents.....</i>	<i>10</i>
3.3.2.	<i>Bottom shear stress under the influence of waves.....</i>	<i>11</i>
3.3.3.	<i>Bottom shear currents under influence of currents and waves.....</i>	<i>12</i>
3.3.4.	<i>Calculation of the bottom roughness</i>	<i>15</i>
4.	ANALYSIS OF THE BOTTOM STRESS MEASUREMENTS.....	20
4.1.	BOTTOM STRESS FROM CURRENT PROFILE.....	20
4.2.	COMPARISON BETWEEN THE THREE MEASURED BOTTOM SHEAR STRESSES.....	20
4.3.	MEAN OF THE BOTTOM SHEAR STRESS MEASUREMENTS	24
5.	COMPARISON OF MODEL RESULTS WITH MEASUREMENTS.....	26
5.1.	INTRODUCTION	26
5.2.	SELECTED DEPLOYMENTS.....	26
5.2.1.	<i>Deployment 025</i>	<i>26</i>
5.2.1.1.	<i>Currents and waves.....</i>	<i>26</i>
5.2.1.2.	<i>Bottom shear stress with constant bottom roughness</i>	<i>27</i>
5.2.1.3.	<i>Bottom shear stress with bottom roughness calculated.....</i>	<i>30</i>
5.2.2.	<i>Deployment 078</i>	<i>31</i>
5.2.2.1.	<i>Currents and waves.....</i>	<i>31</i>
5.2.2.2.	<i>Bottom shear stress with constant bottom roughness</i>	<i>33</i>
5.2.2.3.	<i>Bottom shear stress with bottom roughness calculated.....</i>	<i>35</i>
5.2.3.	<i>Conclusions</i>	<i>37</i>
5.3.	OVERALL RESULTS FOR ALL CAMPAIGNS	37
5.3.1.	<i>Introduction</i>	<i>37</i>
5.3.2.	<i>Bottom stress with constant bottom roughness length</i>	<i>38</i>
5.3.3.	<i>Bottom shear stress with bottom roughness length calculated</i>	<i>39</i>
6.	CONCLUSIONS	41
7.	REFERENCES.....	44
8.	APPENDIX A: STATISTICAL PARAMETERS	46

I. Introduction

The bottom shear stress is an important factor for the calculation of sediment transport. The bottom shear stress determines the erosion and resuspension of the material or the deposition of the material on the sea bed. Furthermore, different total load and bottom load formulae take into account the bottom shear stress. The calculation of the bottom shear stress, under the combined influence of currents and waves, is however not a trivial task. Different methods and techniques are available in literature, sometimes using many parameters, which are not well known. The methods can vary from very simple models to very complex and time-consuming models. Also for the bottom roughness length, one of the main parameters determining the bottom shear stress, different models are available in literature. All these different models can give results that can vary over a large range.

Furthermore the measuring of the bottom shear stress is very complex and reliable bottom shear stress measurements, that could be used to validate the model predictions, are at the moment not available. Different methods are available to “measure” the bottom shear stress. In Francken and Van den Eynde (2010) a method was described, to calculate the bottom shear stress from the measurements from a high frequency point velocity meter (Acoustic Doppler Velocimeter ADV). Using the turbulent velocity spectrum in the high frequency range, the bottom shear stress can be calculated. Also the turbulent kinetic energy, which is calculated from the high frequency velocity variations, can be used to calculate the bottom shear stress. Finally, the bottom shear stress can be calculated from the logarithmic profile of the water currents in the lower water column. These current profiles can be measured using an Acoustic Doppler Profiler (ADP), installed on a bottom lander, or using a bottom mounted Acoustic Doppler Current Profiles (ADCP).

In the present report, some measurements of the bottom shear stress are discussed. Furthermore, a new module is presented to calculate the bottom shear stress, using different methods. This module can be used in the two sediment transport models, which are currently available at the OD Nature. Some first results of the validation of the bottom shear stress are discussed. First of all, the measurements of two deployments are discussed in detail, one offshore and one near shore deployment. Further the overall conclusions from the comparison of the model results with the measurements for all deployments are presented. Some conclusions and plans for further work are given at the end.

2. Measurements of the bottom shear stress

2.1. *Material*

In the framework of different projects (MOMO, ZAGRI, MOZ4, monitoring wind parks), several measuring campaigns were executed since 2005. Measurements were executed with bottom landers that are deployed at the bottom of the sea (see Figure 1 and Figure 2). The frame is equipped with a SonTek ADV Ocean point velocity meter, at 36 cm above the bottom (measuring at 18 cm above the bottom), a downward looking SonTek 3 MHz ADP current profiler, at 228 cm above the bottom, a Sequoia LISST-100X Laser In-Situ Scattering & Transmissometer, at 231 cm above the bottom and a Sea-Bird SBE37 thermosalinograph at 80 cm above the bottom. Furthermore 2 D&A OBS sensors, measuring turbidity, were attached to the frame at 29 cm and 234 cm above the bottom. The LISST measures the particle size distribution in the water column and the volumetric concentration of the material in suspension. During some deployments, the LISST was coupled with a third OBS sensor, measuring the turbidity at 125 cm above the bottom.

Additionally a RDI bottom mounted Acoustic Doppler Current Profiler (ADCP), type Sentinel 1200 kHz Workhorse (see Figure 3), could be deployed. This ADCP measured the current profile in the complete water column. However, these ADCP measurements will not be used in the current study.

As will be explained further in more detail, measurements of the ADP could be used to calculate the bottom stress from the current profile, while the measurements of the ADV could be used to calculate the bottom stress, using the inertial dissipation method or the turbulent kinetic energy method.

2.2. *Overview of the measurements*

In the period 2005-2013 69 measuring deployments with the bottom landers have been executed, mostly (48 deployments, i.e. 69.6 %) near the measuring station MOW1. From 2006 to 2009, 7 deployments were executed near Blankenberge, one deployment at MOW0. In the framework of the monitoring of the effects of the wind farms, 2 deployments were executed at the Gootebank, and 3 on the Bligh Bank in the period 2009-2010. From 2013, 9 campaigns have been executed near the WZ-buoy, near Zeebrugge in the framework of the "terreinproef Zeebrugge". An overview of the deployments, with the position and the starting and ending date is given in Table 1.

The position of the stations is presented in Figure 4.



Figure 1: Tripod bottom lander.



Figure 2: Tripod bottom lander.



Figure 3: Bottom mounted ADCP.

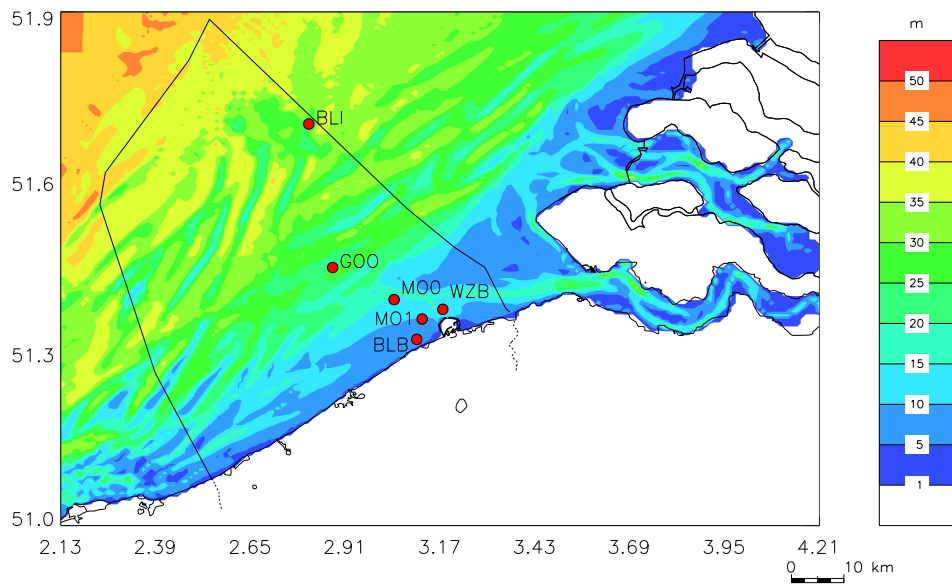


Figure 4: Position of the measuring stations: BLI: Bligh Bank, GOO: Gootebank, MOO: MOW0, BLB: Blankenberge, MOI: MOWI, WZB: WZ-Boei.

Table 1: Overview of the deployments.

	Station	ADP	ADV	Start	End	Model
5	MOW1	X	X	07/02/2005	18/02/2005	
6	MOW1	X	X	04/04/2005	15/04/2005	
7	MOW1		X	22/06/2005	12/07/2005	
8	MOW1	X	X	22/11/2005	05/12/2005	
9	MOW1	X	X	13/02/2006	27/02/2006	
10	MOW1	X	X	27/03/2006	18/04/2006	
11	MOW1	X	X	15/05/2006	15/06/2006	
12	Blankenberge	X	X	08/11/2006	27/11/2006	
13	Blankenberge	X	X	27/11/2006	15/12/2006	
14	Blankenberge	X	X	18/12/2006	07/02/2007	
15	MOW1	X	X	10/07/2007	19/07/2007	X
16	MOW1		X	23/10/2007	28/11/2007	
17	Blankenberge	X	X	28/01/2008	24/02/2008	
18	Blankenberge	X	X	06/03/2008	08/04/2008	
19	Blankenberge	X	X	15/04/2008	05/06/2008	
20	MOW0	X		23/06/2008	11/07/2008	
21	MOW1	X	X	17/11/2008	12/12/2008	
22	MOW1	X	X	09/02/2009	19/03/2009	
23	MOW1	X	X	26/03/2009	29/04/2009	
24	Blankenberge	X	X	04/05/2009	15/06/2009	
25	Gootebank	X	X	23/06/2009	13/07/2009	X
26	Blighbank	X	X	24/06/2009	14/07/2009	X
27	MOW1	X		10/09/2009	21/10/2009	
28	Gootebank	X	X	19/10/2009	09/12/2009	
29	Blighbank	X		21/10/2009	09/12/2009	
30	MOW1	X	X	06/11/2009	08/12/2009	
31	MOW1	X	X	11/12/2009	25/01/2010	
32	MOW1	X	X	25/01/2010	25/03/2010	X
33	MOW1	X	X	25/03/2010	20/05/2010	X
34	MOW1	X	X	20/05/2010	31/05/2010	X
35	MOW1	X	X	31/05/2010	23/07/2010	X
36	Blighbank	X	X	05/05/2010	01/06/2010	X
37	MOW1	X	X	06/09/2010	18/10/2010	X
38	MOW1	X	X	18/10/2010	17/11/2010	X
39	MOW1	X	X	17/11/2010	15/12/2010	X
40	MOW1	X	X	15/12/2010	31/01/2011	X
41	MOW1		X	31/01/2011	21/03/2011	X
42	MOW1		X	21/03/2011	24/03/2011	X
43	MOW1		X	24/03/2011	29/04/2011	X
44	MOW1	X	X	29/04/2011	23/05/2011	X
45	MOW1	X	X	23/05/2011	11/07/2011	X
46	MOW1	X	X	11/07/2011	18/08/2011	X

47	MOW1	X	X	18/08/2011	09/09/2011	X
48	MOW1	X	X	09/09/2011	12/10/2011	X
49	MOW1	X	X	12/10/2011	24/11/2011	X
50	MOW1	X	X	24/11/2011	19/01/2012	X
51	MOW1	X	X	24/02/2012	19/03/2012	X
52	MOW1	X	X	19/03/2012	25/04/2012	X
55	MOW1	X	X	29/06/2012	23/08/2012	X
58	MOW1		X	05/12/2012	24/01/2013	X
59	MOW1	X		24/01/2013	07/03/2013	X
60	MOW1	X	X	07/03/2013	28/03/2013	X
61	WZ Boei	X	X	28/03/2013	23/04/2013	X
62	MOW1	X	X	28/03/2013	22/04/2013	X
63	MOW1	X	X	22/04/2013	17/05/2013	X
64	WZ Boei	X	X	25/04/2013	16/05/2013	X
65	MOW1	X	X	17/05/2013	27/06/2013	X
66	WZ Boei	X		10/03/2013	27/03/2013	X
67	MOW1	X	X	27/06/2013	30/07/2013	X
68	WZ Boei	X		28/06/2013	30/07/2013	X
69	MOW1	X	X	24/07/2013	21/08/2013	X
70	WZ Boei	X	X	29/07/2013	21/08/2013	X
71	MOW1	X	X	21/08/2013	27/09/2013	X
72	WZ Boei		X	23/08/2013	09/09/2013	X
73	MOW1	X	X	23/09/2013	16/10/2013	X
74	WZ Boei	X	X	11/09/2013	14/10/2013	X
75	MOW1	X	X	16/10/2013	28/11/2013	X
77	WZ Boei	X	X	13/11/2013	27/11/2013	X
78	MOW1	X	X	28/11/2013	09/12/2013	X
79	WZ Boei		X	27/11/2013	10/12/2013	

2.3. *Measurements of the bottom shear stress*

For the measurement of the bottom shear stress, different methods are available, using either the current profile above the bottom, or using high frequency measurements of the currents. Giardino and Monbaliu (2006) describe four methods, with are the “mean flow method”, the “turbulent kinetic energy method”, the “inertial dissipation method” and the “eddy correlation method”. The first three methods are used in this report.

The mean flow method uses the fact that close to the bottom, the current profile is supposed to be logarithmic and can be written as:

$$u = \frac{u_*}{\kappa} \ln \frac{z}{z_0} \quad (1)$$

with	u	horizontal velocity at height z above the bottom
	κ	von Kármán constant = 0.4
	u_*	shear velocity, with $\tau = \rho u_*^2$
	τ	bottom shear stress
	ρ	water density
	z_0	bottom roughness length

By fitting the measured current profile to the logarithmic function, the bottom shear stress (and the bottom roughness) can be calculated.

The turbulent kinetic energy method assumes that the bottom shear stress is linear related to the turbulent kinetic energy, which is calculated from the variance of the high frequency three-dimensional current fluctuations (Andersen et al., 2007; Verney et al., 2007).

The inertial dissipation method finally, uses the spectrum of the current components. In this method, the shear velocity is related to the energy dissipation velocity, which is calculated from the spectrum of the three-dimensional currents in the region where the spectrum decreases with the wave number with the characteristic -5/3 power. Remark that Sherwood et al., 2006 and Trowbridge and Elgar, 2001 adapted the method to take into account the effect of the advection of the waves. More information this last method can be found in Francken en Van den Eynde (2010).

3. Calculation of the bottom shear stress

3.1. *Introduction*

The calculation of the bottom shear stress is the topic of much research. The bottom shear stresses under the influence of currents alone and under the influence of waves alone over a flat bed are quite well known. However, the calculation of the bottom stress under the combined influence of currents and waves, over a rippled sea bed is complex. First of all the calculation of the bottom shear stress under the influence of currents and waves is not the simple vectorial addition of the bottom stress vectors for the currents and the waves alone. Non-linear interactions increase the bottom shear stress.

Furthermore, the bottom roughness length, which is an important factor for the calculation of the bottom shear stress, is influenced by different factors. At the bottom itself, the roughness is a function of the grain size. This bottom shear stress, felt by the sediments is called the skin friction. However, at a distance more than a tenth of the length of the bottom ripples, the bottom roughness is also influenced by the bed load and by the height and the length of the bottom ripples. Further away from the bottom, a new logarithmic profile is followed with an apparently increased bottom roughness. The ratio between the skin bottom roughness and the total bottom roughness varies between 1.5 and 20.

At the OD Nature, two different sediment transport models are at the moment available. The mu-STM model calculates the advection and diffusion of suspended particulate matter. The model was developed to simulate the dispersion of dredged material, but can also be used to calculate the sediment balance for the Belgian Continental Shelf. The mu-SEDIM model calculates the transport of sand, using a total load formula. Erosion and deposition is calculated using the divergence of the local sediment transport.

In both models, the calculation of the bottom shear stress is of great importance. In the mu-SEDIM model, the bottom roughness is calculated in the model, taking in account the grain size, the calculated bottom load and ripple roughness. In the mu-STM model, only the total bottom roughness is taken into account.

3.2. *Calculation of currents and waves*

Both sediment transport models use the currents, calculated by a two-dimensional hydrodynamic model mu-BCZ, or the three-dimensional model OPTOS-BCZ. In the first case, the depth-averaged current has to be used. When using a three-dimensional model, also the current in the lowest layer of the water column can be used to calculate the bottom shear stress.

The waves are calculated with the mu-WAVE model, based on the second generation model HYPAS model, or with the third generation WAM model. These models give the significant wave height, the mean wave period and the wave direction.

3.3. *Calculation of the bottom shear stress*

3.3.1. Bottom stress under the influence of currents

The bottom stress under the influence of currents can be written as:

$$\tau_c = \rho C_D \bar{u}^2 = \rho \left(\frac{\kappa}{\ln \frac{h}{ez_0}} \right)^2 \bar{u}^2 = \rho u_*^2 \quad (2)$$

with τ_c bottom shear stress under the influence of currents
 C_D drag coefficient
 \bar{u} depth averaged current
 h water depth
 e 2.7182

As stated above, for the bottom roughness length, a difference has to be made between the skin bottom roughness, felt by the grains itself at the bottom, and the total bottom roughness that is felt by the currents and that is also influenced by the bottom load and by the bottom ripples, see further.

When a three-dimensional model is used, one can also use the current in the lowest layer of the water column. Assuming a logarithmic profile of the currents over the (lower part) of the water column, the bottom shear stress can be calculated as:

$$\tau_c = \rho \left(\frac{\kappa}{\ln \frac{h_1}{z_0}} \right)^2 u_1^2 \quad (3)$$

with u_1 current in the lowest layer of the water column
 h_1 height above the bottom where u_1 is calculated

3.3.2. Bottom shear stress under the influence of waves

The bottom shear stress under the influence of waves is calculated using the (maximum) orbital velocity at the bottom. Using linear wave theory, the maximal orbital velocity of a monochromatic wave can be calculated as:

$$u_w = \frac{\pi h_s}{T \sinh(kh)} \quad (4)$$

with h_s significant wave height
 T wave period
 k wave number

When calculating the wave orbital velocity of a wave spectrum, most of the time the significant wave height and the mean water period are taken as characteristics, although some other recommendations can be found in literature. The wave orbital excursion A can be calculated as:

$$A = \frac{u_w T}{2\pi} \quad (5)$$

The (maximum) bottom shear stress under the influence of waves is then calculated as:

$$\tau_w = \frac{1}{2} \rho f_w u_w^2 \quad (6)$$

with τ_w bottom shear stress under the influence of waves
 f_w wave factor

Also for the wave factor, different theories or models are available, however, with relative small differences.

3.3.3. Bottom shear currents under influence of currents and waves

For the calculation of the bottom shear stress under the influence of currents and waves, many different models can be found in literature, varying from simple model to very complex iterative models, resolving the stresses in the wave boundary layer and during a complete wave cycle. These very complex models are however very time consuming and not really useful to be used in the current sediment transport models. In Van den Eynde en Ozer (2003), different simple models were compared with each other and with the results of more complex model, as they were presented in Dyer and Soulsby (1988). The Bijker (1966) model was selected as a good model, giving realistic model results. The model however doesn't give realistic results for the bottom shear stress under the influence of waves with very small currents, see further. Additionally, no formulation was given for the mean bottom shear stress over a wave cycle, taking into account the increase in mean bottom shear stress under the influence of currents, when waves are available.

Furthermore, recently, more realistic and simple models for the combined bottom shear stress were proposed in literature. Therefore, three new formulations were implemented and tested.

First of all the Soulsby (1995) formulae was implemented which was the results of a two-coefficient optimisation of a simple model to 131 data points, from more complex theoretical models.

More recent, Soulsby and Clarke (2005) developed a new model, assuming an eddy viscosity varying over the water column, but constant in time. The eddy viscosity varies linearly above the bottom in the thin wave boundary layer and has a parabolic function outside the wave boundary layer. Remark that the eddy viscosity is much higher in the thin wave boundary layer than outside. Furthermore the eddy viscosity in the wave boundary layer is only a function of waves and currents, so that no iterative calculations are needed.

In the wave boundary layer, the shear stress is constant, outside the wave boundary layer, the shear stress varies linearly, to zero at the water surface. A current profile can be calculated, integration of the current profile over the water depth gives the depth-averaged current, giving a quadratic equation that can be used to solve the bottom shear stress. The model of Soulsby and Clarke (2005) gives both a formulation for the maximal bottom shear stress during a wave cycle, and the mean bottom shear stress, averaged over a wave cycle. Furthermore, the theory was developed, both for flow over rough and over smooth bottom.

Finally, Malarkey and Davies (2012) developed the theory of Soulsby and Clarke further to include additional non-linearity in the model, which is present in the more complex theoretical models, but is not found in the Soulsby-Clarke model.

A comparison of the non-linearity in the four models is presented for $z_0/h=0.0001$ and $A/z_0=10000$ in Figure 5. These are the same values as the figure presented in Soulsby (1997).

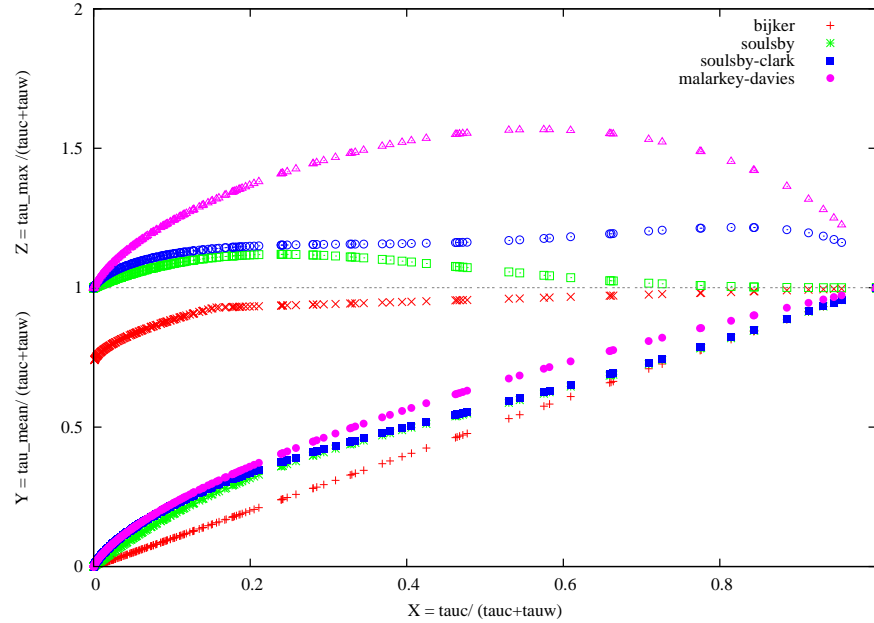


Figure 5: Intercomparison of the four models for the prediction of the mean (τ_{mean}) and maximum (τ_{max}) bed shear stresses due to waves plus currents as a function of the non-dimensional currents and the waves. Results for $z_0/h=0.0001$; $A/z_0=10000$.

One can clearly observe that, at least for these parameters, the Malarkey-Davies formula includes the most non-linearity in the calculated bottom shear stress. For the Bijker formula, the maximum combined bottom shear stress for currents and low waves is clearly below the value that is obtained for bottom shear stress under waves alone.

A comparison between the results of the mean and the maximum bottom stresses as predicted by the four models for $\bar{u} = 1$ m/s in a water depth of 10 m and with a (constant) bottom roughness of 0.053 m for varying wave orbital velocities, is given in Figure 6 and Figure 7. The differences between the models seem not very large, except for the fact that the current implementation of the Bijker formulae has no modelling of the mean bottom stress. It is assumed that the mean bottom stress of the waves, averaged over a wave cycle is zero, so that the mean bottom stress is equal to the bottom stress under the influence of the currents alone.

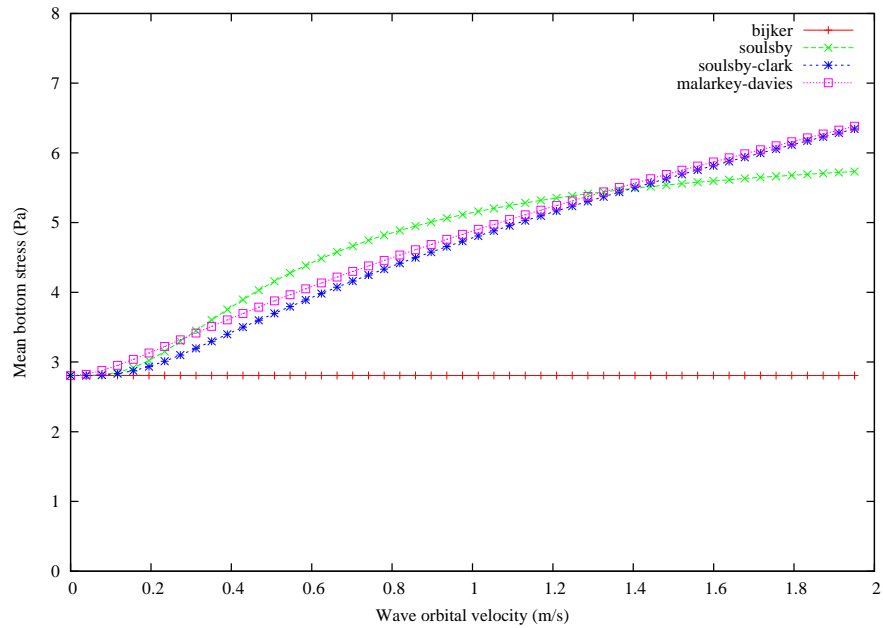


Figure 6: Intercomparison of the four models for the prediction of the mean bed shear stresses due to waves plus currents as a function of the wave orbital velocity for depth-averaged current of 1 m/s, water depth of 10 m and bottom roughness length of 0.053 m.

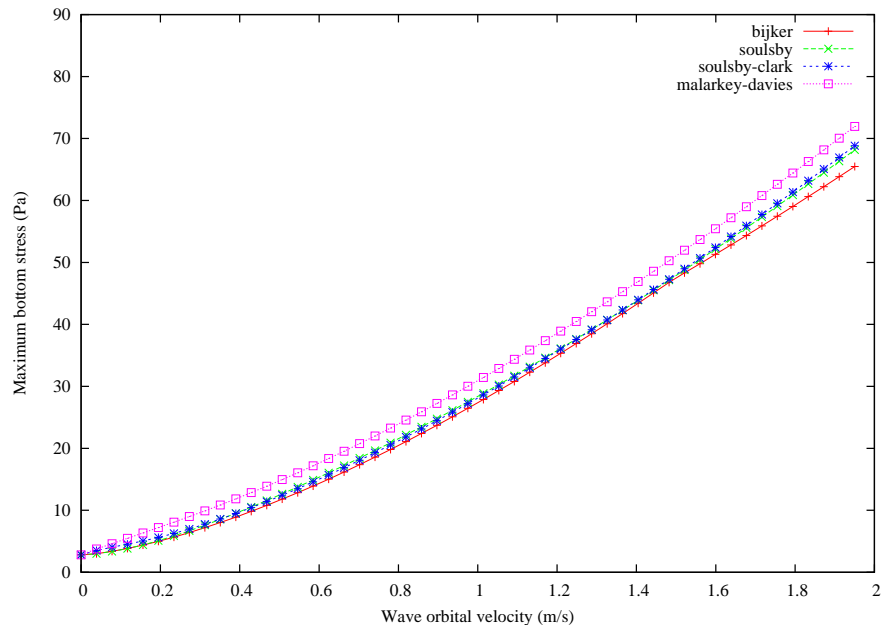


Figure 7: Intercomparison of the four models for the prediction of the maximum bed shear stresses due to waves plus currents as a function of the wave orbital velocity for depth-averaged current of 1 m/s, water depth of 10 m and bottom roughness length = f 0.053 m.

In Figure 8 and Figure 9 the mean and maximum bottom stresses are given as a function of the depth-averaged current for a wave orbital velocity of 0.78 m/s, i.e. for a

significant wave height of 2 m, and wave period of 8 s. The Bijker formulae gives obviously smaller bottom stresses than the three other models. In Figure 9, it can be seen that for low currents, the maximum bottom shear stress in the (implemented) Bijker formula is lower than the bottom shear stress under waves alone, which is of course not realistic. The fact that the maximum bottom shear stress, calculated by the Soulsby-Clarke model is much lower for the case, where the depth-averaged currents is zero, is caused by the fact that this model takes into account the flow regime, and calculates the bottom stress is a different way for laminar flow, turbulent flow with a smooth bottom and turbulent flow with a rough bottom. While in realistic cases, the flow is almost always turbulent with a rough bottom, in this case (for depth-averaged current zero) a laminar flow is modelled, with a much lower bottom stress as a result. Remark that for laminar flow and for turbulent flow with a smooth bottom, the bottom roughness is not accounted for.

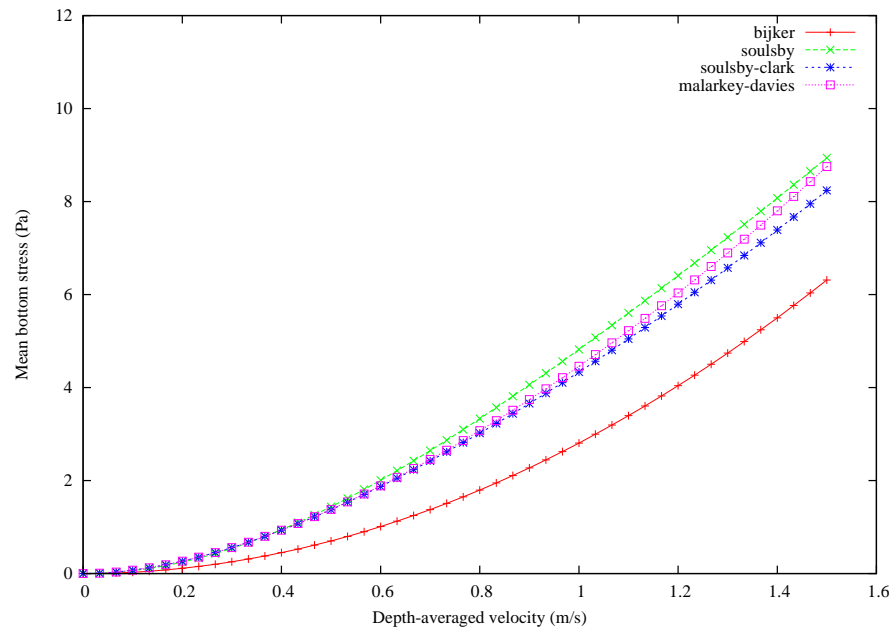


Figure 8: Intercomparison of the four models for the prediction of the mean bed shear stresses due to waves plus currents as a function of the depth-averaged currents for a wave orbital velocity of 0.78 m/s ($h_s=2$ m, $T=8$ s), water depth of 10 m and bottom roughness length of 0.053 m.

3.3.4. Calculation of the bottom roughness

As indicated above, the bottom stress under the influence of currents and waves is a function of the bottom roughness length z_0 (for turbulent flow with a rough bottom). A division has to be made between the bottom roughness length at the bottom itself, the skin bottom roughness, caused by the bottom material itself, and the total roughness, felt by the currents and the waves, which are also influenced by the bottom load and the bottom ripples. The skin and the total bottom roughness can be specified by the user itself, or can be calculated by the model. The bottom roughness length, the height above the bottom where the logarithmic current profiles becomes zero, is normally written as a function of the Nikuradse bottom roughness k_s , of the viscosity of the water ν and the

friction velocity:

$$z_0 = \frac{k_s}{30} + \frac{v}{9u_*} \quad (7)$$

For hydrodynamically rough flows (as is the case in the current flows), the second part of the bottom roughness length can be neglected.

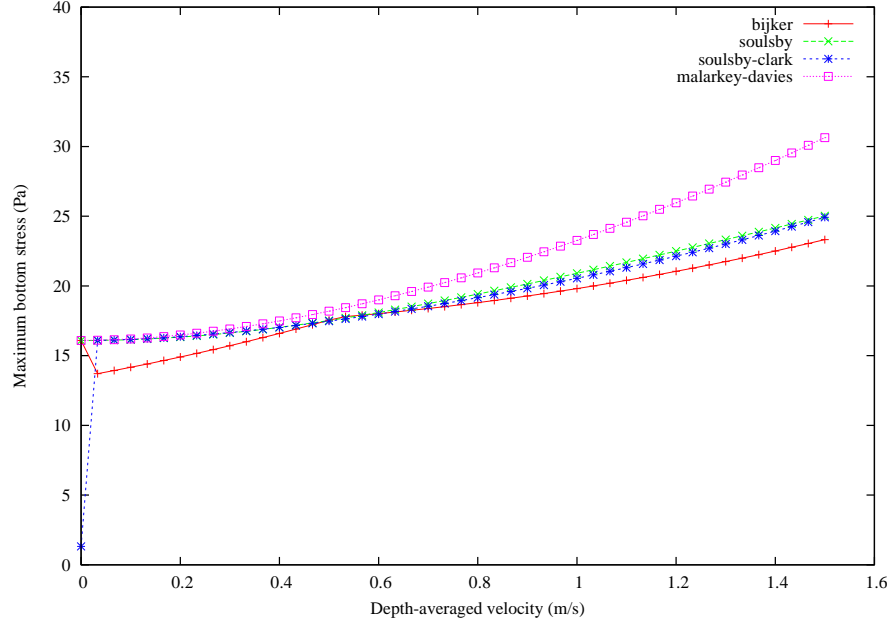


Figure 9: Intercomparison of the four models for the prediction of the maximum bed shear stresses due to waves plus currents as a function of the depth-averaged currents for a wave orbital velocity of 0.78 m/s ($h_s=2$ m, $T=8$ s), water depth of 10 m and bottom roughness length of 0.053 m.

The skin bottom roughness is most of the time written as a function of the grain size distribution. A much used formulation is:

$$k_{ss} = 2.5d_{50} \quad (8)$$

with d_{50} the grain size for which 50 % is smaller.

Values for the total bottom roughness can be found in tables. Typical values, found in literature, are $k_s=0.2$ mm for a mud bottom or $k_s=6$ mm for a rippled sand bottom. They can however be calculated in the model itself.

For the roughness as a function of the bottom load, a division is made between current-domination and wave-domination. For current-domination, the formula, proposed by Wilsen (in Soulsby, 1997) is used. For wave-domination, depending on a flag, five different possibilities are presented, which are: 1) the Grant and Madsen (1982) model; 2) the Soulsby model; 3) the Grant and Madsen (1982), assuming wave-domination ($K=1$); 4) the Nielsen model and 5) the Raudkivi formulation (all in Soulsby, 1997). For the exact formulations, the reader is referred to Soulsby (1997). Due to the fact that bottom roughness, due to bed load, is a function of the skin bottom friction, the

model used to calculate the skin bottom friction influences the calculated bottom roughness. In Figure 10, the bottom roughness length is presented for the Grant-Madsen model and for the different models for the bottom stress. One can see that the bottom roughness length is much smaller for the current-dominated case than for the wave-dominated case (for wave orbital velocities larger than 0.6 m/s). For the wave-dominated case that bottom roughness length can be several orders of magnitude larger than the skin bottom roughness length, which values up to 0.2 m. Furthermore the influence of the bottom stress model is apparent. The fact that the Bijker model gives much lower bottom roughness lengths is due to the fact that the Bijker model gives lower skin bottom stresses than the other models.

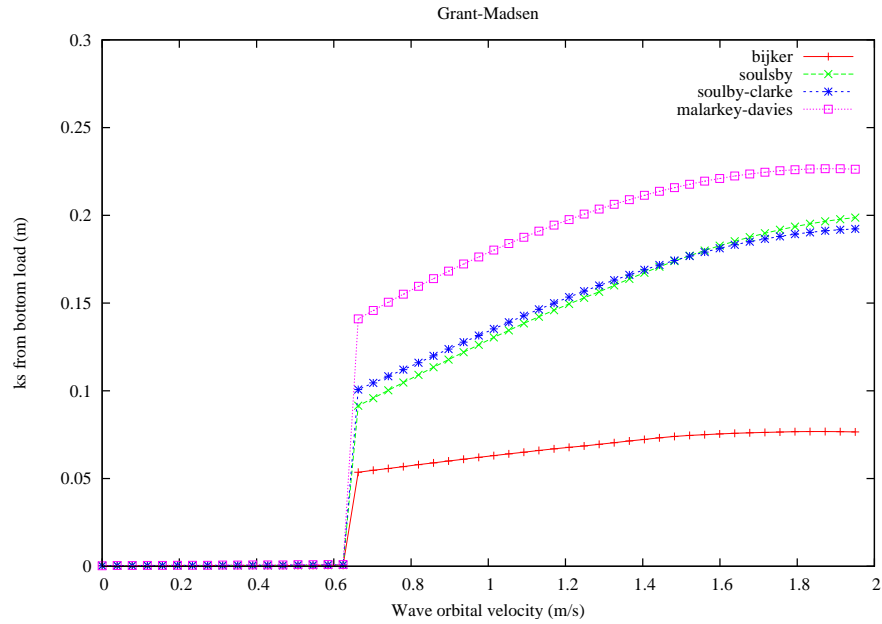


Figure 10: Intercomparison of the bottom roughness length, due to bed load, for the Grant-Madsen formulation (1), when wave-dominated, and for the four different bottom stress models.

In Figure 11, the bottom roughness length for the different formulations available are presented when the Malarkey-Davies formulation is used for the calculation of the bottom shear stress. The Raudkivi formulation gives unrealistic values for larger waves, and is therefore not recommended. The Grant-Madsen model overall gives the largest values, while the Nielsen formulation gives the lowest values for the bottom roughness length, due to bed load.

Finally, the bottom roughness length is a function of the bottom ripples. Normally the bottom roughness, due to bottom ripples is written as:

$$k_{sv} = 27.7 \frac{\eta^2}{\lambda} \quad (9)$$

with η the ripple height
 λ the ripple length

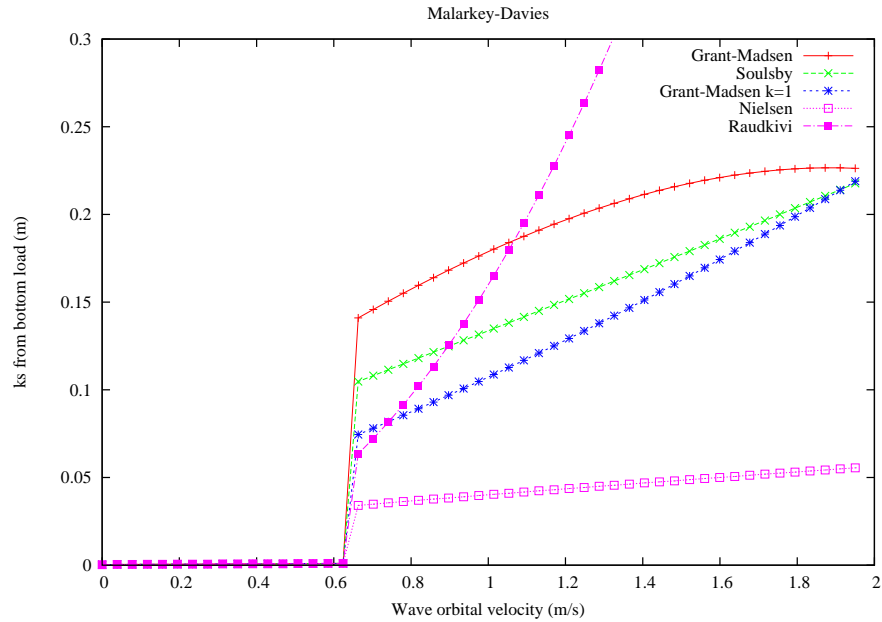


Figure 11: Intercomparison of the bottom roughness length, due to bed load, for the different formulations and for the bottom stress model of Malarkey-Davies.

The ripple geometry itself can be calculated by the model again. Also here, a distinction is made between current-dominated ripples and wave-dominated ripples.

Two models to calculate the ripple geometry were implemented. The first model uses the ripple geometry, proposed by Soulsby (1997) for the current-dominated ripples and the ripple geometry, proposed by Grant and Madsen (1982) for the wave-dominated ripples. More recently, a new ripple predictor was proposed by Soulsby and Whitehouse (2005). The model was validated against many laboratory and field experiment results and has the advantage that the time evolution of the ripples can be accounted for. Furthermore for the current-dominated ripples, sheet flow and ripples that are washed out for larger currents are taken into account. Some results of the bottom roughness length for the two models are given in Figure 12 and Figure 13.

From Figure 12, it is clear that in the Soulsby-Grant&Madsen model, the bottom roughness length in the wave-dominated case is a function of the (calculation of the) bottom shear stress. Furthermore, it is shown that for lower currents and waves and using the Bijker formulation for the calculation of the bottom shear stress, unrealistic values can be obtained. Furthermore, it is shown that the bottom roughness length, due to bed ripples, is larger for current-dominated ripples than for wave-dominated ripples. For larger waves, the bottom roughness length decreases. Figure 13 shows the bottom roughness length for the both models. Both models have a comparable behaviour, but can differ with a factor of 2. Remark that for depth-averaged current of 1.0 m/s, the Soulsby-Whitehouse model assumes that all ripples are washed out.

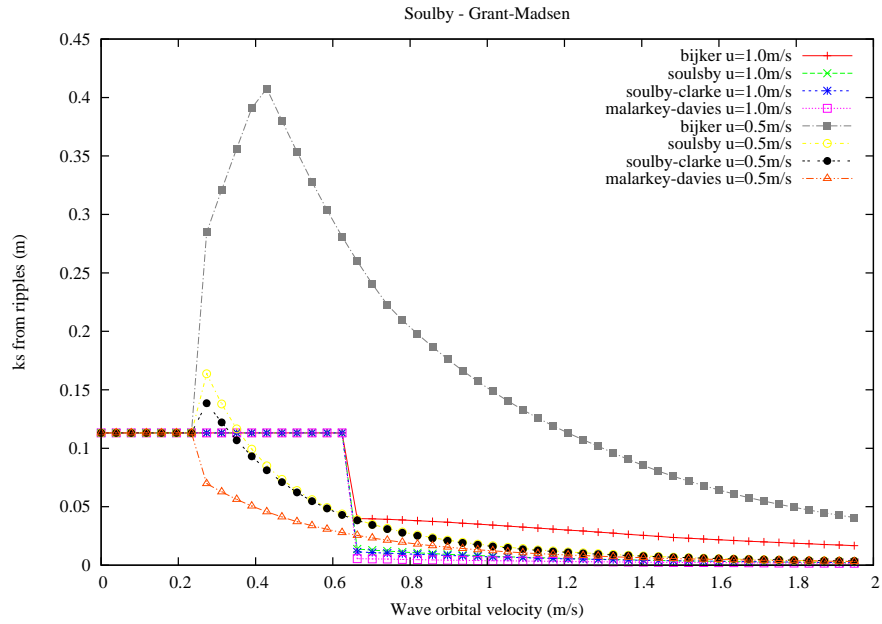


Figure 12: Intercomparison of the bottom roughness length, due to bed ripples, for the Soulsby-Grant&Madsen model and for different bottom stress models, for depth-averaged currents of 1 m/s and 0.5 m/s as a function of the wave orbital velocity. (T2/para05)

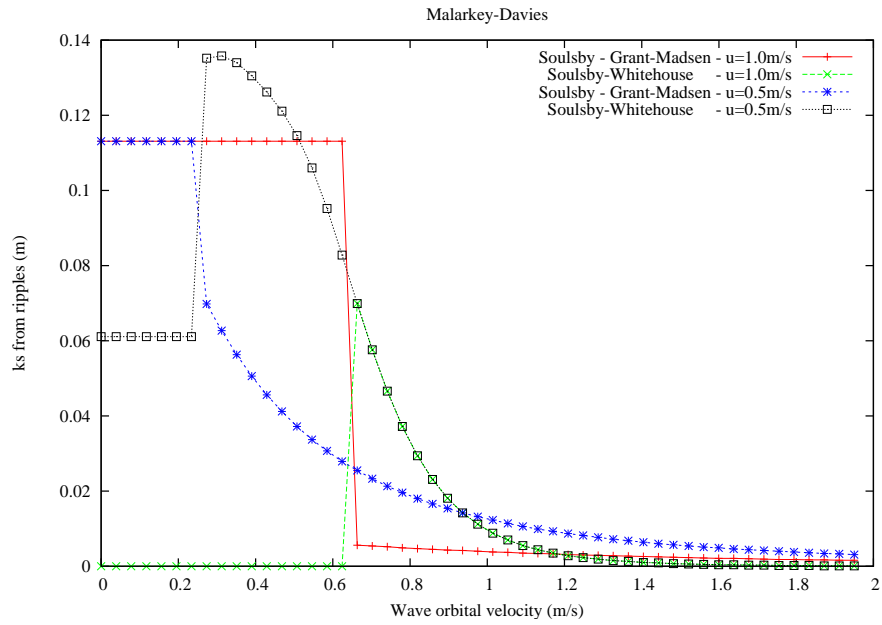


Figure 13: Intercomparison of the bottom roughness length, due to bed ripples, for the Soulsby-Grant&Madsen model (using the Malarkey-Davies model for the calculation of the bottom stress) and for the Soulsby-Whitehouse model, for depth-averaged currents of 1 m/s and 0.5 m/s as a function of the wave orbital velocity.

4. Analysis of the bottom stress measurements

4.1. *Bottom stress from current profile*

As explained in section 2.3, the bottom shear stress can be measured using different methods, including using the current profile, which is assumed to be logarithmic in the lower part of the water column. However, it is important to realise that the measured profile does not always show a logarithmic profile. This is illustrated in Figure 14, where, as an example, the measured profiles for the first 8 minutes of the measuring campaign 025 on the Gootebank are shown, together with the logarithmic regressions. One can clearly see that sometimes the profile is not logarithmic at all (see profiles 1 (left, row 1), 6 (right, row 3) or 7 (left, row 4)). The changes around 1 m above the bottom could be due to the influence of the tripod frame and the instruments itself, more especially of the acoustic transponder (yellow ball – see Figure 2), that was installed on the tripod during the first years of the deployments.

Furthermore, the height above the bottom, where the ADP was mounted varied over time, as well as the number of bins and the bin size. Where in the beginning, the currents were measured at 12 heights above the bottom, later deployments sometimes used 16 bins. The height, where the currents, closest to the bottom was measured, varied over the campaigns between 0.05 m and 0.25 m. Furthermore, sometimes the lowest bin was below the sea bottom, while for other deployments, the lowest bin measured was above the bottom.

When measurements were taken very close to the bottom, the lowest currents could sometimes be less reliable. This is shown in Figure 15, where for deployment 025 at the Gootebank, the U-currents are shown for the 7th bin, at 0.33 m above the bottom, and the 8th bin, at 0.08 m above the bottom. It can be seen that the currents, measured in the 8th bin show much more noise than the current in the 7th bin.

The number of points taken into account to calculate the logarithmic profile can be important and can influence the results quite drastically. This is shown in Figure 14, where 4 different logarithmic profiles are presented, and in Figure 16, where the bottom shear stress averaged over 30 minutes, calculated with 7 points is compared with the averaged bottom stress, calculated with 8 points, including the current measured at 0.08 m above the bottom for the first days of campaign 025. The two time series show the same tidal cycle, but the bottom shear stress, calculated with 8 points, is a factor 2 to 3 lower. It is a priori not clear which is the most realistic result.

4.2. *Comparison between the three measured bottom shear stresses*

In this report, three different techniques are used to measure the bottom shear stress, i.e., 1) the bottom stress, calculated from the current profile, 2) bottom stress, calculated from the turbulent kinetic energy, or 3) bottom stress, calculated using the inertial dissipation method. Unfortunately, the bottom shear stresses, calculated using the different methods, do not correlate with each other very well.

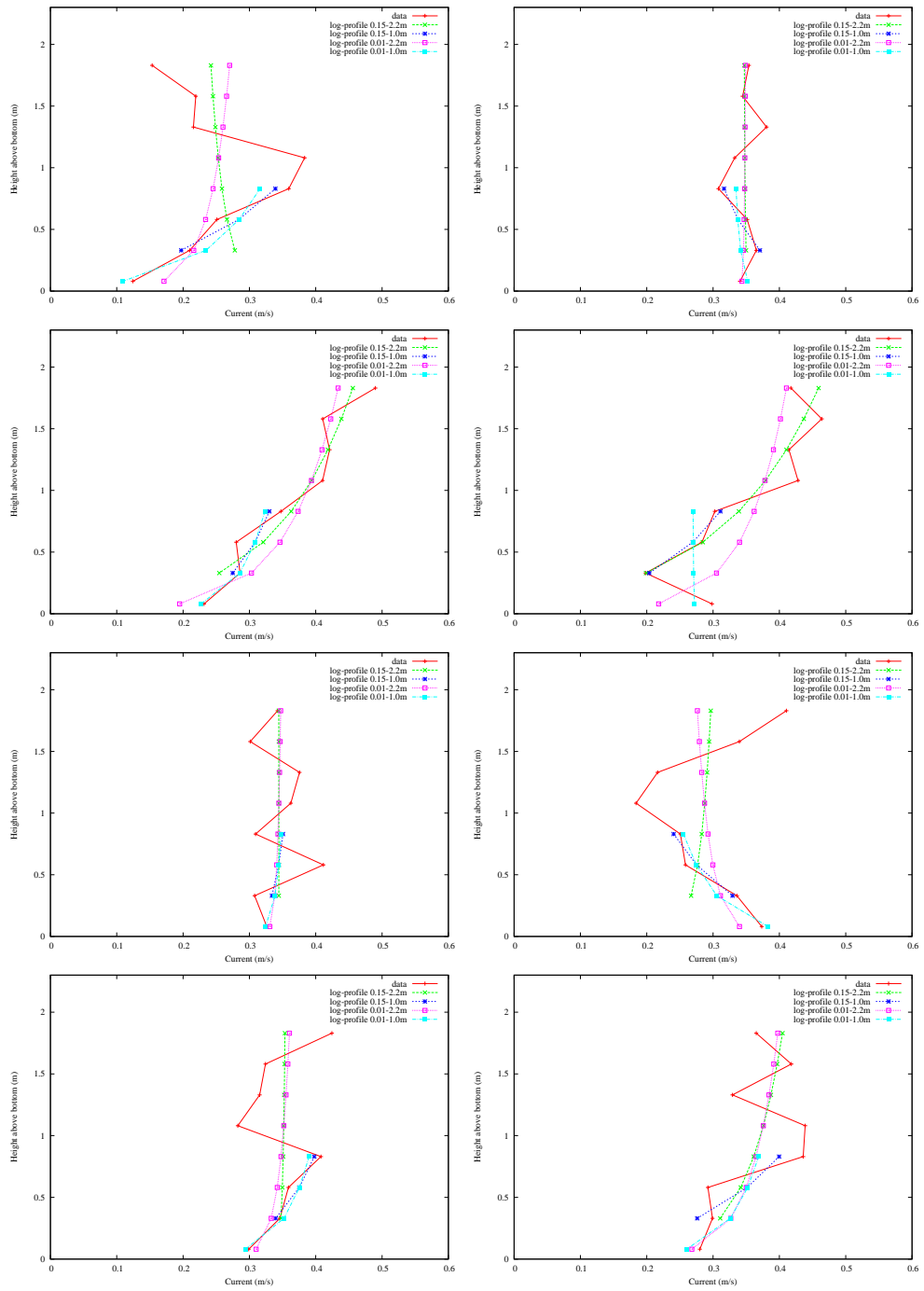


Figure 14: Profiles of currents and logarithmic regression for the currents at the Goetbank from 2009/06/23 18:29:50 till 2009/06/23 18:36:50.

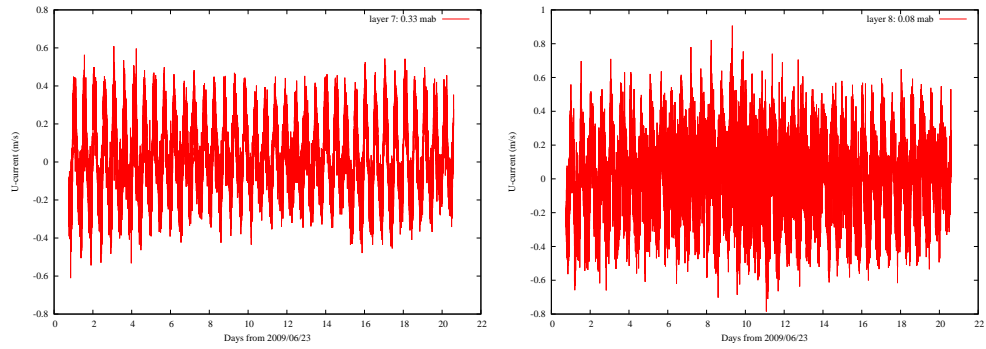


Figure 15: U-currents measured during campaign 25 at the Gootebank, in the layer 7, at 0.33 m above the bottom (left) and the layer 8, at 0.08 m above the bottom (right).

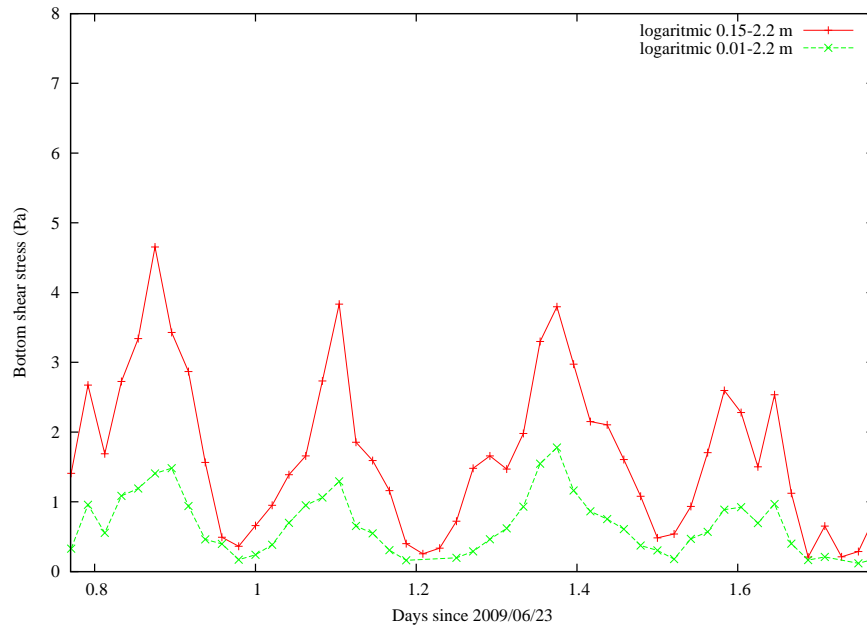


Figure 16: Bottom shear stress (averaged over one half hour) for the first days of campaign 025, calculated with or without the lowest measured point (at 0.08 m above the bottom) taken into account.

First tests showed that the mean correlation (over all deployments) between the bottom stress calculated using the turbulent kinetic energy or the bottom stress using the inertial dissipation method on the one side and the bottom stress, calculated using the current profile on the other side, is the highest when the current measurements between 0.01 m and 2.2 m are used, thus taking all data into account. The mean bias however is the lowest when the data between 0.15 m and 2.2 m are used. Remark however, that the correlation between the different bottom shear stress measurements is very low, while the bias can be considerable. This is illustrated in Figure 17 and Figure 18 where the correlation coefficient and the bias are presented for the different deployments between the measured bottom shear stresses, using the different techniques.

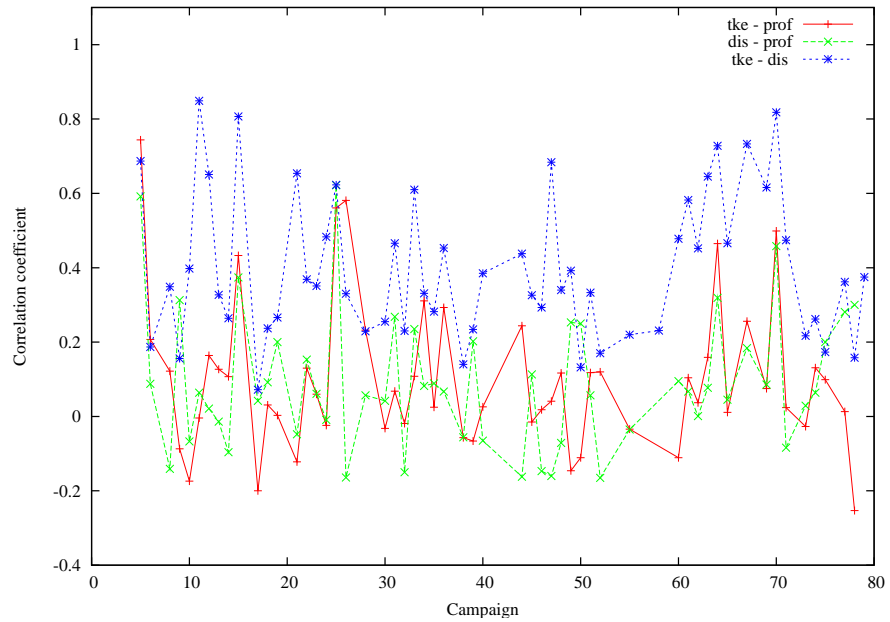


Figure 17: Correlation between the measured bottom shear stresses, using the turbulent kinetic energy method (tke), using the inertial dissipation method (dis) or from the current profile (prof).

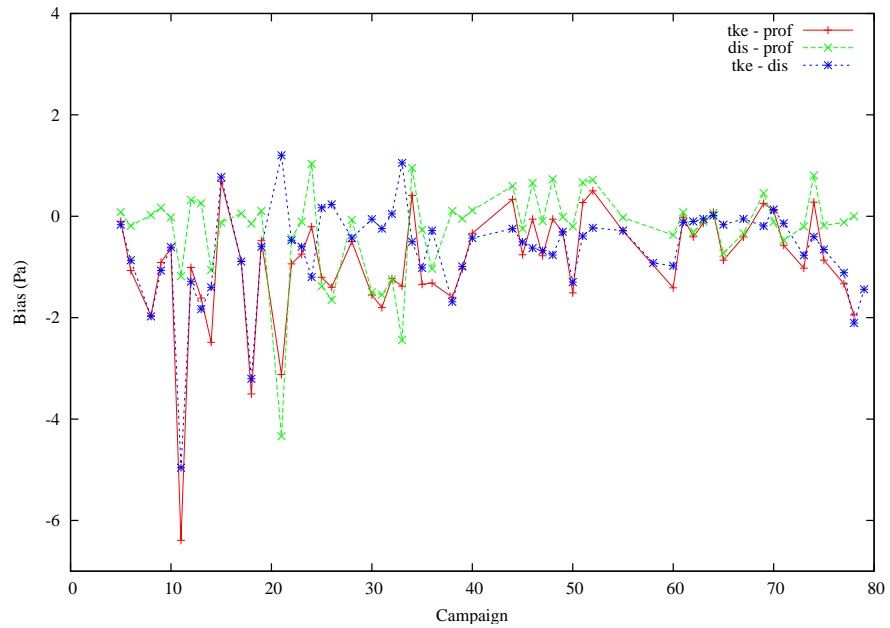


Figure 18: Bias between the measured bottom shear stresses, using the turbulent kinetic energy method (tke), using the inertial dissipation method (dis) or from the current profile (prof).

It is clear that the correlation between the measured bottom shear stress, using the turbulent kinetic energy method and the measured bottom shear stress, using the current profile, is very low and lies around 0.10. Only for the campaigns 5, 15, 25, 26, 64 and 70, the correlation coefficient is higher than 0.40. Also the correlation between the

bottom shear stress, calculated using inertial dissipation method and bottom shear stress, calculated using the current profile, is very low.

The correlation between the measured bottom shear stresses, using the turbulent kinetic energy method and the measured bottom shear stress, using inertial dissipation method, is higher. The mean correlation over all campaigns is 0.40. However, the bias between the bottom shear stresses is again rather high, with variations between -2 Pa and +2 Pa. Overall it is clear that the measured bottom stresses, using the different techniques, do not correlate very well with each other. It is therefore not clear which measurement should be used to validate the model results.

4.3. Mean of the bottom shear stress measurements

As mentioned in section 2.2, 48 of the deployments have been executed at the station MOW1, near the harbour of Zeebrugge, starting in 2005, until the end of 2013. In this case it is possible to get (longer) time series of the mean of the measured bottom shear stress over the deployments, for the different methods of measurements. This is presented in Figure 19. One can see that before 2010, the mean of the bottom shear stress, measured using the turbulent kinetic energy method or the inertial dissipation method, can vary over a larger range. This is probably due to the fact that the burst of the high frequency (25 Hz) measurements with the Acoustic Doppler Velocimeter (ADV) was probably not long enough to get reliable measurements of the bottom shear stress. Starting from campaign 037, in September 2010, the burst for the measurements was changed from 400 s to 7500 s, with more consistent results from then onwards.

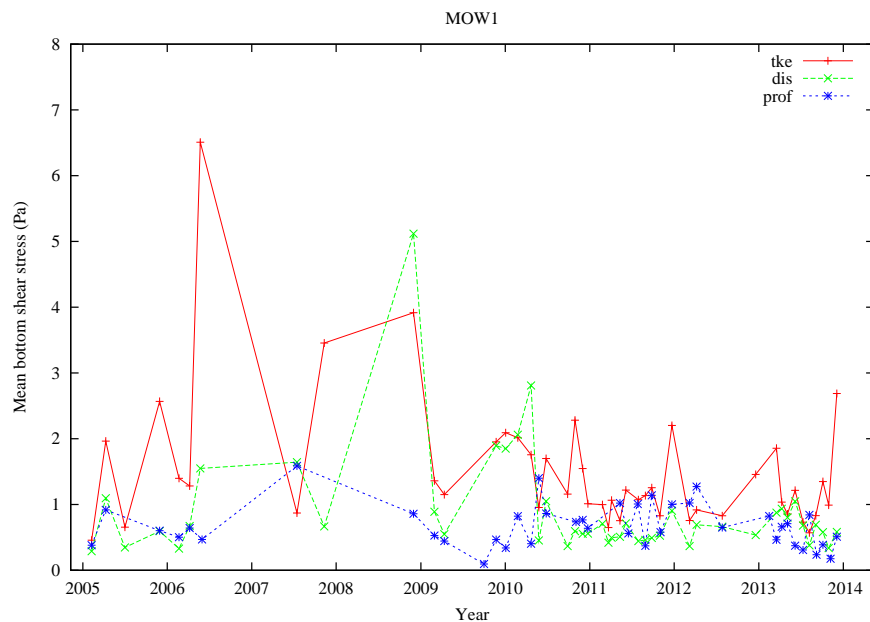


Figure 19: Mean (over deployment) bottom shear stress, measured using the turbulent kinetic energy method (tke), using the inertial dissipation method (dis) or from the current profile (prof) over the years, for the measurements in station MOW1.

Remark that the higher mean bottom shear stress in the measurements, using the

turbulent kinetic energy method, is mainly due to the larger influence of the waves on the measured bottom shear stress. This is illustrated in Figure 20 where the mean bottom shear stress is plotted as a function of the mean significant wave height for the deployments from September 2010. It is clear that a good correlation exists between the mean significant wave height and the mean bottom stress, measured using the turbulent kinetic energy method, with a slope of 1.87 Pa/m and a correlation coefficient of 0.831. For the mean bottom stress, measured using the inertial dissipation method, or using the current profile, this relation is not clear. This could be an indication that the bottom shear stress, using the turbulent kinetic energy, could be the most reliable and should be used to validate the model results.

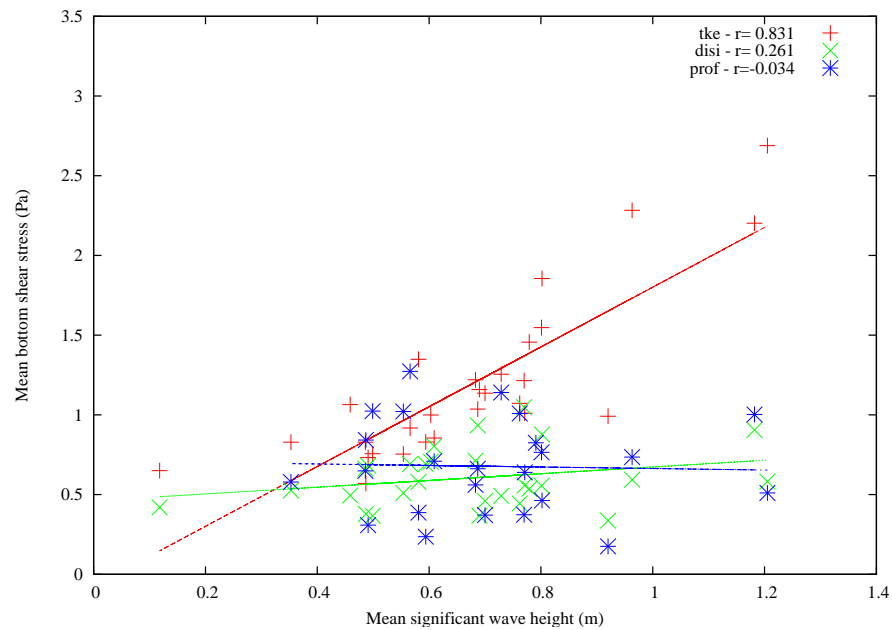


Figure 20: Correlation between the mean (over deployment) significant wave height and the mean (over deployment) bottom shear stress, measured using the turbulent kinetic energy method (tke), using the inertial dissipation method (dis) or from the current profile (prof) over the years, for the measurements in station MOW1.

5. Comparison of model results with measurements

5.1. *Introduction*

In this section the different models results will be compared with the measured bottom shear stresses. It is clear from the previous that, since the different measured bottom shear stresses are not similar, an important uncertainty exists in the “real” bottom stress that should be used to validate the model results. Since the measured bottom shear stress, using the turbulent kinetic energy method, has a clear relation with the mean significant wave height in the shallow waters of the coastal station MOW1, this seems to be the most reliable measurements. Remark that the burst length was increased from 400 s to 7500 s, from September 2010, to increase the reliability of the measurements. Therefore, the emphasis will be on the measurements from campaign 037 onwards.

In the next section, some model results will be discussed in more detail, for two deployments. For the deployment 025, there is a high correlation between the measured bottom shear stresses, using the different techniques. The deployment was executed in deeper offshore waters, at the Gootebank for a period of about 20 days, with low wave activities. The other campaign that will be discussed in more detail is the 078 deployment at MOW1, near the harbour of Zeebrugge, in a water depth of about 10 m. During this campaign of about 11 days, high waves occurred with a significant wave height up to 3 m.

In the last section, a more general discussion of the overall results is presented, investigating which model gives the best results, compared to the measurements. A difference is made between the model results, when a constant total bottom roughness is used, and the model results, where the bottom roughness is calculated by the model itself, based on empirical relations for the bottom roughness as a function of the bed load and of the bottom ripples.

Remark that to evaluate the agreement between the measurements and the model results, the root-mean-square error, the scatter index and the correlation coefficients can be used. These parameters are described in Appendix A. The lower the root-mean-square error or the scatter index, the better the agreement between the measured and the modelled bottom shear stresses. Remark that the scatter index is influenced by the magnitude of the measured bottom shear stresses.

The model simulations will be executed with a model with a constant total bottom roughness length and with the bottom roughness length, calculated in the model, using the different formulations for the bottom roughness length, as a function of the bed load and of the bottom ripples. For the constant total bottom roughness length, the values 0.004 m, 0.007 m, 0.01 m, 0.03 m, 0.07 m, 0.1 m, 0.2 m, 0.3 m, 0.4 m, 0.5 m, and 0.6 m are used.

5.2. *Selected deployments*

5.2.1. *Deployment 025*

5.2.1.1. *Currents and waves*

Campaign 025 was selected because for this deployment, the correlation between the measured bottom shear stress, using the turbulent kinetic energy method and the

measured bottom shear stress, from the current profile was relatively high, i.e. 0.561. The deployment was executed at the Gootebank, in the offshore waters of about 23 m water depth over the period 23 June 2009 till 13 July 2009. The currents modelled by the OPTOS-model and the waves modelled by the WAM model are presented in Figure 21 and Figure 22, together with some measurements. For the currents the measurements by the ADP were multiplied by a factor 1.5, to obtain the depth averaged currents from the currents at only 1.83 m above the bottom. Remark that this factor 1.5 is relatively high, but the figure indicates that the currents behaviour is well modelled by the model. The correlation coefficient between the model and the measurements are 0.801. For the waves, measurements from the Meetnet Vlaamse Banken were used at the A2-buoy. The correlation between the modelled and measured waves is 0.89, the bias -0.013 m. Remark that the waves remain relatively small over the period, with a maximum of 1.5 m, in a water depth of 23 m. The influence of the waves will therefore be limited.

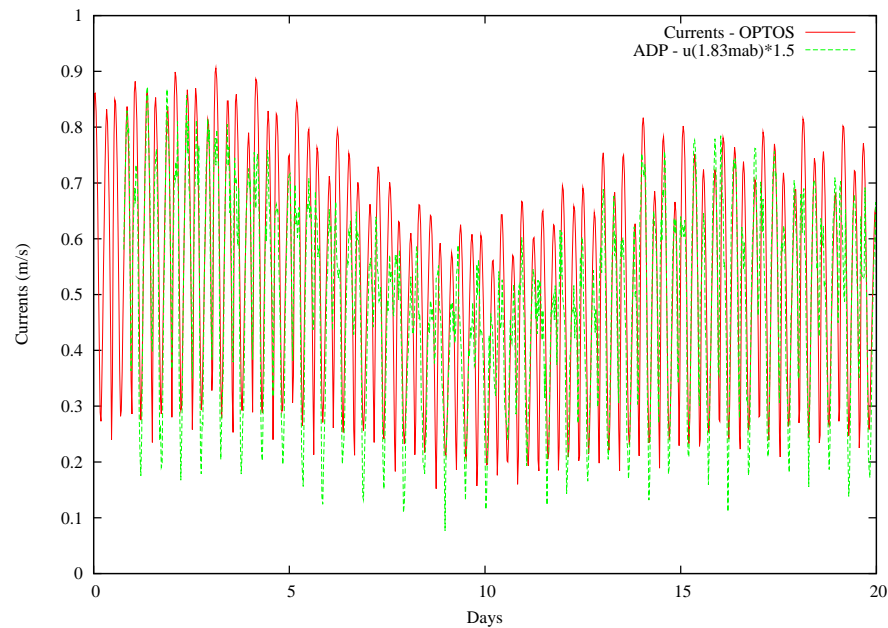


Figure 21: Currents modelled and measured for campaign 025 at the Gootebank for the period 23 June 2009 till 13 July 2009.

5.2.1.2. Bottom shear stress with constant bottom roughness

In the case the (total) bottom roughness is constant, good agreement between measured bottom stresses and model results is found for the bottom stress, derived from the current profile between 0.01 and 2.2 m, and the bottom stress, calculated using the Soulsby model with a constant total bottom roughness of 0.004 m. In this case, a bias is found of -0.052 Pa, a correlation coefficient of 0.748. This is shown in Figure 23 and Figure 24 (detail). For the measured bottom stress, using the turbulent kinetic energy method, the best agreement is found using the Soulsby model with a constant bottom roughness of 0.600 m (bias=-0.219 Pa, $r=0.696$ – see Figure 25). The measured bottom shear stresses are here much higher, resulting in a quite high bottom roughness. Also when the bottom shear stress is derived from the current profile between 0.15 m and

2.2 m (not taking into account the lowest more unreliable measured current value), the bottom shear stresses are much higher (as already mentioned in section 4.1).

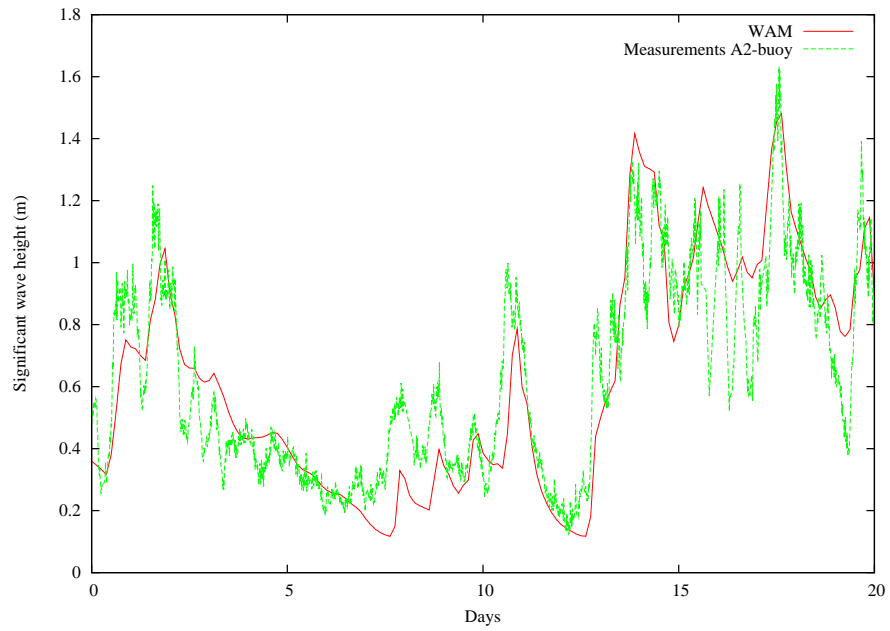


Figure 22: Waves modelled and measured for campaign 025 at the Gootebank for the period 23 June 2009 till 13 July 2009. Measurement at the A2-buoy from Meetnet Vlaamse Banken.

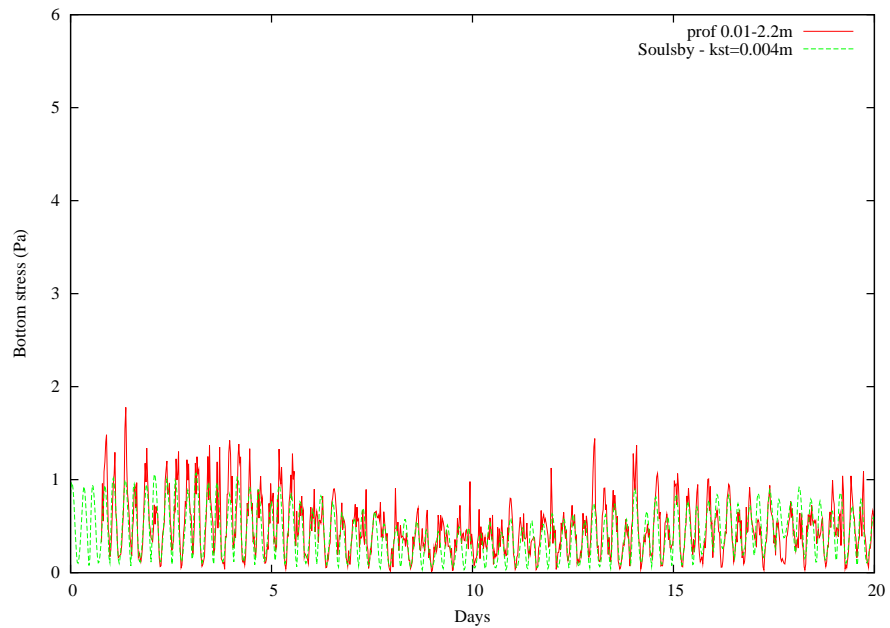


Figure 23: Bottom shear stress, modelled and measured for campaign 025 at the Gootebank for the period 23 June 2009 till 13 July 2009: measurements: bottom stress from current profile 0.01-2.2m, model: Soulsby, bottom roughness length = 0.004 m.

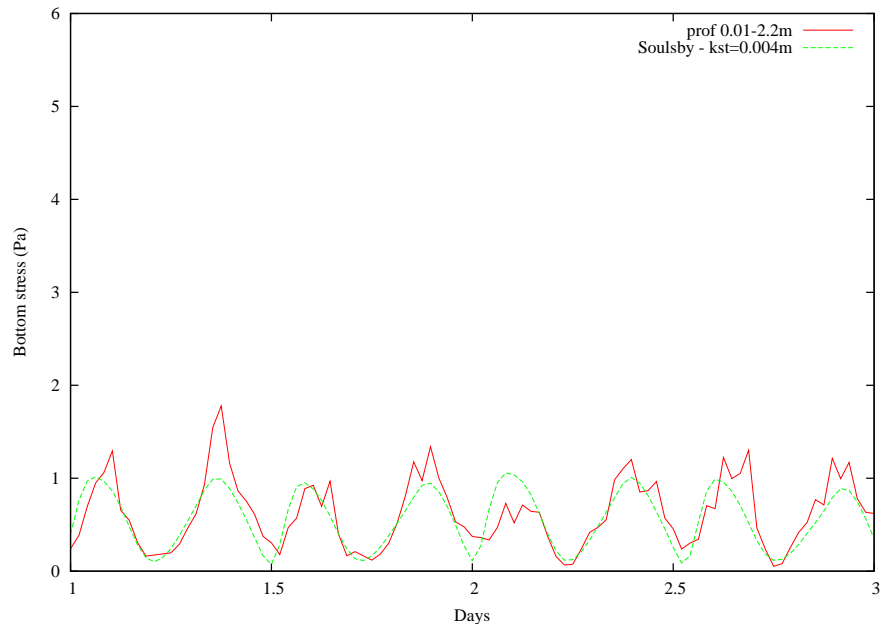


Figure 24: Bottom shear stress, modelled and measured for campaign 025 at the Gootebank for the period 23 June 2009 till 13 July 2009: measurements: bottom stress from current profile 0.01-2.2m, model: Soulsby, bottom roughness length = 0.004 m (detail).

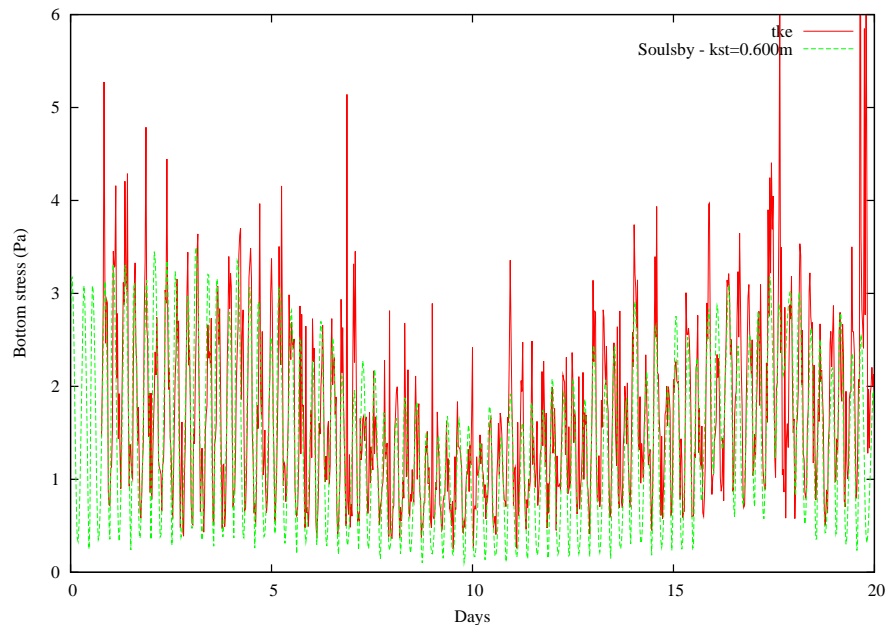


Figure 25: Bottom shear stress, modelled and measured for campaign 025 at the Gootebank for the period 23 June 2009 till 13 July 2009: measurements: bottom stress from turbulent kinetic energy, model: Soulsby, bottom roughness length = 0.600 m.

Also for the other bottom stress models, good agreement can be found, when an appropriate constant bottom shear stress is selected. Remark that for the Malarkey

model, in general a lower bottom roughness is used. This is probably due to the larger non-linearity included in the model and the resulting higher bottom stresses.

5.2.1.3. Bottom shear stress with bottom roughness calculated

As mentioned in section 3.3.4, the bottom roughness can be calculated in the model itself, accounting for skin bottom roughness, bottom roughness from bed load and from bottom ripples. When comparing the result with the bottom roughness, calculated from the current profile between 0.01 and 2.2 m, the modelled results seems to be too high (see Figure 26). The bias is 0.324 Pa, with a correlation coefficient of 0.678. For the bottom stress, calculated from the current profile between 0.15 and 2.2 m and for the bottom stress, using the turbulent kinetic energy model, on the other hand, the modelled bottom shear stresses are too low (not shown).

Remark that the bottom roughness length in this case is mainly driven by the bottom roughness, caused by the bottom ripples. Both the skin bottom roughness as the bottom roughness, caused by the bed load is an order of magnitude lower. When the Soulsby-Grant&Madsen model is used, the bottom roughness length varies around 0.1 m, while for the Soulsby-Whitehouse model, the bottom roughness length varies around 0.06 m (see Figure 27).

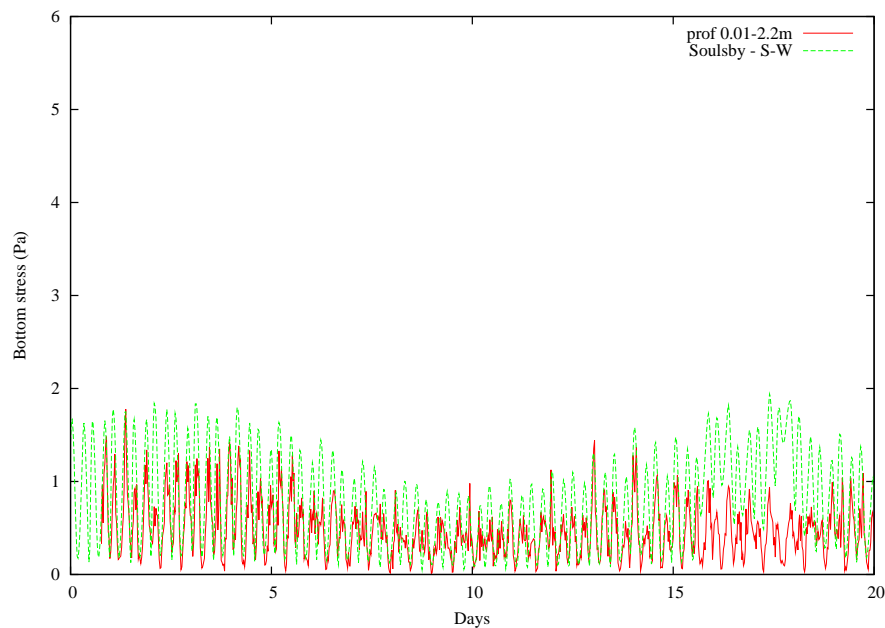


Figure 26: Bottom shear stress, modelled and measured for campaign 025 at the Gootebank for the period 23 June 2009 till 13 July 2009: measurements: bottom stress from current profile 0.01-2.2m, model: Soulsby, ripples calculated with Soulsby-Whitehouse model.

It is clear that there results are less good than the results with a constant bottom roughness, but in that case, there was an additional freedom in choosing a good value for the bottom roughness. Therefore, this additional freedom was included in the model as well, by multiplying the calculated total bottom roughness with an independent factor *convkst*. In this case, the total bottom roughness can be scaled, but the roughness

can vary over time, dependent on the bed load and the bottom ripples. Simulations were executed with 10 possible scaling factors, varying from 0.0001 to 10. Good results are obtained when comparing the bottom shear stress from the current profile between 0.01 and 2.2 m, with the bottom stress calculated by the Soulsby model, using the Soulsby-Whitehouse ripple model and multiplying the total bottom roughness with 0.1 (see Figure 28). In that case a bias of -0.013 Pa is obtained, a RMSE of 0.209 Pa and a correlation coefficient of 0.743. One must observe that these values are comparable with the results obtained with a constant bottom roughness. Since the bottom roughness doesn't really vary a lot over time (see Figure 27), this could be expected.

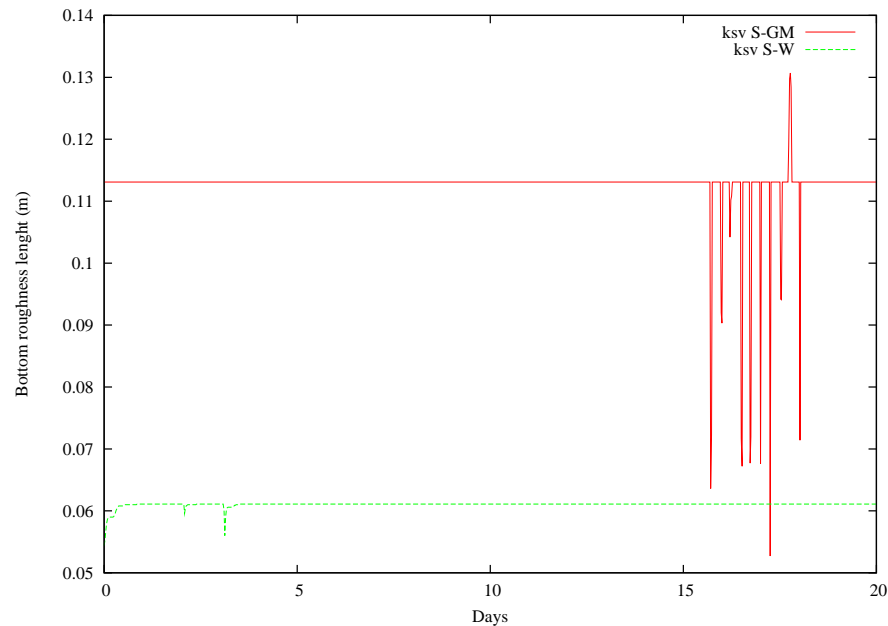


Figure 27: Variation of the bottom roughness length, due to the bottom ripples for campaign 025 at the Gootebank for the period 23 June 2009 till 13 July 2009: S-GM: Soulsby-Grant&Madsen model; S-W: Soulsby-Whitehouse model.

5.2.2. Deployment 078

5.2.2.1. Currents and waves

Deployment 078 was a deployment at the station MOW1, where almost 70 % of the deployments have been executed. The station is in a near shore area, near the harbour of Zeebrugge, in a water depth of about 10 m. During the campaign, which was executed from 28 November 2013 till 9 December 2013, high waves occurred with a significant wave height up to 3 m.

The currents modelled by the OPTOS-BCZ model and the waves modelled by the WAM model are presented in Figure 29 and Figure 30 respectively, together with some measurements. For the currents, the measurements by the ADP were multiplied by a factor 1.1, to obtain the depth averaged currents from the currents at only 1.9 m above the bottom. The currents are well modelled by the model, with a correlation coefficient between the model and the measurements of 0.761. For the waves, measurements from

the Meetnet Vlaamse Banken were used at the A2-buoy (see Figure 30). The correlation between the modelled and measured waves is 0.972, the bias is 0.093 m.

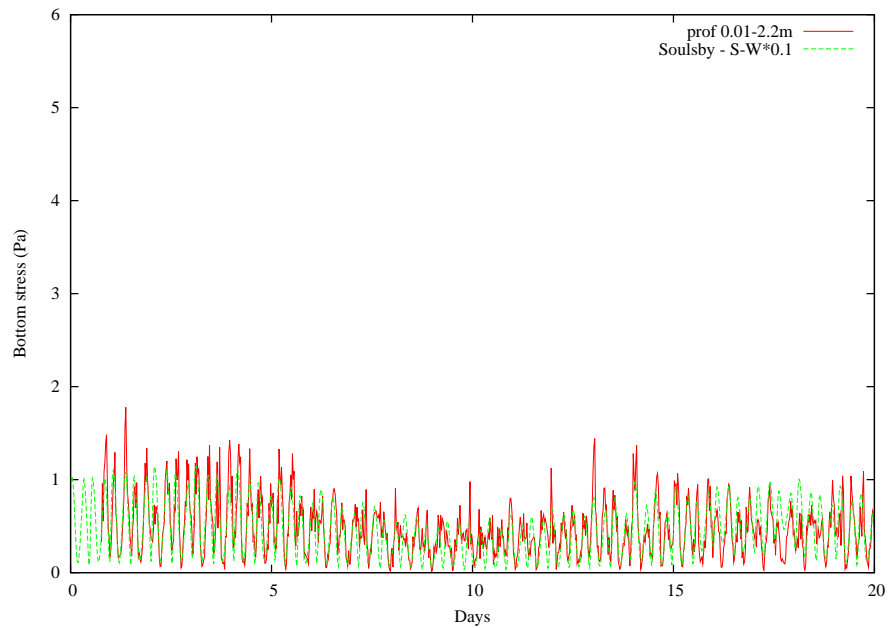


Figure 28: Bottom shear stress, modelled and measured for campaign 025 at the Gootebank for the period 23 June 2009 till 13 July 2009: measurements: bottom stress from current profile 0.01-2.2m, model: Soulsby, ripples calculated with Soulsby-Whitehouse model, total bottom roughness *0.1.

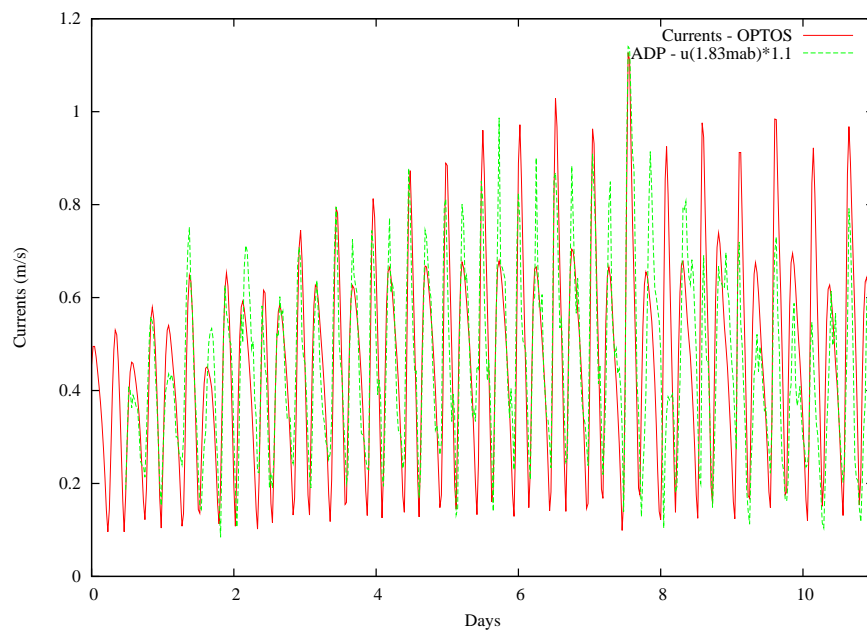


Figure 29: Currents modelled and measured for campaign 078 at MOWI for the period 28 November 2013 till 9 December 2013.

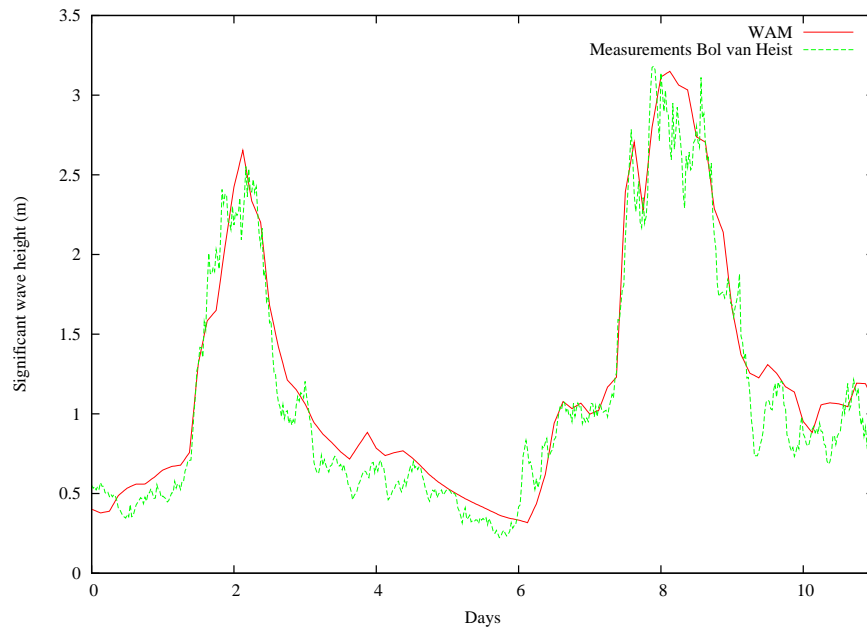


Figure 30: Waves modelled and measured for campaign 078 at MOWI for the period 28 November 2013 till 9 December 2013. Measurements from the station Bol van Heist are from the Meetnet Vlaamse Banken.

5.2.2.2. *Bottom shear stress with constant bottom roughness*

Where for the campaign 025, with low waves, good agreement could be found between the model results and the bottom shear stress, derived from the measured current profile, this is not the case for campaign 078. Good agreement is only found between the model results and the bottom shear stress, derived from the turbulent kinetic energy. This is shown in Figure 31 and Figure 32. The bottom shear stress, derived from the turbulent kinetic energy is well modelled by the models. In both results the influence of the waves on the bottom shear stress in shallow waters is very clear. For the Soulsby-Clarke model with a bottom roughness length of 0.01 m, a bias of -0.22 Pa is found, and a correlation coefficient of 0.931. The constant bottom roughness length is in this case much lower than for the results of the campaign 025.

The bottom stresses, derived from the current profile or derived using the inertial dissipation method, are much lower and don't show a very clear influence of the waves. It is unclear at the moment why these measurements seem less reliable. This should be investigated in the future.

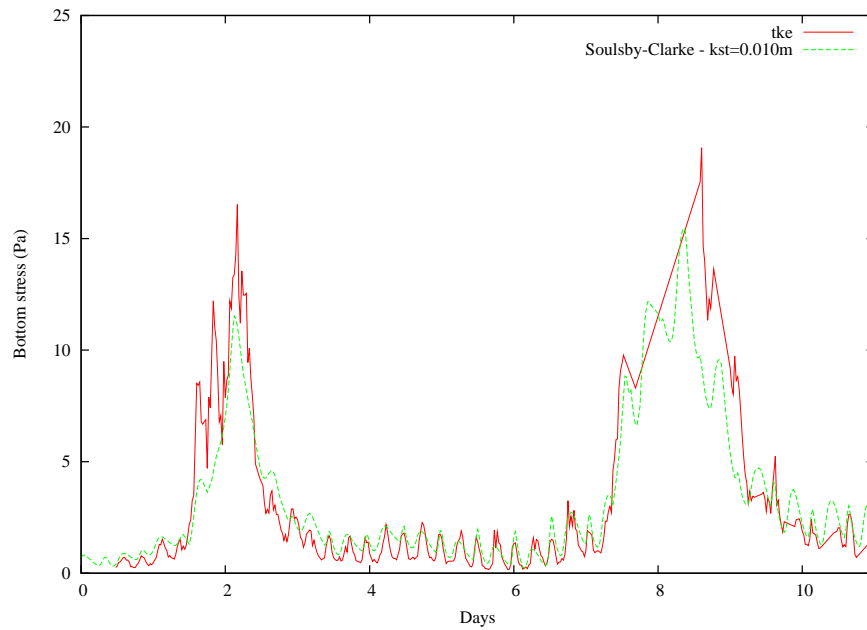


Figure 31: Bottom shear stress, modelled and measured for campaign 078 at MOW1 for the period 28 November 2013 till 9 December 2013: measurements: bottom stress from turbulent kinetic energy, model: Soulsby-Clarke, bottom roughness length = 0.010 m.

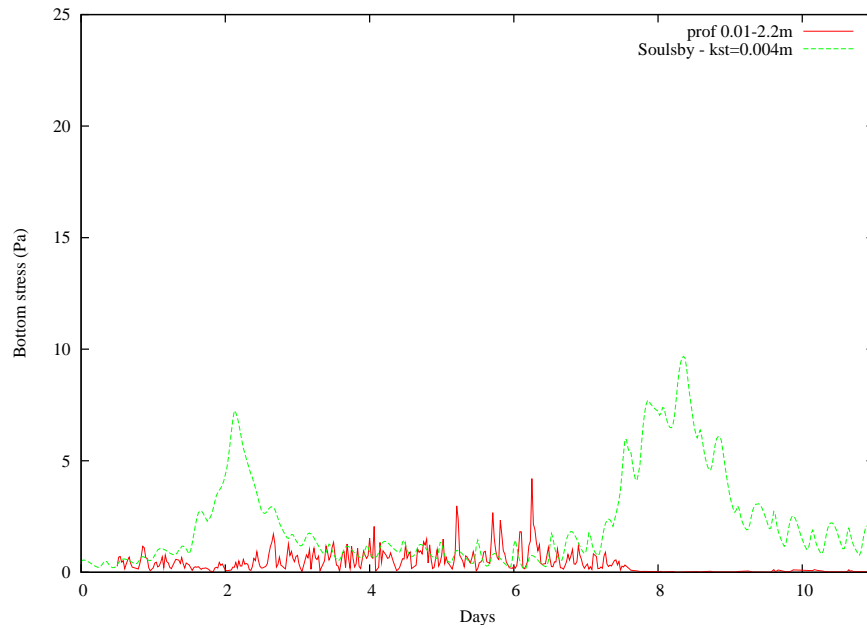


Figure 32: Bottom shear stress, modelled and measured for campaign 078 at MOW1 for the period 28 November 2013 till 9 December 2013: measurements: bottom stress from current profile between 0.01 and 2.2 m, model: Soulsby-Clarke, bottom roughness length = 0.004 m.

5.2.2.3. Bottom shear stress with bottom roughness calculated

Also for campaign 078, the modelled bottom shear stresses are much too high, when the bottom roughness length is used, as calculated by the model itself. However, when the calculated bottom roughness length is again multiplied with a scaling factor, good results are obtained, comparing the model results with the bottom shear stress, derived from the turbulent kinetic energy. This is shown in Figure 33 for the Soulsby-Clarke model, when the calculated bottom roughness length is multiplied with a factor 0.1. In this case the bias is only -0.02 Pa and the correlation coefficient 0.910. Also the RMSE of 1.44 Pa is lower in this case than the RMSE, obtained with a constant bottom roughness length (of 0.01 m).

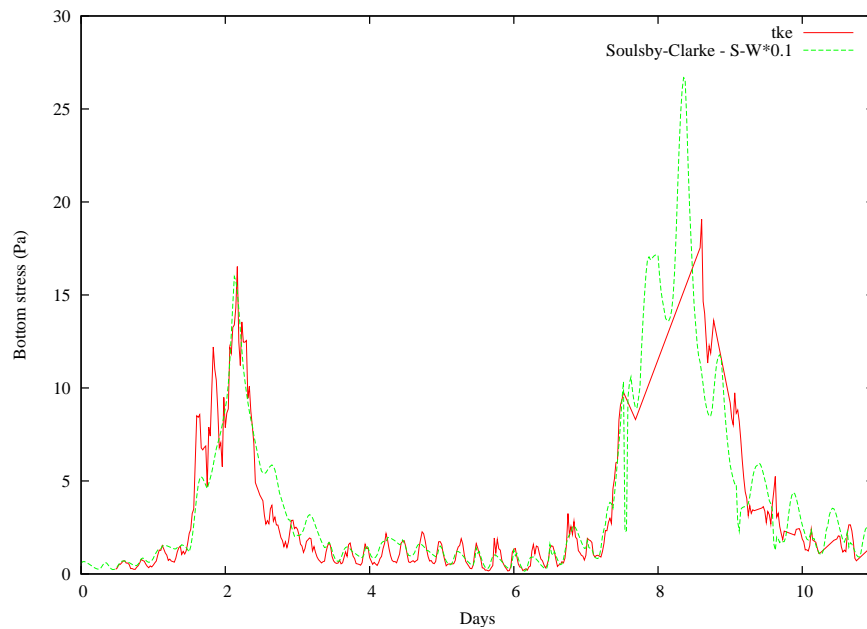


Figure 33: Bottom shear stress, modelled and measured for campaign 078 at MOW1 for the period 28 November 2013 till 9 December 2013: measurements: bottom stress from turbulent kinetic energy, model: Soulsby-Clarke, ripples calculated with Soulsby-Whitehouse model, total bottom roughness *0.1.

Remark that in this case the bottom roughness, due to bed load can be higher and comparable in magnitude as the bottom roughness, due to the ripples. In the case of high waves, the wave ripples are washed out and the bottom roughness, due to the bed load becomes more important. This is illustrated in Figure 34. The bottom roughness, due to ripples, calculated by the Soulsby-Grand&Madsen model and by the Soulsby-Whitehouse model have some differences, but have the same order of magnitude and show more or less the same behaviour (Figure 35).

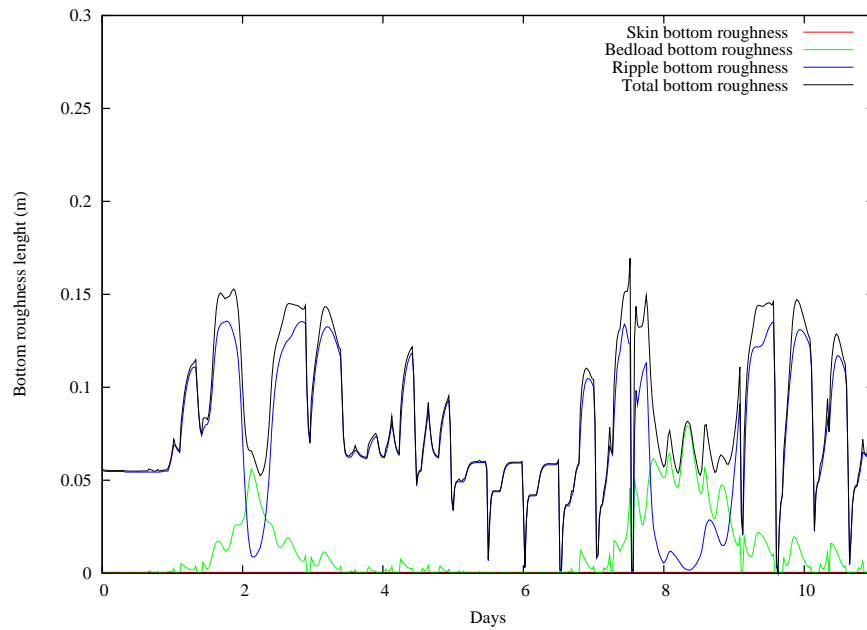


Figure 34: Variation of the skin, bed load, ripple and total bottom roughness length for campaign 078 at the station MOW1 for the period 28 November 2013 till 9 December 2013 for the Soulsby-Clarke model. Bed load roughness by Grant-Madsen, $k=1$; ripple roughness calculated with Soulsby-Whitehouse model.

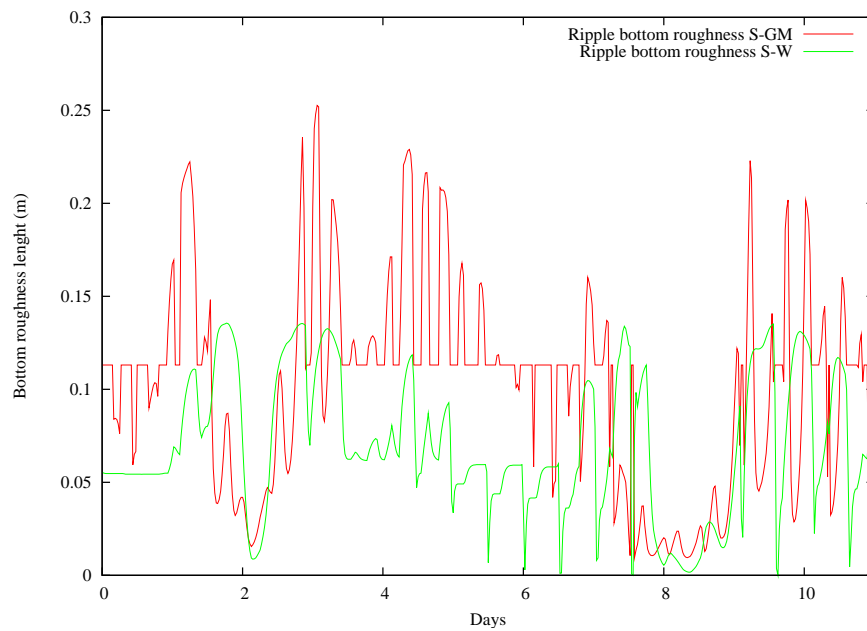


Figure 35: Variation of the bottom roughness length, due to the bottom ripples for campaign 078 at the station MOW1 for the period 28 November 2013 till 9 December 2013: S-GM: Soulsby-Grant&Madsen model; S-W: Soulsby-Whitehouse model.

5.2.3. Conclusions

For two deployments the comparison between the measurements and the model results were evaluated more in detail. The first deployment was executed offshore in deeper waters, with low wave activity, while the second deployment was executed more near shore in a water depth of only 10 m and with waves up to 3 m.

First of all, it was shown that the bottom shear stresses, measured with different techniques didn't show at all similar results. It is therefore difficult to assess what bottom shear stress the model results should be compared to, which of course makes the comparison difficult and the results ambiguous.

However, for the campaign with the low wave activity, when comparing the modelled bottom stress with the bottom stress, derived from the current profile 0.01-2.2 m, good results were obtained with a constant bottom roughness length of about 0.004 m. When using the bottom roughness length, calculated in the model, the bottom roughness length should be multiplied with a factor 0.1 to get good results. When comparing the model results with the bottom roughness, derived from the current profile 0.15-2.2 m, or with the bottom roughness, derived from the turbulent kinetic energy, very high bottom roughness lengths have to be used, due to the fact that the measured bottom stresses are much higher.

For the deployment with high waves, clearly the best measurement are obtained using the turbulent kinetic energy method. In this case, the model results agree well with the measurements, including the strong increase in bottom stress during high wave activity. The best results are obtained using a bottom roughness length of 0.01 m. When using the bottom roughness length, calculated by the model, again a scaling factor of 0.1 should be used. In this case the bottom stresses, calculated from the current profile, or using the inertial dissipation method, give much too low values.

5.3. Overall results for all campaigns

5.3.1. Introduction

In this section, results for all deployments will be evaluated in general. For all deployments, the measurements for which the best agreement exists, between measurements and model results, will be selected. For those measurements, first the optimal bottom roughness length is selected for the different campaigns, when a constant bottom roughness is used in the bottom shear stress models. In this way, a first estimate can be made for the optimal bottom roughness length to be used. The same can be done for the model results, when the bottom roughness is calculated in the model itself, taking into account the scaling factor.

To decide which model gives the best agreement with measured values, a new quality parameter is defined, which combines the effect of the bias, to be as low as possible, and the correlation coefficient, that has to be as high as possible. The quality parameter is thus defined as:

$$QP = \frac{\text{abs}(bias)}{r^2}$$

with $bias$ bias between the measurements and the observations
 r correlation coefficient

In this case the best agreement is determined by the lowest value of the QP . It is clear that using other parameters, like the RMSE, to define the best agreement could influence the results. However, the overall conclusions will not be changed drastically.

Remark that the model predictions are not executed for all deployments. As described above, emphasis was given to the deployments, starting from deployment 037, from September 2010, since from that moment, the burst length was increased, giving more reliable estimations of the bottom stress, using the turbulent kinetic energy method or the inertial dissipation method. Also for the deployments 015 and 025 model simulations were executed, since for these deployments, relatively high correlations were found between the bottom stresses, using different measurements techniques. Furthermore also deployment 26 was included, which was for the same period as deployment 025 and was a more offshore station. Finally all the other deployments from 2010 were included in the study. In total, model calculations were performed for 45 deployments. The deployments for which model simulations were executed are indicated in Table 1.

5.3.2. Bottom stress with constant bottom roughness length

For the models with a constant bottom roughness, the best agreement between the model results and the measured bottom stresses were obtained when the measured bottom stress, was derived from the turbulent kinetic energy. For the 45 deployments, for which the comparison was made, for 30 deployments, this was the case. Remark furthermore that 6 of the deployments for which better agreement was found with the bottom shear stress, derived from the current profile, were before deployment 037, where the bottom stresses derived from the turbulent kinetic energy were less reliable, due to too short burst lengths. Furthermore, for 3 deployments (059, 066 and 068), the ADV was not available. It is therefore clear that in this study, the best results are obtained by comparing the model results with the bottom stress, derived using the turbulent kinetic energy method.

When the bottom shear stress, measured using the turbulent kinetic energy method, is used as the measured bottom shear stress, one can investigate the best model to simulate the bottom shear stress, using a constant bottom roughness length. The results for the mean bias, RMSE and correlation (over all deployments) using the different models is presented in Table 2. The best results (lowest bias and RMSE, highest correlation) was found for the Soulsby model, followed closely by the Soulsby-Clarke model. For the Soulsby model the constant bottom roughness length that was most used to obtain the best results was 0.010 m. For the Soulsby-Clarke, the bottom roughness length that was most used was 0.007 m (16 deployments) or 0.01 m (13 deployments). As remarked earlier, when using the Malarkey-Davies model, lower bottom shear stresses should be used.

When the results of the Soulby model, with a constant bottom roughness length of 0.01 m are compared with the bottom shear stress, derived from the turbulent kinetic energy, for all deployments, a mean bias is found of 0.25 Pa, a RMSE of 1.21 Pa and a correlation coefficient of 0.72. In more the 88 % of the campaigns, the correlation is higher than 0.5. This is clearly satisfactory.

Table 2: The mean (over all campaigns) bias, RMSE and correlation coefficient for the different model results, when comparing the model results, using a constant bottom roughness length, to the measured bottom shear stress, using the turbulent kinetic energy method. Kst: the bottom roughness length that was most used to obtain the best results.

Model	Bias	RMSE	Correlation	Kst
Bijker	0.16	1.20	0.70	0.010 m
Soulsby	0.09	1.14	0.72	0.010 m
Soulsby-Cl.	0.10	1.16	0.72	0.007 m
Malarkey-D.	0.12	1.19	0.70	0.004 m

5.3.3. Bottom shear stress with bottom roughness length calculated

Also in the case the bottom roughness length is calculated by the model itself, taking into account the bottom roughness, due to bed load and bottom ripples, the bottom stress models have the best agreement with the measured bottom shear stress, using the turbulent kinetic energy method. Again in 30 of the 45 campaigns, the best results are obtained using that measured bottom shear stress. However the bias and the RMSE are much higher in this case, due to an over prediction of the bottom roughness length in the model. This was already shown in the two deployments, discussed in more detail in the previous section.

Therefore, also here the scaling factor is applied, to scale the calculated bottom roughness length, but allowing it to vary over time.

For the four different models, the best model results, compared to the bottom stress, derived from the turbulent kinetic energy, were selected. The results are presented in Table 3, where the Quality Parameter, calculated using the overall bias and correlation coefficient, together with the overall bias, RMSE and correlation coefficient are given. Furthermore also the best models to calculate the bottom roughness, due to bed load and bottom ripples, are given in the table. One can again conclude that the best results are given by the Soulsby model. It can be mentioned that, although the Raudkivi model to calculate the bottom roughness, due to bed load, gives non-realistic results in some cases (see 3.3.4), the model gives the best results for the Soulsby model. The bottom ripples roughness is best predicted by the model of Soulsby-Whitehouse. Remark however that the differences between the results of the different models for the bottom roughness length due to bed load and bottom ripples, is very small. Finally the scaling factor that is used to obtain the best results is a factor of 0.1.

Finally, the results are calculated for all deployments when comparing the measured bottom shear stress, using the turbulent kinetic energy method with the bottom stress, calculated using the Soulsby model with bottom roughness length, due to bed load, calculated with the Raudkivi model, the bottom roughness length, due to bottom ripples, with the Soulsby-Whitehouse model and with a scaling factor of 0.1. The overall bias is 0.27 Pa, with a RMSE of 1.28 Pa and a correlation of 0.72. These results are comparable with the results using a constant bottom roughness length, but are not better. At the moment, it is therefore recommended to use a constant bottom roughness length of 0.01 m.

Table 3: The QP, the mean (over all campaigns) bias, RMSE and correlation coefficient for the different model results, when comparing the modelled bottom stress, using the bottom roughness length calculated by the model and a scaling parameter, to the measured bottom shear stress, using the turbulent kinetic energy method. BRM: bottom roughness model that was used to obtain the best results: Raud: Raudkivi, Souls: Soulsby for bottom roughness from bed load; S-W: Soulsby-Whitehouse for bottom roughness from bottom ripples. Convkst: the scaling parameter that was most used to obtain the best results.

Model	QP	Bias	RMSE	Correlation	BRM	<i>convkst</i>
Bijker	0.33	0.17	1.20	0.71	Raud/S-W	0.1
Soulsby	0.24	0.12	1.20	0.72	Raud/S-W	0.1
Soulsby-Cl.	0.26	0.13	1.19	0.72	Raud/S-W	0.1
Malarkey-D.	0.31	0.15	1.17	0.71	Souls/S-W	0.1

6. Conclusions

The bottom shear stress is an important parameter for the calculation of the sediment transport. The erosion and deposition of the material is determined by the bottom shear stress. It is therefore important to have an accurate calculation of the bottom shear stress under the influence of the currents and the waves and to compare the model results with bottom shear stress measurements.

The measurements of the bottom shear stress have been executed during a series of 70 deployments going from 2005 to 2013, during which the current profile near the bottom and the high frequency velocities near the bottom were recorded. Three different techniques were used to determine the bottom shear stress. A first method uses the measured current profile near the bottom, which is assumed to be a logarithmic profile, governed by the bottom shear stress and the bottom roughness length. Further, the turbulent kinetic energy, which can be derived from the high frequency variations of the currents, is assumed to be linearly related to the bottom shear stress. Finally, the bottom shear stress can be derived using the inertial dissipation method. In this method, the velocity spectrum, and more specifically, the high frequency part of the spectrum, that is showing a decay with the wave number following a characteristic $-5/3$ power, is related to the turbulent kinetic energy dissipation and further to the bottom shear stress.

To model the bottom shear stress, four different models were implemented and tested. Normally, a constant bottom roughness length can be applied. However, the bottom roughness length also can be modelled as a function of the currents and the waves. In the framework of this report, different new models were implemented for the calculation of the bottom roughness length, under the influence of the bed load and two models for the calculation of the bottom roughness length, as a function of the bottom ripples. The model results were compared with bottom shear stress measurements to validate the model results.

When comparing the measurements for the bottom shear stress, using the different techniques, it was clear that no correlation between the different measurements of the bottom shear stress was found. Furthermore, it was clear that the bottom shear stress, calculated from the current profile, was highly dependent on the number of current measurements that were taken into account. Since the measurements were not correlating and sometimes had large differences in their values occurred, it was not clear which measured bottom shear stress was the best approximation of reality and should be used to validate the model results. However, the fact that the bottom shear stress, derived from the turbulent kinetic energy, clearly was influenced by the wave height, while the other bottom shear stresses had no correlation with the significant wave height, gave some indication that this technique gave the best results and should be used to validate the model results. Furthermore, it was shown that the most reliable results were obtained from deployment 037 from September 2010, since the burst length seemed to be too short before that date.

The validation of the model results first was executed more in detail for two specific deployments, i.e. deployment 025, on the Gootebank in a water depth of 23 m, over a period with low wave activity, and deployment 078, near the station MOW1 in a water depth of about 10 m and during a period of high wave activity with waves with a significant wave height up to 3 m.

It was first shown that the hydrodynamic and the wave models gave good results for the two deployment periods. For the deployment 025, a large difference was found between the bottom shear stress, derived from the current profile between 0.01 m and 2.2 m, and the bottom shear stress, derived from the turbulent kinetic energy or derived from the current profile between 0.15 and 2.2 m. A quite low constant bottom roughness length of 0.004 m was used to have a good agreement between the model results and the bottom shear stress, derived from the current profile between 0.01 and 2.2 m. In the other case, a very high bottom roughness length of 0.6 m had to be used to give a good agreement between the model results and the measured bottom shear stress. When the bottom roughness was calculated in the model itself, it was observed that the calculated bottom roughness length was a factor 10 too high, to give good agreement with the bottom shear stress, derived from the current profile between 0.01 and 2.2 m.

For the deployment 078, clearly the best results were obtained when comparing the model results with the bottom shear stress, derived from the turbulent kinetic energy. When using the Soulsby-Clarke model and a constant bottom roughness length of 0.01 m, a small bias was found of -0.22 Pa, and a correlation coefficient of 0.93. When using the bottom roughness, calculated in the model, good results were obtained when the total bottom roughness length was again multiplied by a factor 0.1. In this case the results were better than the results with a constant bottom roughness length.

When looking at the best agreement between the model results and the measured bottom shear stress for all deployments, more or less the same conclusions could be put forward. The best results are when comparing the model results with the bottom shear stress, derived from the turbulent kinetic energy. Furthermore, overall the Soulsby model gives the best results, when using a constant bottom roughness length of 0.01 m. When using the bottom roughness, calculated by the model, a scaling factor of 0.1 should be used to lower the calculated bottom roughness. The Soulsby or the Soulsby-Clarke or model gives the best results, when the Soulsby-Whitehouse formulation is used to calculate the bottom roughness length, due to bottom ripples. Remark that the model results with the calculation of the bottom roughness in the model doesn't give necessarily better results than using a constant total bottom roughness. It is, for now, therefore recommended to use in the sediment transport model a constant bottom roughness length.

Overall, one can conclude that using these parameters, good results can be obtained, modelling the bottom shear stress, for most of the deployments. However, one has to take into account that the fact that the measured bottom shear stress, using different techniques doesn't correlate at all with each other, does make the results of this study still uncertain. It is clear that more research has to be done to evaluate the measurements and to obtain in the future high quality measurements of the bottom shear stress. Only in this way, a solid validation of the model results can be achieved.

In the future, the results of the different deployments will be analysed in more detail. Furthermore, an analysis will be made on the dependency of the best bottom roughness length on the water depth, the maximum current or the significant wave height. Unfortunately, all measurements since September 2010 were executed in shallow, near shore waters (MOW1 and WZ-buoy). It could be useful to obtain new, high quality, measurements in deeper waters. Finally, one must remark that apart from the ADV and ADP measurements, also some ADCP measurements are available. An

analysis of these results is foreseen.

7. References

- Andersen, T.J., J. Fredsøe and M. Pejrup, 2007. In situ estimation of erosion and deposition thresholds by Acoustic Doppler Velocimeter (ADV). *Estuarine, Coastal and Shelf Science*, 75, 327-336. doi:10.1016/j.ecss.2007.04.039.
- Bijker, E.W., 1966. The increase of bed shear in a current due to wave motion. In: *Proceeding 10th Conference on Coastal Engineering, Tokyo*, 746-765.
- Dyer, K.R. and R.L. Soulsby, 1988. Sand transport on the continental shelf. *Annual Review of Fluid Mechanics*, 20, 295-324.
- Francken, F. and D. Van den Eynde, 2010. Calculation of current and wave induced turbulence from high frequency ADV measurements. MUMM report, Brussels, 14 pp.
- Giardino, A. and J. Monbaliu, 2006. Shear stress effects on sand bank morphodynamics and sand sorting. In: *Tubielewicz, A. (ed.), Coastal dynamics, geomorphology and protection. EuroCoast - Littoral 2006*, Faculty of Management and Economics, Gdansk University of Technology: Gdansk, 88-96.
- Grant, W.D. and O.S. Madsen, 1982. Movable bed roughness in unsteady oscillatory flow. *Journal of Geophysical Research*, 87, C1, 469-481.
- Malarkey, J. and A.G. Davies, 2012. A simple procedure for calculating the mean and maximum bed stress under wave and current conditions for rough turbulent flow based on Soulsby and Clarke's(2005) method. *Computers and Geosciences*, 43, 101-107.
- Sherwood, C.R., Lacy, J.R., Voulgaris, G., 2006. Shear velocity estimates on the inner shelf off Grays Harbor, Washington, USA. *Cont. Shelf Res.* 26, 1995-2018.
- Soulsby, 1995. Bed shear-stresses due to combined waves and currents. In: *Advances in Coastal Morphodynamics*. M.J.F. Stive, H.J. de Vriend, J. Fredsøe, L. Hamm, R.L. Soulsby, C. Teisson and J.C. Winterwerp (eds.), 4-20 to 4-23. Delft Hydraulics, The Netherlands.
- Soulsby, R., 1997. *Dynamics of marine sands. A manual for practical applications*. Telford, London, 249 pp.
- Soulsby, R.L. and S. Clarke, 2005. Bed shear-stresses under combined waves and currents on smooth and rough beds. Report TR 137. HR Wallingford, Wallingford, United Kingdom, 42 pp. (http://www.estproc.net/EstProc_library.htm).
- Soulsby, R.L. and R.J.S. Whitehouse, 2005. Prediction of ripple properties in shelf seas. Mark 2 Predictor for Time Evolution. Final Technical Report. Prepared for US Office of Naval Research, Contract No. N00014-04-C-0408. Report TR154, HR Wallingford, 41 pp + App.
- Trowbridge, J. and S. Elgar, 2001. Turbulence Measurements in the Surf Zone. *Journal of Physical Oceanography*, 31, 2403-2417.
- Van den Eynde, D. en J. Ozer, 1993. *Sediment-Trend-Analyse: berekening van sedimenttransport met behulp van een mathematisch model*. Studie uitgevoerd in opdracht van HAECON NV, betreffende de 'Sediment-Trend-Analyse' (STA) Activiteit 1. Beheerseenheid Mathematisch Model Noordzee, Brussel, 111 pp.

Verney, R., J. Deloffre, J.-C. Brun-Cottan and R. Lafite, 2007. The effect of wave-induced turbulence on intertidal mudflats: Impact of boat traffic and wind. *Continental Shelf Research*, 27, 594–612.

8. Appendix A: Statistical parameters

For the validation, the statistical parameters bias, root mean square error (RMSE), the systematical and unsystematical RMSE and the correlation coefficient can be calculated.

Hereafter, the measurements series will be presented as x and the model results (that is subject to the test) as y .

The mean values of the time series are represented by \bar{x} (reference) and \bar{y} (subject to test):

$$\bar{x} = \frac{1}{N} \sum_{i=1}^N x_i$$
$$\bar{y} = \frac{1}{N} \sum_{i=1}^N y_i$$

where N is the length of the time series.

The bias is the difference between the mean of the modelled and the measured time series:

$$bias = \bar{y} - \bar{x}$$

The closer the bias is to zero, the better both time series correspond. A positive bias value means that the modelled time series are an overestimation of the observed time series. A negative bias value means that the modelled time series are an underestimation of the observed time series.

The root mean square error (RMSE) is a measure for the absolute error and is defined as:

$$RMSE = \sqrt{\frac{\sum_{i=1}^N (y_i - x_i)^2}{N}}$$

Corresponding time series will result in RMSE values close to zero.

Furthermore, a systematical RMSE ($RMSE_s$) and an unsystematical RMSE ($RMSE_u$) can be defined, that evaluate respectively, the (absolute) error, which is generated by the deviation from the linear regression of the modelled time series from the measurements, and the error that is generated by the deviation from the individual model results from the linear regression itself. While the systematical RMSE could be reduced by applying a correction, using the linear regression, the unsystematical RMSE is the error which is inherent from the variation from the results themselves. These parameters can be calculated as:

$$RMSE_s = \sqrt{\frac{\sum_{i=1}^N (\hat{y}_i - x_i)^2}{N}}$$
$$RMSE_u = \sqrt{\frac{\sum_{i=1}^N (y_i - \hat{y}_i)^2}{N}}$$

with \hat{y}_i is defined from the linear regression

$$\hat{y}_i = mx_i + b$$

with slope m and intercept b calculated from:

$$m = \frac{N \sum x_i y_i - \sum x_i \sum y_i}{N \sum x_i^2 - (\sum x_i)^2}$$

$$b = \bar{y} - m\bar{x}$$

The correlation between both signals is given by Pearson's correlation coefficient, defined as:

$$r = \frac{\sum_{i=1}^N (x_i - \bar{x})(y_i - \bar{y})}{\sqrt{\sum_{i=1}^N (x_i - \bar{x})^2} \sqrt{\sum_{i=1}^N (y_i - \bar{y})^2}}$$

The scatter index is a measure for the relative error and is defined by:

$$S.I. = \frac{RMSE}{\bar{x}}$$

© COLOPHON

This report was issued by Operational Directorate Natural Environment in February 2015.

The reference code is ZAGRI-MOZ4/1/DVDE/201501/EN/TR2.

Status draft
 final version
 revised version of document
 confidential

Available in English
 Dutch
 French

If you have any questions or wish to receive additional copies of this document, please send an e-mail to Dries.VandenEynde@mumm.ac.be, quoting the reference, or write to:

Royal Belgian Institute of Natural Sciences
Operational Directorate Natural Environment
100 Gulledele
B-1200 Brussels
Belgium
Phone: +32 2 773 2111
Fax: +32 2 770 6972
<http://www.mumm.ac.be/>

Royal Belgian Institute of Natural Sciences
Operational Directorate Natural Environment
Suspended Matter and Seabed Monitoring and Modelling Group



The typefaces used in this document are Gudrun Zapf-von Hesse's *Carmina Medium* at 10/14 for body text, and Frederic Goudy's *Goudy Sans Medium* for headings and captions.

Annex D

TSHD technical specifications

This Annex forms part of the report:

Van Lancker, V., Baeye, M., Evangelinos, D. & Van den Eynde, D. (2015). Monitoring of the impact of the extraction of marine aggregates, in casu sand, in the zone of the Hinder Banks. Period 1/1 - 31/12 2014. Brussels, RBINS-OD Nature. Report <MOZ4-ZAGRI/I/VVL/201502/EN/SR01>, 74 pp. (+5 Annexes).

Annex D. TSHD technical specifications

Table D-1. Technical specifications of the trailing suction hopper dredgers operating in the Belgian part of the North Sea.

THSD	Hopper volume (m ³)	Length OA (m)	Length BP (m)	Width (m)	Depth (m)	Draft loaded (m)	Speed loaded (kt)	Total power (kW)	Dredging depth (m)	# dredging pipes	Suction pipe diameter (m)	Built in
Alexander von Humboldt	9000	120.5		24.4		8.95	14	13980		1	1.3	1998
Antigoon	8400	115	109.95	22.4	9.8	8.68	14	10853	33	1	1.2	1990
Arco Adur	2406	98.3	92.7	17.35	7.93	6.7	12	2940	45	1		1988
Arco Back	2600											
Arco Bourne	2600											
Argo 1	1150	79.79	75	11.1	5.21	4.12	10					1983
Arteveld	3679											
Banjaard	1320	78.59	74.9	12.32	4.42	3.6	13		20	1		1963
Bartolomeu Dias	14000	147.8		30		10	15.3	15,960	43.8/52	1	1.3	2012
Breughel	11650	122.9		28		8.15			43	1	1.2	2011
Charlemagne	5000	101.22	92.5	20.8	9.2	8.52	13.4	5883	40/60 extended	1	0.7	2002
Christophorus	967	80.8	77.85	9.77	4.58	3.3		909	20		0.6	1969
DC Vlaanderen 3000	2600	89.2	84.98	14	7.35	6.7	11	2300	35	1	0.8	2002
Delta	778	67.1	64.93	9.43	3.87	3.17	10	906				
Deo Gloria	1300	70.36		14.33	3.8	3.13	9	1060				1978
Hydra	1035										0.3	1908
Interballast 1	1680	84.61	77.98	13.03	7.6	6.9	12	2206		2		1957
Interballast 3	1400	70	65.3	13.2	6.4	5.4		1717				1981
Jade River	3281	98.5	91.6	16.42	8.21	7.33	11.9	8556	27/29	1	0.9	1979
Lange Wapper	13700	129.8	122.1	26.98	10.8	9.45	14.2	14978	28/50	1	1.2	1999
Orisant	2600	89.2	84.98	14	7.35	6.7	11	2300	35	1	0.8	2002
Reimerswaal	1600	82	77.3	11.5	5.1	4.7			30	1	0.65	1994
Rio	2430	69.1	64	14.3	7.4	4.25	10.8	2104	35	1	0.55	1986
Ruyter	1600	82	77.3	11.5	5.1	4.7		1880	30	1	0.65	1994
Saeftinge	752	75.06	71.75	9.45	3.95	3.05	11	1099		1		1979
Sand Fulmar	4920	99.9	95.4	19.5	10	7.78	12.5	4920	33	1	0.85	1998
Scelveringhe	3880	116.5	110	18.6	8.3	6.4	13		33.5	1	0.85	2004
Schotsman	1500	89.97	87.57	12.03	6.8	6.05		2850	25	1	0.6	1983
Swalinge	1800	81.7		14.45	6.46	5.34	12.5	1802				1977
Taccola	4400	95.3	84.7	21	8.5	7.3	12.6	6330	25	1	0.9	2003
Uilenspiegel	13713	142.8	126.5	26.82	10.8	9.45	14.2	13860	28	1	1.2	2002
Victor Horta	5000	99.9	92.5	20.8	9.2	8.5	14	5906	40	2	0.7	2011
Vlaanderen 20 (XX)	5072	106.45	101.02	21.49	7.57	6.65	14.4	10451	30/35 extended	2	0.8	1982
Vlaanderen 21	1751	76.02	72.5	14.52	5.01	4.58	11.4	3496	30/23 extended	1	0.65	1983
Vlieree	600	75.7	70.5	10	5.4	4.3				1		1955

Table D-2. Additional technical specifications of some TSHDs.*Following Miedema & Van Rhee (2007).

Hopper Class	TSHD	Length (m)	Width (m)	Capacity (m ³)	Pipe diameter (m)	Mixture Density (ton m ⁻³)	Flow (m ³ s ⁻¹)
Small	Rio	69.1	14.3	2430	0.55	1.3	3.2*
Small	DC Vlaanderen 3000	89.2	14	2600	0.8	1.3	3.2*
Medium	Taccola	95.3	21	4400	0.9	1.3	7.2*
Large	Alexander Von Humboldt	120.5	24.4	9000	1.3	1.3	10
Large	Breughel	122.9	28	11650	1.2	1.3	10

Table D-3. Per extraction event, estimated release of sediment fractions for each TSHD hopper class taking into account a relative fine seabed substrate (see Table x. for the comparison of values when coarse seabed characteristics are considered).

Hopper Class	Year	Capacity (m ³)	Pipe diameter (m)	16µm (kg)	63µm (kg)	250µm (kg)	500µm (kg)
Small	2012	± 2500	0.8	1349	674	48	73
Medium	2012	± 4500	0.9	4608	2304	186	161
Large	2012	± 10000	1.3	7939	3969	411	318
Small	2013/2014	± 2500	0.55	1130	565	21	32
Large	2013/2014	± 10000	1.2	14427	7213	531	503

Table D-4. Cumulative amount of the release of fines per TSHD hopper class.

Hopper Class	Capacity (m ³)	Year	Months	Extraction events	16µm (kg)	63µm (kg)
Small	± 2500	2012	Feb-Mar	9	12141	6066
Medium	± 4500	2012	Mar-May	83	382464	191232
Large	± 10000	2012	May-Jun	63	500157	250047
Small	± 2500	2013	Mar-Jun	76	85880	42940
Large	± 10000	2013	Oct-Dec	78	1125306	562614
Small	± 2500	2014	Feb-Mar	56	63280	31640
Large	± 10000	2014	Jan-Mar	143	2063061	1031459

Table D-5. Estimated release (kg) of sediment fractions (μm) for a single extraction event, as calculated with the TASS software. The outcome depends on the input of *in-situ* sediment characteristics: the fine core represents the finest sediments sampled in Sector 4c; the coarse core, the averaged sampled sediments in Sector 4c.

DC Vlaanderen 3000 {Small TSHD}			Rio {Small TSHD}		
Fraction (μm)	Fine core (kg)	Coarse core (kg)	Fraction (μm)	Fine core (kg)	Coarse core (kg)
16	1349	0	16	1130	0
63	674	0.2	63	565	0.02
125	0	0	125	0	0
250	48	14	250	21	6
500	73	38	500	32	16
1000	7	32	1000	7	14
2000	0	2.5	2000	0	1.2
Taccola {Medium TSHD}					
Fraction (μm)	Fine core (kg)	Coarse core (kg)			
16	4608	0			
63	2304	0.13			
125	0	0			
250	186	19			
500	161	51			
1000	11.5	43			
2000	0	3			
Alexander Van Humboldt {Large TSHD}			Breughel {Large TSHD}		
Fraction (μm)	Fine core (kg)	Coarse core (kg)	Fraction (μm)	Fine core (kg)	Coarse core (kg)
16	7939	0	16	14427	0
63	3969	0	63	7213	0.64
125	0	0	125	0	0
250	411	35	250	531	60
500	318	89	500	503	156
1000	19	74	1000	37	131
2000	0	6	2000	0	10
Charles Darwin {Jumbo TSHD}					
Fraction (μm)	Fine core (kg)	Coarse core (kg)			
16	43797	0			
63	21905	8.2			
125	0	0			
250	1916	210			
500	1718	545			
1000	127	455			
2000	0	35			

Annex E

Publications

This Annex forms part of the report:

Van Lancker, V., Baeye, M., Evangelinos, D. & Van den Eynde, D. (2015). Monitoring of the impact of the extraction of marine aggregates, in casu sand, in the zone of the Hinder Banks. Period 1/1 - 31/12 2014. Brussels, RBINS-OD Nature. Report <MOZ4-ZAGRI/I/VVL/201502/EN/SR01>, 74 pp. (+5 Annexes).

Annex E. Publications

Abstracts and Proceedings (poster/oral presentations)

- Van Lancker, V., Baeye, M., Francken, F., Van den Eynde, D., Evangelinos, D., De Mesel, I., Kerckhof, F., Van den Branden, R., Naudts, L. (2014). Working together on innovative monitoring strategies: adapting to nature, huge demands and grand challenges, *in: Mees, J. et al. (Ed.) (2014). Book of abstracts – VLIZ Young Scientists' Day. Brugge, Belgium, 7 March 2014. VLIZ Special Publication, 67: pp. 110. (poster) see: <http://www.vliz.be/nl/imis?module=ref&refid=234107>*
- Van Lancker, V., Baeye, M., Evangelinos, D., Van den Eynde, D., De Mesel, I. and Kerckhof, F. (2014). Use of Wave Glider monitoring for assessing changes in habitat integrity. GeoHab Conference (Marine Geological and Biological Habitat Mapping). Lorne (Australia), 5-9/5/2014. (oral presentation)
http://geohab.org/wp-content/uploads/2014/09/a0999b_5c562e0fe3fe4e1382315ac63acc6ff0.pdf
- Van Lancker, V. (2014). Grondstoffenexploitatie in de Noordzee. Uitstraling Permanente Vorming UPV Theme Resources. Oostende, 23/5/2014. (invited oral presentation)
- Van Lancker, V., Baeye, M., Evangelinos, D., Francken, F., Van den Eynde, D., De Mesel, I., Kerckhof, F., Norro, A., Van den Branden, R. (2014). Integrated monitoring of sediment processes in an area of intensive aggregate extraction, Hinder Banks, Belgian part of the North Sea, *in: De Mol, L. et al. (Ed.) (2014). 'Which future for the sand extraction in the Belgian part of the North Sea?'. Study day, 20 October 2014, Belgium Pier - Blankenberge. pp. 59-71. (oral and poster presentation) <http://www.vliz.be/nl/imis?module=ref&refid=242226>*
- Evangelinos, D., Baeye, M., Bertrand S., Van den Eynde, D., and Van Lancker, V. (2015). Dispersion and deposition of sediment plumes, resulting from intensive marine aggregate extraction. 11th Panhellenic Symposium on Oceanography and Fisheries. Mytilene, Lesvos island (Greece), 13-17/5/2015.

Submitted A1 publication

Van Lancker, V. & Baeye, M. (submitted). Wave Glider monitoring of sediment transport and dredge plumes in a shallow marine sandbank environment. Plos ONE.

Msc thesis

Evangelinos, D., (2014). Dispersion and deposition of sediment plumes, resulting from intensive marine aggregate extraction. Thesis submitted in partial fulfilment for Master degree in Marine and Lacustrine Science and Management (Free University Brussels, Ghent University, University of Antwerp), 42 p.